APPLICATION OF DETERMINISTIC AND STOCHASTIC ANALYSIS OF FAULT SEAL INTEGRITY IN BAKA FIELD, NIGER DELTA.

BY

NJOKU, IKECHUKWU ONYEMA

(B.TECH. Geology FUTO, M.SC Petroleum Geology UNIPORT)

REGISTRATION NUMBER: PhD/20099698668

A THESIS SUBMITTED TO THE POSTGRADUATE SCHOOL FEDERAL UNIVERSITY OF TECHNOLOGY, OWERRI

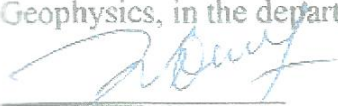## IN PARTIAL FULFILLMENT OF THE REQUIREMENTS FOR THE AWARD OF THE DEGREE OF DOCTOR OF PHILOSOPHY (Ph.D.)

IN

GEOPHYSICS

DECEMBER, 2015

CERTIFICATION

This is to certify that this research work reported in this thesis, " **Application of Deterministic and Stochastic Analysis of Fault Seal Integrity in 'Baka Field', Niger Delta**" was carried out by **Njoku Ikechukwu Onyema (Ph.D/20099698668)** in partial fulfillment for the award of the Degree of Doctor of Philosophy (Ph.D) in Geophysics, in the department of Geology, Federal University of Technology, Owerri.

17/07/2016

Prof. N. N. Onu   Date
Principal Supervisor

11/07/2016

Dr. A. I. Opara   Date
Supervisor

11/7/16

Dr. C. C. Z. Akaolisa   Date
Supervisor

11/7/16

Dr. C. C. Z. Akaolisa   Date

Head of Department

29/7/2016

Prof. B. Anusionwu   Date

Dean, School of Physical sciences

_____   Date

Prof. (Mrs.) Nnenna N. Oti

Dean, Post-Graduate School

26/5/16

Prof. Okwueze, E.E.   Date
External Examiner

ii

DEDICATION

This thesis is dedicated to the glory of God Almighty whose mercy and favor upholds me.

ACKNOWLEDGEMENT

TABLE OF CONTENTS

LIST Of TABLES

LIST Of FIGURES

APPENDIXES

ABSTRACT

Fault seal analysis in fault dependent reservoirs were carried out at different reservoir levels in the Baka Field, Niger Delta. These involved stratigraphic correlation, 3-D seismic interpretation of faults and horizons, time-depth conversion of all interpreted faults and structural maps using both check-shot and synthetic seismogram. Also, static models of all interpreted reservoir levels, and 3-D deterministic and stochastic fault seal integrity models were carried out. The deterministic approach applied in this study is sensitive to uncertainties associated with mapping of horizons in the proximity of faults and the inherent uncertainties in the static fault interpretation in both position and fault zone properties complexity. However, the integration of stochastic approach captured the uncertainties in the position of the reservoirs at all interpreted faults by allowing multiple realizations of stacking geometries relative to their lateral reservoir distribution. All hydrocarbon bearing reservoir levels and faults were interpreted in detail on seismic and a structural framework model was built for juxtaposition analysis and fault shale gouge ratio calculation. The interpreted hydrocarbon columns of the reservoirs in the field are mostly controlled by structural spill points, implying that the faults affecting the accumulation must be effectively sealed which is evident from calculated high SGR values. Some reservoirs are under filled, indicating that the faults are leaking. It was shown that these fault intervals have relatively low SGR. There is high degree of conformity between field hydrocarbon column heights and the stochastic column heights predicted from the shale gouge ratio. The calculated shale gouge ratio quite matched with the shale gouge ratio related column height distribution used in exploration. Top shale thickness played a role (impede up dip fluid conduit), but not a major factor in the Baka reservoirs as regards to column controls. Also, faults in the Baka Field leaks at <20% shale gouge ratio with varying weak points, mainly 20 – 35% shale gouge ratio and more. Good fault seal capacity exists in the Baka Field at >40% shale gouge ratio. Shale gouge ratios are higher at the boundary fault.

Key words: Fault seal, Shale Gouge ratio (SGR), Hydrocarbon column Height, Stratigraphic Juxtaposition, Structural Spill Points and Leaking points.

Chapter One: Introduction

1.1. Background Information:

The study involved fault seal analysis of Baka Field, Niger Delta. This encompassed stratigraphic, structural and petrophysical interpretations in the delineations of fault zone mixed clastic architecture as well as implications to the across fault pressure differentials. The Baka Field is located within the coastal swamp depobelt of the Cenozoic Niger Delta basin. This field is characteristic of different reservoir levels with diverse structural styles. The different structural styles include the faulted roll-over, collapse crest, horst and grabben that resulted in flexural styles in the field. The faults in the field are predominantly growth faults due to the listric normal faults with varying fault throws. These faults in the field however have direct relationship to the sedimentary infill and stratigraphic differences within the field and as such depicts fault dependent reservoir structures. Although faults may be of great importance in a reservoir (sealing faults), some others may egress away fluid and as such detailed interpretation of the faults to ascertain the geological imprints and connotations will reduce drilling of many potentially dry holes thereby saving cost, enhance early decision making, and clues to accuracy in well placement.

Fault seal analysis is the study of the likelihood of fault to allow fluids to move across the fault plane (leak) or not (seal); (Lashin and Abd El-Aal 2004). Fault seal analysis had been carried out by many researchers including Needham et al. 1996, Yielding et al. 1992, Yielding 1997, 1999a & b, Yielding 2002, Knai and Knipe 1998, Manzochi et al. 1999, Fristad et al. 1997, Fisher and Knipe 1998, Lindsay et al. 1993, Manzocchi et al. 1999 and 2000, Lehner and Pilaar 1997, Freeman et al. 1998 & 2004, Hesthammer and Fossen 2000, Bretan et al. 2003, Gibson and Bentham 2003, James et al. 2004, Knipe et al.2004, Hermanrud et al. 2005, etc.

The Baka Field fault seal analysis involved using known column height in the Baka Field to calibrate the traditional exploration column height prediction tool – mainly fault seal. Also, structural spill points and leak points controlled by juxtaposition, shale gouge ratio calculations, column height controls and fault seal capacity were evaluated.

Seal capacity determination is a critical element and a key prerequisite for reliable and successful exploration and production forecast. Geologically, for hydrocarbon accumulation to exist there must be reservoir rocks, seals, trap, and hydrocarbon charge. In spite of considerable researches and publications on the controls on fault seal capacity, there is still a conspicuous lack of precision regarding the

implications of fault zone architecture, the distribution of fault rock heterogeneity within the fault zone, and its capacity to seal. Therefore, it is paramount to understand from the first principle, the key parameters controlling fault surface interplay and its integrity to seal involving seal parameter, spill points, weak point, hydrocarbon column height, and stratigraphic juxtaposition of the fault surface.

Some of the useful terms in this study include: **(1) Spill point:** simply means the structurally lowest point in a hydrocarbon trap that can retain hydrocarbons. Once a trap has been filled to its spill point, further storage or retention of hydrocarbons will not occur for lack of reservoir space within the trap. The hydrocarbons spill or leak out, and they continue to migrate until they are trapped elsewhere.

(2) Weak point: is the location on the fault that exhibits the lowest capillary entry pressure and thus the most likely connected path for hydrocarbons to escape from the trap. Therefore, weak point is the lowest Shale Gouge Ratio value with the shortest column at the shallowest depth. That is the largest pore throat nearest to fault zone edge that provides access to a leak path in the fault zone. Any additional hydrocarbon added to the trap at OWC, would cause an increase in buoyancy pressure that would exceed Critical Fault Displacement Pressure (Pd,

seal capacity) causing excess oil to migrate out of trap and along the fault zone. This means that, at weak point, buoyancy pressure equals the fault entry pressure; (Filbrandt et al. 2007).

(3) Closure: is the area within the deepest structural contour that forms a trapping geometry.

(4) Trap: is a geologic structure or stratigraphic feature that allows the accumulation of hydrocarbons. Trap may be any of the following, (i) Structural traps; hydrocarbon traps that form in geologic structures such as folds and faults. (ii) Stratigraphic traps; results from changes in rock type or pinch-outs, unconformities, (iii) Strati-structural or combination trap; have aspects of both structural and stratigraphic traps.

(5) Seal: is a relatively impermeable rock, commonly shale, anhydrite or salt that forms a barrier or cap above and around reservoir rock such that fluids cannot migrate beyond the reservoir. Also, it may be defined as a sediment, rock or immobile fluid with a high to very high capillary entry pressure which will dam or trap hydrocarbon.

(6) Barrier: is a type of seal lithology within a reservoir that prevents fluid flow during production.

(7) Baffle impedes flow.

1.2. Statement of Problem:

Poor knowledge of the Estimate of Hydrocarbon in a Reservoir, its Sealing Capacity and poor understanding of the Petroleum Migration Trend in a Reservoir. These may prompt the fear of Prospect Risking, improper Field Unitization and wrong placement of well(s) thereby resulting to drill Loss (Dry Hole).

1.3. Aim and Objectives:

Aim: Presentation of deterministic and stochastic 3-dimensional fault seal model in a brittle/ductile (sand/shale) sequence, through interpretation of seismic and well log data from the Baka Field.

Objectives: Assessment of Fault Seal Integrity in a Fault Dependent Petroleum Reservoir, Reserves Estimation and Risk Assessment / Mitigation of Drill loss. These involved detailed integrated interpretations of well log and seismic data, (depth conversions with check-shot, synthetic seismogram, velocity models, faults and horizon mapping, time structural and depth structural maps, 3D structural modeling, property modeling of the petrophysical parameters, stratigraphic juxtaposition modeling, column height calculations, seal integrity predictions, leak and weak points determination, overlying shale top seal evaluations, deterministic and stochastic 3D model assessments).

1.4.   justification of Study:

Considering the huge loss of money in the cause of drilling a dry well, it is paramount the oil industry has to take into account fault seal analysis before drilling is approved. Where a discovery has been made in a development scenario, the oil industry requires not only to know the faults that have compartmentalized the reservoir but also how many wells needed to extract the hydrocarbon. The study of fault seal bridges the gap between divers disciplinary studies of petroleum.

Fault seal analysis enables us to understand the major control on hydrocarbon distribution and accumulation. It provides basis for risking undrilled fault dependent prospects. It provides test of predictive methods. Its model provides a replication of the hydrocarbon condition in a trap. It provides a means for conducting sensitivity analysis and therefore leads to improved prospect risking. Fault seal workflow allows rapid assessment of the value of exploration prospects with a high probability of compartmentalization and informed decisions to be taken at an early stage. It provides information on hydrocarbon column height that could support against fault and what expected volume the oil industry might have. It aid in reservoir management considering where to be putting injectors

and producers, in determination of baffle to fluid flow. Depending on the nature of the baffling, how it's trapped the oil, it actually improves recovery efficiency. Thus far, it must be noteworthy that fault seal deserve special study and should be taken as an integral and indispensable first priority in the oil industry.

1.5. Scope of Study:

The scope of this work covered faults / structural interpretation, seismic to well tie using well 5 velocity data and well 5 check-shot data, horizon mapping (depth conversion and building 3D grid), stratigraphic juxtaposition, structural/saddle spill points and leak points controlled by juxtaposition, fault spill points, shale gouge ratio calculations, column height controls, fault seal capacity, using known field column heights (based on petrophysical fluid contact and reservoir vertical relief) to calibrate the traditional exploration column height prediction method – mainly fault seal (based on shale gouge ratio as seal attribute) for prospect evaluation and application.

1.6. Location and Physiography:

Presently, the Niger Delta occupies about $75,000km^2$ of the sedimentary basin of the southern Nigeria. It is situated in the eastern corner of the Gulf of Guinea which is at the intersection of the triple R junction from which the separation and rifting of the South America and Africa was initiated in the middle Cretaceous time. The subsequent instability and subsidence along rift zones led to a marine transgression which terminated in the late middle Cretaceous times. In the late Cretaceous a proto Niger Delta developed which ended with a major transgression in the Paleocene. From Eocene onwards, regression occurred with the deposition of a wedge of fluvio-deltaic sediments which built out into the South Atlantic as the modern Niger Delta (Stoneley, 1966; Short and Stauble, 1967; Burke, 1972). The study location in this research is the Baka field, located in the coastal swamp depo-belt, Niger Delta, Nigeria.

A few publications had been made concerning the hydrocarbon reservoir seal studies in the Niger Delta. Such findings includes but not limited to the work of Yielding 2002 (as part of his world wide basin studies), Bashir et al. 2003, Filbrandt et al. 2007 etc.

1.7.1. Niger Delta Stratigraphy:

Short and Stauble (1967), defined three stratigraphic units in the tertiary Niger Delta based on the dominant environmental influence. The main sedimentary environments are the continental environment, the transitional environment and the marine environment. The three environments as said earlier are stratigraphically superimposed. The basal parts of the stratigraphic sequence are massive marine shales. The part lying in-between the upper and lower stratigraphic sequence is represented by inter-bedded shallow marine and fluvial sands, silt and clays which are typical of parallic setting. The sequence is capped by a section of massive continental sands.

Based on the history or relative unbroken progradation throughout the Tertiary, these depositional lithofacies are readily identified despite local facies variations, as three regional and diachronons formations ranging from Eocene to Recent age. The three formations are locally designated (from the bottom) as Akata Formation, Agbada Formation and Benin Formation respectively. Of the three formations, the Agbada Formation constitutes the main reservoir of hydrocarbons in the Niger Delta while the Agbada shales mainly constitute the seals. This formation is therefore given greater attention in this study.

The stratigraphy of Niger Delta outlined below is based on the work of (Short and Stauble 1967; Weber 1971; Weber and Daukoru 1975; lambert-Aikhionbare and shaw 1982).

1.7.2. Akata Formation:

The basal marine pro-delta megafacies Akata Formation is predominantly shale sequence with occasional turbidite sandstones and siltstone. The approximate range of thickness is from 0 – 6000 meters and the formation crops out subsea in the outer delta area but is not seen on shore (Weber and Daukoru 1975). The formation consists of dark grey uniform shale, especially in the upper part. In some areas, it is sandy or silty in the upper part of the formation where it grades into the Agbada Formation.

As defined by paleontological evidence mainly planktonic foraminifera, the marine shale of the Akata Formation range from Paleocene to Holocene in age and are over pressured.

Source rocks of the Niger Delta hydrocarbon have been a subject of some controversy. Some researchers have proposed the shales of the paralic sequence (i.e. Agbada Formation) as the source rock, while others argue that in most parts

of the delta, the Agbada Formation is immature and suggested the source rocks to be the mature shales of Akata Formation that are more mature. Drilling activities have not penetrated the base of Akata Formation probably because of its highly compacted and overpressured nature.

1.7.3. Agbada Formation:

The Agbada Formation consists of alternating sandstones and shales deposited at interface between the lower deltaic plain and marine of the continental shelf fronting the delta. It consists of numerous offlap rhythmic, the sand parts of which constitute the main petroleum reservoirs in the Niger Delta oil fields. The shales constitute seals to reservoirs and as such are of utmost important in this study. The alternations of sandy and argillateous sediments are the result of differential subsidence, variation in the sediment supply and shift in the depositional lobs of the delta. Generally the upper part is sandier than the lower part, indicating a general seaward advancing of the delta. The thickest section of the Agbada is about 10,000ft to 15,000ft (Weber and Daukoru 1975). Obviously thickness will vary from place to place dependent on structural and depositional position and criteria adopted for definition. The age of the formation varies progressively from Eocene in the North to Recent in the South at the present day

surface. Weber (1971): the rhythmic sequences which constitute the Agbada Formation because the separate sections of the rhythms were laid down under a variety of conditions are: (1) Agbada onlap or transgrsssive marine sand, (2) Agbada offlap marine clay, (3) Agbada fluvio-marine barrier foot deposits, (4) Agbada barrier bar deposits, (5) Agbada tidal channel deposits, and (6) Agbada fluviatile deposits.

1.7.4. Benin Formation:

The Benin sand is predominantly a sandstone sequence with a few shale intercalations which become more abundant towards the base. The Benin Formation has been described as "Coastal plain Sands" which outcrop in Benin, Onitsha and Owerri provinces and elsewhere in the delta area. The sediments represent upper deltaic plain deposits. The sands may represent braided stream point bars and channel fills or crevasse splay deposits. The shales are few and thin and they may represent back swamp deposits.

Among the minor components, limonite coating, lignite streaks, hematite and feldspar are common. However, the formation lacks faunal content and this makes it uneasy to date although an Oligocene – Recent age is generally accepted.

Till today, very little oil has been found in the Benin Formation (mainly minor oil show), and the formation is generally water bearing. It is the main source of portable ground water in the Niger Delta area. See figures (1.7.1 and 1.7.2).

Niger Delta

Outer Thrust E&W	Folds E&W	Inner Thrust E&W	Deforme d Zone	Wrench Zone	Shallow Offshore	Coastal Swamp	Central Swamp	Greater Ughelli	Northern Delta	PLAYS
										Pliocene
					412	116				Upper Miocene
						64				Middle Miocene
						128	24			Lower Miocene
							56	85		Upper Oligocene
								82		Lower Oligocene
								77	67	Upper Eocene
									43	Middle Eocene
									31 49	Lower Eocene
										Paleocene
15	29	23	15		412	308	165	226	123	Upper Cretaceous
										Lower Cretaceous

ROLLER ZONE
CRETACEOUS MARGIN
WRENCH ZONE
FOLD WEST
OUTER THRUST BELT WEST
INNER THRUST BELT WEST
NORTHERN DELTA (Eocene)
GREATER UGHELLI (Oligocene)
CENTRAL SWAMP (L-M Miocene)
COASTAL SWAMP
STUDY AREA
SHALLOW OFFSHORE (Pliocene)
INNER THRUST BELT EAST
DEFORMED BELT
FOLD EAST
OUTER THRUST BELT EAST
VOLCANIC BELT

1:601,197

Figure 1.7.1 Structural map Niger Delta Showing Study Location, depobelts, plays and number of wells drilled in them (after Carol and Ejedawe, 2012)
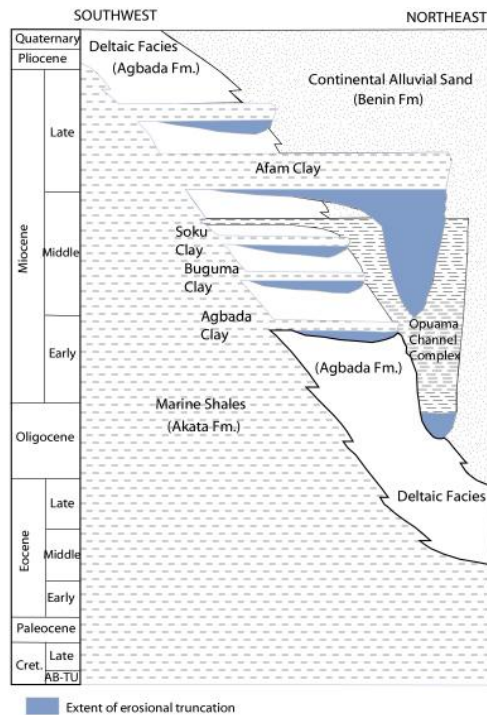
Figure 1.7.2. Stratigraphic column showing the three formations of the Niger Delta. Modified from Shannon and Naylor (1989) and Doust and Omatsola (1990).

1.8. Niger Delta Structure:

The Niger Delta basin is not much disturbed at the surface but the subsurface is affected by large scale synsedimentary features including the growth faults, rollover anticlines and diapirs.

1.8.1   Growth Faults:

Weber and Daukoro described this as a result of rapid sand deposition along the delta edge on top of under-compacted clay which leads to the development of a large number of synsedimentary gravitational faults (Fig. 1.8.1). The termed "growth faults" are also well known from the US Gulf Coast. Based on the theory of soil plasticity, the growth fault origin and shape can be explained.

The spacing between successive growth faults decreases with an increase of depositional slope or an increase in the rate of deposition over the rate of subsidence. Growth faults tend to envelop local depocenters at their time of formation. Their trend is thus an indication of the prevailing sedimentological pattern.

The term "growth fault" derives from the fact that after its formation, the faults remains active and thereby allowing faster sedimentation in the down thrown fault block relative to the up-thrown side. The thickness ratio of a given stratigraphic unit in the up-thrown block is known as the "growth index" which in Nigeria can be as high as 2.5. Basically, growth faults are listric normal faults and thus tend to die out with depth thereby forming bedding plane.

The fault throw at the level of the Akata Formation is often as large as several thousand feet. The enhanced sedimentation along the growth fault causes a rotational movement. This tilts the beds towards the fault thereby forming the "rollover anticlines". Almost all the oil fields discovered in the Niger Delta so far are associated with the rollover anticlines. An important characteristic of Nigerian rollover anticlines is the shift of the crestal position with depth. The Agbada Formation is the most affected by growth faulting in the Niger Delta. The faults of the Niger Delta die out at the upper part of the massive marine Akata shale Formation.

The structural style in the Niger Delta, both on a regional scale and on a field scale can simply be described by the influence of sedimentation ratio to subsidence rates. Thus the following can exist:

(i) Simple unfaulted anticlinal rollover structures

(ii) Faulted rollover anticlines with multiple growth faults or anticlinal faults

(iii)   Complicated collapsed crest structures

(iv)   Sub-parallel growth faults (K-block structure)

(v) Structural closures along the back of major growth faults.

Most of the largest fields in the Niger Delta are of the collapsed crest type and   about half of all the structures of this type are prominent fields. The second best fields are the faulted rollover anticlines while third are the unfaulted rollover structures. Among all other types, only the structures in the upthrown blocks of major growth faults occur with some frequency and appreciable reserves.

1.8.2.   Shale Ridges and Salt Diapirs:

The shale upheaval ridges occurring in Nigeria are of three different kinds (Weber and Daukoru, 1975). The first are the zones behind major growth faults. Secondly, shale bulges in front of growth faults are often observed and these bulges can sometimes act as positive elements, causing collapsed crest structures and unconformities. The third type, are those along the continental slope shale bodies were extruded in a seaward direction as a result of different loading on the plastic marine shale. With continued sedimentation, these offshore clay upheaval ridges are buried but like salt domes, their growth can continue. Finally, the clay ridges may develop into true diapiric structures.
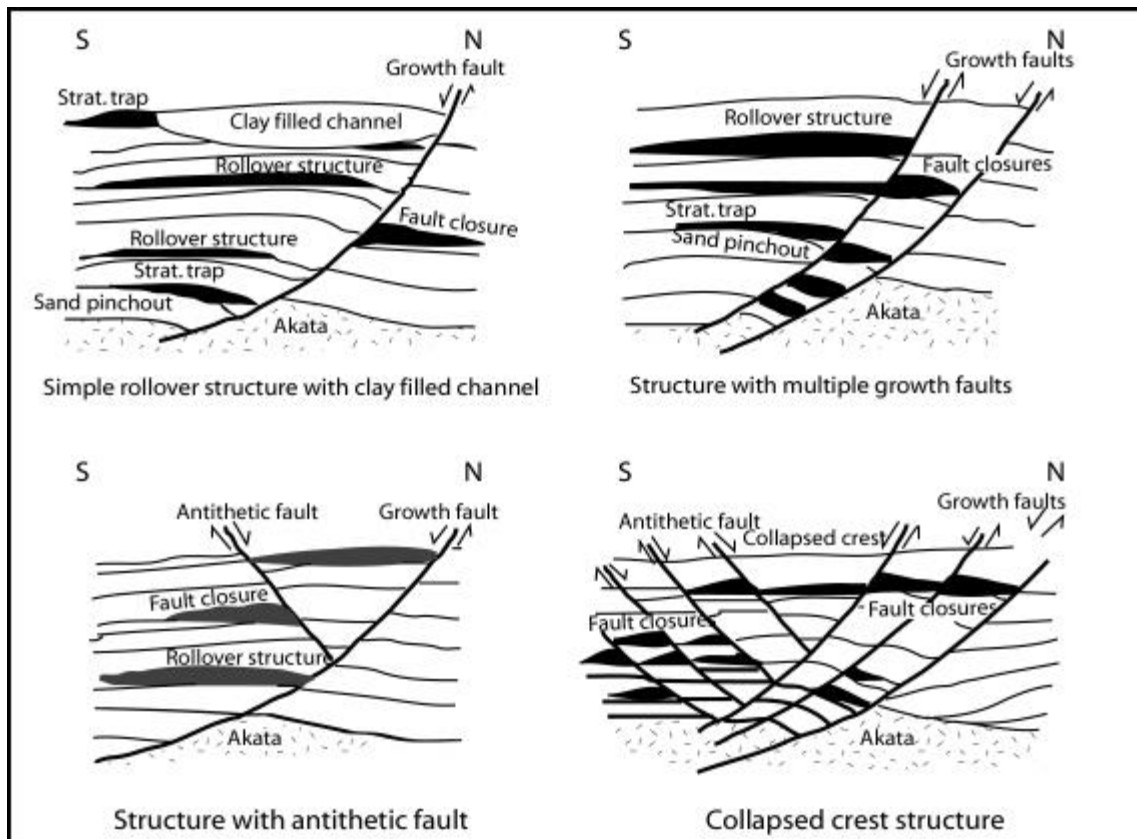
Figure 1.8.1, Example of Niger Delta oil field structure and associated trap types. Modified from Doust and Omatsola (1990) and Stacher (1995).

1.8.3   Niger Delta Petroleum Geology:

The prolific Cenozoic Niger Delta has enormous petroleum reserves estimated at about 30 billion barrels of oil and 260 trillion cubic feet of natural gas. Worldwide ranking marks the Niger Delta as the seventh richest petroleum production with an average of about 1.8 million bbl of oil per day. Nearly 1 billion

barrels of oil and condensate have been discovered in the Rio Del Rey section in Cameroon and 45 million barrels occur in the Equatorial-Guinea sector of the delta (Weber and Daukoru 1975).

In the Niger Basin, oil and gas reserves mainly occur in sandstone reservoirs throughout the Agbada Formation, usually trapped in (faulted) rollover anticlines associated with growth fault. Moreover, growth fault-related structural traps, stratigraphic traps related to palaeo-channel fills, regional sand pinch-outs and truncations occur. Gross reservoir properties are a function of depth, sand / shale ratio and the sealing potential of faults, while the transgressive marine shales form important regional top seals, with faults often providing lateral seals. Due to stacked sand / shale alternations, most oil fields in the Niger Delta have multiple reservoir levels, with oil column heights averaging between 15 to 50m. Exceptionally, longer columns do exist under favorable (fault) sealing conditions, and / or in stratigraphic traps. The mature Eocene to Miocene shales of the Akata and Agbada Formations constitute the major source rocks. Niger Delta crudes originate mostly from land plant material: hence, they are high in resins and waxes, with significant contributions of structureless organic matter from marine source. Nigerian crudes has low sulphur content (below 0.4%) also confirms land

plant source material. Overall consideration showed that two types of crudes are found in the Niger Delta, light paraffinic, waxy crude with pour points of about 20 to 90^{0}F; and naphthenic, non-waxy medium crude with specific gravity of less than 26^{0}API, and pour point below -13^{0}F. Details of the petroleum geology of the Niger Delta is as shown in figure 1.8.3.1.

Niger Delta Depobelts

The Niger Delta has been subdivided into regions based on the tectonostratigraphic development.

These units or depositional belts are bounded by linked growth fault systems.

Legend:
- Pre-Cretaceous Basement
- Outcrop of Cretaceous
- Paleocene Imo Shale Outcrop
- Northern Delta
- Greater Ughelli
- Central Swamp I
- Central Swamp II
- Coastal Swamp I
- Coastal Swamp II
- Offshore (L. Miocene-Pliocene)
- Distal Belt Areas
- Slope Depocentres
- Diapir Belt
- Toe Thrusts

Hooper et al., 2002

Schematic Niger delta regional dip cross-section showing structural belts.

Figure 1.8.3.1 Niger Delta Depobelts and Niger Delta Regional cross-section; showing structural belts (after Hooper et at., 2002).

22

1.9. Theoretical Framework

1.9.1 Different Mechanism of Fault Seal Estimation:

It important not to restrict our understanding regarding fault seal study but also have good knowledge of other seal parameters and the reason why using a particular seal attribute. Some of the common mechanisms are:

(1) **Transmissibility multipliers** (has not been fully understood or defined and therefore do not provide significant confidence that the reservoir fluid simulation model will accurately predict the likely hydraulic behavior of fluid - Lia et al. 1997 and Harris et al. 2002).

(2) **Cataclasis** (which is the crushing of sand grains to produce a fault gouge of finer grained material, again giving the fault a high capillary entry pressure).

(3)**Diagenesis / Cementation:** (when preferential cementation along an originally permeable fault plane may partially or completely remove porosity, ultimately creating a hydraulic seal).

(4) **Reservoir / Non-reservoir stratigraphic juxtaposition** (in which reservoir sands are juxtaposed against a low-permeability unit e.g., shale, with a high entry pressure).

(5) **Clay smear** (i.e., entrainment of clay or shale into the fault plane, thereby giving the fault itself a high entry pressure. This includes clay smear potential (**CSP**), shale smear factor (**SSF**), and shale gouge ratio (**SGR**)).

SGR and **CSP** estimate the likelihood of smear developed fault surface and derived from multiple source beds, where SSF estimates the possibility of specific shale layer being drawn along the fault zone to form a thinned but continuous smear (Fisher and Jolley, 2007).

A key limitation of the CSP and SSF algorithms is that they only provide information on the continuity of clay smears, and do not by themselves provide an estimate of the clay content along a fault when the smear is discontinuous. SSF and CSP relied on the modeler to define and identify the discrete shale layers that are considered as source beds for the smear. SGR provides an estimate of clay content along a fault irrespective of whether or not the clay smear is continuous.

1.9.2. Fault Seal Terminologies:

Watts (1987) recognized two most likely barriers to hydrocarbon flow within rocks over geological timescale as 'membrane' and 'hydraulic' seal. **Membrane seal** are generally classified as the boundary of layer of smaller pore throats, and

therefore capable of allowing the passage of hydrocarbon under certain pressure conditions. Capillary entry pressure determines the effectiveness of membrane seals over geological timescales and is defined as 'the pressure required for hydrocarbon to enter the largest interconnected pore throat in the seal' (Watts 1987, p.278). **Hydraulic seal** have no inter-connected pore space or the pore throats are so small that the rock strength is exceeded before the capillary entry pressure and are thus only breached through fracturing.

A seal which has the capacity to maintain a pressure drop over millions of years is called '**static sealing**', while that which maintains a pressure drop over the life time of a single field is called '**dynamic seal**', (Yielding et al., 1999a,b).

A conceptual fault seal modeling could be a deterministic model, stochastic model or combination of both. **Deterministic models** (are sensitive to the uncertainties associated with mapping of horizons in proximity of faults and the inherent uncertainty in a static fault interpretation in both position and fault zone complexity), since the prediction of the locations of the reservoir overlap is made from the static model of the reservoir horizon and fault geometry (Dee et al 2007). **Stochastic models** capture the uncertainty in the position of the reservoir at the fault by allowing multiple realizations of stacking geometries, where the

principal assumption is that these stacked reservoir zones are laterally continuous covering the entire likely fill area.

1.9.3 Descriptions of Different Fault Seal Concepts

1.9.3.1 Alan Diagram (Stratigraphic Juxtaposition diagram): Alan maps are essentially depth vertical sections along the strike length of a fault showing the locations of stratigraphic units intersecting either side of the fault, (Alan 1989). This method is an effective method of showing all potential juxtapositions of reservoirs across the fault. Juxtaposition gives us the connectivity or "plumbing" between reservoirs. Understanding the juxtaposition area is vital when trying to understand production scenarios. The degree of fault seal or conversely connectivity usually varies greatly at different locations on the fault plane. Illustration of the concept of stratigraphic juxtaposition is shown on figure 1.9.3.1.
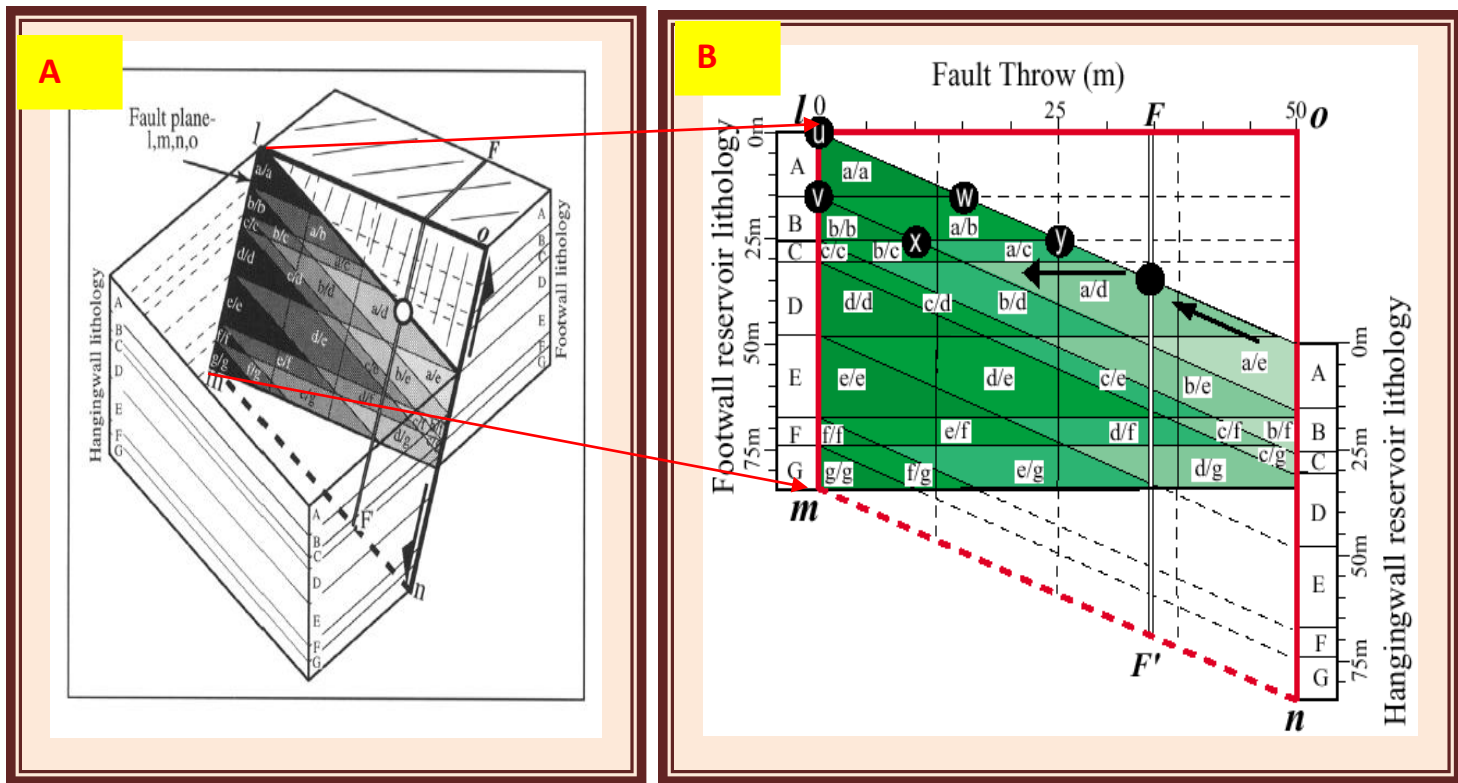
Fig. 1.9.3.1: Illustration of the idea of juxtaposition diagram adopted from (Knipe, 1997,)

1.9.3.2   Shale Smear Factor:

Lindsay et al. (1993) proposed a shale smear factor (SSF) based on their observations of abrasion smears in a lithified sequence as SSF which constrains the continuity of the smear along the fault plane. Fig. 1.9.3.2., shows Lindsay et al. (1993) Shale Smear Factor. They defined Shale Smear Factor (SSF)

as: SSF= $\dfrac{\text{Fault throw}}{\text{Shale layer thickness}}$ ……………….…… (1)
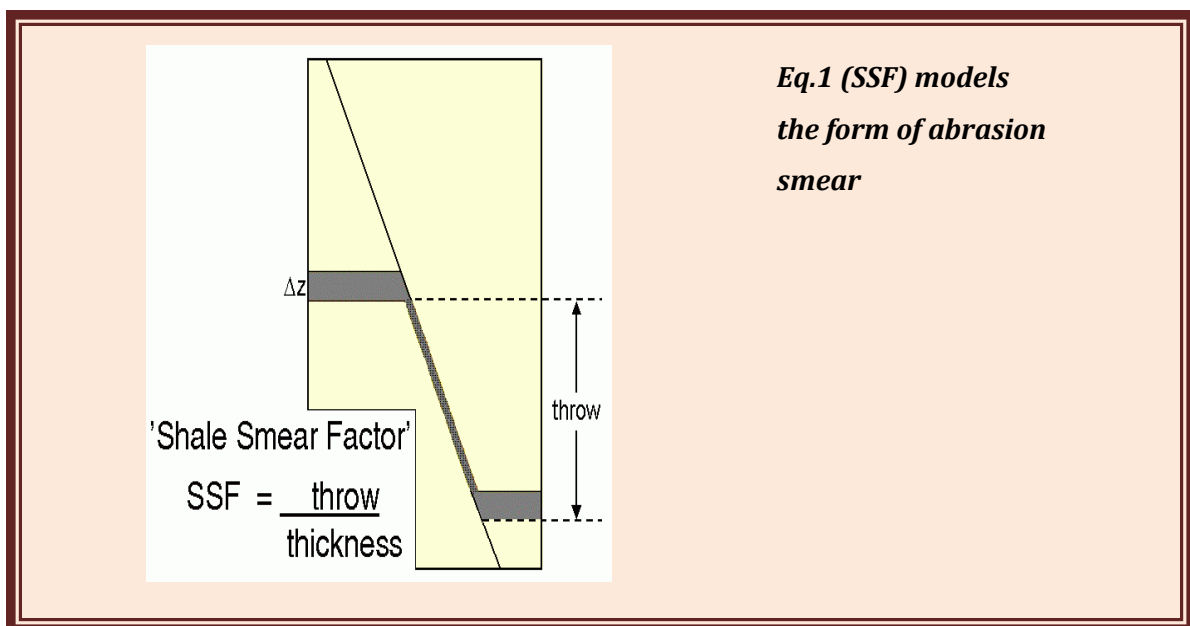
Fig. 1.9.3.2: Shale Smear Factor (SSF) (Lindsay et al., 1993)

1.9.3.3. Clay Smear Potential: Bouvier et al. (1989) define CSP as

$$\text{CSP} = \sum \frac{(\text{Shale bed thickness})^2}{\text{Distance from source bed}} \qquad \text{............. (2)}$$

Eq.1 (CSP) & Eq. 2 (SF) models the distance-tapering of shear-type smears.

Δz

distance

Clay Smear Potential

$$\text{CSP} = \sum \frac{\text{thickness}^2}{\text{distance}}$$
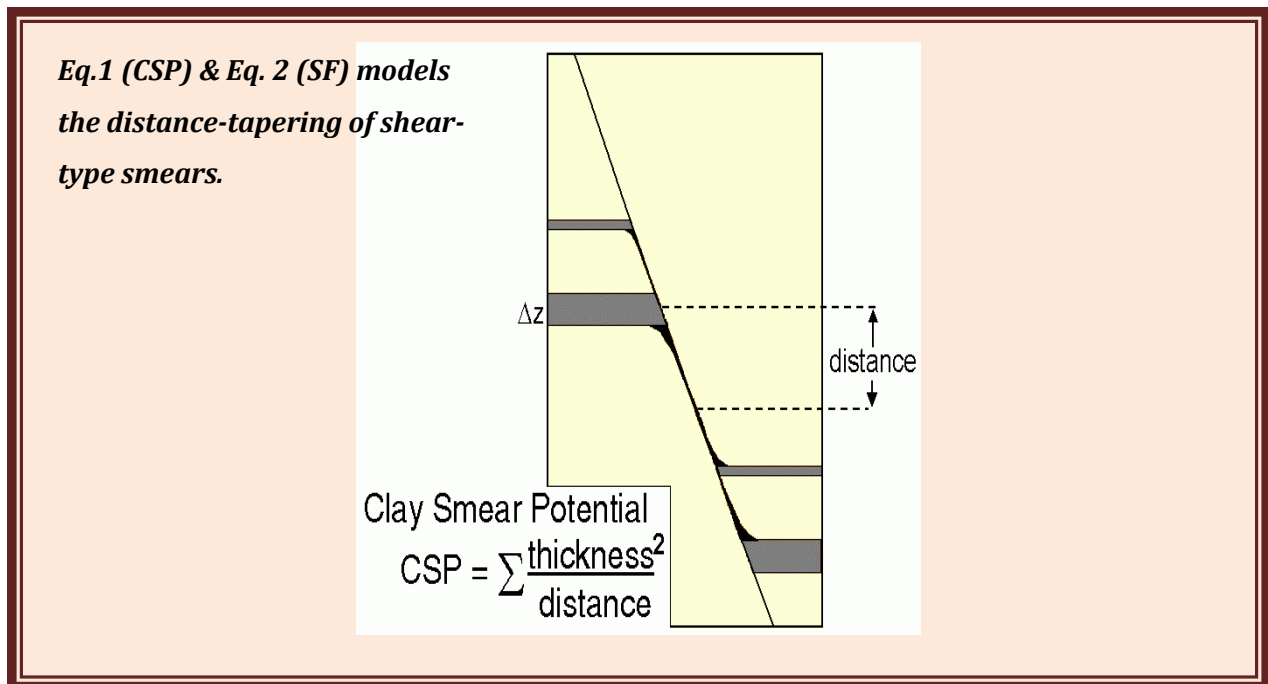
Fig. 1.9.3.3: Clay Smear Potential (CSP) (Bouvier et al., 1989; Fulljames et al., 1996)

1.9.3.4. Shale Gouge Ratio: Yielding et al. (1997) define SGR as

$$\text{SGR} = \sum \frac{\text{(Shale bed thickness)}}{\text{Fault throw}} \qquad \text{................ (3)}$$

That is Shale Gouge Ratio (SGR) represents the proportion of shale or clay that might be entrained in the fault zone by a variety of mechanisms. The shaly wall rocks will increase the amount of shale in the fault zone, hence high capillary pressure. In case of thick reservoir zone (fig.1.9.3.4.) where the faulting affecting a zone of beds rather than individual simple beds another treatment for the Shale Gouge Ratio (SGR) can be used:

$$\text{SGR} = \sum \frac{\text{(Zone thickness) . (Zone clay fraction)}}{\text{Fault throw}} \qquad 100\% \quad \text{...... (4)}$$
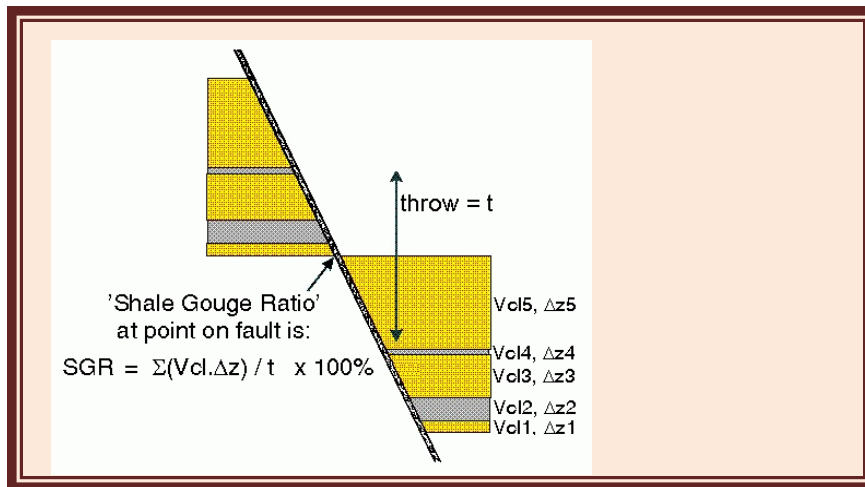
Fig. 1.9.3.4: Shale Gouge Ratio (SGR) (Yielding et al., 1997)

Chapter Two: Literature Review

Koledoye *et al.* (2003) however generated a new process-based methodology for analysis of shale smear along normal faults in the Niger Delta. This involved three-dimensional (3-D) seismic and well-log data from the producing Okan field in the Niger Delta. A working conceptual model derived from field observations and theoretical considerations were used to map the 3-D geometry of a representative normal fault with shale smear. Seismic data showed clear fault segmentation in the dip direction with extensional relays referred to be occupied by smeared shales. Log data helped to identify lithologic horizons throughout the field, and in some cases, where a wellbore crossed the fault, to quantitatively determine the amount of smeared shale within the fault zone. The development of conceptual models provided means for interpretation of crucial details of the fault geometry and the distribution of shaley fault rock beyond the conventional resolution of a 3-D seismic data set. With the combination of seismic data, well-log data, in the conceptual model; they developed a procedure to determine the fault geometry. They assessed the nature of the smeared shales and their evolving configurations as a function of the fault throw, thickness of corresponding shale units, and the thickness of the sand units between the

shales. They said that this work introduced a new and improved technique to visualize fault architecture and to interpret fault rock; both of which lead to constructing a structurally realistic juxtaposition diagram and a physically sound shale-smear analysis in a reservoir.

Shale Gouge Ratio (SGR) - calibration by geohistory was conducted by Yielding (2002) in basins with mixed clastic sequence and dominant extensional faulting which occurred in range of depth 0 -2km. These include Niger Delta, Northern North Sea, Central North Sea, Mid-Norway, Grand Banks, Gulf of Mexico, Columbus Basin, Vietnam, and Gulf of Thailand. The integrated comparison was done to delineate a seal – failure envelope, based on seal attribute and across-fault pressure difference calibration to determine efficiency of the reservoir seal. He concluded that: (i) Shale Gouge Ratio is a robust method for predicting the gross distribution of fault – rock types (cataclastic/frame work phyllosilicate fault rocks / clay smear). (ii) In an exploration / appraisal context, higher values of SGR generally indicate the potential to hold back higher pressures (trap greater hydrocarbon columns) at sand – on – sand juxtaposition. (iii) In a production context, higher values of SGR generally indicate lower fault-zone permeabilities, and hence more resistance to across-fault flows. (iv) In both

exploration and production, all elements of the structural history should be considered in calibrating the calculated Shale Gouge Ratio against expected column height or fault –zone permeability. This is particularly so at lower SGR values, where different burial depths at the time of faulting can produce disaggregation zones or cataclasites, and different maximum burial depths can produce different degrees of cementation. (v) SGR can be used, in conjunction with structural history, to produce a first-pass distribution of transmissibility multipliers for simulation, cutting months off the history-match workflow. (vi) Time needed to be invested in basin- and field-specific refinements of the relationships between SGR, entry pressure and fault-zone permeability to account for local variations (e.g. related to lithologies and / or burial depth), and to explore the sensitivities to unmappable features such as subseismic relay zone. He observed that the Oseberg Syd study suggested an SGR value between15 and 20% represented a threshold value between non-sealing and sealing faults, in an appraisal context. This value also represents the maximum clay content of cataclastic gouge, implying that in this field cataclasite do not form significant seals whereas more clay-rich gouge do. He further said that this threshold had proven to be robust not only in Brenth Province but also in other basins with mixed clastic reservoirs.

Alan, (1989) presented a model that relates faults to petroleum migration and entrapment. The model was based on an assumption that fault is neither a seal nor a conduit. He said that the effect of faulting on both migration and entrapment depends on the rock properties of strata juxtaposed fault blocks. He used fault-plane sections and structural maps to generate a three dimensional view of migration and trapping; and illustrated the interplay of three critical parameters: (1) closure style, that is, unfaulted anticline, faulted anticline, or nose, (2) cross-fault geometry, i.e., the throw and change of throw along a fault, and (3) stratigraphic geometry, i.e., the thickness and spacing of permeable and impermeable units. He said that cross-fault spill-points defined limits of trapping potentials and paths for vertical migration. Synclinal spill points defined stratigraphic tops of vertical migration paths and egress points for lateral migration.

Knipe *et al.* (1998) showed that to model fluid in hydrocarbon reservoir, it is essential to gain a detailed insight into the evolution, structural and properties of faults and fractures. The generation of realistic flow models also requires calibration with data on the fluid distributions and flow rates from hydrocarbon field. They postulated that there are questions that must be answered in order to

generate a geological reasonable and reliable fault-fluid and seal integrity analysis. Such questions include: (1) What is the behavior of this fault? (2) What is the geometry of this fault zone? (3) What are the nature and petrophysical properties of any fault rocks developed and how are they distributed in the subsurface? (4) What impact could the fault zone have on fluid flow through time?" They suggested that properties and evolution of fault zones can be evaluated using the combined result of structural core and down-hole logging, microstructural and physical property characterization, together with analysis of faults from seismic and outcrop studies as well as well test data. They concluded that successful fault analysis depends upon the amalgamation of these data and its incorporation into robust numerical flow model.

Childs *et al.* (2002) carried out a study on the impact of fault seal properties on hydrocarbon migration modeling of the Oseberg-Syd area, Viking Graben. They showed that seal capacity of faults is known to have a major control on hydrocarbon distribution and accumulation. They incorporated fault seal properties into migration modeling and confirmed that this approach provides a stringent test of predictive methods together with the empirical data on which they are based. Their analytical results showed many applications of seal capacity

importance such as: the basis for risking undrilled fault dependent prospects. Its usage provides test of predictive methods. Its model provides a replication of the hydrocarbon condition in a trap. It provides a means for conducting sensitivity analysis and therefore leads to improved prospect risking.

Lashin and Abd El-Aal (2004) presented a study of the juxtaposition and fault seal analysis of some mixed clastic reservoir in Egypt with demonstrated evidences from Nile Delta and Western Desert. The potential sealing parameters were checked in three different fields (West Abu Qir, Abu Sennan and Abu Madi-El Qar'a). In their attempt in showing the role of faults in the creation of hydrocarbon traps, they emphasized on sealing along fault planes arising where reservoir / non-reservoir rocks of different petrophysical characters are juxtaposed against each other, with different hydrocarbon potentialities (gas and oil) as an attempt to model the sealing attributes in these areas. Different qualitative and quantitative techniques (including seismic and well logging attributes) were used in assessing and evaluating the properties of the fault rock seal types along this faulted reservoir. These were followed by numbers of juxtaposition and 3-D property diagrams (permeability, sealing capacity and relative areas of fault rocks) and were constructed along the proposed sealing

planes. Then, shale gouge ratio (SGR) and smear factor parameters i.e. clay smear potential (CSP) and shale smear factor (SSF) were estimated. This was followed by pressure analysis on either side of the faults which cut through the potential reservoirs to calibrate the reservoir zones of known petrophysical and sealing parameters. In Abu Sennan and West Abu Qir areas, the structural control of faults is the main sealing factor. In terms of sealing efficiencies, the analyzed reservoirs showed two different pressure regimes on either side of the studied faults associated with good sealing parameters (SGR 15-20% and SSF<7%). While in Abu Madi-El Qar'a area, sealing was controlled by the combined effect of the deposition of the reservoir (stratigraphic control) and bounding faults (structural control).

Bretan *et al* (2003) demonstrated a study using calibrated shale gouge ratio to estimate hydrocarbon column height. In an exploration context, SGR values can be empirically calibrated with pressure data to define depth-dependent seal-failure envelopes. The seal failure envelope provides a method to estimate the maximum height of hydrocarbon column that can be supported by the fault. Leakage of hydrocarbons across a fault occurs when the buoyancy pressure exceeds the capillary entry pressure of the fault and is not confined to the crest

of the structural or even where the SGR values is lowest. Here, an established calibration diagrams based on across-fault pressure difference have over-generalized the relationship between increasing SGR and increasing pressure support. Calibration diagrams based on buoyancy pressure showed that gas and oil data exhibit a correlation between increasing SGR and increasing buoyancy pressure and this falls between SGR values of 20 and 40%. [No increase in the supportable buoyancy pressure, at SGR values greater than about 40% for both gas and oil data]. However, column heights do not continue to increase in the SGR range between 50 − 100%. Hence, estimation of hydrocarbon column heights using seal attributes depends upon the geologic input to the model, in particular, pressure data, volumetric shale fraction, and the precision of the three-dimensional mapping of reservoir geometry in the vicinity of the fault.

Freeman *et al.* (1998) with the application of gouge ratio method to fault seal prediction disclosed that the reduction in pore throat size attributable to the enhanced clay content in the fault rock between two juxtaposed reservoir bodies supports the production of an efficient seal to hydrocarbon migration. This gouge ratio, when applied to sand − shale sequences, indicates the proportion of phyllosilicate material that is expected to be incorporated into the fault rock,

hence it provides a measure of the seal capacity. Based on their usage, seismically derived geometric data, well-based stratigraphic and compositional data, comparative analysis of SGR was made at the scale of individual faults, and fields at large. This was followed by the examination of fault analysis from the Oseberg Syd Field that is known to produce effective seal and was concluded that SGR of 18% will support across-fault pressure of c.8 bar.

A comparison between deterministic and stochastic fault seal techniques were carried out by Dee et al. (2007). They defined deterministic model as one in which prediction of the locations of reservoir overlaps is made from the static model of the reservoir horizon and fault geometry. Here, their principal aim of deterministic model was to map faulted reservoir overlaps and determined their sealing characters. These were performed using predictive algorithm such as SGR that relates the shale content of the formations that have moved past a point on the fault zone to the sealing capacity of the fault rock. Deterministic model of fault seal are sensitive to the uncertainties associated with mapping horizons in proximity to faults and inherent uncertainty in a static fault interpretation in both position and fault zone complexity. The uncertainty in the static structural model can be addressed by convolving uncertainty in the magnitude of throw with

juxtapositions at the fault. However, this does not address the uncertainty in the distribution of reservoirs on either side of the fault while with the application of stochastic models, multiple realizations of the stratigraphy can be tested. The stochastic models capture the uncertainty in the position of the reservoir at the fault by allowing multiple realizations of stacking geometries, where the principal assumption is that these stacked reservoir zones are laterally continuous covering the entire likely fill area. They also showed that despite the conceptual differences between the two analytical fault seal approaches, comparison of the predictions on the Ling Gu field still showed a surprising degree of conformity.

Yielding *et al.* (1997) presented a quantitative fault seal prediction. The evaluation methodology was based on detailed seismic mapping and well analysis in relation to fault seal arising from reservoir / non-reservoir juxtaposition or by development of fault rock having high entry pressure. Here, two types of lithology dependent attributes were defined (gouge ratio and smear factor). Gouge ratio is an estimate of the proportion of fine grained material entrained into the fault gouge from the wall rocks. Smear factor methods (including clay smear potential and shale smear factor) estimate the profile thickness of shale drawn along the fault zone during faulting. All these applied parameters vary over the fault

surface, implying that faults cannot simply be designated sealing or non-sealing. An important step here was the calibration of these parameters where Across-Fault Pressure Differences are explicitly known from wells on both sides of the fault. The calibration here, showed a remarkable consistent result despite their diverse settings (e.g., Brent Province, Niger Delta, and Columbus Basin).

Jolley *et al.* (2007) carried out a study on fault and sealing in production simulation models in the Brent Province and Northern North Sea. They disclosed as follows: that based on theoretical standpoint and by comparison with historical production data, results showed that systematic modeling of single-phase fault transmissibility multipliers from the cellular model enables rapid application of fault seal to simulation model. On compared with 'traditional' methods, this allows superior production history match results to be achieved with far less manual intervention, and at a fraction of the normal workflow speed. Given the improvement in technical product and speed to achieve history match, this leads to improved confidence and quality of field development and management decisions based on running the models in predictive mode. The Brent Group Field contains a complex arrangement of fault juxtapositions of the well-layered sand-shale reservoir stratigraphy. These juxtapositions are first-order sensitivity on

compartmentalization of pressures and fluid flow within production simulation models of the reservoir. These could be demonstrated in the following ways, via, (i) Geometrical coherence is insured and preserved between the seismic interpretation, static geocellular model and the production simulation model by model building and validation in conjunction with seismic interpretation, and by sensitive upscaling to preserve these geometries for input to the simulator. (ii) Fluid flow properties of the faults are accounted for in the simulator by systematic modeling of fault transmissibility multipliers from the upscaled geocellular geometry / property grids in the model, to produce unique multiplier values for each faulted cell face. (iii) Multipliers calculated on 'amalgamation' datasets, based on global correlations between fault permeability and clay content improved the history match. However, the history match was far better when these multipliers were calculated with reference to fault rock permeability – clay content data, measured from faults present in drill cores within the study reservoir, and / or from similar reservoir within the same stratigraphy in nearby fields in the region. The results are particularly enhanced where these data are measured from rocks that have experienced a similar burial – strain history to the study reservoir.

Hesthammer and Fossen (2000) studied the uncertainties associated with fault seal analysis in the Gullfaks Field, Northern North Sea and revealed uncertainties factors that can render even the most detailed simulation model useless as could be attributed by (i) Variation in lateral continuity of faults, (ii) Properties and thickness of fault zones, (iii) Influence of deformation bands within and outside damage zones, (iv) Subseismic features such as small fault around the fault zone further decrease the confidence level of simulation modeling result. The outcome of this analysis can in many cases be used as input to further enhance models for reservoir simulation in order to increase the validation of the model. This showed that a sound approach to knowledge management for increased oil recovery based on fault seal analysis requires sharing of gained knowledge from many oil and gas fields rather than monopolizing information that cannot be fully utilized by studies from a single field.

Harris *et al.* (2002) presented a study using Shale Gouge Ratio (SGR) to model faults as transmissibility barriers in reservoirs: an example from the Strathspey Field, North Sea. The estimates of clay concentration within fault gouge, mapped across the surface of the Central Fault as Shale Gouge Ratio (SGR) were calibrated with the result of pressure analysis. The calibration showed that

as SGR increases, so does the measured pressure differential across the fault. This positive relationship between SGR and pressure differential suggest that SGR is a guide to potential fluid-flow resistance exerted by faults. They therefore suggested that SGR can potentially be used as a guide to defining differences in permeability within and between faults in a given field. This 'scalability' of SGR as an indicator of fault permeability within a field could provide hitherto unachievable flexibility in the systematic modeling of the hydraulic behavior of fault during fluid flow simulations.

The use of fault-seal analysis in understanding petroleum migration in a complexly faulted anticlinal trap as in Columbus Basin, offshore Trinidad was carried out by Gibson and Bentham (2003). A case study from Mahogany Field, (where interbedded Pliocene – Pleistocene shales and reservoir sands occur in a broad four-way-closed anticline cut by numerous normal faults) was conducted. It was shown that fault seals in this stratigraphic sequence were successfully evaluated using shale gouge ratio (SGR), with a transition between sealing and non-sealing faults occurring in the SGR within the range of 0.15 – 0.25. this has highlighted high net-to-gross ratio of individual sands, low SGR values typically correspond to areas of reservoir self-juxtaposition, whereas good seals (SGR ≥

0.2) exist where different sands are juxtaposed against one another. The distribution of stacked, fault sealed petroleum accumulations in this field was closely control by the larger structural geometry, which changes significantly from the shallow reservoirs to deeper ones. Petroleum column heights in individual fault blocks within the structure are limited either by: (i) a cross-fault spill point at a low-SGR window on the west side of a fault block or (ii) a synclinal spill point within a fault block from which petroleum leaves the overall four-way closure. However, the pattern of hydrocarbon-water contacts in the field suggests that petroleum filled and spilled its way from northeast to southwest across the structure with individual sands acting as a separate flow systems. In spite of the juxtaposition against each other, communication between stratigraphically different sands was minimal. This has further shown that vertical migration of petroleum along faults is not required to explain the distribution of charged sands, and this was consistent with both petrophysical data and the known sealing character of the fault. This petroleum migration model serves as a tool for evaluating charge risk and column heights in untested fault blocks in the area.

Manzocchi *et al.* (1999) incorporated geological conceptualizations of fault zone structure and content into a predictive method for calculating fault zone

transmissibility multipliers. However, this method is based on poorly defined empirical correlations which can only be improved when more data becomes available. With this applied perspective, he concluded that based on numerical and analytical considerations of flow through realistically heterogeneous faults are highlighted as follows: (i) Flow through a representative portion of a heterogeneous fault can be approximated as a function of the harmonic average of the fault zone permeability, provided there is no spatial correlation of permeability and thickness. (ii) Where there is spatial correlation of permeability and thickness, the transmissibility of the fault is a function of the arithmetic average of the permeability / thickness ratio. There is, however, no analytical solution to transmissibility as a function of this ratio. (iii) Extreme flow segregation occurs through realistically heterogeneous faults. This flow segregation is accommodated by tortuous flow in the matrix. (iv) The analytical determination systematically overestimates fault transmissibility at higher transmissibilities and higher fault heterogeneities. The extent of this overestimation is a function of the permeability structure to significant distances down-stream and up-stream of the fault, as this determines the ease of tortuous flow in the matrix and (v) Statistically identical faults do not necessarily have the same transmissibility even if an area larger than the REV is being modeled. In a

system containing statistically identical heterogeneous faults, the more closely spaced faults will have a lower transmissibility.

Trapping capacity of faults in the Eocene Yegua Formation, east south Lake field, southeast Texas was conducted by Kim *et al.* (2003). Evaluation of the trapping capacity of the faults was carried out based on the investigation of the properties of the shear zone in the formation. Interpretation showed that the Yegua sandstone is a prograding delta-front sequence based on the increasing amounts of sandstone upward in the section, the abundant carbonaceous material, and the nature of the sedimentary structures. Rapid deposition at a distal delta-front location induced the sediment instability, resulting in mass movement. Small-scale of normal faults in Yegua Formation disrupt the lateral continuity of the reservoir sandstones and reduce greatly the drainage areas of producing wells. The principal fault-trapping capacity in the Eocene Yegua Formation increases by reduction of porosity and permeability resulting from clay smears, which yields the high capillary displacement pressure.

Cerveny *et al.* (2005) divulged a methodology of reducing uncertainty with fault–seal analysis. They documented that oil and gas reservoir in faulted siliclastic formations are difficult to exploit. With integration of seismic data,

detailed core information, and wellbore and production data, geoscientists can now model fault behavior and incorporate the results into reservoir fluid-flow simulators. They said that the integrated process improved prediction of fault behavior, and reduces the uncertainty and risk associated with complex trap.

Doughty (2003) interpreted clay smear seals and fault sealing potential of an exhumed growth fault, Rio Grande rift, New Mexico. An exhumed growth fault (Calabacilas fault, New Mexico) provided insights on the processes of clay smear formation and the effectiveness of fault seal prediction for faults of this type in the subsurface. The exposed clay smears range from being continuous and having a taper geometry to being semi-continuous and segmented by secondary faults. He reported that in some cases, source beds are truncated at the fault and there was no attached clay smear. Detailed mapping of the fault zone showed that there was a veneer of clay gouge on the fault that is interrupted by multiple gaps that would reduce the ability of the fault to be an effective seal over geologic time scales. However, presence of releasing dip relays in footwall source beds and the evolution of dip relay during the growth of the fault zone primarily control the variability in clay smear type and continuity. The source bed plasticity, composition, and thickness play a secondary role. His observation showed that as

the fault zone grows, the dip relay is breached, and the clay smear is progressively segmented by normal faults that translated it down the fault and eventually truncated it from its source. Smear- type algorithm (CSP, for example) over-predicted the likelihood of fault seal at the base of the source bed, because the clay smear is commonly detached from its source. He concluded that a key threshold for fault seal prediction is the stage of fault growth at which the clay smear tapers become separated from their source beds. Below this threshold, smear-type algorithm work best and above this threshold, abrasion-type algorithm work best.

Brown (2003) used the approach of capillary effects on fault-fill sealing in the study of trap integrity. The study involved capillary–pressure models and concepts to evaluate excess pressure, capillary hysteresis, and relative permeability on fault-fill sealing. Here, overpressure fault fill (fault water pressure higher than reservoir water pressure) always increases the height of the sealed petroleum column. The sealing interface moves into the over-pressured fault fill where water flows from the fault into the reservoir. Under-pressured fault fill decreases petroleum column height only where cross-fault water flow is absent. If water flows across the fault, column height is unaffected. Water cannot flow

across the faults where the reservoir is at irreducible water saturation. The relative permeability smoothes the transition from membrane sealing to leakage, thus, hydraulic-resistance sealing is possible after membrane-seal failure. The height of membrane sealing by homogeneous, water-wet fault fill exceeds the height of hydraulic-resistance sealing at geological leakage rates. Hydraulic-resistance sealing becomes more significant when charge and leakage are both high, when trap life is short, and during production. Moreover, trap leakage rate through a water-wet, fault-fill pore network cannot exceed trap charge rate during initial trap charging slows, leakage exceed trap charge until a new equilibrium column height develops. If charge stops, the seal continues to leak until the petroleum column height is reduced substantially below its original height. Membrane sealing is re-established at low capillary pressure. Theoretically, restored seal capacity is close to the original capacity. Cross-fault pressure and petroleum column height cannot be converted to seal capacities because charge history and seal type influence sealing. Cross-fault pressure data should be analyzed in light of the charge and pressure history so that different controls on fault-fill sealing can be assessed.

Naruk *et al.* (2002) presented a study on common characteristics of proven

sealing and leaking faults. The study involved the use of well and 3D seismic data

in defining both the structural and stratigraphic architecture of the fields, and to

make fault plane juxtaposition diagrams of each sealing or non-sealing fault.

Pragmatically derived interpretation showed that fault in general may seal as a

result of a very wide variety of processes, including juxtaposition, gouge, clay

smear, cementation, grain-size reduction and / or diagenesis. The relative

significance of each mechanism is commonly interpreted on the basis of

theoretical fault models, outcrop studies, or limited field studies. In relatively

shale-rich stratigraphic sections, sand-on-shale juxtaposition is commonly

interpreted to be the primary factor determining whether or not a fault seals

(Allan, 1989). Sealing sand-on-sand fault contacts also occur, however in relatively

shale-rich sections, this sealing capacity is thought to be a function of clay smear

potential (CSP) (Bouvier *et al.,* 1989; Jev *et al.* 1993) or shale gouge ratio (SGR)

(Yielding *et al.,* 1997, 1999). Sealing sand-on-sand fault contacts also occur in

reservoir sections that are essentially devoid of shale or clay, however, and in

these cases the fault seal capacity is attributed to some combination of

orientation, total depth and throw (Knott, 1993), or more specifically the

conditions of faulting and amount of self-healing experienced by the fault rock

(Hippler, 1997; Knipe et al., 1997). Here, the common occurrence of demonstrably sealing sand-on-sand fault contacts, as well as the occurrence of demonstrably leaking sand-on-shale fault contacts, indicates that juxtaposition is not a primary control on fault seal capacity. Global comparisons of known sealing and leaking faults showed positive linear correlations between the retained pressures, and the gouge compositions as described by SGR algorithms in some cases, and the gouge compositions as described by CSP algorithms in other cases. Where net / gross of the faulted section is greater than ~20%, sealing sand-on-sand fault contacts are still common, but the retained pressure showed no correlation with either SGR or CSP algorithm.

The work of Dutzer *et al.* (2006) in their application of the concept of Seismic Fault Distortion Zone (SFDZ) in the investigation of fault seal potential through fault relative seismic volume analysis showed that; seismic data is statistically sufficient to derive accurate information on sealing / non sealing capacities (varying within one fault), provided some calibration additional data (pressure from wells) is given. Therefore delineation of the SFDZ is a key step in further analyzing 3D seismic data to provide information regarding variations in

seismic attributes across a fault that can be used to indicate how juxtaposition of strata influences a potential sealing fault.

Davies *et al.* (2003) presented fault-seal analysis of the South Marsh Island 36 field, Gulf of Mexico. The evaluation was conducted in this heterolithic section of sands and shales. The methods does not rely strictly on the juxtaposition and distribution of fault rock on the fault plane, but include the evaluation of trap geometries and fluid pressure, which provide the necessary data for fault-seal calibration. Analysis of the study showed that: (i) different gas-water contacts across fault and sand-on-sand juxtaposition suggest that the intra-reservoir fault is sealing. (ii) Unique overpressure in the hanging wall and foot wall of the fault (pressure seal) is attributed to the containment of the downthrown reserves. (iii) Shale gouge is the fault-sealing mechanism in the up-thrown fault block. (iv) An estimated shale percent of 45% is estimated as a minimum seal threshold for supporting as much as 80psi (5.51×10^5Pa) capillary pressure and (iv) Production pressure difference across the fault approaches 3000psi (2.06×10^7 Pa) before fault-seal breakdown and gas breakthrough across the fault.

Jones and Hillis (2003) used an integrated, quantitative approach to assessing fault-seal risk. They expressed that a quantitative assessment of fault

risk that integrates parameters from different aspect of fault-seal analysis in a consistent framework may be determined if the risks associated with juxtaposition sealing, deformation process sealing, and reactivation are known. The impact of uncertainty and value of information for each aspect of fault sealing may be determined through the construction of data webs and modification of the equation: FS = {1 − [(1 − a)(1 − b)]} x (1 − c). Where FS represent fault-seal, a, b, and c are the probabilities of deformation process sealing, juxtaposition sealing, and of the fault being reactivated subsequent to the trap being charged with hydrocarbons, respectively. The fault seal risk web profile provides a powerful tool for visualizing each parameter probability of fault sealing and allows rapid comparison with proven success, or failure of prospect cases.

Modeling of shale smear parameters, fault seal potential, and fault rock permeability were shown by Sorkhabi *et al.* (2002). In view of their study, factors involved in the petrophysical properties and flow directions include basin tectonics, fault geometry, fault mode (its timing and activity), fault juxtaposition of sedimentary layers, fault stress field, cataclasis (both grain size reduction and porosity loss due to tectonic composition), shale smear in sandstone-shale sequences, fault diagenesis (precipitation seal), and fault damaged zone (open-

mode fractures versus mineral-filled or mechanically-healed fractures bordering the fault). Understanding each of these processes and factors needs to be followed up by quantifying the relations among them. In spite of strides taken in fault sealing assessment over the past decade, the inherent complexity of faults poses major challenges to experimentalists, geologists, and modelers for years to come. For purposes of practical demonstration in petroleum exploration and production activities, fault geometric reconstruction, juxtaposition, shale smearing parameters, fault rock characterization, and fault stress regime currently provides some important tools for fault sealing assessment.

Quantitative and sensitivity of fault seal parameters demonstrated in an integrated reservoir modeling work flow: a case study on the Njord Field, Halten Terrace, Norway was presented by Ehrlich *et al.* (2006). The study utilized analogue field studies as well as core descriptions and petrophysical well data in order to evaluate the sealing potential of medium to large scale faults that segmented the reservoir. Dynamic data and 4D seismic information was used to calibrate the results. The study was carried out using Fault Seal module of Irap RMS. The focus of the study is the integration of fault seal calculation in a common reservoir modeling workflow in order to quickly investigate the effects

of changing fault seal parameters and algorithms with respect to reservoir performance. The fault seal module of RMS has the ability to create and organize a large number of fault rock property predictions, and to export final results for reservoir simulation. The algorithms include Shale Gouge Ratio (SGR), Shale Smear Factor (SSF), Clay Smear Potential (CSP), and user defined SGR curves, as well as the published algorithms of Manzocchi *et al.* (1999) and Sperrevik *et al.* (2002).

Grollimund and Zoback (2003) gave a study on the impact of glacially induced stress changes on fault-seal integrity of offshore Norway sediments. This study utilized a three-dimensional numerical model of glacially related lithospheric flexure to estimate in-situ stress and pore-pressure changes through time in the Norwagian sector of the northern North Sea. The model results match available borehole measurements of in-situ stress and pore pressure showed a transition from high horizontal stresses at large distances from the coast to lower horizontal stresses in near-coastal areas and associated rotation in stress orientation. In addition to the present-day predictions, the model results provide an estimate for the evolution of stress and pore-pressure during glacial and interglacial periods. They found that the temporally changing stress field might

have induced repeated reactivation of reservoir-bounding faults during the course of the Pleistocene glaciations, especially during Weichselian interglacials. As a result, hydrocarbon fields in the Norwegian offshore areas appear to have been exposed to multiple periods of fault reactivation and potential hydrocarbon leakages.

Egholm *et al.* (2008) used Mohr-Coulumb failure theory based model and presented the mechanics of clay smearing along faults. This was done using discrete element computations in demonstrating of how the model framework can predict the fault smear potential from soil friction angles and layer thickness. They said that a clay- or shale-rich fault gouge can significantly reduce fault permeability. Hence, predictions of the volume of clay or shale that may be smeared along a fault trace are important for estimating the fluid connectivity of groundwater and hydrocarbon reservoir systems. However, they showed that fault smears developed spontaneously in layered soil systems with varying friction coefficients, and presented a quantitative dynamic model for such behavior.

Pelosi, (2009) conducted a study on fault seal prediction and risk evaluation of exploratory prospects: example of Brazilian marginal Basins. A composite methodology involving fault geometry edition and fault throw mapping, structural

modeling, well log analysis, volume of shale determination, stratigraphic juxtaposition diagram and seal attribute analysis (Shale Gouge Ratio and Smear Factor) was evaluated. He said that the structural modeling can be used to evaluate risk of two important aspects: trap closures and migration pathways. Comparative evaluations were made based on one Brazilian marginal basin to estimate different spill points in siliclastic and carbonate prospects. In both cases, fault seal prediction was able to increase the exploratory success. In the carbonate sequences, fault seal was estimated by juxtaposition diagram and porosity logs. In the siliclastic sequences, threshold values of SGR were used to delimitate trap closure, lateral seals and spill points. In another case, fault seal studies evaluated migration risk, where juxtaposition of reservoirs rocks and low gouge ratio showed the most likely oil migration pathway.

According to Cranganu and Villa (2006), their deductions on the study of the capillary sealing as an overpressure mechanism in the Anadarko basin, southwestern Oklahoma has been highlighted. They said that this basin is known to contain - today areas of extensive overpressures (pressure higher than hydrostatic pressure). Explaining the origin and maintenance of overpressured pore-fluids in the basin over long periods of time cannot be achieved by invoking

sealing mechanism that is responsible for both generating and maintaining almost all overpressure observed today in this basin. Capillary forces act at gas-water interfaces between coarse- and fine-grained clastic rocks. Detecting capillary seals and estimating the magnitude of their pressure sealing implies two main aspects: (1) measuring the pore throat radius of coarse- and fine-grained clastic rocks, and (2) detecting the presence of gas-bearing layers using geophysical logs and other data. Measurements by injecting mercury into rock pores allow estimation of the pore throat radii controlling the capillary sealing. It was further discovered that twenty one fine-grained rock samples from the Anadarko Basin were thus measured and their average pore throat radius was found to be 2.5×10^{-8}m. The proposed model also requires the presence of gas-bearing layers interbedded into shale layers. Using a suite of geophysical logs from more than 100 wells, they were able to identify such gas-saturated layers in more than 50 wells. Further calculation indicated that a capillary sealing mechanism in the overpressured area of the basin may produce ~ 80% of the maximum observed overpressure in the basin.

Effect of hydrodynamics and fault zone heterogeneity on membrane seal capacity was carried out by Strand *et al.* (2008). They said that the use of

shale- Gouge-Ratio (SGR) methods to predict across-fault seal capacity relies on a calibration of the methodology against field examples. Existing calibrations have plotted across-fault pressure difference or buoyancy pressure against in situ SGR to define a fault-seal failure envelope. Recent work on hydrodynamics and seal capacity has provided insight on fine-tuning the calibration methodologies that should in turn lead to improved fault seal capacity predictions. A situation not fully addressed, however, is the impact of fault zone heterogeneity on the hydrodynamic characteristics of a fault and thus the membrane seal capacity. For a fault that defines a hydraulic head discontinuity at the reservoir scale, there exists a hydraulic head gradient or distribution within the fault-zone that is determined by the detailed permeability distribution within the fault zone. As a result, the capillary threshold pressure varies across the fault. When compared with the hydraulic head, the fault zone seal capacity can be estimated at various locations within the fault zone. Theoretical examination of membrane seal capacity for various permeability distributions can be used to understand parameters that control the location of the critical leak point for a membrane fault seal. This can also be extended to examine possible up-fault leakage. A range of permeability distributions are examined for a theoretical fault zone. Assuming a given across fault pressure difference in aquifer, the internal fault zone seal

capacity is determined to demonstrate the various controls on a faults critical leak point.

Grattoni *et al.* (2010) presented a study on multiphase flow properties of clay bearing rocks: laboratory measurement of relative permeability and capillary pressure. They emphasized that clay bearing rocks can have a large impact on trapping, reservoir compartmentalization and production oil or gas in a number of ways. With the recognition of faults as being critical for defining the likely sealing or baffling nature of within reservoir systems; the applied approach involved: evaluation of new prospects and reservoir production simulations using fault permeabilities based on estimates of clay distribution. An experimental setup was made to determine the relative permeabilities and capillary pressures with brine, oil or gas. The synthetic plugs were used with controlled amounts of sands and clays that successfully mimic the single phase permeability behavior of phylosiliclastic fault rocks. It is evident that different measurements techniques provided consistent and comparative results. The gas brine capillary pressures of the synthetic plugs agreed well with mercury results. The oil or gas relative permeabilities measured showed a large drop within a very small variation in saturation and at relatively small capillary pressure range. The results indicated

that attempting to model the impact of faults on fluid flow based on single phase permeabilities or using general relative permeability curves could significantly over-estimate fault transmissibility and their impact on reserves evaluation.

Geological risk and uncertainty in the outer fold and thrust belt-deepwater, Niger Delta was carried out by Oluseye *et al.* (2008) using evidences from geochemical analysis of oil samples from OFTB wells. This involved integrated geological and geophysical studies to disclose prospectivity trends. The analytical result showed that they are likely to have been derived from less mature source rocks while the fault seal capacity and source rock maturity appear to be the primary exploration risk elements in the OFTB. They said that the deep water Niger Delta is a prolific hydrocarbon basin containing significant commercial discoveries; and that the hydrocarbon occurrence is not uniform across all the three major structural provinces: Inner Fold and Thrust Belt (IFTB), Detachment Fold Trend (DFT) and Outer Fold and Thrust Belt (OFTB). Most of the discoveries are situated within IFTB and DFT. They predicted that it is most likely we have reached the end of the first phase of exploration successes in terms of discoveries as evident in the Miocene creaming curve. They also said that the OFTB which has not been extensively explored is less prolific in terms of commercial discoveries;

and stated that wells drilled in this structural trend have encountered marginal success with highest discovered volumes reported (HIS) in the range of 150MMBOE.

Haney *et al.* (2004) conducted a study on fault plane reflections as a diagnostic of pressure differences in reservoir: a case study of south Eugene Island Field. They said that differences in pore pressure across the fault gave rise to fault plane reflections. The pressure differences are detectable since pore pressure that exceed the hydrostatic pressure, or overpressure, lower the seismic velocity. Thus, the presence of the reflection points to the fault providing a significant seal. They developed a processing scheme and highlighted the fault-plane reflections which simultaneously removed the reflections from the layered structure. Using processed data set, they extracted the amplitude of the fault-plane reflections on the fault-plane itself. The areas of strong reflection amplitude correlated well with the geology and known areas of overpressure.

Fisher and jolly, (2007) described basic 'rule of thumb' that offer an indication of common uncertainties and pitfalls as well as the analytical methods, data requirements and work elements required to replicate the impact of faults on fluid flow in production simulations models successfully. They said that the

first and most important is to ensure that an accurate structural interpretation is incorporated into the simulation model. In particular that all fault linkages and cross-fault juxtapositions were taken from the seismic interpretation into the simulation grid. They said that fault rock sometimes reduce the rate of cross-fault flow in which case it is important to account for this reduction in flow within simulation models. This is best achieved if database of fault rock properties, measured from the field of interest or nearby similar reservoir, are up-scaled to calculate fault transmissibility multipliers. They said that it is sometimes necessary to consider not just the single-phase permeability but also the capillary pressure and relative permeability characteristics of the fault rocks present. They concluded that all relevant static and dynamic data must be appraised critically and emphasized that the interpretation of such data is usually non-unique and misinterpretation can create errors in the production related fault seal analysis.

Continuity of shale smear and the fault seal capacity along faults was presented by Færseth, (2006). He observed that data from faults with core recovery offshore Norway, outcrops and the onshore demonstrate the development and continuity of smear along large (seismic-scale) faults. He documented that smear along the offset, where the overlap between the

segments creates an extensional dip relay. He demonstrated that rocks type other than shale, such as coal, siltstones and carbonates, may smear and thereby contribute to low permeable fault gouge. He further said that a critical threshold for the shale smear factor (SSF), given by the fault throw divided by the thickness of the shale source layer, is established to separate continuous and discontinuous smears; however this SSF ≤ 4 is likely to correspond to a continuous smear along large faults and thereby to a sealing membrane on the fault surface. He said that small (subseismic) faults, a continuous smear can be maintained for both shale and coal source layers for much higher smear factors compared with large faults. He concluded that the continuity of smear associated with small faults also displays a greater variation (SSF in the range of 1 – 50), to become less predictable than smear along large faults.

Færseth *et al.,* (2007) introduced a methodology for quantifying the risk associated with a seal for fault bounded prospects. The application of this methodology confined aspects of fault seal within four main risk categories. This method allowed comparable criteria to be applied in the risking procedure to reduce uncertainty in fault seal assessments. The methodology integrated onshore and offshore data set from large faults and demonstrated effectively how

architecture and the distribution of fault rocks may influence sealing capacity. Despite the variable and complex structure of fault zones, the observed fault zone characteristics that appear in common to the risking of faults investigated and these factors were considered to be crucial in the risking of fault seal prediction. Evidence from fault in their data-base are typically bounded by extensional slip surfaces, represented two main categories: (1) a layer of shale smear entrained into the fault zone and derived from a thick shale source layer within the sequence offset by the fault and (2) fault zones characterized by internal slip surfaces, slivers of footwall and hanging-wall-derived material rotated along the fault zone and commonly enclosed in a matrix of shaly-silty fault gouge. This study highlights the disparity between the complexity of actual faults and the abrasion-type shale gouge ratio (SGR) algorithm currently used in the industry to estimate sealing capacity of faults, which assumes that the seismically derived throw is concentrated in a single fault plane and how it influence juxtaposition across fault, associated SGR values and fault seal risking.

Freeman *et al.* (2008) presented a workflow, key relationships and results of multiple stochastic fault seal analyses conducted on geocellular geological (static) reservoir grids. The ranges of uncertainties were computed from new and

published datasets for different input relationships (e.g. throw, volume of shale to volume of clay, fault clay prediction, fault rock clay content to permeability); and these were used as input into stochastic modeling process and the impact of each was assessed. Based on the review of fault seal techniques, published data and the potential pitfalls associated with these analyses, they said that having the uncertainties associated with the computation of the transmissibility multiplier, for instance, reduces this range from 7 - 1 and 1.5 order of magnitude of the base-case value (no uncertainty).

Detecting fault-related hydrocarbon migration pathways in seismic data; implication for fault seal, pressure, and charge prediction were presented by (Connolly *et al.* 2008). This method used multiple seismic attributes and neural networks to highlight vertical aligned low-energy chaotic seismic data described as gas chimneys, gas cloud, or seepage pipes. The result is a gas chimney probability volume. They said that when gas chimney probability data were overlain on the fault data, obvious vertical gas chimney can be distinguished. However, subtler fault-related hydrocarbon migration can be seen. They said that hydrocarbon migration is often associated with fault intersections or splinter fault related to shear along the fault. Overlying the chimney information on fault

planes can often indicate which parts of the fault have been migration pathways and which parts of the fault have not.

Needham *et al.* (2008) presented a study on faulting and fault sealing in the TAGI Formation of the Ourhoud Field Algeria. They used the concept of fault geometry, connectivity and fault sealing potential and determined different oil-water contacts suggesting a degree of fault compartmentalization. Fault-rock material from cored wells in the Ourhoud field was analyzed and the type, permeability and capillary threshold pressure was determined. The suite of fault rock present is highly varied, ranging from disaggregation faults and cataclasis in clean sands to clay smears. The observed oil-water contact and pressure differences can all be supported by the dominant fault rocks if their clay content exceeds 20%. Fault-rock data were also used to generate transmissibility multipliers for incorporation into the Ourhoud geological and simulation model. Significant reductions in transmissibility multiplier are generated by more clay-rich fault rocks separating reservoir units with permeabilities ranging from 10mD to 1000mD.

On predicting brittle cap-seal failure of petroleum traps, an application of 2D and 3D distinct element method was presented by Camac *et al.* (2009). Two

case studies were carried out in Penola Trough, onshore Otway Basin, South Australia for assessments of pre-drill seal integrity. Sensitivity studies at prospect scale showed how (1) fault rock strength, (2) fault zone width and (3) the interaction of two fault sets, generated local perturbations in the regional stress field. At the play scale, the depth to which a younger active fault set propagates can be explained by the distribution of stress within the rock mass generated by the present-day far-field stress acting on older regionally significant faults.

Accessing controls on reservoir performance in different stratigraphic settings were carried out by Tveranger *et al.* (2008). Their study attempts to qualify the impact of tectonic parameters on hydrocarbon production in reservoir models representing four clastic depositional environments. Eleven sectors from existing 3D reservoir models, representing fluvial, tidal, shallow marine and deep marine depositional settings, were re-sampled into a fixed-volume, unfaulted model grid. Each sample were permutated into seventy three different faulted model configurations by using predefined combinations of fault patterns, maximum fault throw, shale gouge ratio and shale smear factor. The resulting changes in fluid flow response caused by changing model input parameters. Finally, outcome for each of the four depositional environments were compared.

It was observed that, inadequate database and technical limitations with the input models restricted their ability to draw quantitative conclusions; a number of qualitative interpretations could have been made. The four investigated stratigraphies respond differently to identical fault parameter settings. Thus, there is a link between the depositional model input and the impact that faults have on production parameters. This suggests that sedimentological factors have a significant influence on which and to what extent fault parameter affect petroleum production.

A study of the structural controls on oil recovery from shallow-marine reservoir was presented by Manzocchi *et al.* (2008). Their study was based on a simple predictor of fault juxtaposition and fault-rock heterogeneity combined with two-dimensional considerations from streamline theory in an attempt to capture quantitatively the change in economic reservoir value arising from faults. Despite limitations associated with the three-dimensional role of juxtaposition, the result were encouraging and represents a step towards establishing a rapid transportable predictor of the effects of faults on production.

Combined effects of structural, stratigraphic and well controls on production variability in faulted shallow-marine reservoirs were studied by

Skorstad *et al.* (2008). They said that sedimentological parameters dominated both the production and the discounted production variability, especially the aggradation angle and progradation direction, where as the fault pattern is equally significant for the recovery factor. Continuity of sedimentological barriers were found to contribute less than expected to the production variability for the reservoir models, and the well placements showed a low effect.

Knai and Knipe, (1998) analyzed cores from Heidrun Field and observed three main fault rock types as cataclasites, phyllosilicate framework and clay smears in their study of the impact of faults on fluid flow. The clay content of the host sediment is the controlling factor in determining which fault rock type dominates in the fault zones. Fault plane geometries were assessed from seismic-based juxtaposition analysis for input into the reservoir simulation model. The transmissibility multiplier is a function of fault rock permeability and fault rock width, as well as the matrix (host rock) permeability and dimensions of the grid blocks used in the simulation model. Introducing a quantitative description of the faults had a significant effect on the results of the reservoir simulation runs and had played an important role in the successful modeling and prediction of the observed gas breakthrough and pressure evolution.

Experiments on clay smear formation along faults were carried out by Sperrevik *et al.* (2000) which they concluded that stress conditions allowing shale sample to contract will result in the formation of fluid flow barriers, whereas dilation results in the formation of conduits.

Teige *et al.* (2005) carried out a study on capillary resistance and trapping of hydrocarbons using a laboratory experiment. Their observation disclosed that oil was kept in place by capillary forces while water flowed through the core and the membrane. Accordingly, residual water can move through sandstones that are saturated to S_{wi}. They cocluded that the permeability associated with this residual water is high enough to prevent overpressure in the aquifer below the oil-water contact from pushing oil through a membrane seal. Thus, even for this highly permeable sandstone, the overpressure in the aquifer will not cause capillary seal failure.

An, (2009) presented a study of paleochannel sands as conduits for hydrocarbon leakage across faults: an example from the Wilmington oilfield, California. Evidences showed that oil-water contacts cutting structure depth contours, scattered oil traces, and fault seal analysis all indicate that the channel deposit is responsible for hydrocarbon leakage across the boundary faults.

Structural evaluation of column-height controls at a toe-thrust discovery, deep-water Niger Delta was carried out by Kostenko et al., (2008). They said that column heights do not appear to be limited by capillary entry pressure of the top seal because the buoyancy pressure of the columns are significantly less than typical entry pressure.

Eichhubl *et al.,* (2005) studied structure, petrophysical, and diagenesis of shale entrainment along a normal fault at Black Diamond Mines, California – implications for fault seal. They said that fault seal by shale entrainment involves a variety of structural, textural, and diagenetic processes that require an integrated methodology for improved predictions and fault-sealing capacity.

Knipe *et al.,* (2001) presented applying faulting and seal: progress with prediction, using an integrated approach. Involving amalgamation of detailed microstructural and petrophysical property analysis of fault rocks, characterization of the population and distribution of sub-seismic fault from well, core and outcrop data, and an evaluation of the seismic scale fault array attributes. They said that the ability to quantify the petrophysical properties of fault rocks - the permeability and threshold pressure, which are critical for evaluating seal potential of fault rocks, depend upon (a) the host lithology being

deformed, (b) the conditions and mechanisms of deformation and (c) the post-deformation and geohistory of the fault zone. They said that improving fault seal analysis is difficult but not impossible. Reducing the uncertainty associated with fault zone behavior prediction is achievable if the following are recognized: (1) Seismic resolution places important limitations on the characterization of fault zone architectures needed for flow modeling. (2) Robust databases on fault zone architectures and fault rock properties are required. (3) New and more flexible reservoir modeling packages are required which can incorporate the more detailed and more realistic fault property data. (4) The calibration and validation of fault analysis 'tools' is needed from well constrained situations so that wrong application is avoided.

Quantitative evaluation of synsedimentary fault opening and sealing properties using hydrocarbon connection probability assessment were conducted by Zhang *et al.,* (2010). They said that sealing is only an impressive and time-dependent aspect of the hydraulic behavior of faults, which may act as seals during some periods and as pathways some time later. Therefore, in hydrocarbon migration studies, sealing indices may successfully be used in some cases but not in others. Empirical fault-connectivity probability method was used to assess the

hydraulic connecting capacity of fault for hydrocarbon migration over geologic time scales. The method is based on the recognition that observable hydrocarbon in reservoirs should result from the opening and closing behavior of the fault during the entire process of hydrocarbon migration. Data from Chengbei step-fault zone (CSFZ) in the Qikou depression, Bohai Bay Basin, northeast China, were used. Fluid pressure in mudstones, normal stress perpendicular to fault plane, and shale gouge ratio were identified as the key factors representing fault-seal capacity. They were combined to define a non-dimensional fault opening index (FOI). The values of FOI were calculated from the measured values of the key factors, and the relationship between FOI and fault-connectivity probability on any fault segment was established through statistical analysis. Bases on data from the CSFZ; when FOI < 0.75, fault connectivity probability is zero (0), when FOI ranges from 0.75 to 3.25, the corresponding fault connectivity probability increases from zero (0) to 1, following a quadratic polynomial relationship; when FOI > 3.25, the fault connectivity probability is one (1). They said that the values of fault connectivity probability could be contoured on a fault plane to characterize the variations of hydraulic connective capacity on the fault plane.

Hege and Hermanrud (2003) presented a study of hydrocarbon leakage processes and trap retention capacities, offshore Norway. They said that association between high overpressure and sparse hydrocarbon occurrence are commonly ascribed to hydrocarbon leakage through pressure induced features in the cap rock. However, several hydrocarbon traps in the North Viking Graben area in the North Sea still contain abundant commercial volumes of pressured structures at the Halten Terrace further to the north had leaked hydrocarbons, even at considerable lower overpressure. Investigations to find the possible explanation of the observations were conducted using selected wells in the North Viking Graben and the Helten Terrace areas. Distinct regional differences emerged, as the emptied reservoirs at the Helten Terrace generally have higher retention capacities than the over-pressured discoveries in the North Viking Graben area. Thus, there appears to be a lack of any clear relationship between structures emptied of hydrocarbons and low retention capacities, which could be expected if pressure-induced fracturing of cap rock was the main process of the hydrocarbon leakage. They concluded that the regional differences in retention capacities were mainly attributed to different leakage processes in the two basins. Stress history variations were suggested to be the main controlling factor of these leakage processes.

Fault trap analysis of the Permian Rotliegend gas play, Lauwerszee Trough, NE Netherlands has been critically reviewed and was presented by Corona, (2005). He analyzed thirty (30) fault traps in which twenty two (22) were found to have gas accumulations. He said that trap fill is controlled primarily by Slochteren sand-on-sand juxtaposition leakage across a fault; however, some gas accumulations as mapped appear to be filled deeper than the leak point and required sand-on-sand fault seal. Retained fault-seal gas columns were relatively small and mostly less than 60m with one exception of 95m. Seven potential Slochteren sand-on-sand fault-zone seals were identified. He said that based on the analysis result, three possible criteria that may promote the development of such fault seal are: (1) juxtaposition against a tight, shale-rich interval; (2) small isolated sand-on-sand juxtaposition area ($<25000m^2$) typically associated with fault lengths less than 1km; and/ or (3) occurrence of a complex narrow fault zone. He concluded that some sealing fault segments are associated with structural interpretation/mapping uncertainty.

A study on cross fault sealing, baffling and fluid flow in 3D geological models: tools for analysis, visualization and interpretation were carried out by Freeman *et al.,* (2010). Their methodology involved a pragmatic utilization and

comparison of static proxies (Shale Gouge Ratio, Transmissibility Multiplier, and Effective Cross Fault Transmissibility) for cross-fault fluid flux and visualization of cross-fault fluid flux values derived from either streamline or full flow simulation data. The visualization of the fault and flow related properties include (a) on the fault face; (b) in the grid cells adjacent to the fault face; (c) as vectors; and (d) as fault-wide summations. They said that direct imaging of cross fault derived from their work simulation results allowed a better understanding of how the faults contributes to reservoir flow simulation results.

Clarke *et al.,* (2005) carried out a work on dynamic fault seal analysis and flow pathway modeling in three-dimensional basin models. The technique used geometries of strata that are cut by faults and their physical properties in the construction of 3D models in which the evolution of cross-fault relationships were calculated and the development of fault-zone argillaceous smear predicted. Hydrocarbon migration pathways through faulted structures were investigated with a 4D migration model based on inversion percolation (IP) techniques. The controls on hydrocarbon migration were investigated for fieldwork-derived models of rock volumes from the Moab Fault, Utah, and USA to test the modeling techniques against reality. As a result, predominantly of argillaceous smear,

hydrocarbons are shown to accumulate in the hanging wall of parts of the modeled section of the Moab Fault, but leak across juxtaposed sandstones elsewhere on the fault to produce footwall accumulations. The techniques are then applied to a seismically derived model of the Artemis Field, UK Southern North Sea, to demonstrate how hydrocarbon charging history and pathways are influenced by fault geometries. Multiple model realizations enabled the risk associated with charging of individual fault compartments to be assessed.

Vrolijk *et al.,* 2005 said that reservoir connectivity analysis (RCA) is a series of analysis and approaches to integrate structural, stratigraphic, and fluid pressure and composition data into permissible but non-unique scenarios of fluid contacts and pressure. With the integration of the conventional structural and fault juxtaposition spill concepts with a renewed appreciation of fluid break-over (contacts controlled by spill of pressure driven, denser fluid, like water over a dam) and capillary leak (to define the ratio of gas and oil where capillary gas leak determines the GOC). They defined permissible but non-unique scenarios of the full fluid fill / displacement / spill pathway of a hydrocarbon accumulation comprised of single or multiple reservoir intervals. They concluded that RCA is an integrated technology that challenges the interpreter to evaluate and incorporate

fluid property, composition, and pressure data with stratigraphic and structural interpretations of a reservoir to achieve a deeper, more comprehensive understanding of reservoir compartments and connections between them.

Sapiie et al. 2013 said that evaluating fault seals forms an important component of hydrocarbon exploration, production, and reservoir management. They noted that most of the fault seal analysis workflow and theory is developed for normal fault system. In the case of oblique convergent strike-slip fault deformation, the movement of the block will involve both vertical and horizontal components. Therefore, additional evaluation need to be done for using standard fault seal analysis workflow. This study demonstrated results of fault seal analysis study which show the important relationship between fault geometries, distributions and characteristic in term of sealing and leaking with the reservoir compartmentalization in the Jambi Merang Area, South Sumatra Basin. The results of study revealed several major concerns in particular related to the faulting history due to the deformation history. Deformation history of the study area is dominated by oblique convergent strike-slip fault which means appearance slip or throw on most faults are not total movement history. Consequently, the results of calculation should consider as minimum of fault

sealing capacity. Fault seal is largely controlled by v-shale distributions rather than by throw as demonstrated by faults having small throws. This result suggested that distributions of good quality sand reservoir become the main control of fault sealing capacity.

Lingdong et al. 2014 presented a research carried out on outcrop. Through outcrop observation of the internal structure of volcanic fault zone and in combination with fault sealing mechanism research and lithology juxtaposition evaluation, the paper analyzed the internal structure and lateral fault sealing of a volcanic fault zone of the Xujiaweizi Fault Depression. The "binary structure" of damage zone and fault core is developed inside the volcanic fault zone. The fault does not have the sealing property basically at the juxtaposition of volcanic rock. Lithologic juxtaposition sealing is formed at the juxtaposition of the volcanic rock reservoir stratum and the overlying conglomerate bed and mudstone bed. By improving the traditional Knipe diagram (single-well triangle diagram), a dual-well triangle map is drawn to indicate the influence of strike-slip fault on the lithology juxtaposition. Modeling is established with the dual-well triangle diagram and in combination with the fault lithology juxtaposition diagram to evaluate the fault sealing property. The research showed that the gas pools in the Xujiaweizi Depression are almost in the upside of faults; in the longitudinal, gas-water

contract is almost at the most shallow position of volcanic juxtaposition and the horizontal distribution of gas pools around faults is just like the curve "sine" as the result of the "dolphin effect" of the Xuzhong strike fault.

Alan, et al. 2013 said that slip-tendency analysis is a new technique that permits rapid assessment of stress states and related potential fault activity. The tendency of a surface to undergo slip in a given stress field depends on its frictional characteristics (primarily controlled by rock type) and the ratio of shear to normal stress acting on the surface, here defined as slip tendency (determined by orientation of the surface within the stress field). An interactive computer tool displays the stress tensor in terms of its associated slip-tendency distribution and the relative likelihood and direction of slip on surfaces of all orientations. The technique provides easy visualization and rapid evaluation of stress in terms of its potential for causing slip on individual faults or fault populations for use in seismic-risk and fault-rupture–risk assessment, exploration for high-risk and earthquake-prone blind faults, selection of likely earthquake focal mechanism solutions, and for use in analysis of compatibility of geologic structures.

Lampe et al. 2012 stated that Seismic interpretation and various modeling techniques, including structural modeling, fault-seal analysis, and petroleum

systems modeling, have been combined to conduct an integrated study along a tectonically complex compressional cross section in the Brooks Range foothills of the Alaska North Slope. In the first approach, relatively simple models have been developed to show the interaction and codependency of various parameters such as changing geometry over time in a compressional regime, character and timing of faults with respect to sealing or nonsealing quality, thermal and maturity evolution of the study area, as well as petroleum generation, migration, and accumulation over time, with respect to the geometry changes and the fault properties. Modeling results showed that a comprehensive understanding of all aspects involved in basin evolution is crucial to understand the petroleum systems, to be able to reproduce what is observed in the field, and to ultimately predict what can be expected from a prospect area. This integrated approach allows a better understanding of the complex petroleum systems of the Brooks Range foothills.

Bogdan et al. 2013 presented that the importance of geomechanical factors is increasingly beingrecognized when investigating the feasibility of geological CO_2 storage. Top seal and fault integrity studies have become a common part of feasibility studies of CO_2 storage. Side seal and boundary faults represent weak spots where production-induced mechanical damage or fault re-activation will first occur (storage in depleted reservoirs). Damaged seals provide the initial

pathways for CO2 penetration enhancing fluid-rock chemical interaction (long-term effects). In case of anhydrite caprock, lab and numerical tests indicate that the rock strength can be reduced by ~25% after 50,000 years of exposure

to CO2-reach fluids.

Laurent et al. 2013 said that the Mandurah Terrace in the onshore central Perth Basin Autralia has been proposed as an environmentally suitable site for CO2 injection (i.e. the SW Hub) with the "storage complex" reservoir, primary and secondary seal represented by the Triassic lower Lesueur Sandstone (Wonnerup Member), the Late Triassic upper Lesueur Sandstone (Yalgorup Member) and the Early Jurassic basal Eneabba Formation, respectively.

Prior investigations in the SW Hub region indicate that fault systems affect the target CO2 storage reservoir and the potential top seals and it is known that changes in the pore pressure and stress field induced by fluid injection could alter the initial seal performance of a reservoir by either overcoming the faults membrane seal capacity leading to across- or along-fault circulation of CO2 or by triggering slip on pre-existing faults leading to the potential along-fault circulation of CO2.

This project is integrated with others ANLEC R&D funded projects. It uses stress data from the project *Advanced geophysical data analysis at Harvey-1: storage site characterization and stability assessment* (Pevzner et al., 2013), it uses facies and rock properties defined in the project *Facies-based rock proprieties distribution along Harvey-1 stratigraphic well* (Delle Piane et al., 2013) and it uses 3D facies models from the project *Stratigraphic forward modelling for South West Collie Hub Phase One - Static Model* (Griffith et al., 2012).

The project (*Integration of data from Harvey-1 well to support decision,* 7-1111-0201) relies on the available subsurface data and carries out a first-order assessment of the CO_2 containment potential for the SW Hub. A new geological model consistent with the integration of the latest 2D seismic reflection survey with the vintage seismic surveys and available geophysical data has been built. It integrates five stratigraphic horizons tied to formation tops in the new Harvey-1 data well (Neocomian UC, top basal Eneabba Shale, top Yalgorup, top Wonnerup and top Sabina sandstone) and 13 main faults that can be correlated between at least two 2D-seismic lines that show constancy in dip, strike orientation and offset. This represents a first-order geological model and the acquisition of additional seismic and well data is critical to reduce remaining geological uncertainty and further constrain the structural framework.

The membrane fault seal capacity has been assessed using the Shale Gouge Ratio (SGR) predictive algorithm that can be calibrated to derive an across-fault-seal failure envelop and to calculate a maximum fluid column height capable to be trapped by a fault without leaking. Three across-fault CO_2 migration scenarios are investigated: (1) between two self juxtaposed Wonnerup Members, (2) between the Wonnerup Member and a juxtaposed thief zone in the Yalgorup Member and (3) between the Wonnerup Member and the Eneabba Formation lying above the Yalgorup Member. The likelihood of lateral migration of CO_2 across faults between the Wonnerup Member and any interbedded sandstone thief zone in the Yalgorup Member can be locally high to the south of the SW Hub (faults F1, F11 and 14). The likelihood of lateral migration of CO_2 across faults within the Wonnerup Member can also be locally high to the south of the SW Hub with potential of westward migration beyond F1 if the CO_2 column exceeds the local offset. One fault (F10) juxtaposes the Wonnerup with the overburden Eneabba; however SGR values on the fault plane suggest an "average to low" likelihood of across-fault migration and the supported CO_2 column before breaching the membrane seal is between 110 and 1100m.

The relationship between the modelled faults and the present-day stress field has been investigated to define critically stressed fault segments most at risk of

reactivation and failure with pore-pressure build-up due to injection. It is assumed that a reactivated fault will be associated with an increase in structural permeability (i.e., along-fault flow). The slip tendency values are minimum for faults striking parallel to SHmax and Shmin (105^0 and 195^0 respectively) and increase for strike orientation 50^0-80^0 (SW-NE) and 130^0-160^0 (SSE-NNW). However the slip tendency magnitude for the SSE-NNW-oriented faults in the SW Hub are low (typically between 0.15 and 0.3) suggesting a low risk of fault failure under the present-day stress. The critical pore pressure perturbation required to induce failure on any particular fault orientation is primarily depth-dependent as a result of an increase in depth resulting in an increase in stresses. This will have the effect of preventing failure to occur. Therefore the smallest critical pore pressure perturbations required to reach failure stress are located to the north of the SW Hub along faults F1, F2 and F10 and once converted to an equivalent of CO_2 column height represent 1200 m or 1000 m of CO_2 column. However this corresponds to fracture stability values slightly <10MPa and empirical data from the Timor Sea suggest that below 10 MPa faults have a higher likelihood of experiencing onset of reactivation and leakage of hydrocarbons over geological times.

The cumulative frequency distribution of fault throws suggests that the geological model underestimates the number of faults with throw smaller than 120 m. A first-order fracture modelling suggests dominant shear failures with a maximum density of fractures in the central and eastern part of the SW Hub, adjacent to fault F10. The stress state of these small faults and fractures suggests that there is an average-low likelihood of failure under the present-day in-situ stress field. However the pore pressure increase required to reach failure stress decreases down to <10MPa to the west of the SW Hub where the Wonnerup and Yalgorup Members are the shallowest.

In light of the first-order assessment at the CO_2 containment for the SW Hub it is recommended to (1) acquire additional subsurface data, especially seismic reflection data in order to decrease uncertainties on the subsurface architecture and constrain the structural framework; (2) constrain the local stratigraphic framework by acquiring additional data to calibrate the Vsh models and the distribution of geomechanical and petrophysical properties; (3) acquire pressure data from within multiple fault compartments to constrain the across-fault pressure difference and calibrate the membrane fault seal calculations; and eventually (4) sample fault zones and define the geomechanical and petrophysical properties of faults to constrain the geomechanical fault seal assessment.

Maunde et al. 2013 stated that faults in the subsurface generally have compartmentalization and sealing properties, the sealing properties of the faults were determined using Shale Gouge Ratio, Shale Smear Factor and the changes in pressure across the faults. Two fields (A and B Fields) in the Nile Delta were analysed, the fields were mostly dominated by structural traps where faults play an important role in trapping of hydrocarbons. A threshold of > 20% SGR and < 7 SSF was used as threshold for faults to seal. Five faults in A field and two faults in B field were analysed, faults in both fields were characterised by Sand-Shale juxtaposition in the footwall while the hanging wall is characterised by Sand-Sand juxtaposition and Shale–Sand juxtaposition. Five traps were identified in A field and 2 traps were identified in B Field, traps analysis shows that 4 of the traps in A field are structural spill point controlled traps (Spill point >Leak point). The faults in these traps are sealing with potential of over 200m hydrocarbon column height, the last trap in the field is a fault leak trap (Spill point <Leak point) and would not trap hydrocarbons. In B field, trap analysis for the main trap of the field shows a structural spill controlled trap (Spill point >Leak point), however the leak point of this trap is in the oil leg. The second trap in this field is a fault leak controlled trap and would not trap hydrocarbons.

Tan and Lothar 2012 said that recent advances in computing power have led to vast improvement on static modeling for both fault modeling and fault seal prediction. Nevertheless, there are still many uncertainty factors that are being built into the seal models and need to be addressed in order to come up with a reliable risking. The paper is dealt with a major water wet fault of a clastic oil reservoir. Consequently, it's possible sealing is based on capillary entry pressure. The first part of the paper discusses the estimation of the shale/clay content of the fault. Based on the upscaled well data the shale distribution is modeled using multiple stochastic realization as well as different interpolation algorithm. This approach tries addressing fundamental issues of juxtaposition uncertainty. The shale/clay contents of the fault are estimated based on different algorithm (e.g. Vshale cutoff, Shale Gauge Ratio, Shale Smear Factor etc). The impact of each approach is assessed and reviewed. The results are compared to the simplistic approach of triangulating the Vshale/Vclay of the wells to the fault.

The second part of the paper discusses the estimation of the permeability and the capillary entry pressure using different published empirical algorithm. Again, emphasis is laid on the attempt to estimate the uncertainty range of the properties. The final result is presented by three scenarios representing the low, base and high case. Based on the limited pressure data the pressure difference

across the fault resulting from the oil buoyancy is estimated and the sealing likelihood of the fault evaluated.

Kondal et al. 2013 presented a carefully planned 4D seismic survey. This was executed and interpreted on the Ravva Field. An integrated multidisciplinary workflow was successfully implemented for understanding and reducing uncertainty in 4D seismic interpretations. The qualitative and quantitative 4D interpretation has helped in identifying by-passed oil areas. The multi-disciplinary integration has reduced the uncertainty associated with locating and designing infill wells. All these results are being used to update the reservoir model for continued optimal reservoir management and development. Also the detailed 3D mapping of faults has provided a comprehensive understanding of 3D fault geometries and their linkages across the field. Mapping has revealed that the main faults that delineate and compartmentalize the Ravva Field are the result of early gravitational collapse of the shelf margin and two sets of rotational fault systems interact to produce the fault patterns observed today (McClenaghan et al., 2012). Final fault and horizon models have been combined with well, tracer and pressure data to investigate fault sealing characteristics of the main faults in the field. Vertical sections across the key faults in the 4D volume and respective horizons reveal the impact of an intra-block fault structuration on fluid flow and

show a potentially unswept fault compartment. Then 4D seismic amplitudes were

restricted to the fault F2 due to the possible fault sealing in production time

scales.

Chapter Three: Methodology

The methodology used in this study, utilized tools such as 123DI software, Petrel software, and Stochastic Trap Analysis and Risking (STAR) module of Petrel software. Details of the workflow are:

3.1.   Data Collection and Quality Control:

The data used in this study are: (1) Well Data: well logs (gamma ray logs, resistivity logs, neutron logs, density logs, volume of shale logs and net to gross logs), well tops and bases, and well path. (2) Seismic Data: Pre-stack Time Migration Seismic data.

All log data were corrected for spikes using de-spike algorithm, log splicing were carried out at log inconsistent values, washed out logs and cycle skipping were also corrected. The seismic data were enhanced using semblance edge with plane confidence threshold integrated in structurally enhanced dip guided Gaussian Vangough.

3.1.1 Stratigraphic Correlation:

An open end transect line (fig. 3.1.1) was used for the stratigraphic correlation which involved correlation of wells that are closest to themselves for better stratigraphic relationship. This was constrained chronostratigraphicaly within genetic packages using maximum flooding surfaces (MFS 9.5Ma in the shale above D1000 sand top, MFS 10.4Ma in the shale above G2000 sand top and MFS 11.5Ma in the shale above K2000 sand top. However, fault heaves were noted and their changes down dip in respect to the fault throw values were used to capture stratigraphic short section and missing sections across the reservoirs.

3.2. Detail Faults / Structural Interpretation:

Faults and structural interpretations were carried in a Pre-stack Time Migration Seismic data using 123DI software. The faults were interpreted in the seismic in-lines using 123DI Travers window and map window. An aid to the original seismic data for enhanced and better imaging and clear understanding of faults and structural interpretations were performed using semblance map and vangogh. A 10 by 10 milliseconds pacing was used in the fault mapping while areas of fault connections and truncations were confirmed using narrower pacing so as to capture faults relationship; which is paramount for a realistic and reliable

structural framework building in fault seal analysis. The interpreted faults and structures include growth faults, synthetic faults, antithetic faults, faulted anticlines, and collapsed crest structures within Baka field, back-to-back (counter regional faults) and horst structure around Baka North-West.

3.3. Seismic to Well Tie:

Well 5 check-shot data was used for the seismic to well tie. This was complemented with generation of synthetic seismogram: The Time to Depth conversions performed by generating a velocity function utilized the extraction of spectra/synthetic wavelet from seismic by creating synthetic RFC (reflectivity seismogram) using density and sonic log from well 5. Then, synthetic RFC and synthetic wavelet were convolved.

3.4. Horizon Mapping:

Thirteen (13) different horizons were interpreted using 10 by10 milliseconds pacing both in the in-lines and the cross-lines of the seismic data as delineated by the reservoir sand tops of the wells. The interpreted horizons are F1000, G2000, G4000, G6000, G8000, G9000, H7100, H8000, K2000, K3200, K5000, K6400 and K7000. The oil reservoirs are F1000, G4000, G6000, G8000, G9000, H7100, and H8000. The gas reservoirs are G2000, K2000, K3200, k5000, K6400 and K7000.

After each horizon interpretation, fault polygons were drawn using exclusive function in 123DI software to delineate all the interpreted fault gaps. Then, completed horizon interpretations in time value were made after each horizon interpretation using flirt function at 98% confidence level in 123DI software.

3.4.1. Depth Conversion: The mapped horizons and faults in time values (time structural maps) were depth converted using well 5 velocity data to generate depth structural maps. This was followed by depth conversions of all the interpreted faults. Then, all depth structural maps, faults (in depth values) and fault polygons were exported from 123DI software to Petrel software; ready for 3D grid building. Both depth surfaces and faults (in depth values) were exported as ASCII 123DI/Charisma/Petrel while fault polygons were exported using export to petrel function. All horizons interpreted are within exploration scale (not more than 30ft difference after depth conversion) before exporting them to Petrel software for depth shift correction.

3.4.2. Building of Petrel 3D Grid:

The faults were imported into petrel software as Charisma fault sticks (ASCII) (*.*). The horizons were imported as petrel points with attribute (ASCII) (*.*), while the fault polygons were imported into Petrel software as IESX fault polygons (ASCII).

As a first step is the Fault Modeling, for structural and fault seal analysis purpose, faults frame work of interest were modeled by retaining the original trends and styles of faults and fault to fault relationship so as to depict the exact geological conditions that had prevailed over time. This was done to ascertain the controlling factor and predict possible scenario. The fault pillars were first converted to faults in the fault model window from the input window of the Petrel software. Then, the faults in the fault model were constrained to the top and base limits of the surfaces used for the model. Fewer pillars were used where possible and no alteration of the original fault trends was made to avoid losing the real geology of the Baka field. Equal spacing of fault pillars were made, and fault truncations and fault connections were also considered at their exact locations. Then, horizons in the model were built using the mapped surfaces.

Then isochors were generated for the model intervals of interest. Zones were generated by complimenting the modeled horizons with respective isochors. Then, layers within each zone were modeled with minimum of 20ft zone thickness.

3.5 Stratigraphic Juxtaposition Models: As a first step in fault seal analysis, stratigraphic juxtaposition is a quick way to check the juxtaposition between individual stratigraphic zones across faults of interest. These are depth vertical sections along the strike length of a fault showing the locations of stratigraphic units intersecting either side of the fault. Only those parts of the faults that share the same stratigraphic interval on both sides are made visible in the display window. Typical explanation of the stratigraphic juxtaposition model is as shown below Knipe (1997).
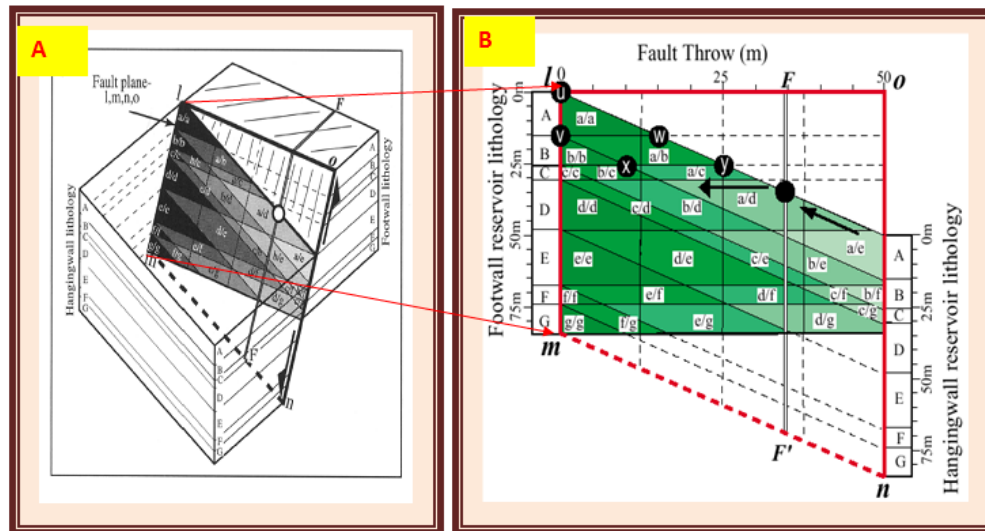
Figure 3.5. Illustration of the idea of juxtaposition diagram adopted from (Knipe, 1997).

3.6   Structural Spill Points and Leak Points Controlled by Juxtaposition:

Structural spill points were captured at structurally lowest points in the hydrocarbon traps that can retain hydrocarbons. Migration trends were also captured where further accumulation could not occur in some hydrocarbon traps due to traps attaining their maximum capacity. Leak points assessments were based on underfilled reservoir and low average SGR of the fault planes where there are hydrocarbon communications across the fault and locations of reservoir sand on sand juxtaposition.

3.7   Petrophysical Models:

3.7.1 Geometrical Model of Cell volume: Important for volume calculations and in mathematical operations between petrophysical properties.

3.7.2 Scale Up of Volume of Shale Log: When modeling petrophysical properties, the modeled area is divided up by generating a 3D grid. Each grid cell has a single value for each property. As the grid cells are often much larger than the sample density for well logs, well log data must be scaled up before they can be entered into the grid. That is blocking of well logs.

3.7.3 Volume of Shale Models: The volume of shale modeling was done using moving average function. The moving average function takes an average value for each unsampled location based on input data, and calculates weights according to distance from wells. The volume of shale calculations involved an initial determination of gamma ray index, then integrating GRI into volume of shale algorithm of either consolidated or unconsolidated sandstones as the case may be. Then volume of shale were incorporated into Lerinov equation. The details of the equations are outlined below.

$$\text{Gamma Ray Index GRI} = \frac{GR\,value(log) - GR(min)}{GR(max) - GR(min)}$$

Where GR value(log) is the value of the gamma ray reading,

GR(min) is the gamma ray minimum value, while

GR(max) is the gamma ray maximum value.

Then, the GR_I values were incorporated into V_{sh} algorithm based on either

consolidated or unconsolidated sandstone categories.

V_{sh} = 0.33(2^2Vsh - 1) That is Volume of Shale for Pre-Tertiary Consolidated Rocks.

While,

V_{sh} = 0.083($2^{3.7}$Vsh - 1) For Tertiary Unconsolidated Rocks, like those in the Niger

Delta.

The Vsh for Unconsolidated Rocks predominates in the study area and were all

calculated in percentage.

The Net to Gross calculated is as shown below:

NTG = 100 - Vsh

VOLUME OF SHALE		
Well	Log used	Method
Baka-001		
Baka-002		
Baka-003		
Baka-004		Larinov (Tertiary Rocks)
Baka-005	GR, Neutron and Density	Non Linear Method and
Baka-006		Minimum Indicator Method
Baka-007		
Baka-008		
Baka-009		
Baka-NW		

$$I_{sh} = \frac{Gr\ Log - Gr\ Min}{Gr\ Max - Gr\ Min}$$

Ish(IGR)= Shale or GR radioactivity index.

Linear	$V_{sh} = I_{sh}$
Steiber	$V_{sh} = \dfrac{I_{sh}}{I_{sh} + A(1 - I_{sh})}$, commonly $A = 2$
Clavier	$V_{sh} = 1.7 - \sqrt{3.38 - (I_{sh} - 0.7)^2}$
Larinov Old Rock	$V_{sh} = \dfrac{2^{I_{sh}} - 1}{3}$
Larinov Tertiary Rock	$V_{sh} = 0.083(2^{3.70 I_{sh}} - 1)$

Larinov (Tertiary Rocks) Non Linear Method and Minimum Indicator Method were used for Vshale estimation as the GR alone is not always a reliable Volume of shale estimator. The non-linear functions were used as they attempt to compensate for density effects on numbers of detected gamma rays.

Figure 3.7.3. Summary chat of algorithm used for volume of shale calculations

3.8   Shale Gouge Ratio Calculation: Shale Gouge Ratios were calculated using Stochastic Trap Analysis and Risking (STAR) module of SHELL Petrel software. These were used to evaluate the fault zone rock property heterogeneities and displayed on a detailed layer cake with hanging wall and foot wall stratigraphic juxtapositions to predict the seal capacity of the faults of interest. The Shale Gouge Ratio calculations are as shown in figures 3.8 and 3.8.1.
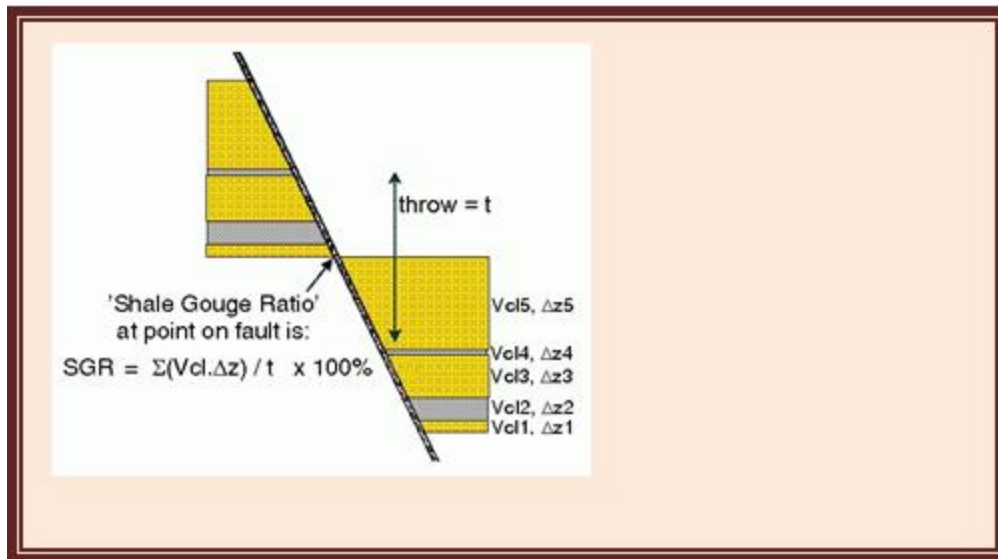
Figure 3.8. Shale Gouge Ratio (SGR) (Yielding et al., 2002 and 2008)

$$\text{SGR at point A} = \frac{(Vsh1*T1)+(Vsh2*T2)+(Vsh3*T3)}{Throw}$$
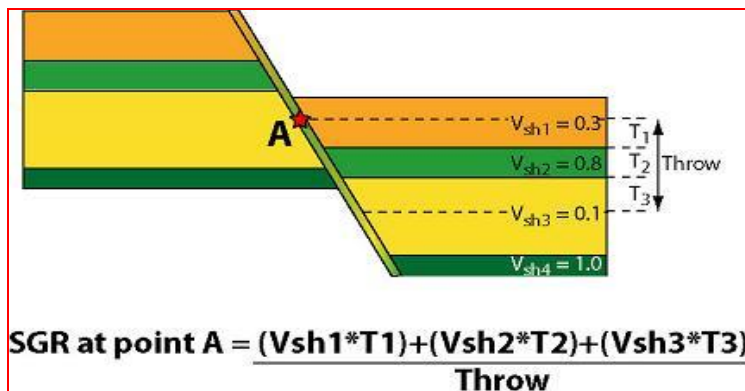
Figure 3.8.1. Shale Gouge Ratio (after Yielding et al., 1997)

3.9.0 Column Height Controls: Hydrocarbon column height controls were evaluated based on reservoir hydrocarbon relationship with structural controls (saddle point) and leaking fault surface.

3.9.1 Fault Seal Capacity: Average Shale Gouge Ratio and stratigraphic juxtapositions were used in the assessment of the actual geologic conditions that had prevailed during the hanging wall and foot wall displacement of the Baka faults.

3.9.2 Fault Seal Capacity, Hydrocarbon Column Height and Across Fault Pressure Algorithm Relationship: The fault seal integrity were ascertain through SGR and across fault pressure relationship adopted from seal-failure envelope plots established by Yielding et al. 2008 and 2014. These are as shown in figures 3.9.2.1 and 3.9.2.2.
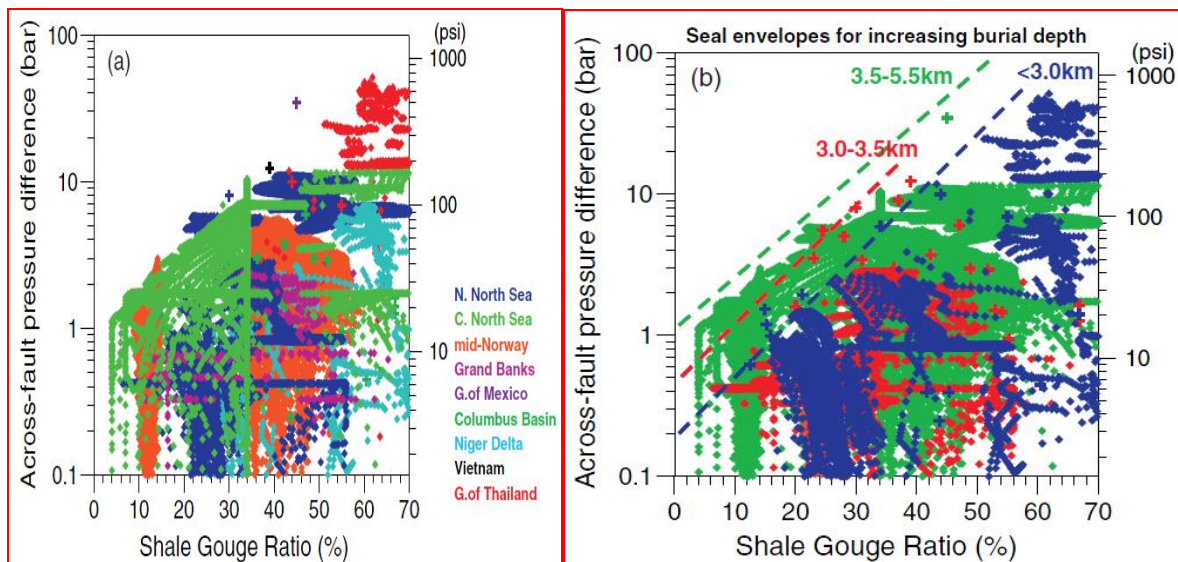
Figures 3.9.2.1. Seal-failure envelope from multiple subsurface studies from basins around the world (Yielding et al. 2008 and 2014).
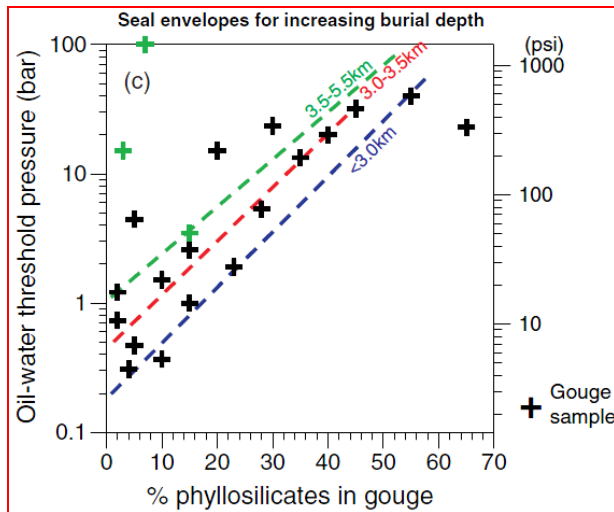
Figures 3.9.2.2. Seal-failure envelope from multiple subsurface studies from basins around the world showing Attributes (Yielding et al. 2008 and 2014).

The algorithm used are as follows:

The Shale Gouge Ratio (SGR) relationship utilized Yielding 2008 approach as oulined in fig. 3.9.2.2 above. The Across Fault Presure Difference implications to hydrocarbon column supports were determined using yielding et al. 2008,

AFPD(bar) = 10$^{(SGR/27-C)}$ Where **C = 0.5 at Burial Depth <3.0km, C = 0.25 at Burial Depth 3.0-3.5km, and C = 0 at Burial depth 3.5-5.5km.** The empirical relationship for Hydrocarbon Column Height calculation was used as follows:

H = AFPD
————
g(ρw – ρh)
                 That is Schowalter 1979, Vavra et al., 1992.

Where **g=gravity, ρw=density of water, ρh=density of hydrocarbon, and**

1bar = 14.5psi = 10^5pa

However, Capillary pressure can be calculated by: $P_c = (\rho_w - \rho_{nw})gh$ or $P_c = \dfrac{2\sigma\cos\theta}{r_c}$

Where **ρ_w= specific gravity of wetting, ρ_{nw}= specific gravity of non-wetting,**

g=acceleration due to gravity, h=Height of non-wetting phase above Free water

level, σ =Interfacial tension,

Θ= Contact angle between fluids and the Capillary tube,

r_c =radius of the capillary i.e. pore throat size

In field units, this is expressed as

$$P_c = 0.433 \times (\rho_w - \rho_{nw}) \times h$$

or $\boxed{h = \dfrac{P_c}{WaterGradient - HydrocarbonGradient}}$

Where, P_c is in psi.

ρ_w **and** ρ_{nw}**=** specific gravities (g/cm^3) of the wetting and non-wetting fluids at ambient conditions, 0.433= water gradient psi/ft, and h is in feet.

Chapter Four: Results and Discussion

4.1 Stratigraphy and Fluid Contact Interpretation

The Baka Field showed varying stratigraphy with diverse depositional environment which include shore face deposits and channels. The stratigraphy of the field in many parts of the field are affected by the faults and as such, the accommodation space are greatly dependent on these faults. In the log scale correlations, these stratigraphic representation of the field were constrained chronostratigraphicaly within genetic packages guided with open ends correlation transect line. Typical of the correlation transect line used for stratigraphic delineations is as shown in figure 4.1.
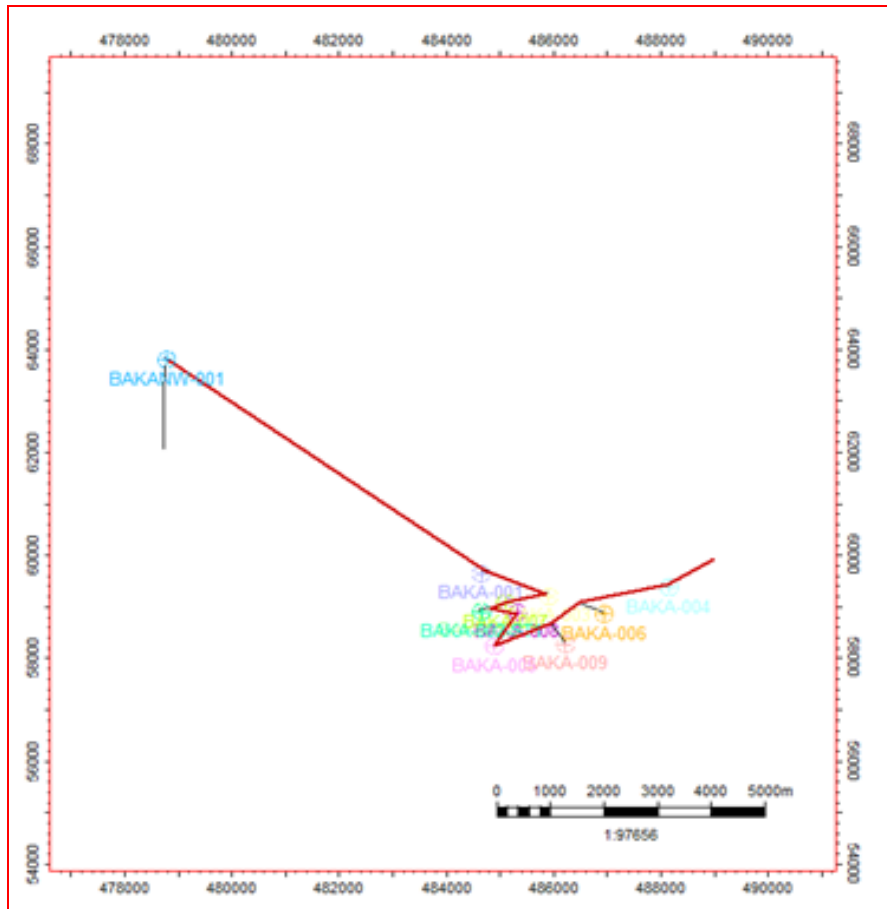
Figure 4.1. Open ends correlation transect line.

The stratigraphy of the field range from clean sand reservoirs to mixed clastic reservoirs. The thickness of the individual sand reservoirs varies depending on the available accommodation space created by the faults. These event disparities resulted to thin reservoirs in some parts of the field and amalgamated multi story sand reservoirs in other parts. The rock and fluid properties also vary within and across the reservoirs and such a particular reservoir may contain hydrocarbon in some parts and none in other parts, or none at all or completely filled with

hydrocarbon. Typical fluid property distribution of gas-down-to the base of the

reservoir is as shown in figure 4.1.1 using G2000 channel reservoir sand. These

utilized the gamma ray motif, neutron and density logs complemented with the

resistivity logs.
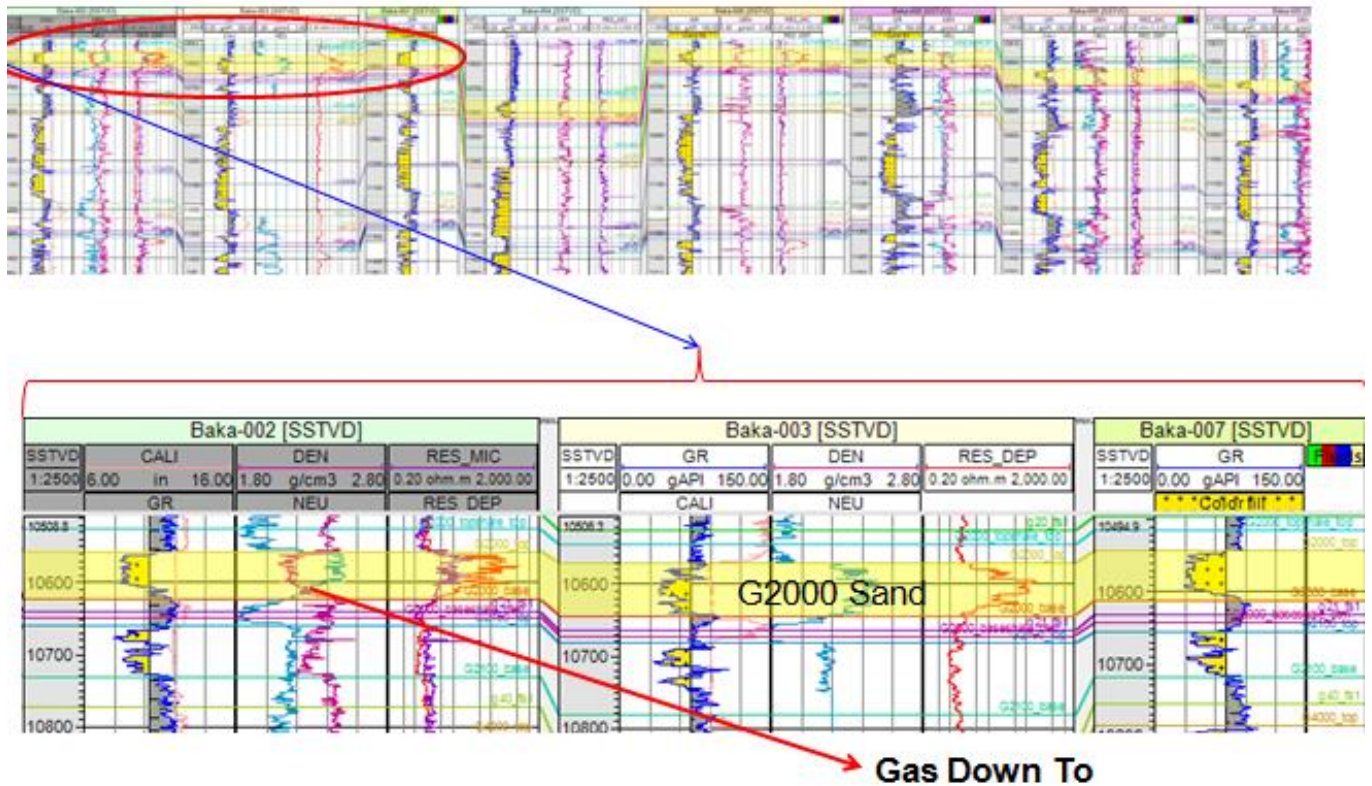
Figure 4.1.1. Correlation of G2000 Gas bearing sand reservoir

Other fluid distribution type in this field is where both oil and water filled the

same reservoir. Typical of this fluid distribution type can be seen in the G6000

reservoir as shown using figure 4.1.2. The G6000 reservoir is also a good example

of the amalgamated multi-story channel reservoir sand.
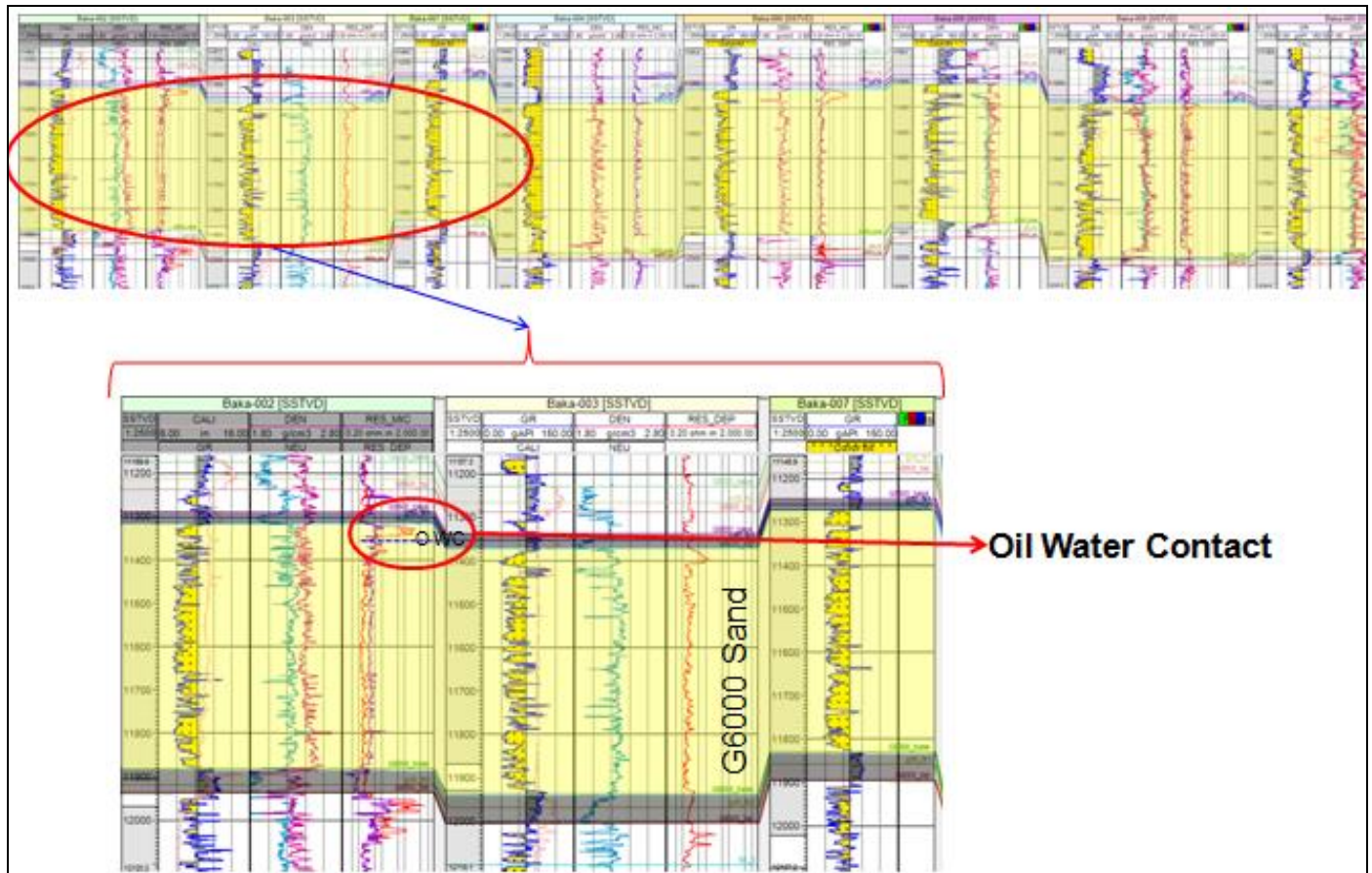
Figure 4.1.2. Correlation of G6000 Oil bearing sand reservoir

The different reservoirs architecture and their different fluid types are interpreted

and represented as oil-water-contact, oil-down-to, and gas-down-to, (figures

4.1.3, 4.1.4 and 4.1.5).
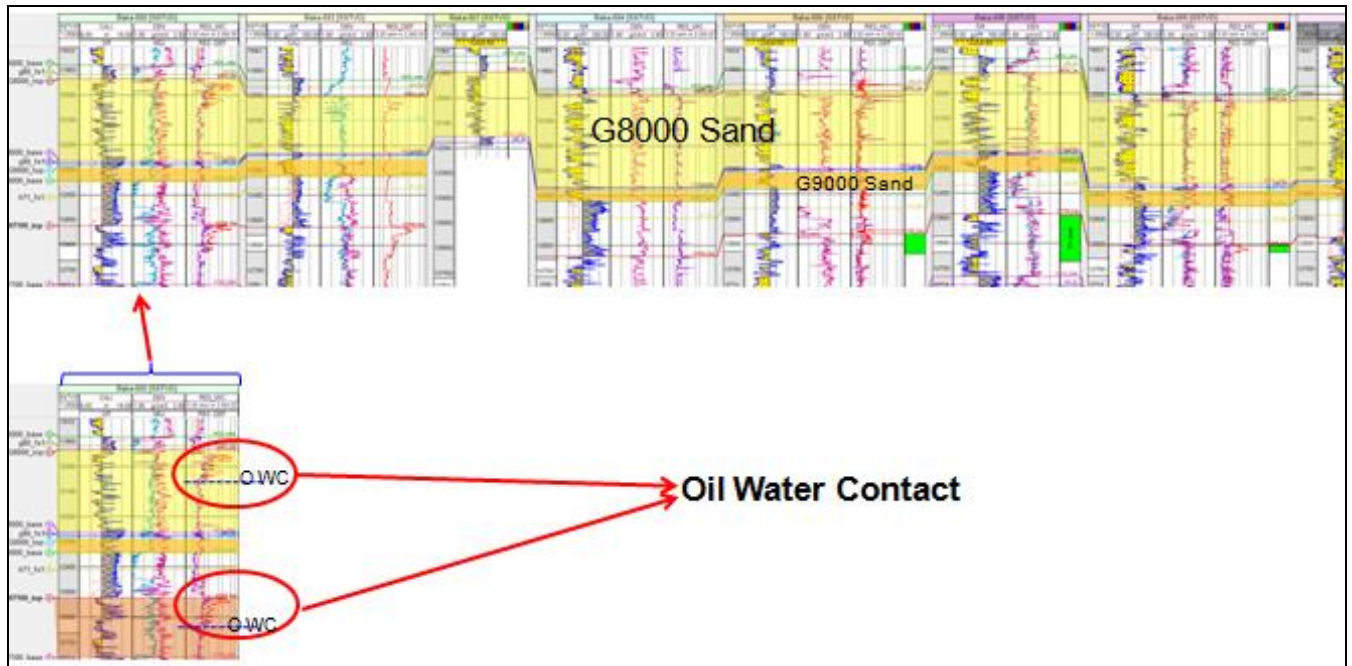
Figure 4.1.3. Correlation of G8000 and H7100 Oil bearing sand reservoir
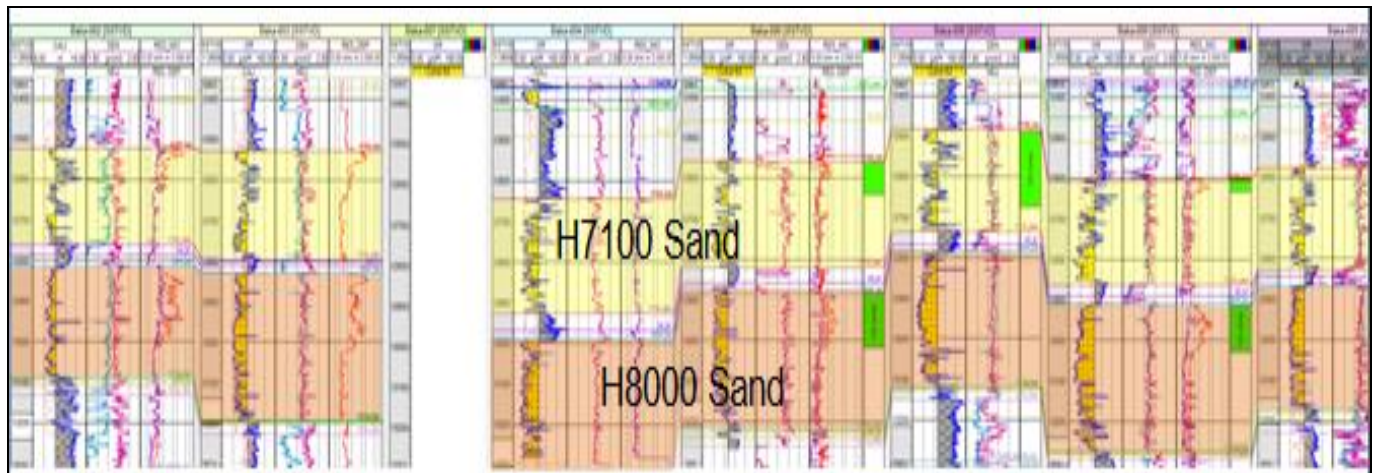
Figure 4.1.4. Correlation of H7100 and H8000 Oil bearing sand reservoir
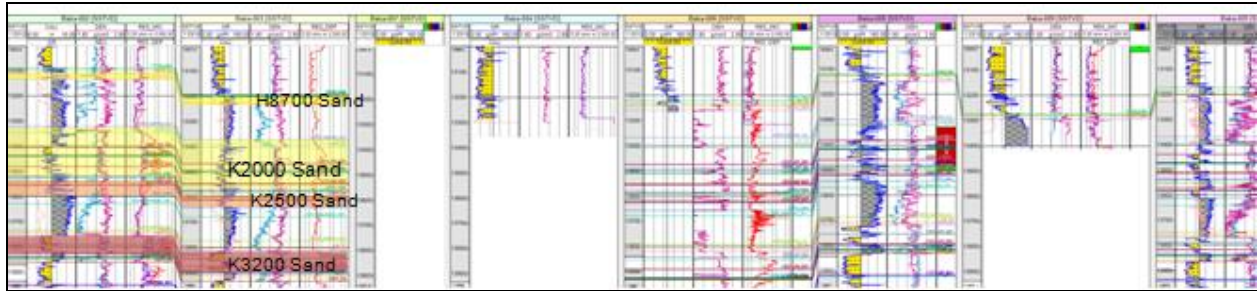
Figure 4.1.5. Correlation of H8700, K2000, K2500 and K3200 Oil bearing sand reservoir

4.2 Seismic Interpretation

The seismic interpretation encompassed fault mapping, horizon mapping and time - depth conversions.

4.2.1. Fault Mapping and Horizon Mapping

The interpretations of faults in this field utilized extraction of dip guided semblance map (figure 4.2.1) from the seismic volume and this showed that the field is predominantly of the growth fault system with diverse structural styles (figure 4.2.2). The semblance map showed that the lateral extensiveness of the faults in the field also varies. The smaller faults died at shallow depths in some of the reservoirs while some other faults like the boundary fault penetrated to the deeper prospects. The semblance map in figure 4.2.1 indicates that the boundary fault formed fault plays and as such good site for investigation of fault bounding reservoirs. The semblance map at varying time slices indicates that shallower reservoirs are more faulted compared with deeper reservoirs. These faults as can

be seen in both (figures 4.2.1 and 4.2.2) may be sealing faults or conduits and as

such a subject of great interest in this study.
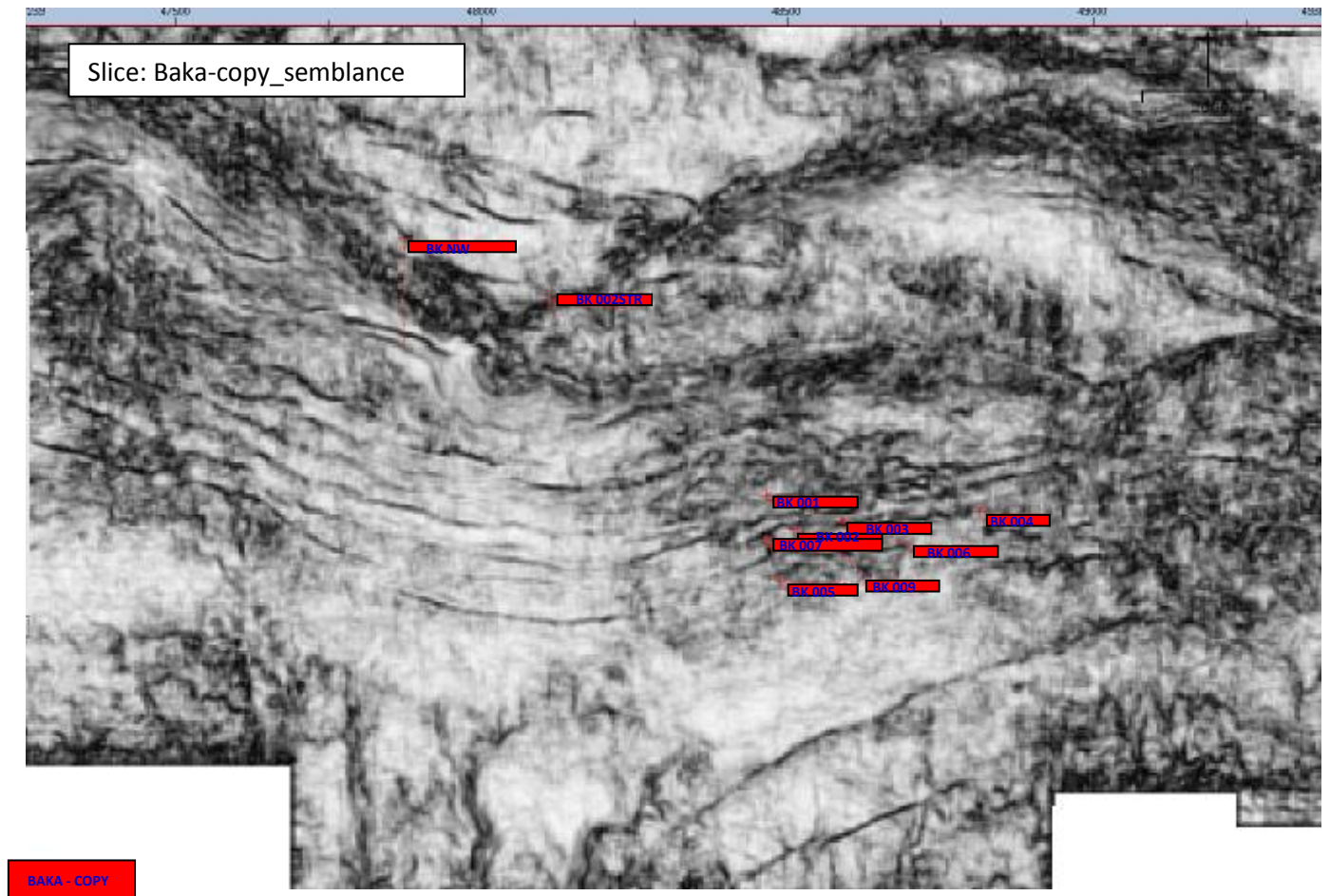
Figure 4.2.1. Extracted Dip Guided Semblance Map of Baka Field

Typical of the structural distributions in the field is as shown in (figure 4.2.2). This

growth fault system within a faulted roll-over indicates that stratigraphic

thicknesses are more concentrated in the hanging walls of the fault blocks

compared to the foot wall sides. The question of which of the blocks have the

trapping capacity with fluid concentration remains paramount and as such subject

to investigation in this study.
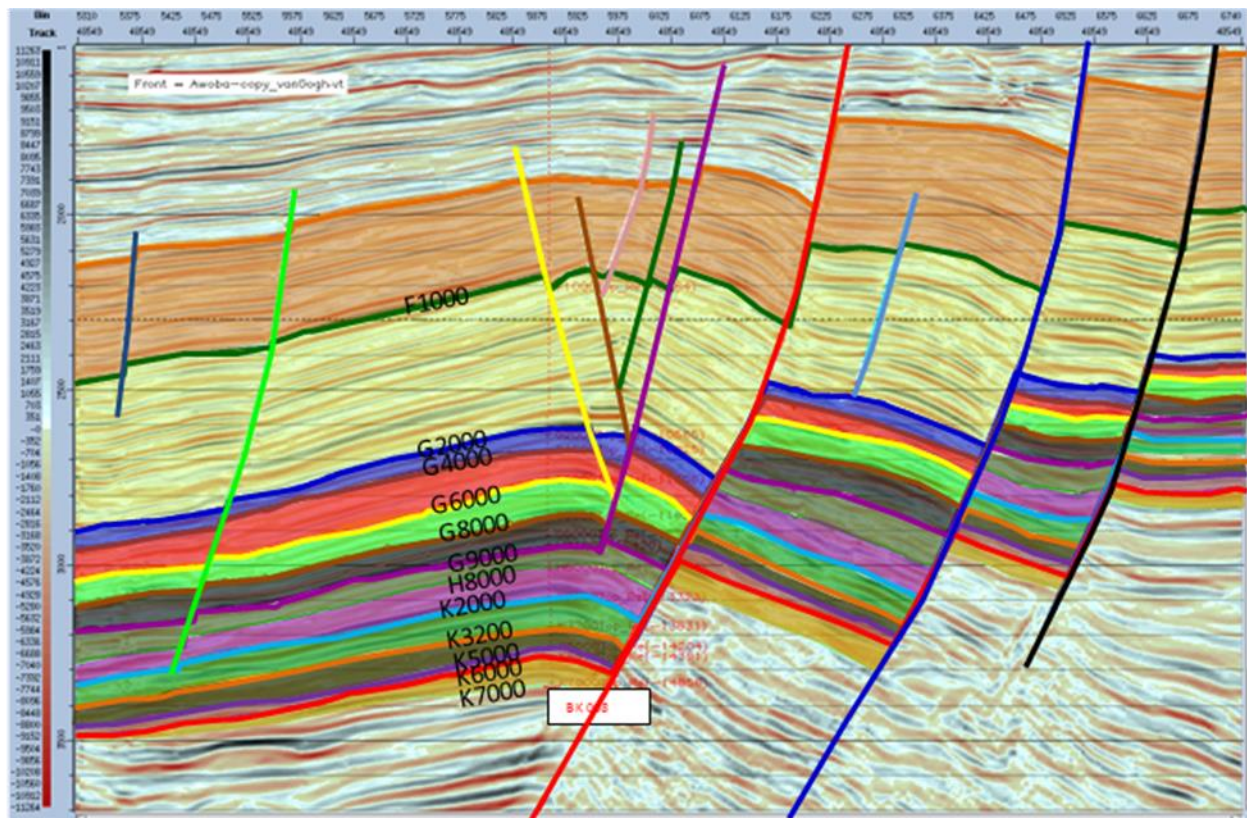
Figure 4.2.2: Faults and Horizon Interpretation from Seismic Data In-Line

The lateral stratigraphic disseminations in the field as shown in (figure 4.2.3) using

Vangogh seismic cross line are within sub-parallel reflections pattern with little

indications of chaotic incursion. The structural saddle spill points are also shown

as areas of limits of the reservoir capacities. The lateral faults shapes and extensiveness varies as a result of different prevailed geologic events in the field.
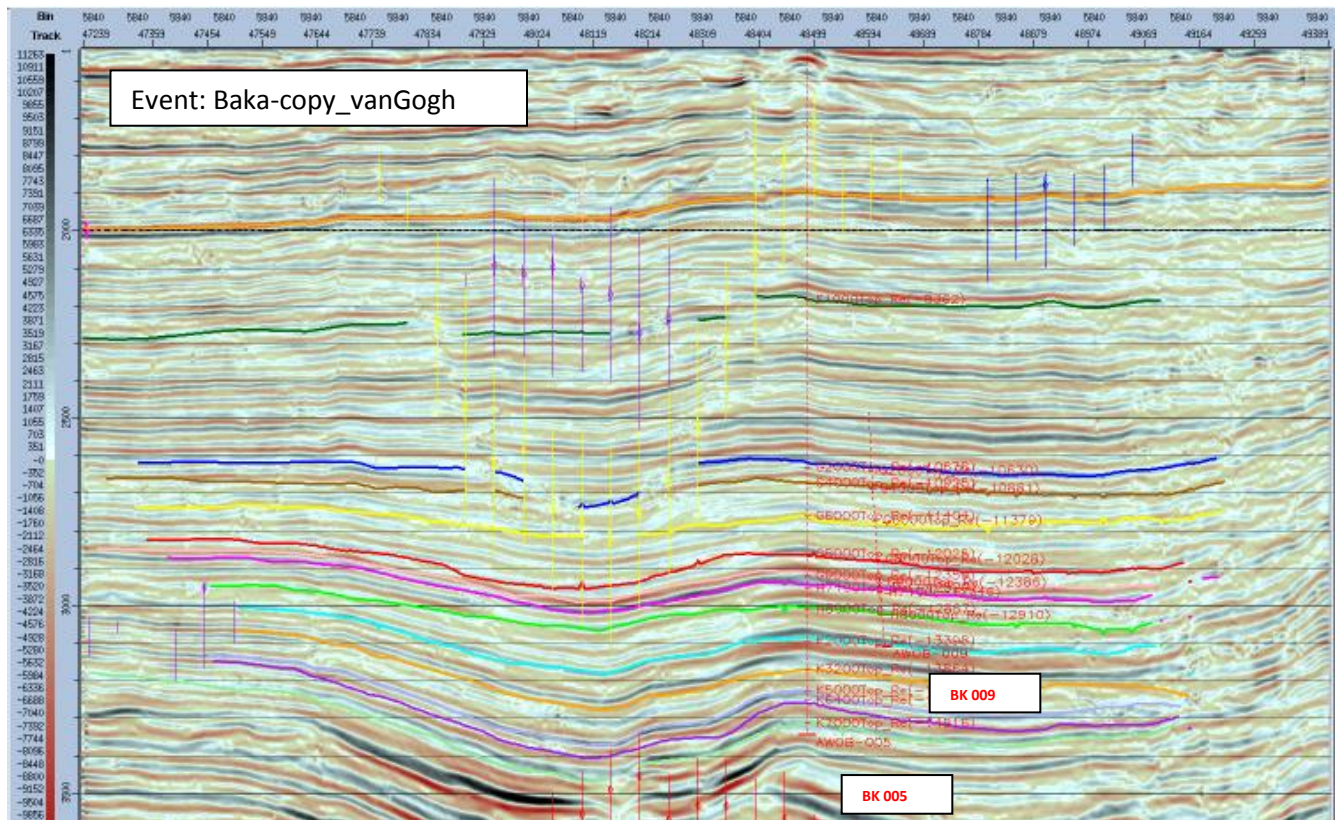
Figure 4.2.3: Faults and Horizon Interpretation from Seismic Cross-Lines

The resultant prevailed geologic events in the field is credence to structural relay defined from Southern part of the field to the North-West part of the field. The Baka North-West structural features entirely changed with impressions of back-to-back faults, horst and grabben and flexural faulted collapse crest structures as can be seen in (figure 4.2.4).
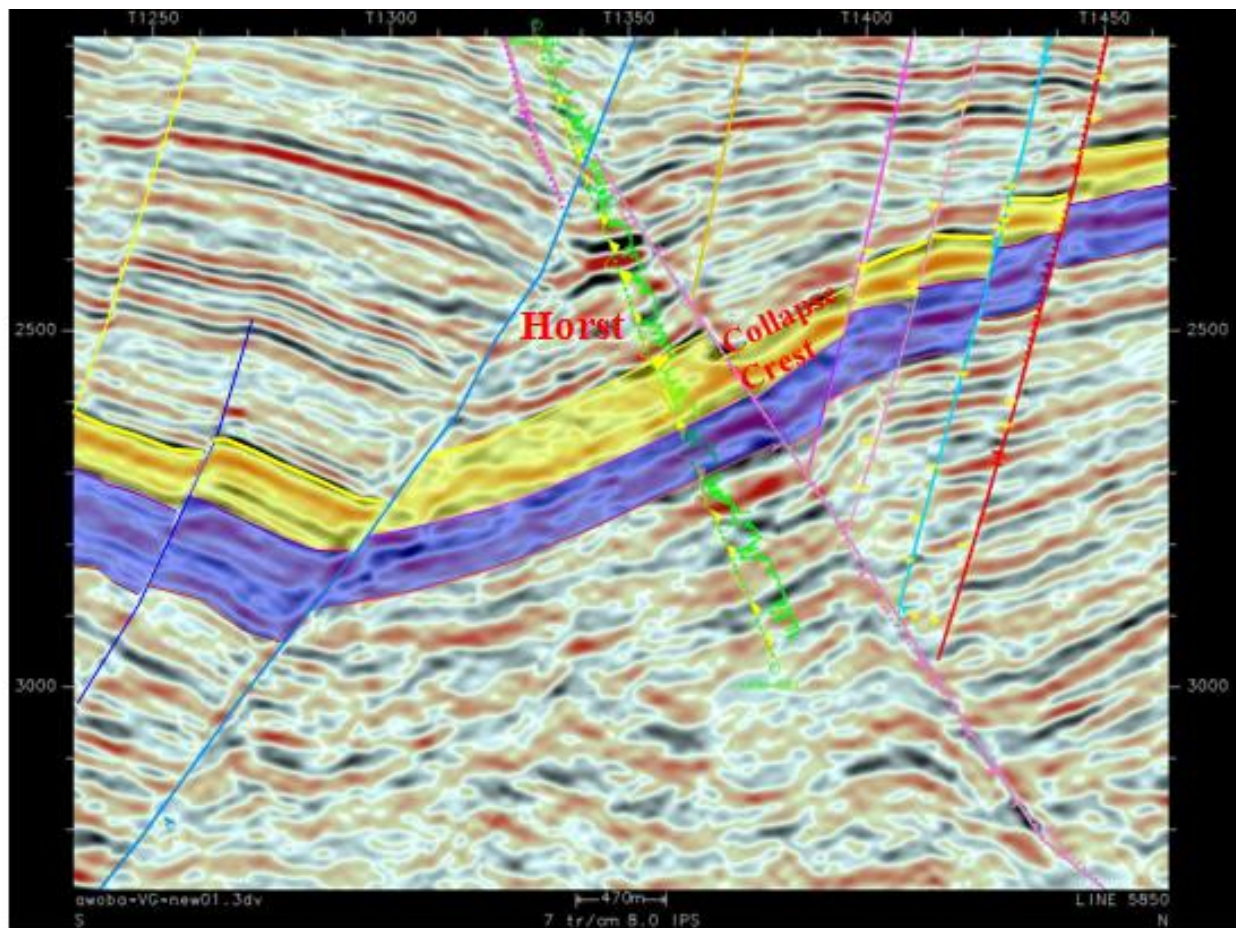
Figure 4.2.4: Baka North-West Interpretation on Seismic Data (Inline 5850ms)

Typical of the stratigraphic variations with respect to the structural styles in the field is represented as horizon interpretation using F1000 reservoir (figure 4.2.5). The overlay of the horizon on the semblance map is to established stratigraphic representation with structural connotations. The fault polygons as used in (figure 4.2.5), denotes the fault gaps, heaves and throws depending on the usage and applications and orientations of the structures.
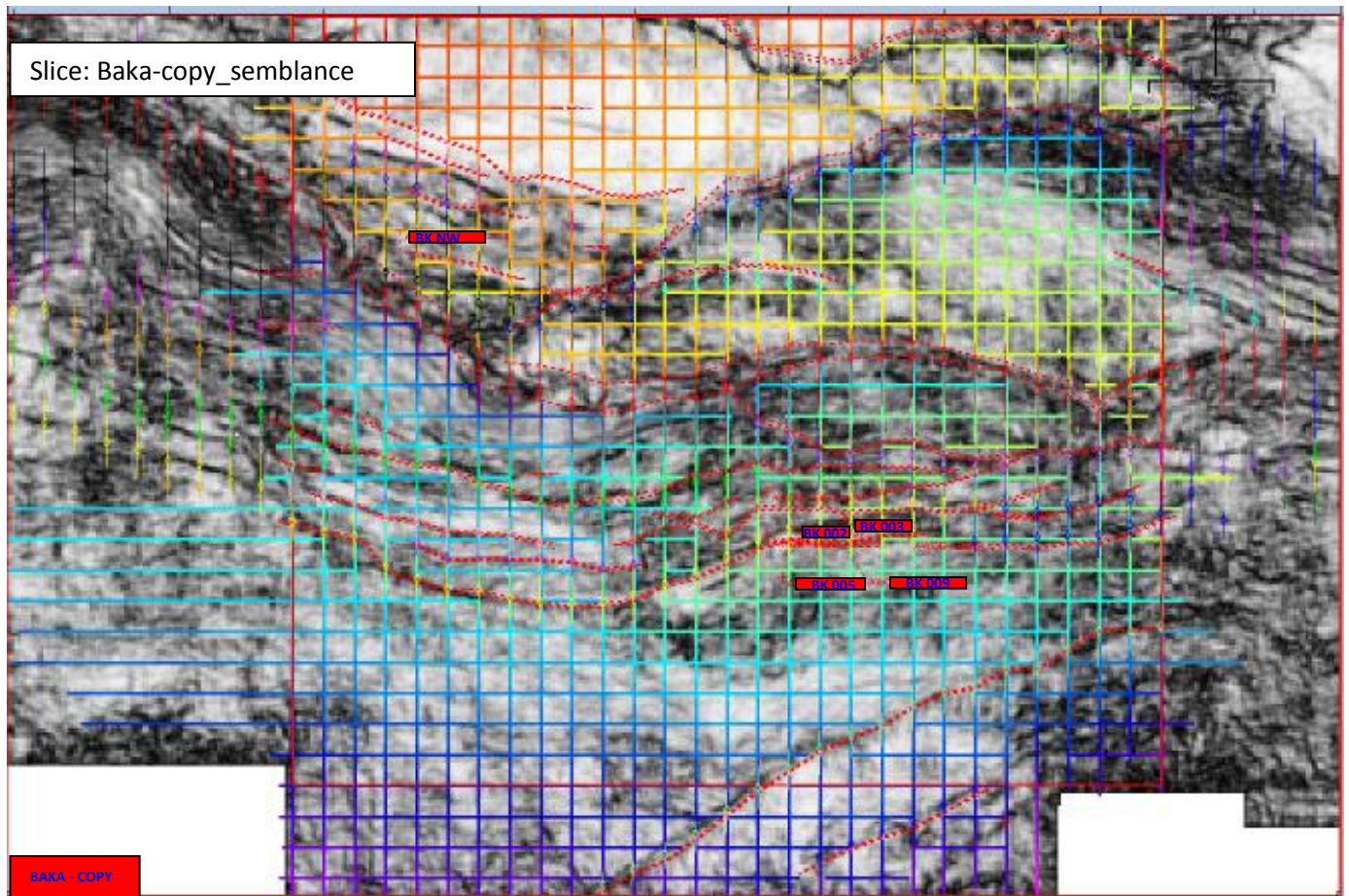
Figure 4.2.5: Horizon F1000 Interpretation on Semblance Map with Fault Polygons

The field can be described as predominantly of the stacked faulted role-over geometry as can be seen in the inline - cross line representation of the field in (figure 4.2.6). The hanging wall side of the faults are thicker compared with the foot walls and as such indicates that more accommodation space were created and more sediments deposited within the hanging walls. Either sides may be the site of the hydrocarbon accumulations depending on the source rock generation,

depth of hydrocarbon expelled and the available trapping mechanism of the

reservoirs.
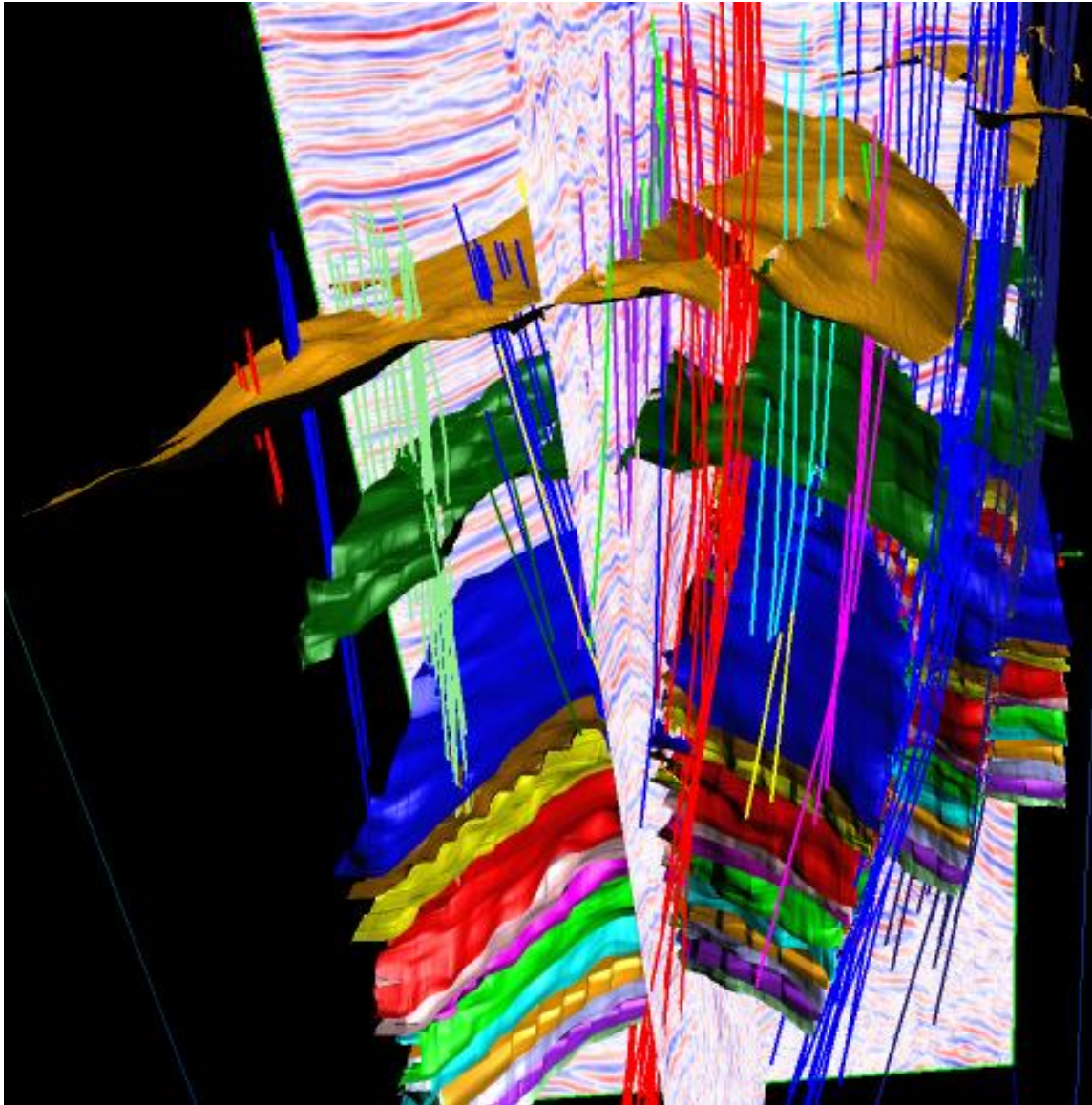
Figure 4.2.6: Seismic Volume showing interpreted In-lines and Cross-lines

Horizons as Faulted Roll-Over Anticline

Typical of the edited and calibrated check-shot used and the associated synthetic seismogram generated from the seismic is displayed in (figure 4.2.7). Time to depth conversions or vice versa used in this study were ascertained as shown in (figure 4.2.7).
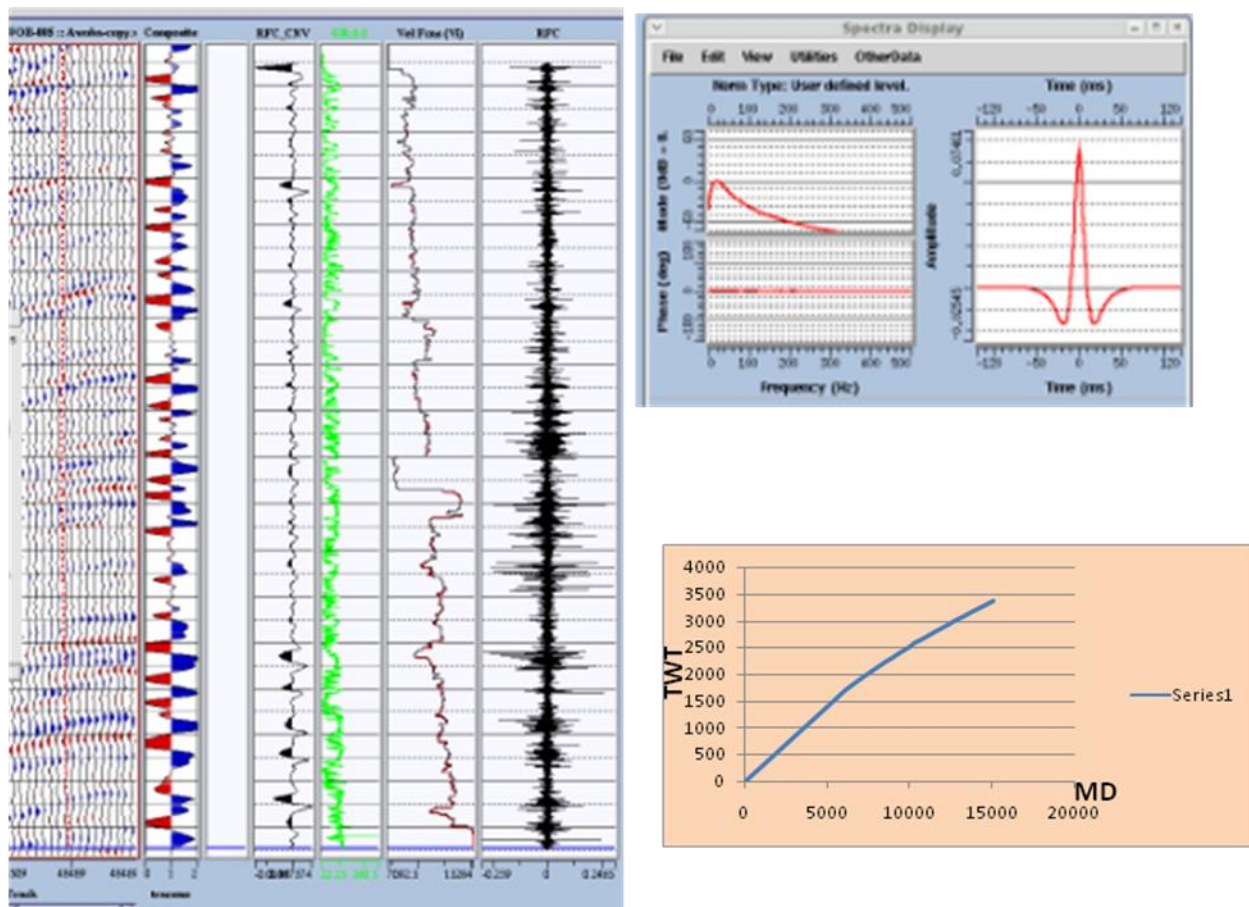
Figure 4.2.6: Synthetic Seismogram and Check-Shot Curve used in the interpretation

Episodic geologic events in field triggered different faults which emanated at some depths and died out at some depths while some other faults penetrated to the deeper reservoirs. Typical different faults penetrations in the reservoirs are shown in (figure 4.2.7). The hanging wall block relative to the boundary fault indicates that at shallower depths, reservoirs such as G2000 and G6000 are more faulted while some of these faults died out at G8000 and K2000 reservoir depths. The disparities in structural styles has implication in the reservoirs as which of the faults is trapping or not. Also, in (figure 4.2.7), the reason why hydrocarbon accumulation are concentrated within the hanging wall fault block relative to the foot wall is attributed to these faults influences and as such detail understanding of the faults needed to be carried out as will be seen in subsequent sections.
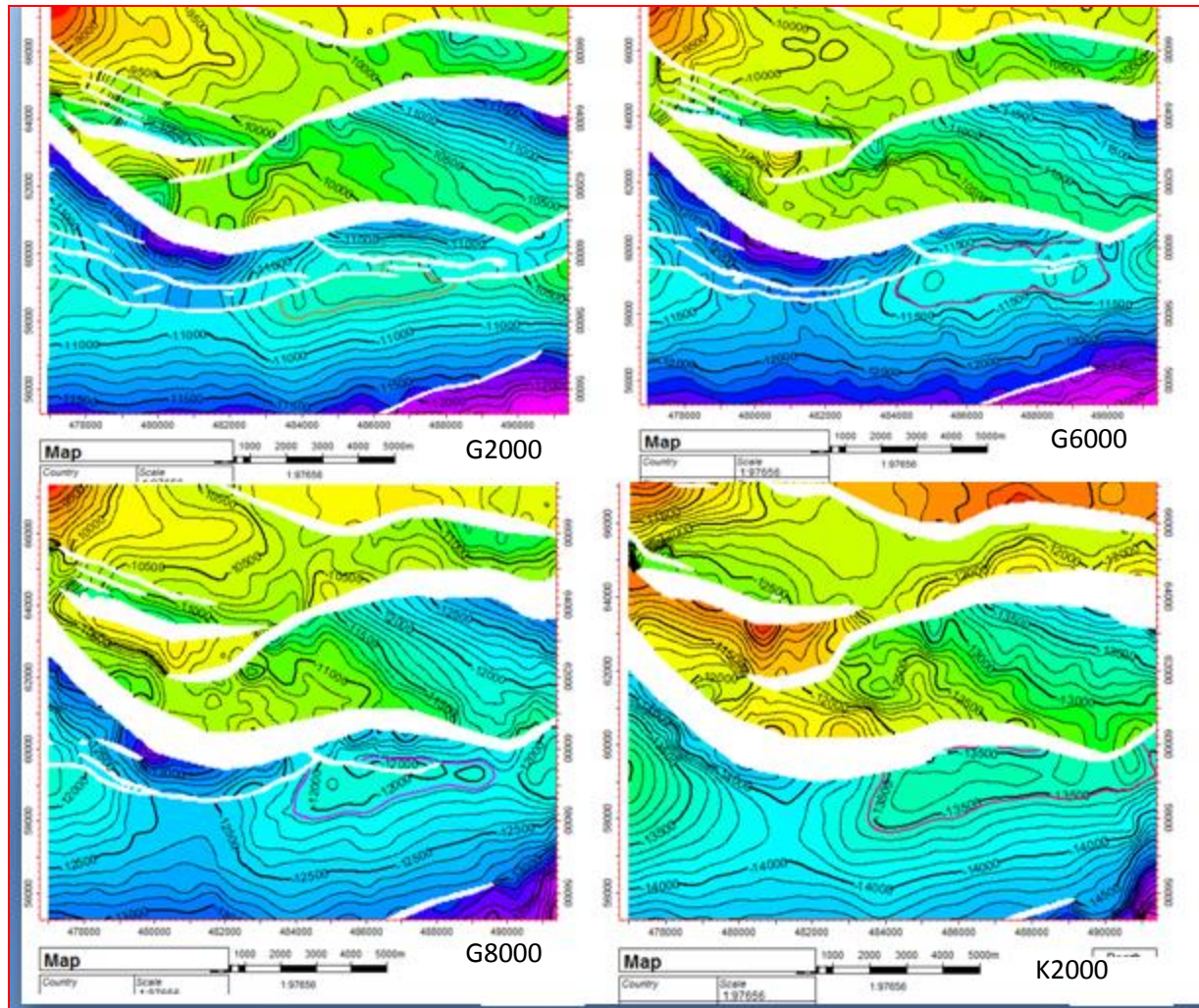
Figure 4.2.7: Structural variations at different stratigraphic depths

4.3. 3D Structural Model, Property Models and Stratigraphic Juxaposition Model

The 3D models in this study utilized direct conversion of seismic interpretations to 3D grid models and structural framework models to avoid compromising the prevailed structural features. The mapped faults as integrated in the models were

122

constrained using the top, mid and base skeleton model methods (figure 4.3 and

4.31) as a guide to the imprints of the faults structural framework (figure 4.3.2).
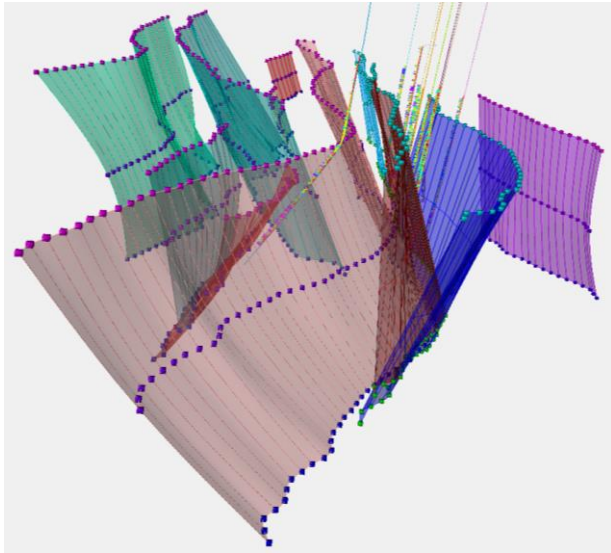
Figure 4.3: Fault Modeling (Fault Sticks)
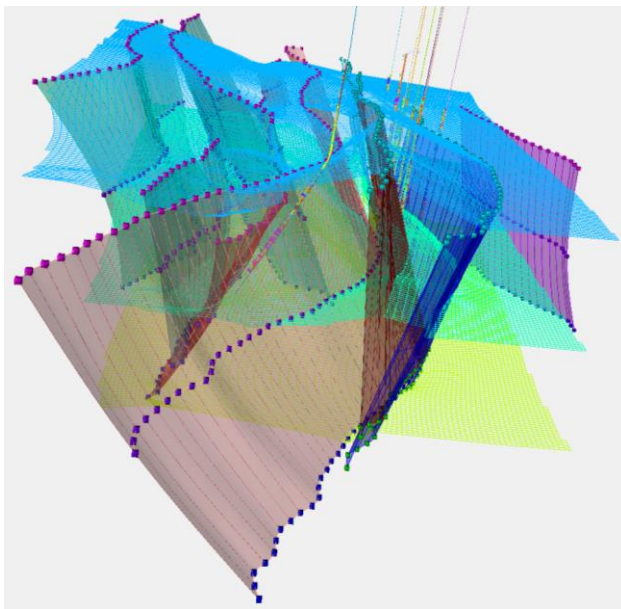
Figure 4.3.1: Fault Modeling and Pillar Gridding at all Mapped Horizons

The interpreted structural framework model of the field is as shown in (figure 4.3.2). This indicates that the field is composed of different fault styles such as back-to-back faults, synthetic and antithetic faults and faults of varying depths of penetrations. The boundary fault as can be seen in (figure 4.3.2) delineates the major boundary between the hanging wall and the footwall block of the field. The trends of these faults and the degree of penetrations of the faults has influences on the stratigraphy, fluids and pressure differentials relative to either sides of the faults.
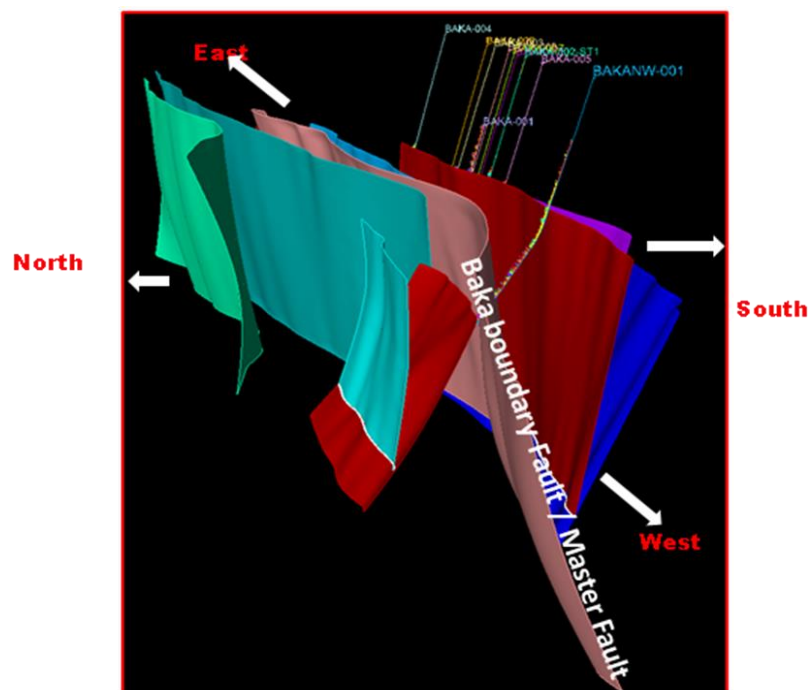
Figure 4.3.2: 3D Structural Framework Model

Typical of the fault penetrations and structural segments defining the major fault blocks are represented in (figures 4.3.3 and 4.3.4). In both figures it is glaring that some faults are more laterally extensive compared with other faults and as such has implications to the reservoir fault seal. Also, fault throw variations virtually exist in all the interpreted faults in the field and as such may lead to cataclasis, gouge formations, smearing of fluidized shale and their pressure disparities relationships. Such evidences were investigated in the subsequent interpretations.
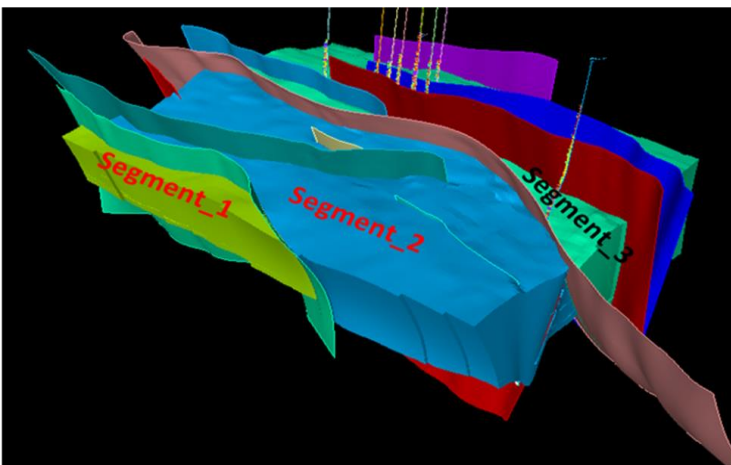
Figure 4.3.3 : 3D Structural Segment Model with faults penetrations
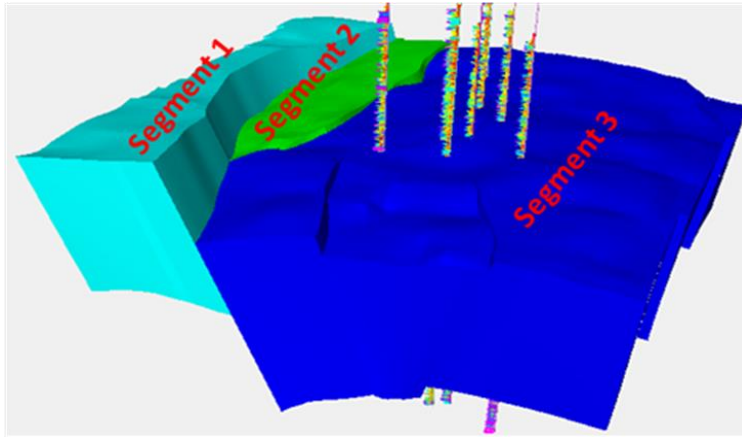
Figure 4.3.4: 3D Structural Segment Model at shallow reservoirs (F1000-G4000) showing structural blocks

The determination of the structural limits of the reservoir capacities gives credence to the accuracy of the interpreted fault seal capacities. The structural saddle spill points that defines the structural lowest points in a reservoir that is capable to harbor fluid were delineated using intersection planes as shown in (figure 4.3.5). The evidence of the structural lowest points capable of holding fluid provides direct meaning to the reservoir vertical relief as the entirety of the capacity capable of holding fluid can be clearly seen in (figure 4.3.5)
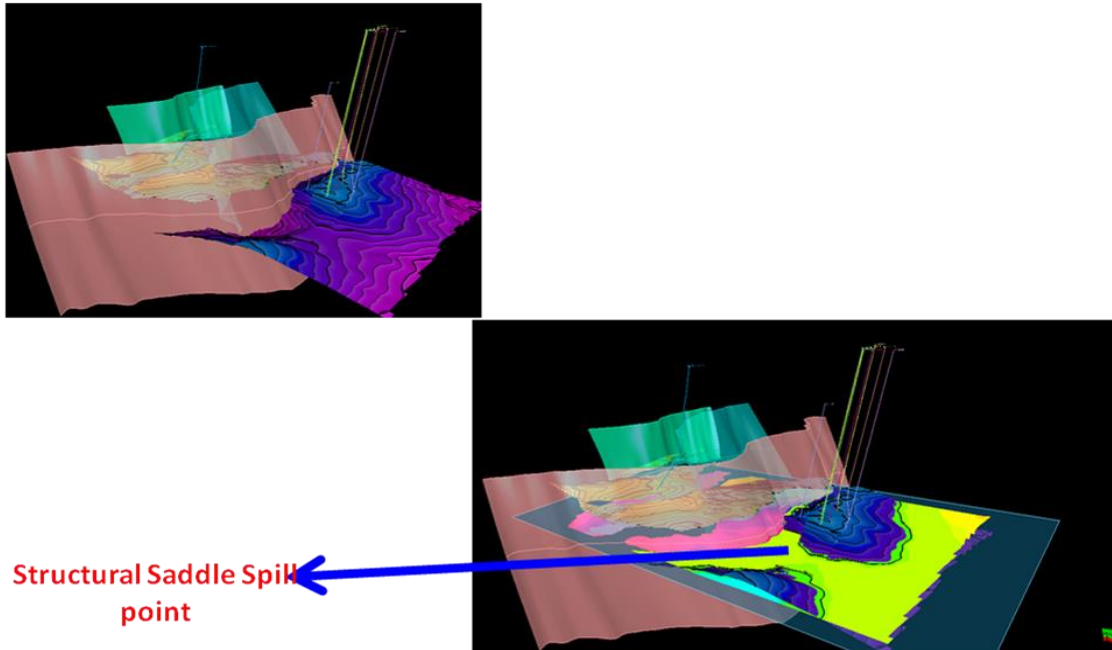
Figure 4.3.5: 3D Interpretation of Structural Saddle Spill Point

The study field was investigated at 3D horizon and zone modeling stages as shown in (figure 4.3.6) using fine scale gridding methods to capture and investigate both micro and macro reservoir information's for optimal reservoir quality predictions. Interpretations were carried out the gross reservoirs and the net reservoir depths. The individual reservoir quality ascertained by measurable parameters such as volume of shale, net to gross, fault throw profile analysis, and shale gouge ratio were then integrated in the 3D reservoir property models (figure 4.3.7) for detail reservoir quality results predictions.
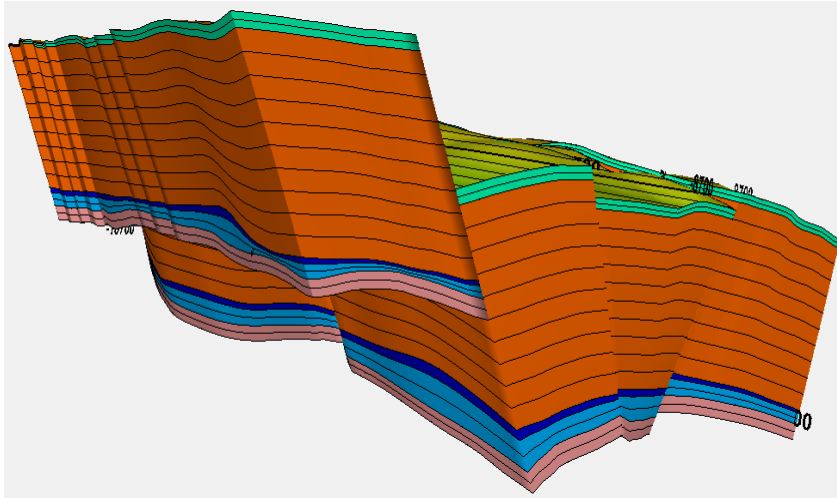
Figure 4.3. 6: 3D Horizon and Zone Modeling

Typical of the reservoir property distribution in a 3-dimentional view is as shown in (figure 4.3.7). The question of the processes that led to faulting and its implication and representations were then extracted as fault stratigraphic juxtaposition models.
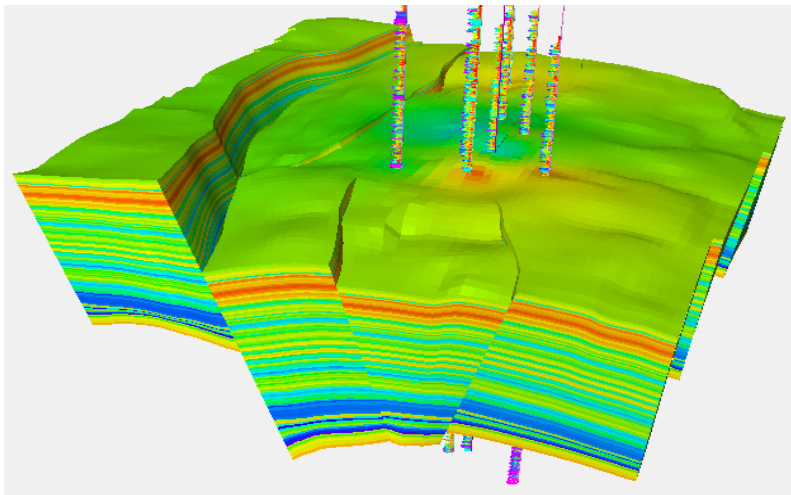
Figure 4.3.7: Petrophysical Model of Volume of Shale

The stratigraphic variations within the fault surfaces are entirely different at the same depth compared to the depth equivalent of the nearby stratigraphy and as such good indication of diverse prevailed processes of geologic events. The cataclasis, smearing of shales, shale gouge, rock pore throat and contact angle relationships, capillary pressure, bouyancy pressure and across fault pressure differences can be ascertained at different hanging walls and footwal blocks as shown in (figure 4.3.8).
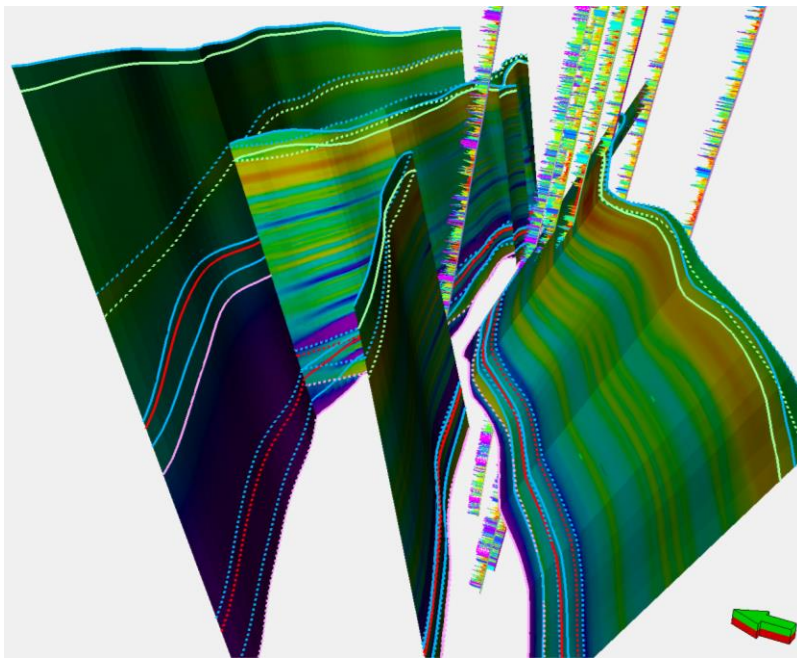
Figure 4.3.8: Fault Surface Relationships: Hanging Wall – Foot Wall

    Stratigraphic Juxtaposition modeling

4.4   Fault Seal Analysis

Thirteen (13) different horizons interpreted in this study includes the oil bearing reservoir sand bodies (F1000, G4000, G6000, G8000, G9000, H7100, and H8000); and the gas reservoirs (G2000, K2000, K3200, K5000, K6400, and K7000). Reservoirs interpreted in Baka Field are fault dependent - faulted anticlinal reservoirs. Hydrocarbons in the faulted anticlinal reservoirs are trapped at the crest of the anticline dependent on the fault(s). The reservoir fluid contact is determined in the field scale using neutron logs, density logs and resistivity logs. However, the mixed clastic heterogeneous fault zone properties were used to determine the fault seal fluid contacts based on stochastic shale gouge ratio approach. Details of the individual reservoir fault seal capacity, spill points and leak points, field column height distributions and calibrations with stochastically predicted column heights based on average shale gouge ratios of the fault surface stratigraphic juxtapositions are as follows:

4.5. Interpretations of Fault Dependent Oil Reservoirs

4.5.1 Horizon F1000 (Under Filled Fault/Dip Dependent Closure Oil Reservoir)

F1000 reservoir is an under-filled oil reservoir in a fault/dip dependent closure within a faulted anticline considering the column height and the vertical relief of 237ft. E. of the field. The F1000 reservoir crest is at 8,258ft with an oil column height of 86ft based on field evaluation. The saddle spill point of this reservoir is at 8,495ft towards the east. Based on stochastic fault seal analysis using shale gouge ratio in column prediction, 89.42ft oil column height is predicted from P85 (that is at low column SGR prediction) and this showed high degree of conformity with F1000 field columns. The average shale gouge ratio values range from 16 – 38.7% (low class, based on exploration classification) with fault leak points at <20% SGR. The oil column height control in this reservoir is due to fault leak as shown by the fault plain strtigraphic juxtaposition in figure 4.5.1.1. The P85 predicted the most consistent and high degree of conformity with the observed field columns of the F1000 under-filled reservoir. Details of the fault seal analysis results are shown in figures (4.5.1.1 and 4.5.1.2.).
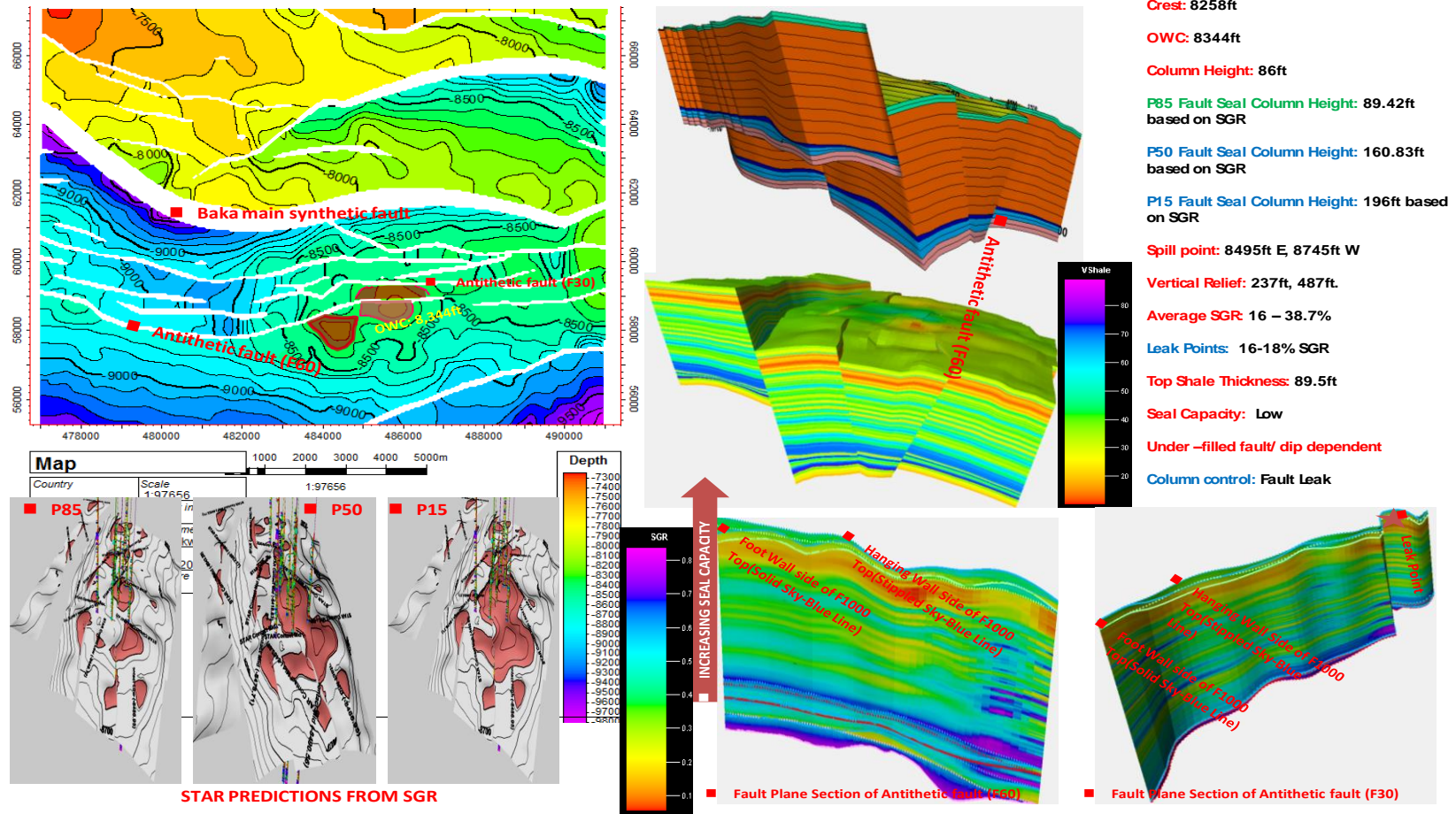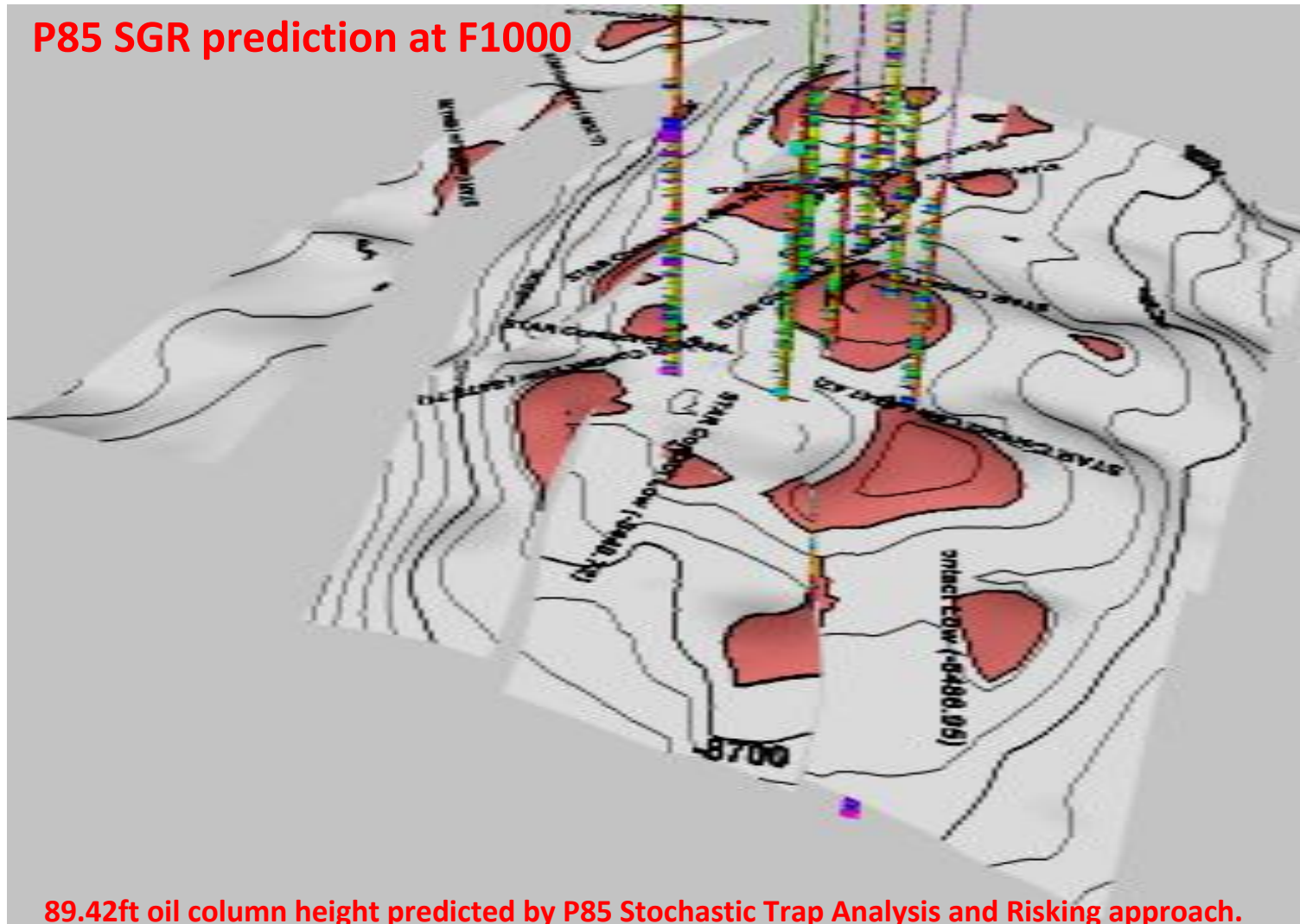
F1000 (UNDER FILLED RESERVOIR)

Crest: 8258ft

OWC: 8344ft

Column Height: 86ft

P85 Fault Seal Column Height: 89.42ft based on SGR

P50 Fault Seal Column Height: 160.83ft based on SGR

P15 Fault Seal Column Height: 196ft based on SGR

Spill point: 8495ft E, 8745ft W

Vertical Relief: 237ft, 487ft.

Average SGR: 16 – 38.7%

Leak Points: 16-18% SGR

Top Shale Thickness: 89.5ft

Seal Capacity: Low

Under –filled fault/ dip dependent

Column control: Fault Leak

STAR PREDICTIONS FROM SGR

Fault Plane Section of Antithetic fault (F60)

Fault Plane Section of Antithetic fault (F30)

Figure 4.5.1.1: Detailed Result of F1000 Fault Seal Analysis and Known Field Column Height
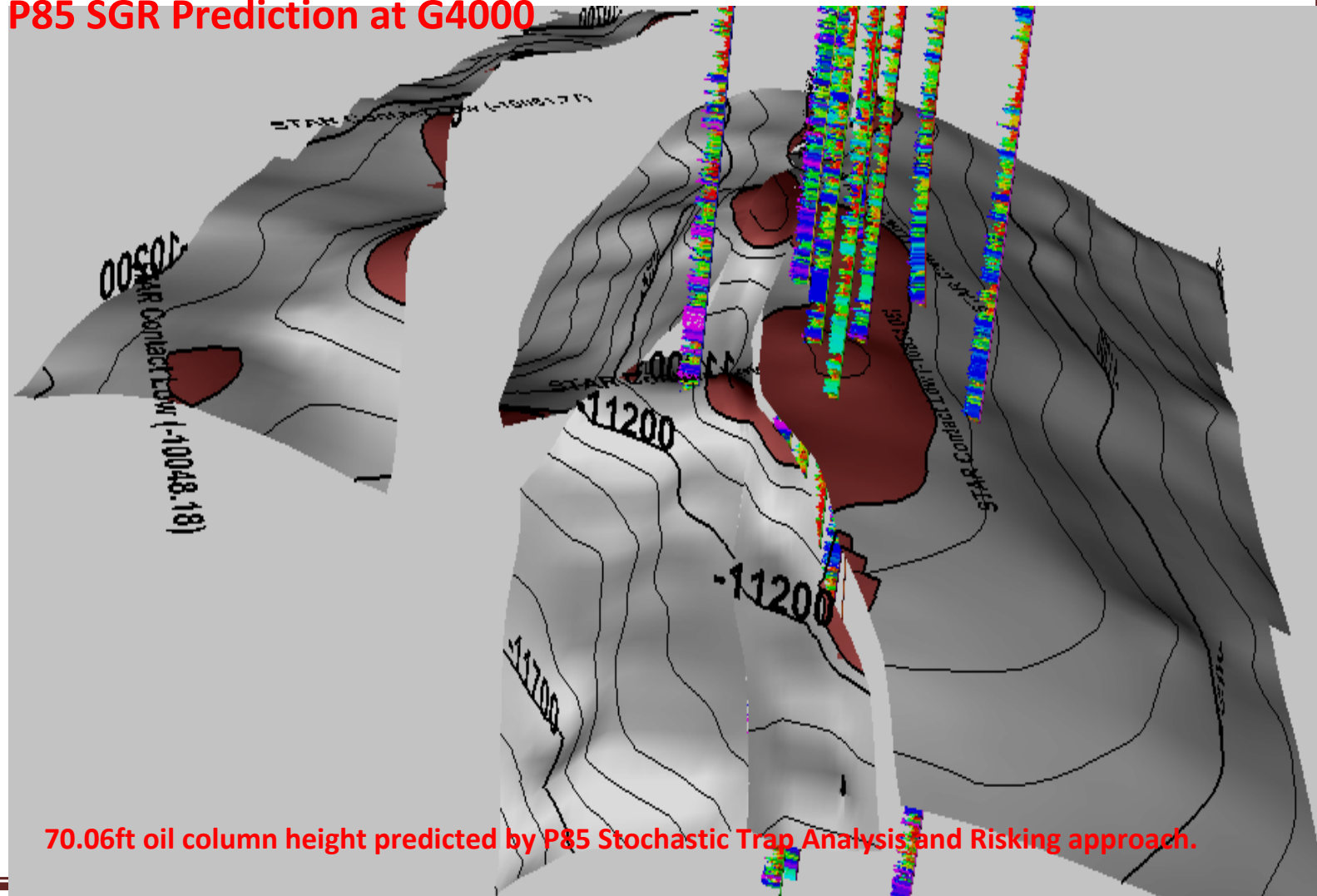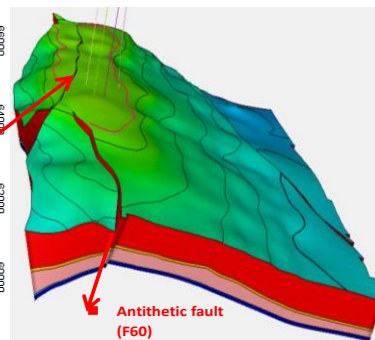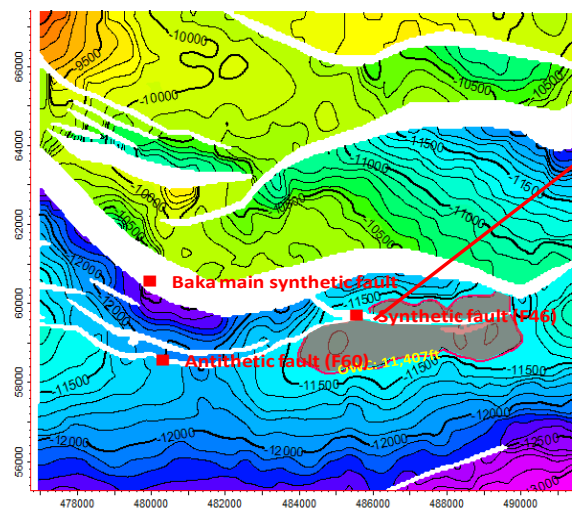
Figure 4.5.1.2: P85 Oil Column Height Predicted by Stochastic Trap Analysis at F1000 Reservoir

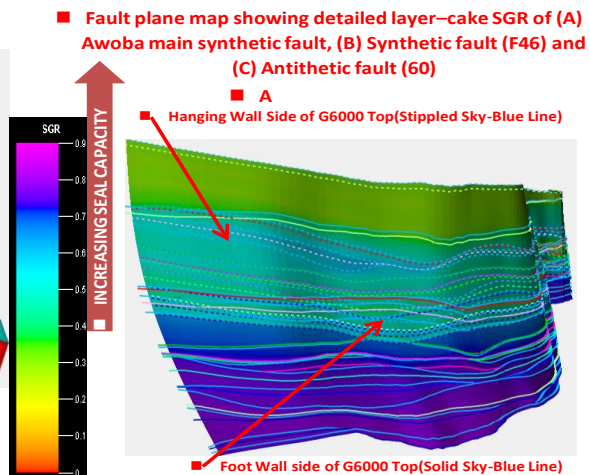### 4.6.2 Horizon G4000 (Under Filled Fault Dependent Closure Oil Reservoir)

G4000 reservoir is an under-filled reservoir considering the vertical relief and column height difference. This reservoir is a fault dependent closure and an oil bearing reservoir within a faulted anticline. The oil column height based on field evaluation is 55ft with reservoir crest position at 10,784ft and oil water contact of 10,839ft. Based on Stochastic column height derived from SGR, P85 predicted that faults at G4000 reservoir levels could seal up to an oil column height of 70.06ft. The column height predicted from a stochastic approach in comparison with field column height showed good degree of conformity. The average shale gouge ratio within the hanging wall and foot wall stratigraphic juxtaposition range from 14.5 – 39% (low SGR class based on exploration classification). Leak points exists in the antithetic fault (F60) at <20% SGR as shown on figure 4.6.2.1. The under filled is attributed to low SGR mainly due to reservoir sand juxtaposing reservoir sand. The G4000 faults have low seal capacity based on SGR range classification used in exploration. Oil column height control in this reservoir is the fault leak. P85 oil column height predicted by the SGR showed high degree of conformity with the observed field column at the under-filled

G4000 reservoir. Details of the fault analysis and observed field column heights

are shown in figures 4.6.2.1 and 4.6.2.2.

G4000 (UNDER FILLED RESERVOIR)

Crest: 10,784ft

OWC: 10,839ft

Column Height: 55ft

P85 Fault Seal Column Height: 70.06ft. Based on SGR

P50 Fault Seal Column Height: 158ft based on SGR

P15 Fault Seal Column Height: 159ft based on SGR

Spill Points: 11,006ft.E and 11,209ft.W

Vertical Relief: 222ft, 425ft.

Average SGR: 14.5 – 39%

Seal Capacity: Low Seal

Leak Points: <20% SGR at F60

Top Shale Thickness: 89.89ft

Column Control: Fault Leak

■ **Baka main synthetic fault**

■ **Synthetic fault (F46)**

■ **Antithetic fault (F60)**

OWC: 10,839ft

■ **Fault Plane Section of Synthetic fault (F46)**　■ **Fault Plane Section of Antithetic fault (F60)**

Map

Country

Scale 1:97656

1:97656

Depth

■ P85　■ P50　■ P15

INCREASING SEAL CAPACITY

SGR

Hanging Wall Side of G4000 Top(Stippled Sky-Blue Line)

Foot Wall side of G4000 Top(Solid Sky-Blue Line)

Leak Point

STAR PREDICTIONS FROM SGR

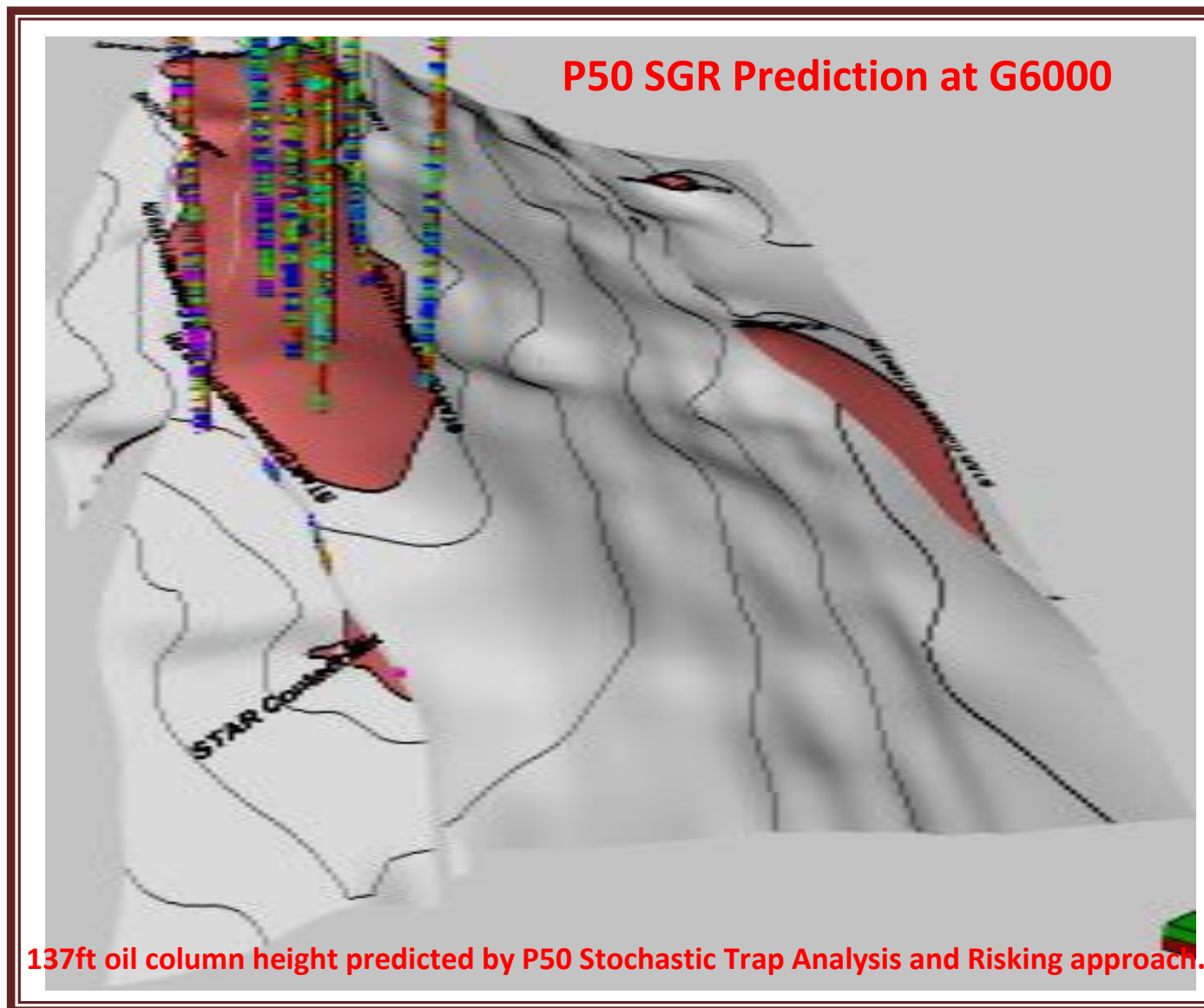**Figure 4.6.2.1: Detailed Result of G4000 Fault Seal Analysis and Known Field Column Height**

Figure 4.6.2.2: P85 Oil Column Height Predicted by Stochastic Trap Analysis at G4000 Reservoir

4.7   Horizon G6000 (Full To Spill Fault Dependent Closure Oil Reservoir)

G6000 reservoir is a full to spill fault dependent closure - anticlinal reservoir

segmented by fault and bounded at one of its proximal anticline flank by the Baka

Field boundary fault. Oil column height in this reservoir filled up to the structural

saddle spill point covering almost the entirety of the vertical relief. Field

evaluation at structural crestal position of 11,271ft and oil water contact of

11,407ft points at 136ft oil column height. The stochastic trap analysis and risking

showed that the shale gouge ratio within the hanging wall – foot wall

stratigraphic juxtaposition of the three faults of interest as shown in figure 4.7.1,

indicates that the SGR values are higher compared with faults of under-filled

reservoirs. Seal capacities of the three faults are quite good and could seal up to

137ft oil column height based on stochastic prediction of the SGR at mid column

height (P50). The structural saddle spill point is the main oil column control in this

reservoir. The oil column height evaluated from the field and the stochastically

predicted column heights showed high degree of conformity. The P50 predictions,

showed high degree of conformity with the observed field column height at full to

spill reservoirs in the Baka Field. Details of the G6000 reservoirs field column

height calibrations with the predicted fault seal column heights at different

percentile levels are shown in figures 4.7.1 and 4.7.2.

G6000 (FULL TO SPILL RESERVOIR)

■ Fault plane map showing detailed layer–cake SGR of (A) Awoba main synthetic fault, (B) Synthetic fault (F46) and (C) Antithetic fault (60)

■ A

■ Hanging Wall Side of G6000 Top(Stippled Sky-Blue Line)

■ Foot Wall side of G6000 Top(Solid Sky-Blue Line)

Baka main synthetic fault

Synthetic fault (F46)

Antithetic fault (F60)

Antithetic fault (F60)

Crest: 11271ft

OWC: 11407ft

Column Height: 136ft
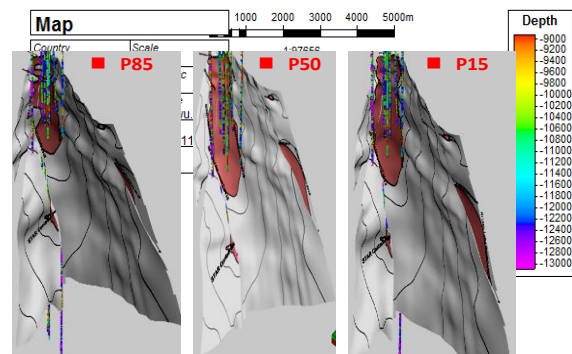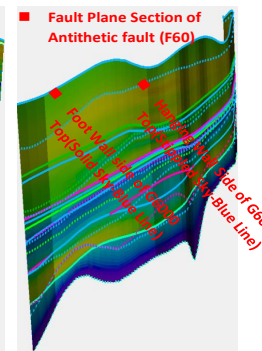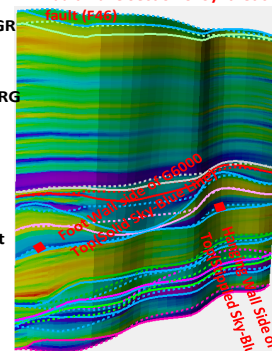
P85 Fault Seal Column Height: 107.43ft based on SGR

P50 fault seal column height: 137ft based on SGR

P15 Fault Seal Column Height: 146.27ft. Based on SRG

Spill point: Full to Spill

Vertical Relief: 159ft

Closure Type: Fault dependent closure

Average SGR: 45 – 51% at boundary fault, 45 – 49 at F46 and 36 -40 at F60

Seal Capacity: Good Seal

Column Control: Spill Point

Map

■ P85   ■ P50   ■ P15

STAR PREDICTIONS FROM SGR

■ Fault Plane Section of Synthetic fault (F46)

■ Fault Plane Section of Antithetic fault (F60)

Figure 4.7.1: Detailed Result of G6000 Fault Seal Analysis and Known Field Column Height

140

P50 SGR Prediction at G6000

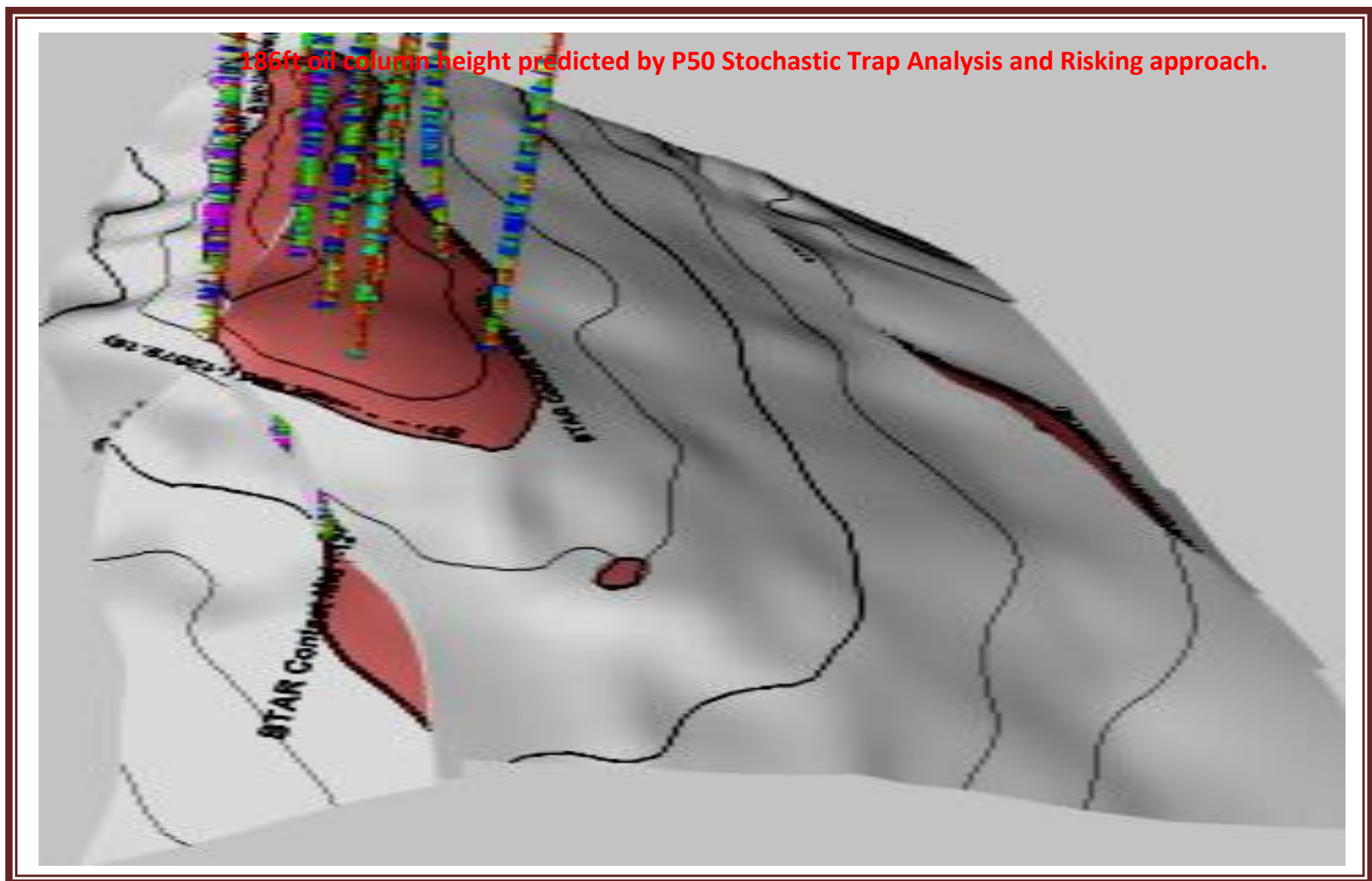**137ft oil column height predicted by P50 Stochastic Trap Analysis and Risking approach.**

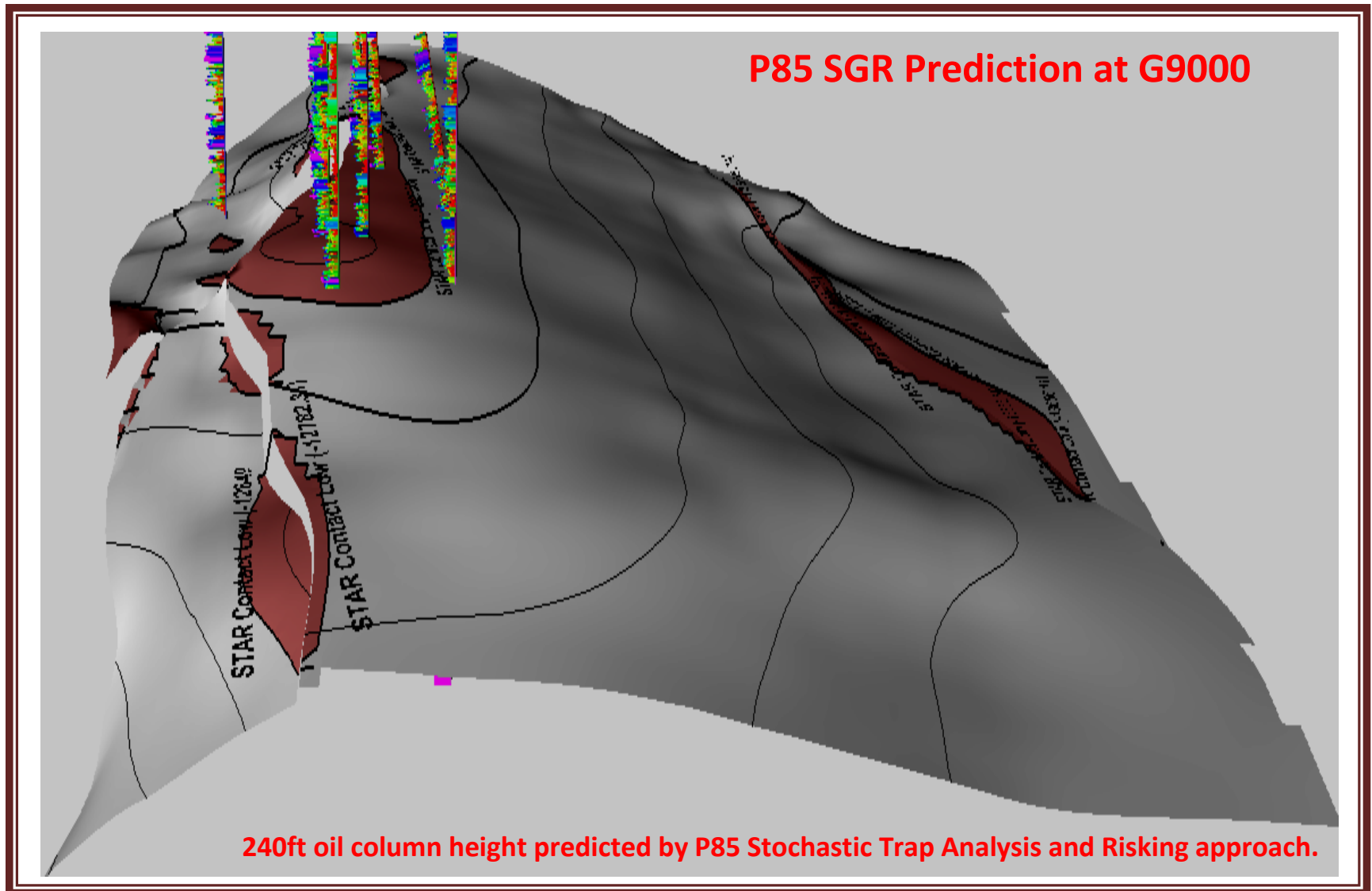**Figure 4.7.2: P50 Oil Column Height Predicted by Stochastic Trap Analysis at G6000 Reservoir**

4.8   Horizon G8000 (Full To Spill Fault Dependent Closure Oil Reservoir)

G8000 reservoir is a full to spill fault dependent closure oil reservoir. This reservoir has an oil column height of 177ft from a crestal position of 11,891ft and oil water contact of 12,068ft covering almost the entirety of the vertical relief with oil. The oil in this reservoir filled down to the lowest structural contour that defined the structural trap reaching the maximum capacity of the reservoir at the structural saddle spill point based on field evaluation. Application of stochastic approach using fault shale gouge ratio as the seal parameter indicates that the fault could seal up to 186ft oil column height at the mid column prediction of the faults (P50). Both the observed field column height and the fault seal column height showed high degree of conformity. The shale gouge ratio's of the faults (that is within the hanging wall and foot wall stratigraphic juxtaposition of the synthetic fault-F46 and the antithetic fault-F60 range from 41 – 52% SGR). Both faults have good sealing capacity with no indication of fault leak points. The shale gouge ratio as predicted from the heterogeneous fault rock properties (SGR) are within the medium class shale gouge ratio based on the exploration scale. The oil column height control in this reservoir is the structural spill point.

G8000 (FULL TO SPILL RESERVOIR)

Crest: 11891ft

OWC: 12068ft

Column Height: 177ft

P85 Fault Seal Column Height: 119.79ft. Based on SGR

P50 Fault Seal Column Height: 186ft. Based on SGR

P15 Fault Seal Column Height: 188.91ft. Based on SGR

Spill point: 12080ft. E Shallow, 12550ft. W Deep

Vertical Relief: 189ft, 659ft

Closure Type: Fault dependent closure

Average SGR: 41 – 52% at both Fault F46 and F60

Top Shale Thickness: 75ft Average

Seal Capacity: Good Seal

Column Control: Spill Point

■ Fault plane map showing detailed layer–cake SGR of (A) Synthetic fault (F46) and (B) Antithetic fault (60)

Baka main synthetic fault

Synthetic fault (F46)

OWC: 12,068ft

Antithetic fault (F60)

STAR PREDICTIONS FROM SGR

■ Fault Plane Section of Synthetic fault (F46)

■ Fault Plane Section of Antithetic fault (F60)

Figure 4.8.1: Detailed Result of G8000 Fault Seal Analysis and Known Field Column Height

143

186ft oil column height predicted by P50 Stochastic Trap Analysis and Risking approach.

Figure 4.8.2: P50 Oil Column Height Predicted by Stochastic Trap Analysis at G8000 Reservoir

4.9   Horizon G9000 (Under Filled Fault Dependent Closure Oil Reservoir)

The G9000 oil reservoir is an under-filled fault dependent closure with faulted crest anticline. Both flaks of the faulted anticline are under filled considering the reservoir vertical relief and the accumulated oil column height. This reservoir has 210ft oil column height based on field observation. The crest of this reservoir is at 12,087ft and the oil water contact is at 12,297ft. Predictions based on stochastic trap analysis using shale gouge ratio as the seal attribute indicates that the synthetic fault (F60) could seal up to 240ft oil column height at P85. Both the observed field column height and the fault seal column height showed high degree of conformity. The shale gouge ratio captured at the hanging wall and foot wall stratigraphic juxtaposition range from 17.31 – 70%. Fault leak zone at this reservoir exists around 17.31 - <20% SGR and had leaked oil into the nearby structure. The thin overlying shale thickness of about 19.58ft at this reservoir is also attributed to the under-filled. The oil column height control in this reservoir is clearly the fault leak points.

G9000 (UNDER FILLED RESERVOIR)

Crest: 12,087ft

OWC: 12,297ft

Column Height: 210ft

P85 Fault Seal Column Height: 240.05ft. Based On SGR

P50 Fault Seal Column Height: 299ft. Based on SGR

P15 Fault Seal Column Height: 323.94ft. Based on SGR

Spill Points: 12,425ft.E Shallow and 12,860ft. W. Deep.

Vertical Relief: 338ft, 773ft

Average SGR: 17.31 – 70%

Leak Point: 17.3 -18% SGR

Top Shale Thickness: 19.53ft

Seal Capacity: Low

Column Control: Fault Leak

Top Shale Thickness of 19.53 is also attributed to the under filled.

STAR PREDICTIONS FROM SGR

INCREASING SEAL CAPACITY
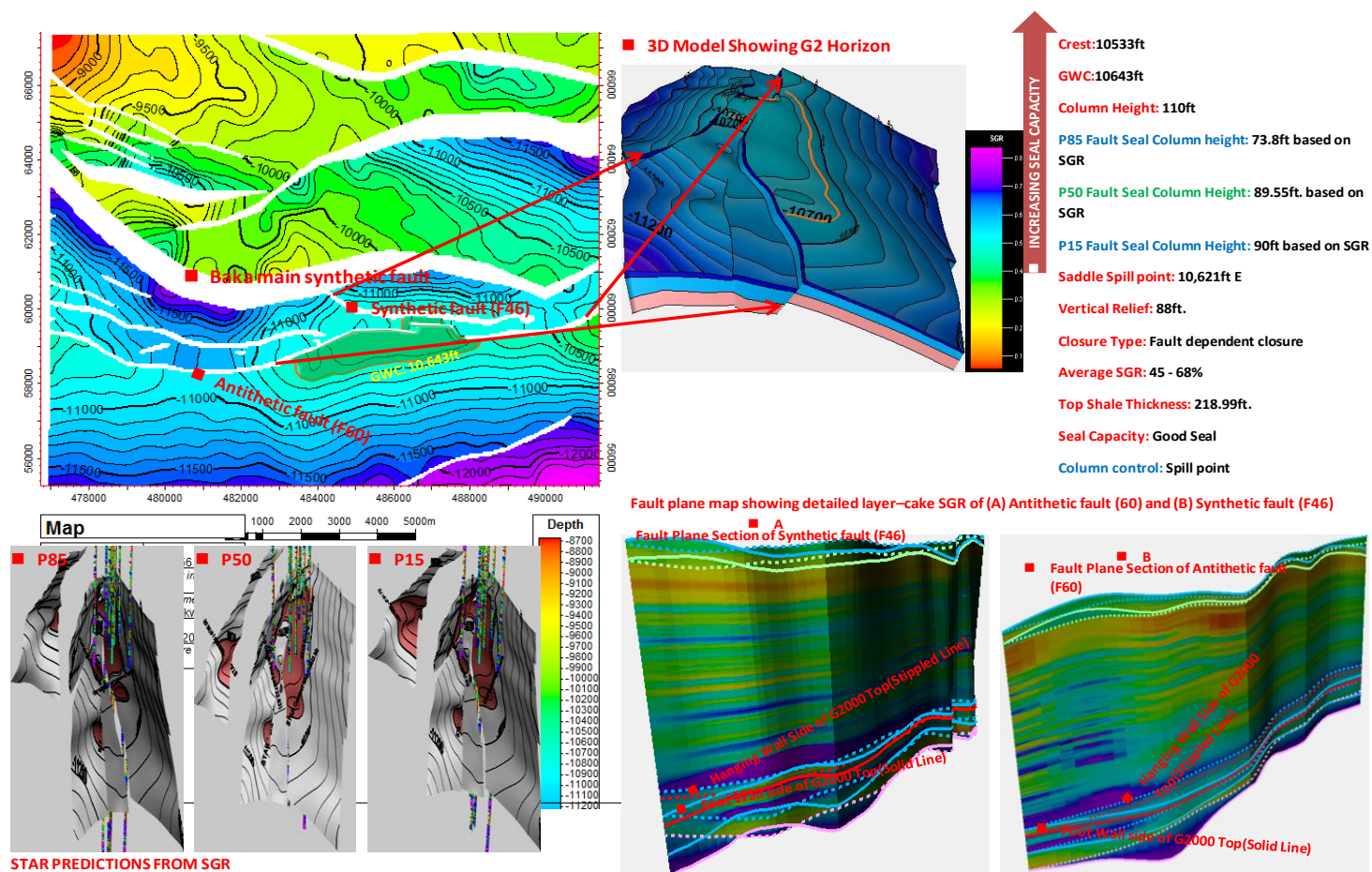
Figure 4.9.1: Detailed Result of G9000 Fault Seal Analysis and known Field Column Height

Figure 4.9.2: P85 Oil Column Height Predicted by Stochastic Trap Analysis at G9000 Reservoir

4.10   Horizon H7100 (Full To Spill Fault Dependent Closure Oil Reservoir)

The H7100 oil bearing reservoir is a full to spill fault dependent closure with faulted crest anticline. This reservoir is filled to the maximum capacity at the structural saddle spill point and as such oil will start migrating to a nearby reservoir if further charged by the source rock. The reservoir crest is at 12,408ft and the oil water contact is at 12,645ft. The oil column height measured from field evaluation is 237ft. Fault seal prediction based on stochastic trap analysis and risking using shale gouge ratio algorithm indicates that the reservoir faults (synthetic fault-F46, antithetic fault-F60 and Baka boundary fault) is capable of sealing and sustaining an oil column height of 268.83ft. The shale gouge ratio at the three faults varies, ranging from 62 – 67% SGR in F46, 51 – 66% in F60 and 45 – 73% at the Baka boundary fault. The three faults of this reservoir has good fault seal capacities with F46 and F60 in the exploration medium class of SGR and the boundary fault within the medium to high SGR classification based on exploration scale. No fault leak points were encountered in any of the three faults. The oil column height control in this reservoir is the structural saddle spill point at about 12,650ft depth.

H7100 (FULL TO SPILL OIL RESERVOIR)

Synthetic fault (F46)

Antithetic fault (F60)

Baka main synthetic fault

Synthetic fault (F46)

Antithetic fault (F60)

OWC: 12645ft

Awoba main synthetic fault

Foot Wall side of H7100 Top(Solid Sky-Blue Line)
Hanging Wall Side of H7100 Top(Stippled Sky-Blue Line)

Map

Country	Scale 1:97656

1:97656

P85   P50   P15

STAR PREDICTIONS FROM SGR

Depth

SGR

INCREASING SEAL CAPACITY

Crest: 12408ft

OWC: 12645ft

Column Height: 237ft.

P85 Fault Seal Column Height: 100.83ft. Based on SGR

P50 Fault Seal Column Height: 268.83ft. Based on SGR

P15 Fault Seal Column Height: 487.12ft. Based on SGR

Spill point: Full to Spill (12650ft)

Vertical Relief: 242ft

Average SGR: 62-67% in F46, 51-66% in F60 and 45 – 73% at boundary fault

Top Shale Thickness: 108.455ft

Seal Capacity: Good

Column Control: Spill point

Fault Plane Section of Synthetic fault (F46)

Fault Plane Section of Antithetic fault (F60)

Figure 4.10.1: Detailed Result of H7100 Fault Seal Analysis and known Field Column Height

149

P50 SGR Prediction at H7100
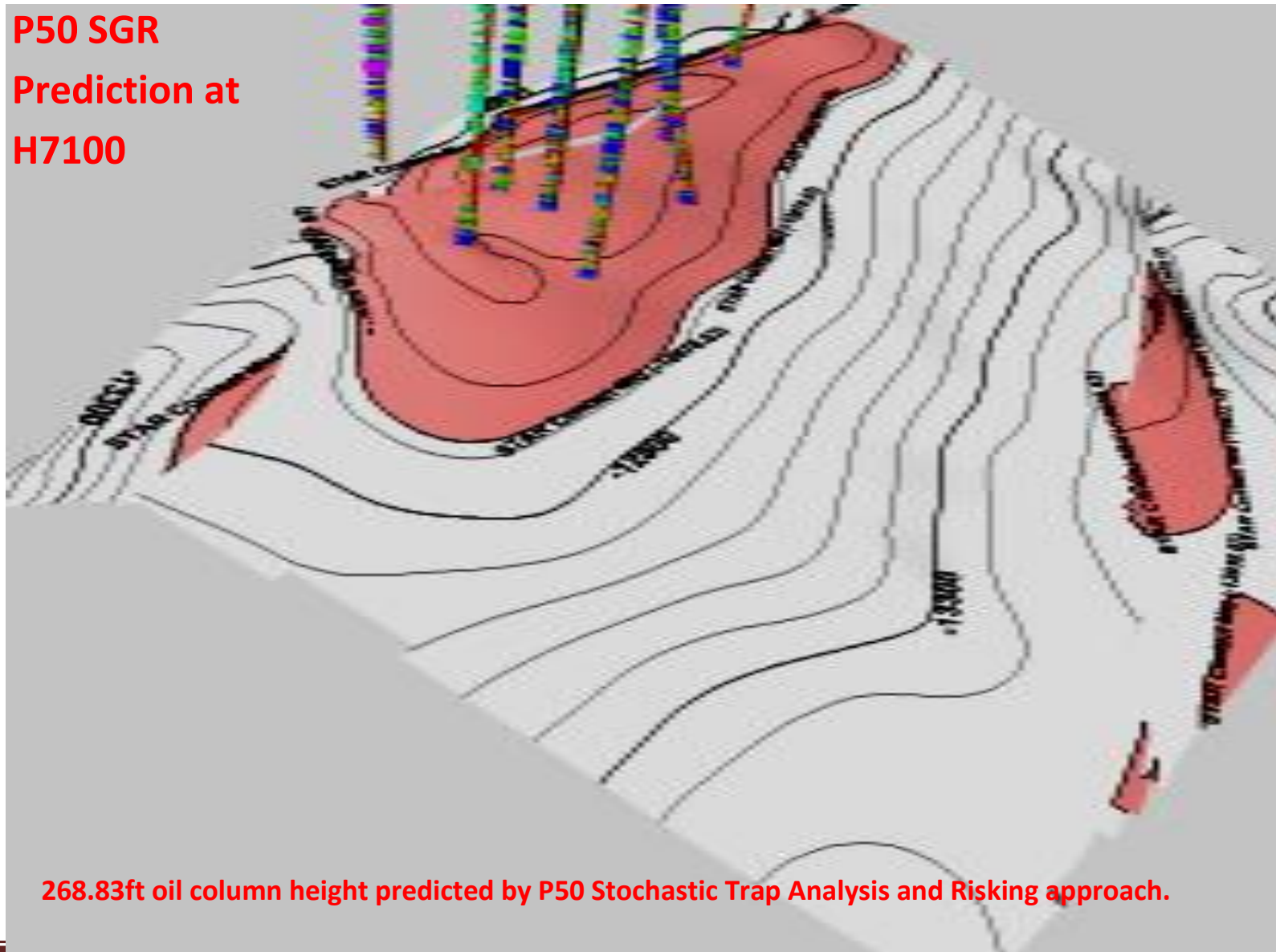
268.83ft oil column height predicted by P50 Stochastic Trap Analysis and Risking approach.

Figure 4.10.2: P50 Oil Column Height Predicted by Stochastic Trap Analysis at H7100 Reservoir

4.11 Horizon H8000 (Under Filled Fault / Dip Dependent Closure Oil Reservoir)

H8000 reservoir is an under-filled fault/dip dependent closure in a faulted anticlinal reservoir. The reservoir crestal position is at 12,780ft with oil water contact at 13,039ft. Field evaluation indicates that this reservoir is capable of having an oil column height of 259ft. The reservoir spill point is at a depth of 13,190ft west of the reservoir. Considering the reservoir vertical relief and the oil in the reservoir, it is evident that this reservoir had leaked away oil from the reservoir. Indication from a stochastic fault seal analysis and risking using shale gouge ratio showed that the boundary fault could seal up to a column height of 290.57ft at P85. The antithetic fault F60 has low fault seal capacity and leaks away oil from the reservoir at about 19.1% SGR; that is at and near F60 connection with the boundary fault and as such fault F60 is termed a conduit at this reservoir level. The oil column control in this reservoir is the fault leak.

H8000 (UNDER FILLED RESERVOIR)

Baka main synthetic fault

Anthetic fault (F60)

OWC: 13,029ft

Awoba main synthetic fault plane

Foot Wall side of H8000 Top(Solid Sky-Blue Line)

Hanging Wall Side of H8000 Top(Stippled Sky-Blue Line)

Antithetic fault (F60)

Map

| Country | Scale 1:97656 | 1:97656 |

P85 P50 P15

SGR

INCREASING SEAL CAPACITY

Depth

STAR PREDICTIONS FROM SGR

Crest: 12780ft

OWC: 13039ft

Column Height: 259ft

P85 Fault Seal Column Height: 230.28ft. Based on SGR

P50 Fault Seal Column Height: 230.28ft. Based on SGR

P15 Fault Seal Column Height: 230.28ft. Based on SGR

Spill point: 13,190ft W.

Vertical Relief: 410ft.

Average SGR: 19.1 – 69%

Leak Points: <20% SGR at Fault F60

Top Shale Thickness: 50.75ft

Seal Capacity: Low – Medium

Column Control: Fault Leak

Figure 4.11.1: Detailed Result of H8000 Fault Seal Analysis and Known Field Column Height

152

P85 SGR Prediction at H8000

230.28ft oil column height predicted by P85 Stochastic Trap Analysis and Risking approach.
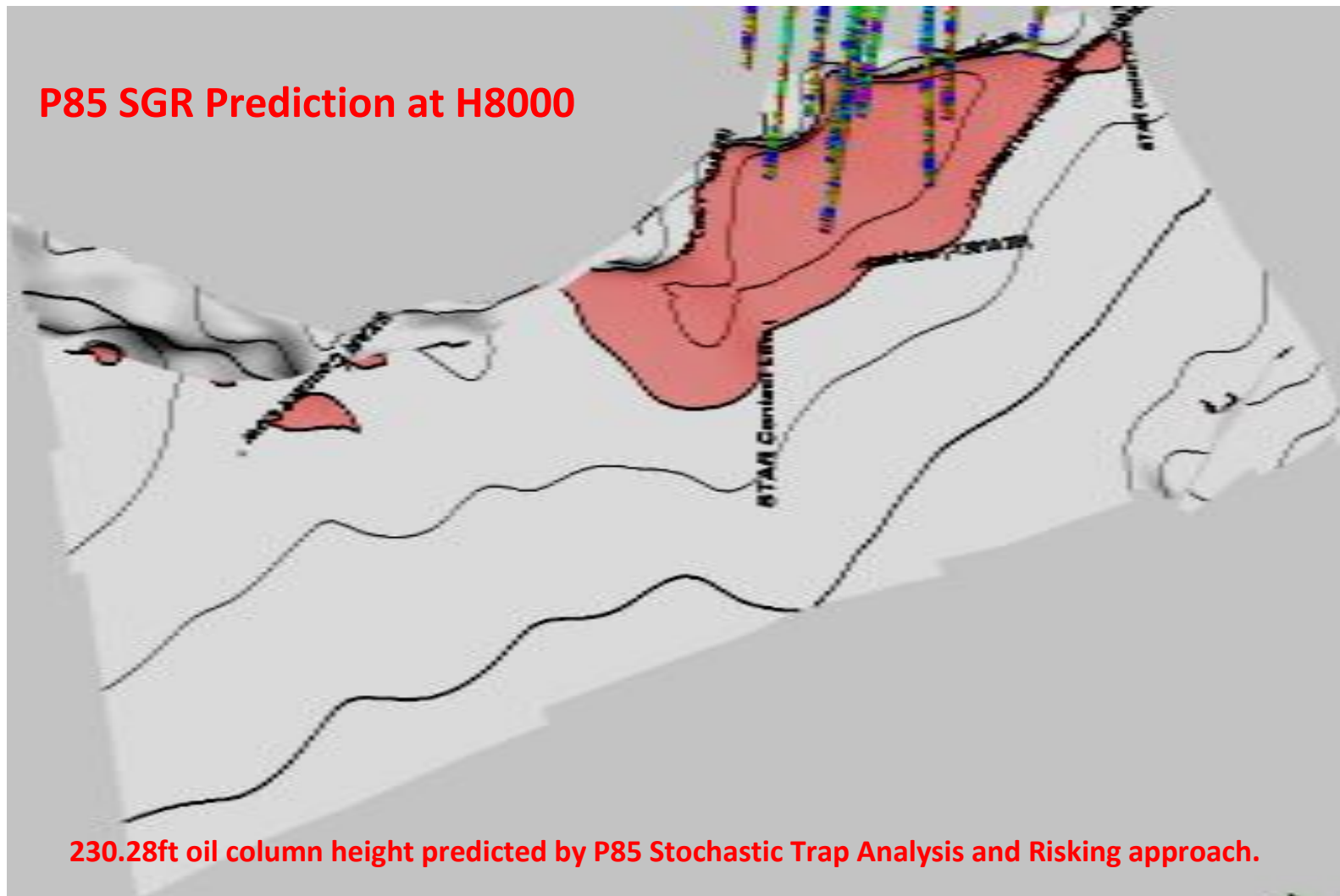
Figure 4.11.2: P85 Oil Column Height Predicted by Stochastic Trap Analysis at H8000 Reservoir

4.12   Interpretations of Gas Reservoirs

4.12.1 Horizon G2000 (Under Filled Fault Dependent Closure Gas Reservoir)

The G2000 reservoir is a full to spill fault dependent closure oil reservoir. The reservoir crestal position is at a depth value of 10,533ft and the gas water contact depth at 10,643ft. Field observation indicates a gas column height of 110ft in the reservoir. The faults shale gouge ratio's indicates that the faults of this reservoir could seal up to a gas column height of 89.55ft at P50 based on stochastic SGR approach. The observed field gas column height and the predicted fault seal gas column height showed high degree of conformity. The shale gouge ratio as predicted by the hanging wall and foot wall stratigraphic juxtaposition of the faults range from 45 – 68%SGR (within medium SGR class based on exploration SGR classification). Both faults F46 and F60 have good seal capacity at G2000 level. The gas column height control in this reservoir is the structural saddle spill point.

G2000 (FULL TO SPILL RESERVOIR)

- **3D Model Showing G2 Horizon**

- **Baka main synthetic fault**
- **Synthetic fault (F46)**
- **Antithetic fault (F60)**
- GWC:10,643ft

Crest:10533ft

GWC:10643ft

Column Height: 110ft

P85 Fault Seal Column height: 73.8ft based on SGR

P50 Fault Seal Column Height: 89.55ft. based on SGR

P15 Fault Seal Column Height: 90ft based on SGR

Saddle Spill point: 10,621ft E

Vertical Relief: 88ft.

Closure Type: Fault dependent closure

Average SGR: 45 - 68%

Top Shale Thickness: 218.99ft.

Seal Capacity: Good Seal

Column control: Spill point

Map

- P85
- P50
- P15

STAR PREDICTIONS FROM SGR

Fault plane map showing detailed layer–cake SGR of (A) Antithetic fault (60) and (B) Synthetic fault (F46)

- A
- **Fault Plane Section of Synthetic fault (F46)**

- B
- **Fault Plane Section of Antithetic fault (F60)**

Figure 4.12.1: Detailed Result of G2000 Fault Seal Analysis and Known Field Column Height

P50 SGR Prediction at G2000

89.55ft Gas column height predicted by P50 Stochastic Trap Analysis and Risking approach.
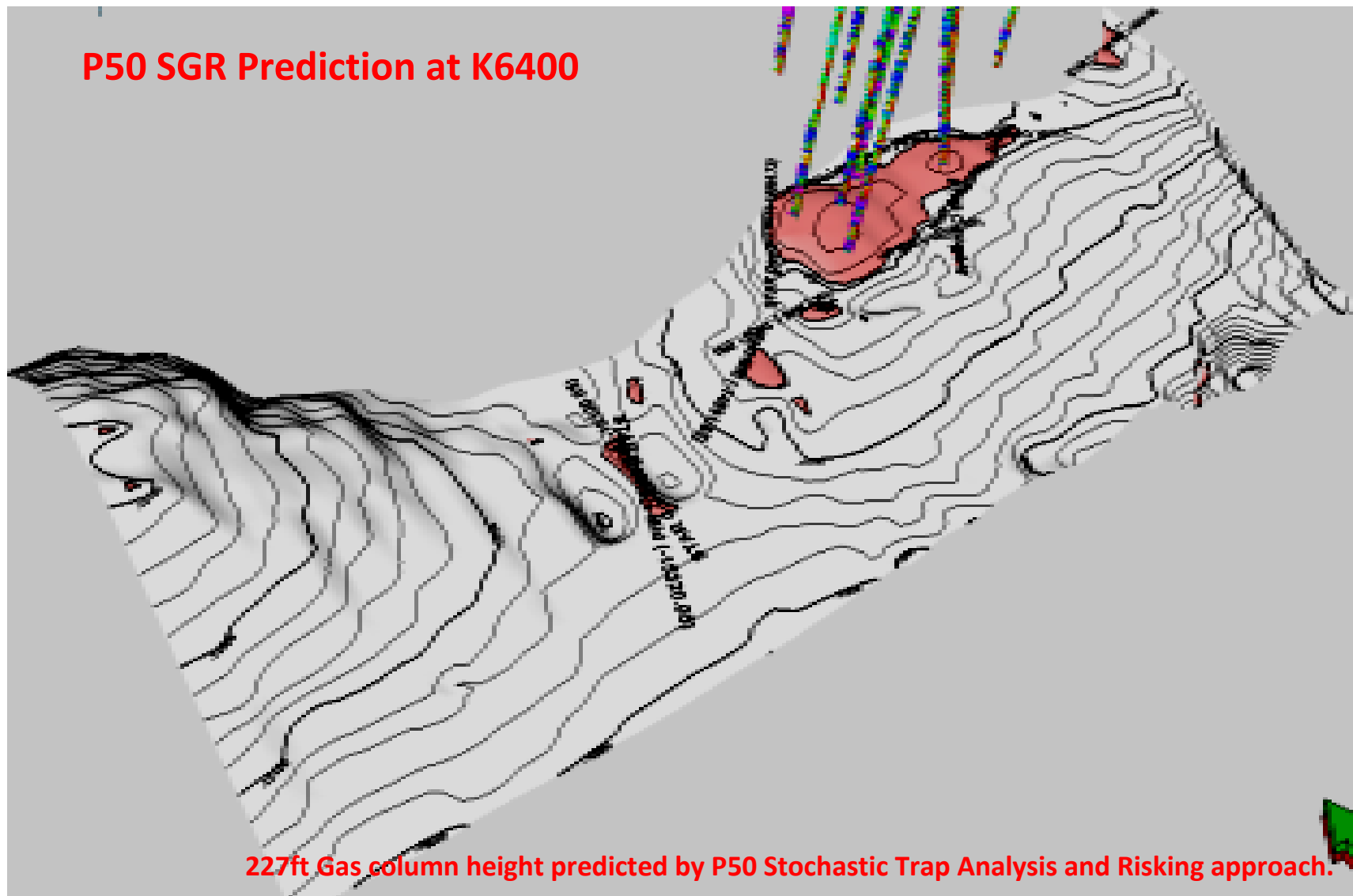
Figure 4.12.2: P50 Gas Column Height Predicted by Stochastic Trap Analysis at G2000 Reservoir

156

4.13 Horizon K2000 (Full to Spill Fault Dependent Closure Gas Reservoir)

The K2000 reservoir is a full to spill fault dependent closure gas reservoir. The reservoir crestal position is at 13,301ft with gas-water contact at a depth of 13,535ft. The gas column height from field observation is 234ft filling entirely the reservoir vertical relief. The stochastic trap analysis and risking approach using shale gouge ratio indicates that the Baka boundary fault at this reservoir level is capable of sealing a gas column height of 170.08ft. Both the observed field column height and the fault seal column height showed some degree of conformity at P50. The Baka boundary fault at this level has good seal capacity with no indication of any leak points. The hanging wall and foot wall stratigraphic juxtaposition of the fault surface at this reservoir level, range from 45 – 77% SGR (medium – high SGR class based on exploration SGR classification).
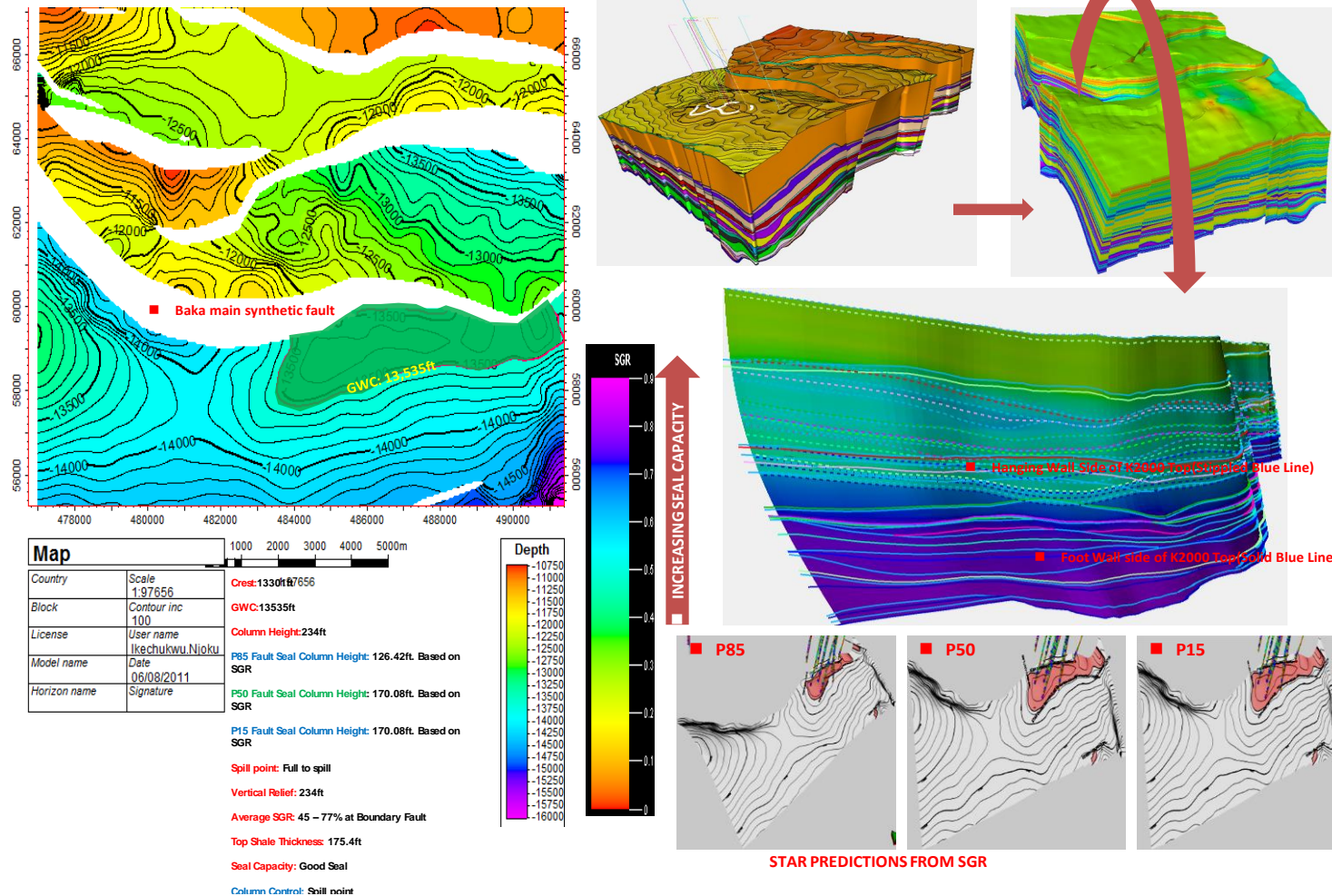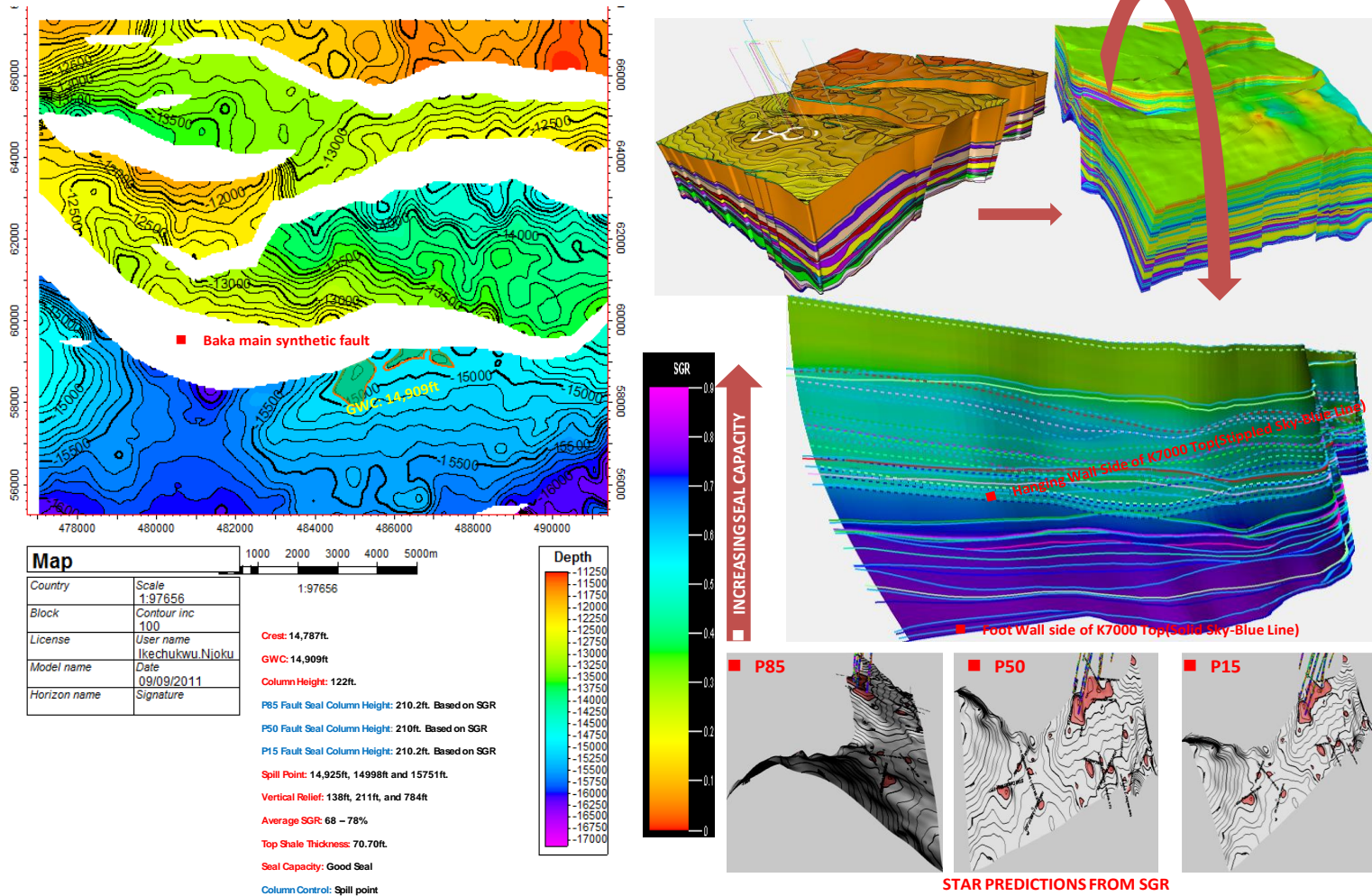
Figure 4.13.1: Detailed Result of K2000 Fault Seal Analysis and Known Field Column Height
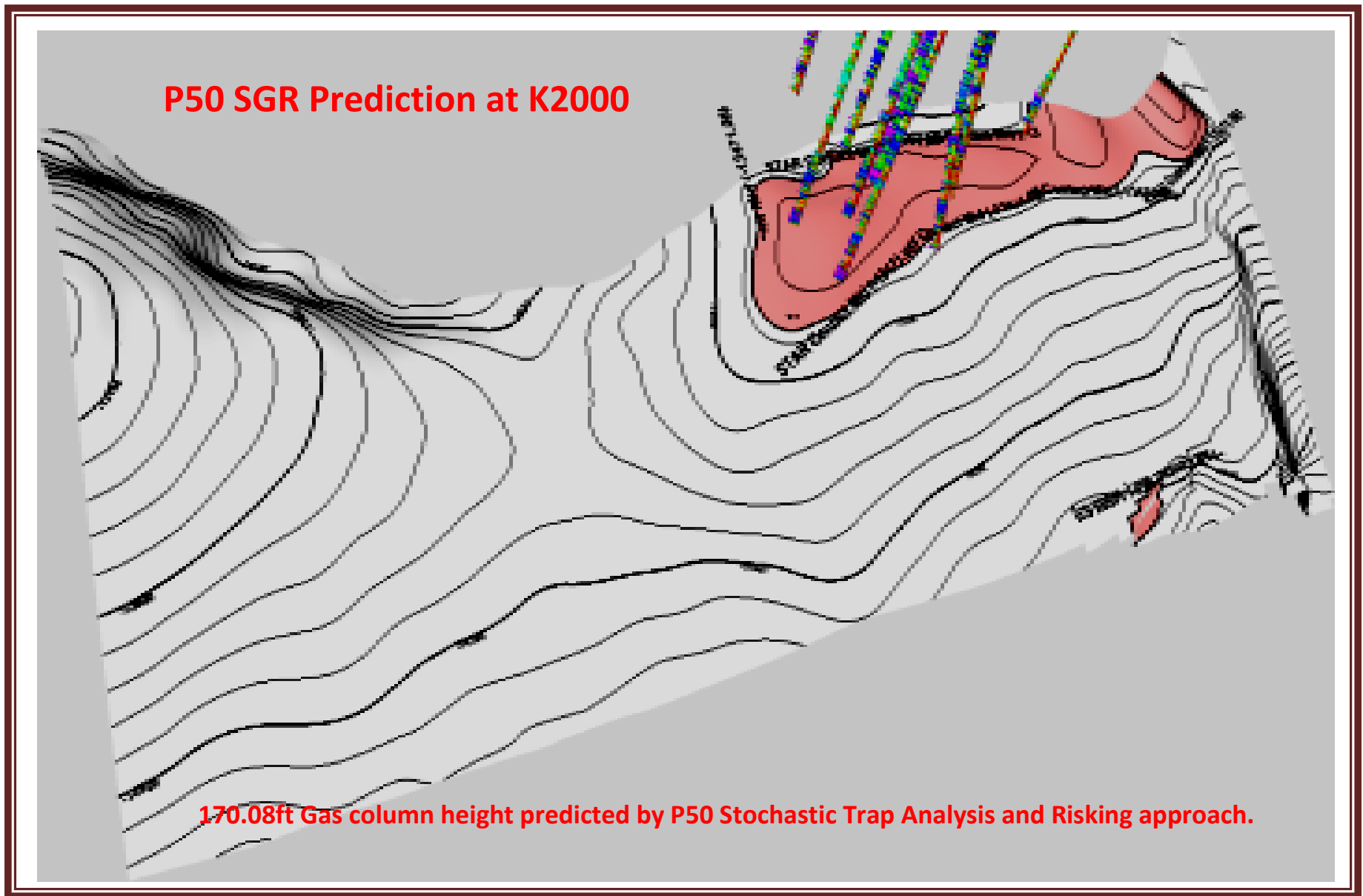
Figure 4.13.2: P50 Gas Column Height Predicted by Stochastic Trap Analysis at K2000 reservoir

4.14 Horizon K3200 (Filled below dip closure, fault Dependent Closure Gas Reservoir)

The K3200 reservoir is an over filled fault dependent closure gas reservoir. Based on field evaluation, this reservoir is said to be over-filled in this study (having column below structural closure) with gas-water contact depth of 13,974ft and reservoir crestal position of 13,733ft depth. The field gas column height at this reservoir level is about 241ft filling below the lowest structural point that defined the trap. This is termed impossible occurrence in this study and it is advised that the fluid contact value at this reservoir level should be revisited. Also, fluid contacts delineated using porosity logs and the resistivity logs will have to be quality checked and edited. The fault shale gouge ratio based on stochastic fault seal analysis predicted that the hanging wall and foot wall stratigraphic juxtaposition at the Baka boundary fault is capable of sealing and supporting a column height of 200ft at P50. The Baka boundary fault has 45 – 77% shale gouge ratio at K3200 level (medium – high SGR class based on exploration SGR classification). The fault has good seal capacity at this reservoir and the gas column height control in this reservoir is the structural saddle spill point.

K3200: ABOVE SPILL POINT (COLUMNS BELOW DIP CLOSURE)

Baka main synthetic fault

Crest: 13733ft

GWC: 13974ft

Column height: 241ft.

P85 Fault Seal Column Height: 200ft. Based on SGR

P50 Fault Seal Column Height: 200ft. Based on SGR

P15 Fault Seal Column Height: 200ft. Based on SGR

Spill Point: (13,935ft)

Vertical Relief: 202ft

Average SGR: 45 -77%

Top Shale Thickness: 38.13ft.

Seal Capacity: Good Seal

Column Control:

Map	
Country	Scale 1:97656
Block	Contour inc 100
License	User name Ikechukwu.Njoku
Model name	Date 06/08/2011
Horizon name	Signature

INCREASING SEAL CAPACITY

Hanging Wall Side of K3200 Top(Stippled Sky-Blue Line)

Foot Wall side of K3200 Top(Solid Sky-Blue Line)

P85   P50   P15

STAR PREDICTIONS FROM SGR

Figure 4.14.1: Detailed Result of K3200 Fault Seal Analysis and known Field Column Height

P50 SGR Prediction at K3200

200ft Gas column height predicted by P50 Stochastic Trap Analysis and Risking approach.
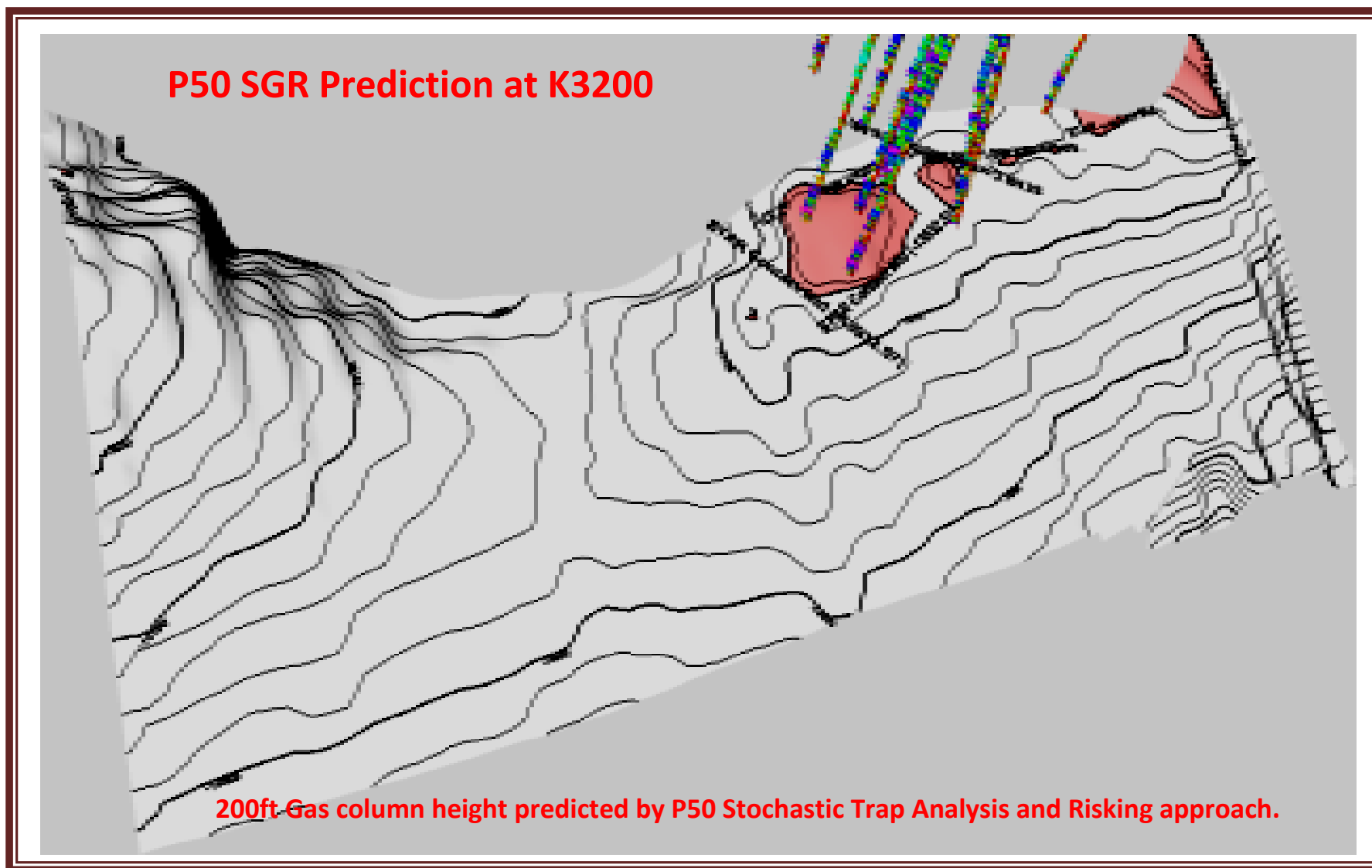
Figure 4.14.2: P50 Gas Column Height Predicted by Stochastic Trap Analysis at K3200 Reservoir

4.15 Horizon K5000 (Full to Spill fault Dependent Closure Gas Reservoir)

The K5000 reservoir is a full to spill fault dependent closure gas reservoir that had spilled gas within the reservoir. Observation from the field indicates that the gas column height in the reservoir is 166ft, filling almost the entirety of the reservoir's vertical relief (179ft). The crest of the reservoir is at 14,136ft and the gas water contact is at a depth of 14,302ft. Prediction from a stochastic trap analysis and risking approach using shale gouge ratio showed that the Baka boundary fault at K5000 level is capable of sealing and sustaining a column height of 216.15ft at P50. The shale gouge ratio of the Baka boundary fault at K5000 horizon; range from 46 – 80% SGR (medium – high SGR class, based on exploration SGR classification). The gas column height control in K5000 reservoir is the structural saddle spill point.

K5000 (SPILL WITHIN RESERVOIR) – AT SHALLOW SPILL POINTS

Map	
Country	Scale 1:97656
Block	Contour inc 100
License	User name Ikechukwu.Njoku
Model name	Date 06/08/2011
Horizon name	Signature

1000 2000 3000 4000 5000m

1:97656

Crest: 14,136ft & 14,112ft

GWC: 14,302ft

Column Height: 166ft

P85 fault Seal Column Height: 216ft. Based on SGR

P50 Fault Seal Column Height: 216ft. Based on SGR

P15 Fault Seal Column Height: 216.15ft. Based on SGR

Spill Point: 14,315ft Shallow,14,355ft Shallow, 14645ft.

Vertical Relief: 179ft.

Average SGR: 46 – 80%

Top Shale Thickness: 50.69

Seal Capacity: Good Seal

Column Control: Spill point

Baka main synthetic fault

GWC: 14,302ft

INCREASING SEAL CAPACITY

Hanging Wall Side of K5000 Top(Stippled Sky Blue Line)

Foot Wall side of K5000 Top(Solid Sky Blue Line)

P85   P50   P15

STAR PREDICTIONS FROM SGR

Figure 4.15.1: Detailed Result of K5000 Fault Seal Analysis and Known Field Column Height

P50 SGR Prediction at K5000

216.15ft Gas column height predicted by P50 Stochastic Trap Analysis and Risking approach.
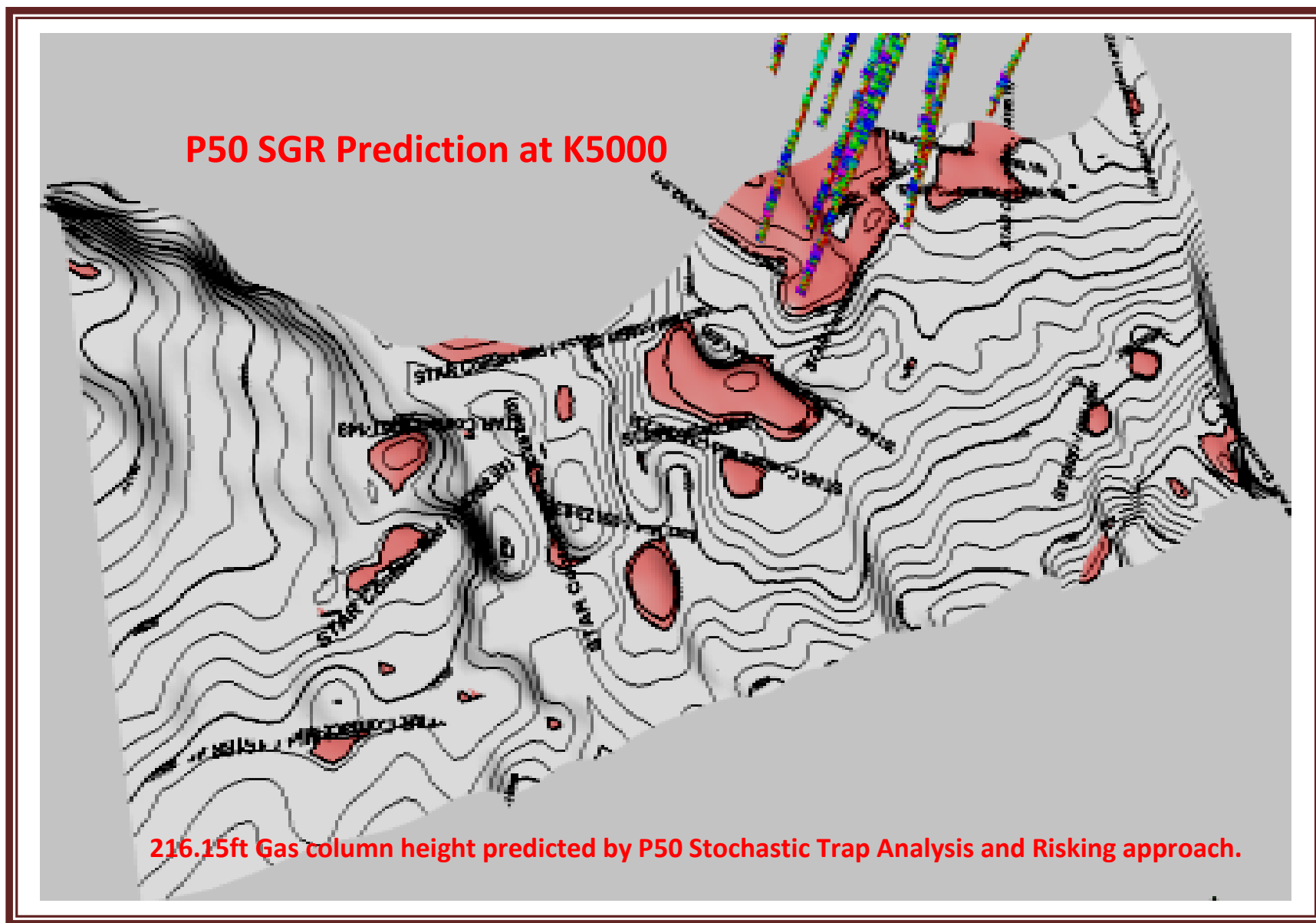
Figure 4.15.2: P50 Gas Column Height Predicted by Stochastic Trap Analysis at K5000 Reservoir

4.16   Horizon K6400: Above Spill Point – Column Below Dip Closure (Fault Dependent Gas Reservoir)

The K6400 reservoir is a fault dependent closure gas reservoir. Observation from field evaluation showed that this reservoir is gas filled below structural closure (? 408ft gas column height). It is recommended that fluid contact at the K6400 reservoir be re-visited. The reservoir crest is at 14,322ft and gas water contact depth at 14,730ft. A stochastic trap analysis and risking approach using shale gouge ratio as the seal attribute predicted that the Baka boundary fault is capable of sealing and sustaining a gas column height of 227ft at P50. The shale gouge ratio of the hanging wall and foot wall stratigraphic juxtaposition range from 45 – 80% SGR (medium – high SGR class based on exploration SGR classification). The boundary fault at K6400 level has good seal capacity with no indication of any leak points. The column control in K6400 reservoir is the structural saddle spill point.

K6400: ABOVE SPILL POINT (COLUMNS BELOW DIP CLOSURE)
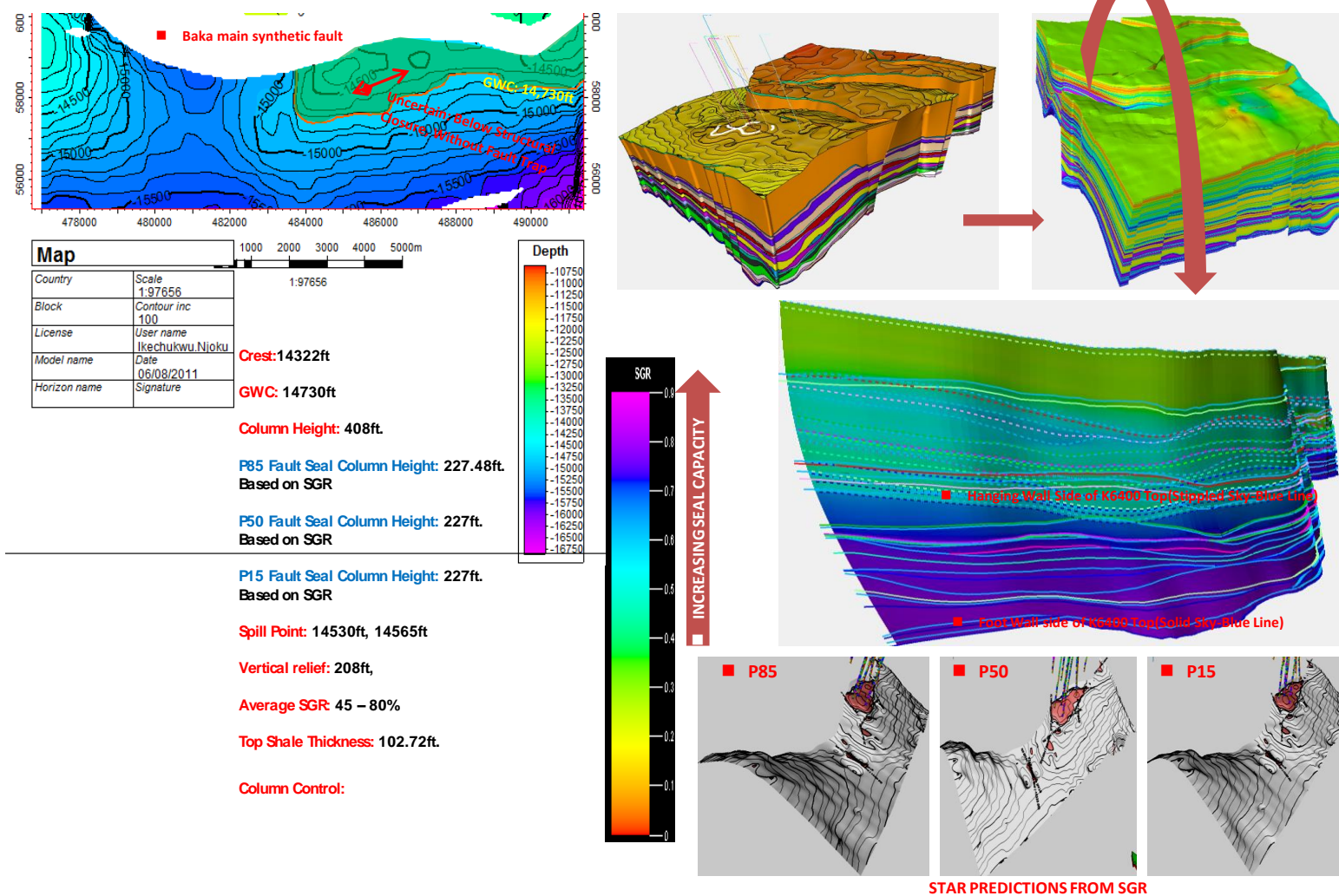
Figure 4.16.1: Detailed Result of K6400 Fault Seal Analysis and Known Field Column Height

Figure 4.16.2: P50 Gas Column Height Predicted by Stochastic Trap analysis at K6400 reservoir

4.17 Horizon K7000 (Full to Spill Fault Dependent Closure Gas Reservoir)

The K7000 reservoir is a full to spill fault dependent anticlinal reservoir. The reservoir crestal position is at 14,787ft and the gas water contact is at 14,909ft depth. Observation from field evaluation showed a gas column height of 122ft filling almost the entirety of the vertical relief. A stochastic fault seal analysis and risking approach using shale gouge ratio as the seal parameter predicted that a gas column height of 210ft is trapped at P50. The average shale gouge ratio of the boundary fault at K7000 horizon; range from 68 – 78% SGR (high SGR class based on exploration SGR classification). The boundary fault at K7000 level has good seal capacity with no indication of any fault leak points. The column height control in the K7000 reservoir is the structural saddle spill point.

Figure 4.17.1: Detailed Result of K7000 Fault Seal Analysis and known Field Column Height

P50 SGR Prediction at K7000

210ft Gas column height predicted by P50 Stochastic Trap Analysis and Risking approach.
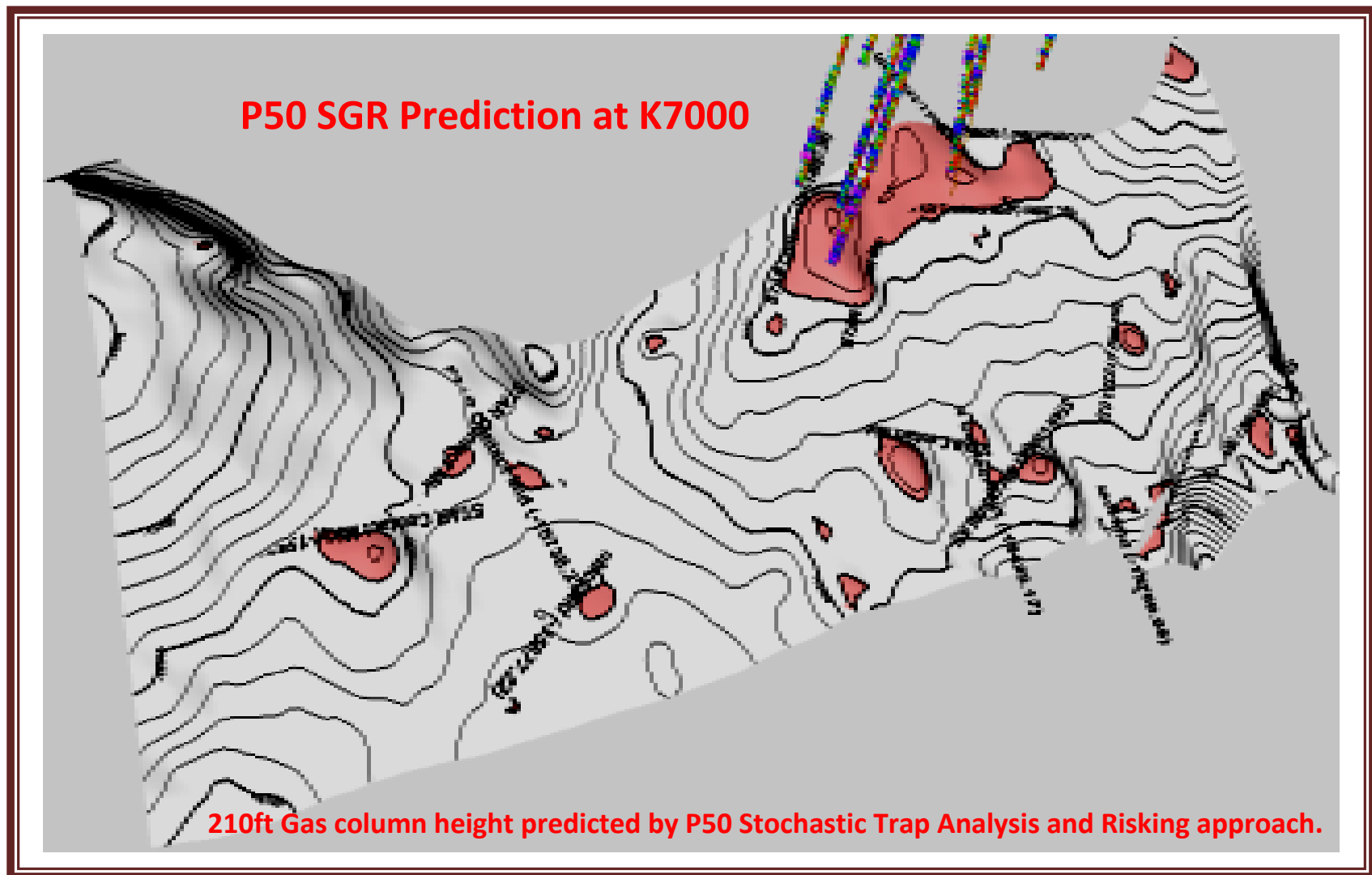
Figure 4.17.2: P50 Gas Column Height Predicted by Stochastic Trap Analysis at K7000 Reservoir

4.18 Column Heights Conditions in Baka Field

Table 4.18.1 Column Heights Distributions in Baka Field

Mapped Levels for Oil reservoirs	Full to Spill	Underfilled	Overfilled
F1000		■	
G4000		■	
G6000	■		
G8000	■		
G9000		■	
H7100	■		
H8000		■	
Mapped Levels for Gas reservoirs			
G2000	■		
K2000	■		
K3200			■
K5000	■		
K6400			■
K7000	■		

- **Full to Spill Reservoir in the studied Baka Field (G6000, G8000, H7100 Oil Reservoir and G2000, K2000, K5000, and K7000 Gas Reservoir):** Good Fault Seal Capacity with generally >40% Average SGR. The higher shale gouge ratio here are mainly due to the non-reservoir rocks juxtaposing reservoir rocks. This influenced the across fault pressure difference leading to the higher capillary entry pressure relative to reservoir fluid buoyancy pressure.

- **Under-Filled Reservoir in the studied Baka Field (F1000, G4000, G8000, G9000, and H8000 Reservoirs):** Generally due to fault leak points at <20%

average shale gouge ratio within the fault surface and its attributed to sand on sand juxtaposition.

- **Over-Filled Reservoir (K3200 and K6400):** Impossible occurrence (it is recommended that fluid contacts at these reservoir levels be re-visited.

Also, overlying shale thicknesses of all the studied reservoir sand were analyzed relative to the hydrocarbon column height (figure 4.3.1) and these showed that top seal played a role (impeded up-dip hydrocarbon migration). However, is paramount to note that top seal in the Baka Field is not a major factor regarding hydrocarbon column height control. This simply means that in as much as the up-dip hydrocarbon is being impeded by the top seal in the studied field, the thicker shale top seal sequences are never indicative of higher hydrocarbon columns in the study area. The study area with evidences of mixed clastic heterogeneous fault zone properties as attributed to variable shale gouge ratio showed evidences of fault controls (both sealing and leaking) - supported with structural saddle spill points.
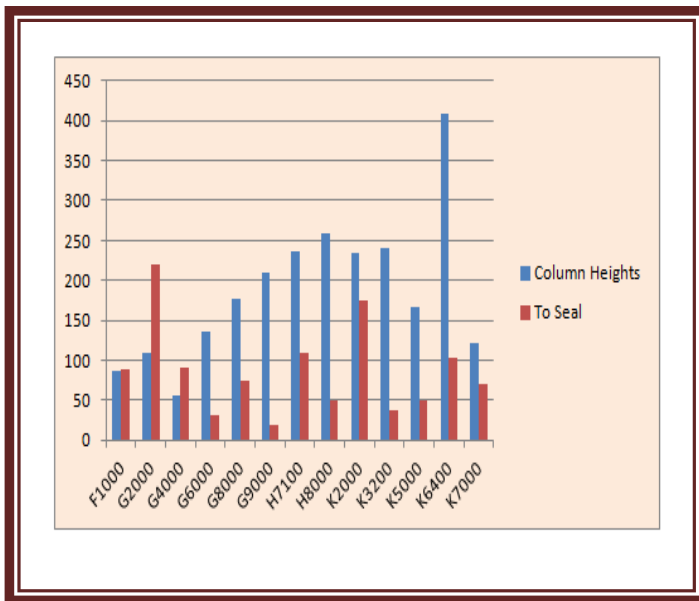
Figure 4.18.1: Field Column Heights Distributions versus Top Shale Thickness in Baka Field

4.19 Field Column Heights Calibration with Fault Seal Column Height in Baka Field
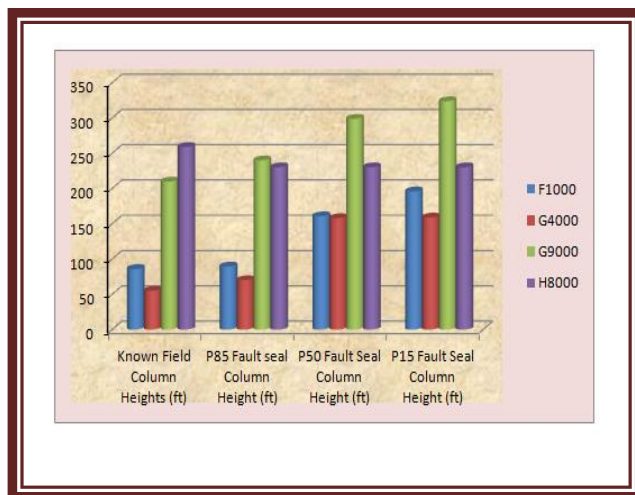
Figure 4.19.1 Field Column Height versus Fault Seal Column Height at Under-Filled Reservoir

174
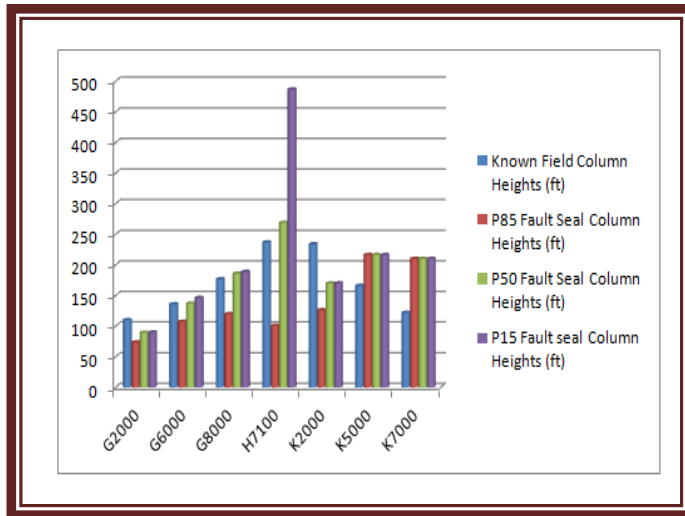
Figure 4.19.2 Field Column Height versus Fault Seal Column Height at Full to Spill Reservoir

- The field column height showed high degree of conformity with P85 fault seal column height predicted by shale gouge ratio at the under-filled reservoirs.

- At the full to spill reservoir, the field column height showed high degree of conformity with P50 fault seal column height predicted by shale gouge ratio.

All the interpreted results as shown previously in chapter four are summarized in tables 4.19.2 and 4.19.3. Also the exploration SGR classifications is shown in figure 4.9.4 which showed high degree of conformity with the present study.

Table 4.19.2 Detailed Result of Under-filled Reservoir Fault Seal Analysis

Horizon	Crest (ft)	Known Field Column Height (ft)	P85 Fault Seal Column Height (ft)	P50 Fault Seal Column Height (ft)	P15 Fault Seal Column Height (ft)	Average SGR	Exploration SGR Class
F1000	8,258	86	89.42	160.83	196	16 - 38.7	Low
G4000	10,784	55	70.06	158	159	14.5 - 39	Low
G9000	12,087	210	240.05	299	323.94	17.3 - 70	Low - Medium
H8000	12,780	259	230.28	230.28	230.28	19.1 - 69	Low - Medium

Table 4.19.3 Detailed Result of Full to Spill Reservoir Fault Seal Analysis

Horizon	Crest (ft)	Known Field Column Height (ft)	P85 Fault Seal Column Height (ft)	P50 Fault Seal Column Height (ft)	P15 Fault Seal Column Height (ft)	Average SGR (%)	Exploration SGR Class
G2000	10,533	110	73.8	89.55	90	45 - 68	Medium
G6000	11,271	136	107.43	137	146.27	45 - 51	Medium
G8000	11,891	177	119.79	186	188.91	41 - 52	Medium
H7100	12,408	237	100.83	268.83	487.12	62 - 67	Medium
K2000	13,301	234	126.42	170.08	170.08	45 - 77	Medium - High
K5000	14,136	166	216.51	216.51	216.51	46 - 80	Medium - High
K7000	14,787	122	210.2	210.2	210.2	68 - 78	Medium - High

Table 4.19.4: Exploration SGR Classification

Low	Medium	High
0.0 0.4	0.4 - 0.7	0.7 - 1.0
Mean Column: 59ft	Mean Column: 102ft	Mean Column: 160ft
Max Column: 250ft	Max Column: 450ft	Max Column: 600ft

Chapter Five: Conclusion and Recommendation

5.1   Summary

Fault seal analysis is an integral part of petroleum studies that give high degree of certainty of the occurrence, accumulation and trapping of hydrocarbon which gives credence to early and accurate decision making. The applied perspective reduces the risk of drilling of many wells and thereby saves cost of drilling dry holes.

5.2   Conclusions

Baka reservoirs are fault dependent closure reservoirs. The Hydrocarbon column heights in the Baka Field are mostly controlled by spill points. Shale Gouge Ratio of the Baka faults generally matched with the Shale Gouge Ratio related column height distribution, used in exploration. Top seal (top shale thickness) played a role (impeded vertical up-dip migration). However, top seal is not a major factor as regards to column control in the studied field.

Through this method, it is now note worthy that fault seal analysis application is of paramount value in any reservoir study and it is easy to apply as well as cost effective.

5.3   Prospect Applications:

Faults in the Baka Field generally leaks at <20% Shale Gouge Ratio.

Weak points on faults in the Baka field varies; mainly 20 – 35% and more. Good

fault seal in the Baka Field generally exist at >40% Shale Gouge Ratio. Low Fault

seal in the Baka Field range between <40% - ≥20% Shale Gouge Ratio and mostly

associated with leak points.

Shale Gouge Ratio is greater at the Baka boundary fault and – good seal capacity.

The approach used in this study can be applied in other fields and as such of great

value to uncertainty reduction and risk mitigation.

5.4   Recommendation:

It is recommended from this integrated fault seal studies that any reliable and

efficient reservoir studies should deem it necessary to incorporate fault seal

analysis for efficient sealing component predictions and realistic fluid

estimations. Also, it is advised that the applied approach from this study should

remain the top priority in any reservoir risk assessment to save cost due to

money lost in drilling dry wells.

5.5   Contribution to knowledge:

This study reduces the incidence of drilling of dry holes as better understanding of the reservoirs and their capacity to harbor hydrocarbon is achieved thereby saving money worth millions of US dollars.

Fault Seal as used in this study answers the question of how many wells are needed to extract the hydrocarbon and which of the reservoirs is to be targeted as well as providing better information where directional well(s) should be penetrated.

The Fault Seal analysis as seen in this study enabled us to understand the major control on hydrocarbon distribution and accumulation in the Baka Field and this study can be carried out in other oil fields in any part of the world.

This study has provided us with basis for risking undrilled fault dependent prospects with high degree of confidence.

Its model provides a replication of the hydrocarbon condition in a trap.

It provides a means for conducting sensitivity analysis and therefore leads to improved prospect risking.

Fault seal workflow allows rapid assessment of the value of exploration prospects with a high probability of compartmentalization and informed decisions to be taken at an early stage.

It provides information on hydrocarbon column height that could support against fault and what expected volume the oil industry might have.

The study of fault seal in the Baka Field has improved hydrocarbon recovery efficiency in the field as the hydrocarbon accumulation and seal integrity of the faults were determined as shown in chapter four and this gives direct clue for its applicability in other oil fields of the world.

REFERENCES CITED

Alan M., David A. F., and Brent D. H ., 2013. Slip-tendency analysis and fault

   reactivation. Introduction to American Association of Petroleum Geologists

   Bulletin thematic issue on fault seals. V.3, no. 4, p. 41 - 46.

Allan, U. S., 1989. Model for hydrocarbon migration and entrapment within

   faulted structures. American Association of Petroleum Geologists Bulletin,

   v. 73, p. 803-811.

An, L. Y., 2009. Paleochannel sands as conduits for hydrocarbon leakage across

   faults: An example from the Wilmington oil field, California. American

   Association of Petroleum Geologists Bulletin, v. 93, no. 10, p. 1263-1279.

Bashir, A. K., Atilia, A., and Eric, E., 2003. A new process-based methodology for

   analysis of Shale Smear along normal faults in the Niger Delta. V.87, p. 445 -

   463.

Bogdan O., Jan ter H., Brecht W., Mariëlle K., Laura W., and Edésio M.

B., 2013. Analysis of caprocks for CO2 storage- sealing capacity. *Applied R&D organization technology development contract R&D non-routine consulting special tasks (Geological Survey of The Netherlands).* Netherlands Organization for Applied Scientific Research. p1-16.

Bouvier, J. D., Kaars-Sijpesteijin, C. H., Kluesner, D. F., Onyejekwe, C. C., and

Van Der Pal, R. C., 1989. Three-dimensional seismic interpretation and fault sealing investigation, Num River field, Nigeria. American Association of Petroleum Geologists Bulletin, v. 73, p. 1397-1414.

Bretan, P., Yielding, G., and Jones, H., 2003. Using calibrated shale gouge ratio to

estimate hydrocarbon column heights. American Association of Petroleum Geologists Bulletin, v. 87, p. 397-413.

Brown, A., 2003. Capillary effects on fault-fill sealing. American Association of

Petroleum Geologists Bulletin, v. 87, p. 381-395.

Burkel, K. C., 1972. Longshore drift, submarine canyon and submarine fans in

development of Niger delta. In: Reijers, T. J. A., Petters, S. W., and Nwajide,

C. S. The Niger delta basin. Selected chapters on geology. P. 103-117.

Camac1, B. A., Hunt2, P. S., and Boult3, P. J., 2009. Predicting brittle cap-seal

failure of petroleum traps: an application of 2D and 3D distinc element

method. EAGE / Geological Society of London, v. 15. p. 75 -89.

Carol, C.M. and Ejedawe, J. (2012). Nigeria Potential Waiting To Be Tapped. AAPG
Explorer Issue.

Cerveny, K., Davies, R., Dudley, G., Kaufman, P., Knipe, R., and Krantz, B., 2005.

Reducing uncertainty with fault-seal analysis. Oilfield Review, p.38-51.

Childs, C., Sylta[2] Ø., Moriya[1], S., Hermansen[3], D., Strand[1], J., and Walsh[1], J. J.,

2002. The impact of fault seal properties on hydrocarbon migration

modeling of the Oseberg-Syd area, Viking Graben. American Association of

Petroleum Geologists Hedberg Conference, p.1-4.

Clarke, S. M., Burley, S. D., and Williams, G. D., 2005. Dynamic fault seal analysis

and flow pathway modeling in three-dimensional basin models. Petroleum

Geology Conference Series 2005; v.6; p.1275-1288.

Connolly1, D. L., Brouwer1, F., and Walraven2, D., 2008. Detecting fault-related

hydrocarbon migration pathway in seismic data: Implications for fault-seal,

pressure, and charge prediction. Gulf Coast Association of Geological

Societies Transactions, v. 58, p. 191 -203.

Corona, F. V., 2oo5.Fault trap analysis of the Permian Rotliegend gas play,

Lauwerszee trough NE Netherlands. Geological Society, London, Petroleum

Geology Conference, p. 327 – 335.

Cranganu1, C., and Villa1, M. A., 2006. Capillary sealing as an overpressure

mechanism in the Anadarko basin. American Association of Petroleum

Geologists, Search and Discovery article #40187 (2006)

Davies, R. K., An, l., Jones, P., Mathiis, A., and Cornette, C., 2003. Fault-seal

analysis of the South Marsh Island 36 field, Gulf of Mexico. American

Association of Petroleum Geologists Bulletin, v. 87, p. 479-491.

Dee, S. J., Yielding, G., Freeman, B., and Bretan, P., 2007. A comparison between

   deterministic and stochastic fault seal techniques. Geological Society,

   London, Special Publications, v. 292, p. 259-270.

Delle P, C., Olierook, H.K.H., Timms, N.E., Saeedi, A., Esteban, L.,   Razaee,   R.,

   Mikhaltsevitch, V., and Lebedev, M., 2013. Facies-Based Rock Properties

   Distribution Along The Harvey 1 Stratigraphic Well, CSIRO Report Number

   EP133710.

Doughty, P. T., 2003. Clay smear seals and fault sealing potential of an exhumed

   growth fault, Rio Grande rift, New Mexico. American Association of

   Petroleum Geologists Bulletin, v. 87, p. 427-444.

Doust, H., and Omatsola, E., 1990. Niger delta. In: Edwards, J. D., and

   Santogrossi, P. A., eds, Divergent / passive Margin Basins, AAPG Memoir 48:

   Tulsa, American Association of Petroleum Geologists, p. 239-248.

Dutzer[1], J., Basford[2], H., and Purves[2], S., 2006. Investigation of fault seal

   potential through fault relative seismic volume analysis. World Count, v.

   3121, p. 1-16.

Egholm1, D. L., Clausen1, O. R., Sandiford2, M., Kristensen3, M. B., and

Korstgard1, J. A., 2008. The mechanics of clay smearing along faults.

Geological Society of America, v. 36, p. 787-790.

Ehrlich[1, 3] R., Sverdrup[1, 3] E., Øye[2] V., Sjøholm[2] J., Lien[2] K. S., and Færseth[2] 2006.

Quantification and sensitivity of fault seal parameters demonstrated in an

integrated reservoir modeling work flow. A case study on the Njord Field,

Halten Terrace, Norway   Vortrag. TSK 11 Göttingen, p. 1-4.

Eichhubl, P., D'Onfro, P. S., Aydin, A., Waters J., and McCarty, K., 2005.

Strcuctural, petrophysical, and diagenesis of shale entrained along a normal

fault at Black Diamond Mines, California – implications for fault seal.

American Association of Petroleum Geologists Bulletin, v. 89, no. 9, p. 1113-

1137.

Færseth, R. B., 2006. Shale smear along large faults: continuity of smear and the

fault seal capacity. Journal of the Geological Society London, v. 163, p. 741

– 751.

Færseth, R. B., Johnsen, E., and Sperrevik, S., 2007. Methodology for risking fault seal capacity: Implications of fault zone architecture. American Association of Petroleum Geologists Bulletin, v. 91, no. 9, p. 1231-1246.

Filbrandt, J., Naruk, S., Wilkins, S., Dula, F., and Ganz, H., 2007. Fault Seal Analysis using Shale gouge Ratio: Basic principles and guidelines for SGR calibration and column height prediction. SPDC exploration report. p. 1-53.

Fisher, Q. J., and Knipe, R. J., 1998. Fault sealing processes in siliciclastic sediments. In: Dee, S. J., Yielding, G., Freeman, B. and Bretan, P. (2007): A comparison between deterministic and stochastic fault seal techniques. Geological Society, London, Special Publications, v. 292, p. 259-270.

Fisher[1], Q. J., and jolly[2], S. J., 2007. Treatment of faults in production simulation models. In: Jolley, S. J., Barr, D., Walsh, J. J., and Knipe, R. J. (eds) Structurally complex reservoirs. Geological Society, London, Special Publications, v. 292, p. 219 – 233.

Freeman, B., Yielding, G., Needham, D.T., and Badley, M. E., 1998. Fault seal

prediction: the gouge ratio method. Geological Society, London, Special

Publications, v. 127, p. 19-25.

Freeman, S., Harris, S., Knipe, R. J., and Davies, R., 2004. Rapid

approaches to mapping and interpreting fault seal properties within

reservoir modeling packages. Ex. Abs., 19th April, American

Association of Petroleum Geologists, Annual Convention, Dallas.

Freeman, S. R., Harris, S. D., and Knipe, R. J., 2008. Fault seal mapping –

incorporating geometric and property uncertainty. In: Robinson, A.,

Griffiths, P., Price, S., Hegre, J., and Muggeridge, A. (eds) The future of

geological modeling in hydrocarbon development. The Geological Society,

London, Special Publications, v. 309, p. 5 – 38.

Freeman, s. R., Harris, S. D., and Knipe, R. J., 2010. Cross-fault sealing, baffling

and fluid flow in 3D geological models: tools for analysis, visualization and

interpretation. The Geological Society, London, Special Publications, v. 347,

p.2 57 – 282.

Fristad, T., Groth, A., Yielding, G., and Freeman, B., 1996. Quantitative fault seal

prediction – a case study from the Oseberg Syd area. In: Yielding, G.,

Freeman, B., and Needham, D. T. (1997): Quantitative fault seal prediction[1].

American Association of Petroleum Geologists Bulletin, v. 81, p. 897-917.

Fristad, T., Groth, A., Yielding, G., and Freeman, B., 1997. Quantitative fault seal

prediction – a case study from Oseberg Syd. In: Jolley[1], S. J., Dijk[1,2], H.,

Lamens[1,3,] J. H., Fisher[4], Q. J., Manzochi[5], T., Eikmans[1], H. and Huang[1,2], Y.

(2007): Faulting and fault sealing in production simulation models: Brent

Province, northern North Sea. Petroleum Geoscince, v. 13, p. 321-340.

Fulljames, J. R., Zijerveld, J. J., Franssen, R. C. M. W., Ingram, G. M., and Richerd,

P. D., 1996. Fault seal processes, in Norwagian Petroleum Society, eds.,

hydrocarbon seal- Importance for exploration and production. (Conference

abstracts) Oslo, Norwegian Petroleum Society, p. 5.

Gibson, R. G., and Bentham, P, A., 2003. Use of fault-seal analysis in

understanding petroleum migration in a complexly faulted anticlinal trap,

Columbus Basin, offshore Trinidad. American Association of Petroleum

Geologists Bulletin, v. 87, p. 465-478.

Grattoni[1], C. A., Guise[1], P., Fisher[1], Q. J., and Knipe[1], R. J., 2010. Mutiphase flow

properties of clay bearing rocks: laboratory measurement of relative

permeability and capillary pressure. American Association of Petroleum

Geologists bulletin, Search and Discovery article #405229 (2010)

 Griffiths, C. M., Seyedmehdi, Z., Salles, T., and Dyt, C., 2012. Stratigraphic

Forward   Modelling for South West Collie Hub Phase One - Static Model.

Anlec R&D   Project *7-0411-0129;* CSIRO Report Number EP13068.

Grollimund, B., and Zoback, M. D., 2003. Impact of glacially induced stress

changes on fault-seal integrity offshore Norway. American Association of

Petroleum Geologists Bulletin, v. 87, p. 493-506.

Haney[1], M., Sheiman[2] J., Snieder[1] R., Naruk[2], S., Busch[2], J., and Wilkins, S.,

   2004. Fault-palne reflections as a diagnostic of pressure differences in

   reservoirs: A case study of Eugen Island Block 330.

Harris[1], D., Yielding[1], G., Levine[3], P., Maxwell[2], G., Rose[4], P. T., and Nell[1], P., 2002.

   Using shale gouge ratio (SGR) to model fault as transmissibility barriers in

   reservoir: an example from the Strathspey Field, North Sea.   Petroleum

   Geoscience, v. 8, p. 167-176.

Hege, M. N. B., and Hermanrud, C., 2003. Hydrocarbon leakage processes and

   trap retention capacities offshore Norway. EAGE / Geological Society of

   London. Petroleum geosciences, v.9, p. 321 – 332.

Hermanrud, C., Bolas, H. M. N., and Teige, G. M. G., 2005. Seal failure related to

   basin scale processes. In: Cavanagh: A Leakage through faults.

Hesthammer, J., and Fossen, H., 2000. Uncertainties associated with fault

   sealing analysis. Petroleum Geoscience, v. 6, p.37-45.

Hippler, S. J., 1997. Microstructures and diagenesis in North Sea fault zone:

implication for fault seal potential and fault migration rates. In: Naruk[1], S. J.,

Dula[1], W. F., Couzens-Schultz[1], B. A., Garmezy[1], L., Griffiths[2], H., Gunst[1], A.

M., Hedlund[2], C. A., McAllister[1], E., Onyeagoro[1], U. O., Ozumba[3], B. M., and

Younes[1], A. (2002): Common characteristics of proven sealing and leaking

faults.

Hooper, R. J., Fitzsimmons, R. J., Grant, N., and Vendeville, B. C., 2002. The role

of deformation in controlling depositional patterns in the South-Central

Niger Delta, West Africa. Journal of Structural Geology, v. 24, p. 847 – 859.

James, W. R., Fairchild, L. H., Nakayama, G. P., Hippler, S. J., and Vrolijk, P. J.,

2004. fault-seal analysis using a stochastic multi-fault approach. In: Dee, S.

J., Yielding, G., Freeman, B. and Bretan, P. (2007): A comparison between

deterministic and stochastic fault seal techniques. Geological Society,

London, Special Publications, v. 292, p. 259-270.

Jennings, J. B., 1987. Capillary pressure techniques; application to exploration

and development geology. In: Brown, A. (2003): Capillary effects on fault-

fill sealing. American Association of Petroleum Geologists Bulletin, v. 87, p.

381-395.

Jev, B. I., Kaars-Supesteijn, C. H., Peter, M. P. A. M., watts, N. L., and Wjlkie, J. T.,

1993. Akaso field, Nigeria: use of integrated 3D seismic, fault-sealing, clay

smearing and RFT pressure data on fault trapping and dynamic leakage. In:

Freeman, B., Yielding, G., Needham, D.T. and Badley, M. E. (1998): Fault

seal prediction: the gouge ratio method. Geological Society, London,

Special Publications, v. 127, p. 19-25.

Jolley[1], S. J., Dijk[1,2], H., Lamens[1,3,] J. H., Fisher[4], Q. J., Manzochi[5], T., Eikmans[1], H.,

and Huang[1,2], Y., 2007. Faulting and fault sealing in production simulation

models: Brent Province, northern North Sea. Petroleum Geoscince, v. 13, p.

321-340.

Jones, R. M., and Hillis, R. R., 2003. An integrated, quantitative approach to

assessing fault-seal risk. American Association of Petroleum Geologists

Bulletin, v. 87, p. 507-524.

Kim, J., Berg, R. R., Walkins, J. S., and Tieh, T. T., 2003.Trapping capacity of faults

in the Eocene Yegua Formation, east south Lake field, southeast Texas.

American Association of Petroleum Geologists Bulletin, v. 87, p. 415-425.

Knai[1], T. A., and Knipe[2], R. J., 1998. The impact of faults on fluid flow in the

Heidrun field. In: Jones, G., Fisher, Q. J. and Knipe, R. j. (eds) Faulting, fault

sealing and fluid flow in hydrocarbon reservoir. Geological Society, London,

Special Publications, 147, 269 – 282.

Knipe, R. J., 1997. Juxtaposition / seal diagrams to facilitate fault seal analysis of

hydrocarbons. In: Aref, L. and Muhamed, A. (2004): Juxtaposition and fault

seal analysis of some mixed clastic reservoir in Egypt. Egyptian Geophysical

Society Journal, v. 2, p. 165-184.

Knipe, R. J., Fisher, Q. J., Jones, G., Clennel, M. R., Farmer, A. B., and Harrison,

A., Kidd, B., McAllister, E., Porter, J. R., and White, E. A., 1997. Fault seal

analysis: Successful methodologies, application and future directions. In: P.

Moller-Pedersen and Koestler, A. G., (eds), Hydrocarbon seal: Importance

for exploration and production. NPF Special Publications, v. 7, p. 15 – 40.

Knipe, R. J., Jones, G., and Fisher, Q. J., 1998. Faulting, fault seal and fluid flow in

hydrocarbon reservoirs: an introduction. In: Jones, G., Fisher, Q. J., and

Knipe, R. J., (eds) Faulting, fault sealing and fluid flow in hydrocarbon

reservoirs. Geological Society, London, Special Publications, v. 147, p. 7 -21.

Knipe, R. J., Freeman, S., Harris, S., and Davies, R., 2004. Structural uncertainty

and scenario modeling for fault seal analysis. In: Aref, L. and Muhamed, A.

(2004): Juxtaposition and fault seal analysis of some mixed clastic reservoir

in Egypt. Egyptian Geophysical Society Journal, v. 2, p. 165-184.

Knipe, R. J., Fisher, Q. J., Jones, G., McAllister, E., Needham, D. T., Davies, R.,

Kay, M., Edwards, E., Li, A., Porter, J. R., Harris, S. J., Ellis, J., and Odling, N.,

2001. Faulting and fault seal: Progress with prediction. Canadian Society of

Petroleum Geologists, p. 137.

Knott, S. D., 1993. Fault seal analysis in the North Sea. In: Naruk[1], S. J., Dula[1],

W. F., Couzens-Schultz[1], B. A., Garmezy[1], L., Griffiths[2], H., Gunst[1], A. M.,

Hedlund[2], C. A., McAllister[1], E., Onyeagoro[1], U. O., Ozumba[3], B. M., and

Younes[1], A. (2002): Common characteristics of proven sealing and leaking

faults. American Association of Petroleum Geologists Hedberg Research

Conference, p. 71-74.

Koledoye, A. B., Aydin, A., and May, E., 2003. A new process-based

methodology for analysis of shale smear along normal faults in the Niger

Delta. American Association of Petroleum Geologists Bulletin, v. 87, p. 445-

463.

Kondal R., Kausik S., Susanta M., Challapalli R., Vivek S., and Arvind K., 2013

    Reducing the uncertainty in 4D seismic interpretation through an

    integrated multi-disciplinary workflow: A case study from Ravva field, KG

    basin, India. 10th Biennial International Conference & Exposition. p.227.

Kostenko O. V., Naruk, S. J., Hack, W., Poupon, M., Meyer, H., Mora-Glukstad,

    M., Anowai, C., and Mordi, M., 2008. Structural evaluation of column-

    height controls at a toe-thrust discovery, deep-water Niger Delta.

Lambert-Aikhionbare, D. O., and Shaw, H. O., 1982. Significance of clay in the

    petroleum geology of the Niger delta. Clay Mineralogy, v.17, p. 19-103.

Lampe, C., Bird, K. J., Moore, T. E., Ratliff, R. A., and Freeman, B., 2012,

    Modeling[3]: Integrating structural modeling, fault property analysis, and

    petroleum systems modeling—an example from the Brooks Range foothills

    of the Alaska North Slope, *in* K. E. Peters, D. J. Curry, and M. Kacewicz,

    eds., Basin Modeling: New Horizons in Research and Applications: AAPG

    Hedberg Series, no. 4, p. 119–136.

Langhi, L., Ciftci, B., and Strand, J., 2013. Fault seal first-order analysis –SW Hub.

    CSIRO earth Science and Resource Engineering, Australia. p.1-60.

Lashin, A., and Abd El-Aal, M., 2004. Juxtaposition and fault seal analysis of some

mixed clastic reservoir in Egypt. Egyptian Geophysical Society Journal, v. 2,

p. 165-184.

Laurent G., Caumon G.,Bouziat A.,Jessell M., 2013.A parametric method to model

3D displacements around faults with volumetric vector   fields.

Tectonophysics, v. 590, p.83-93.

Lehner, F. K., and Pilaar, W. F., 1997. The emplacement of clay smears in

synsedimentary normal faults. In: Bashir, A. K., Atilla, A. and Eric, M.

(2003): A new process-based methodology for analysis of shale smear

along normal faults in the Niger Delta. American Association of Petroleum

Geologists Bulletin, v. 87, p. 445-463.

Lia, O., More, H., Tjelmeland, H., Holden, L., and Egeland, T., 1997. Uncertainties

in reservoir production forecast. In: Harris1, D., Yielding1, G., Levine3, P.,

Maxwell2, G., Rose4, P. T. Nell1, P. (2002): Using shale gouge ratio (SGR) to

model fault as transmissibility barriers in reservoir: an example from the

Strathspey Field, North Sea. Petroleum Geoscience, v. 8, p. 167-176.

Lindsay, N. G., Murphy, F. C., Walsh, J. J., and Watterson, J., 1993. Out crop

    studies of shale smears on fault surfaces. In: Davies, R. K., An, L., Jones, P.,

    Mathis, A., and Cornette, C. (2003): American Association of Petroleum

    Geologists Bulletin, v. 87, p. 479-491.

Lingdong, M., Xiaofei, F., Yachun, W., Xiaoling, Z., Yibo, J., and

    Hongsong, Y., 2014. Internal structure and sealing properties of the

    volcanic fault zones in Xujiaweizi Fault Depression, Songliao Basin, China.

    Petroleum Exploration and Development Journal, v.41, p.165-174.

Manzocchi[1], T., Walsh[1], J. J. Nell[1], P., and Yielding[2], G., 1999. incorporated

    geological conceptualizations of fault zone structure and content into a

    predictive method for calculating fault zone transmissibility multipliers.

    Petroleum Geosciences, V. 5, p. 53-63.

Manzocchi, T., Heath, A. E., walsh, J. J., and Childs C., 2000. Fault-rock capillary

    pressure: extending fault seal concepts to production simulation. In:

    Yielding, G. (2002): Shale gouge ratio – calibration by geohistory.

    Netherland, Elsevier, Norwegian Petroleum Society NPF Special Publication,

    11, P. 1-15.

Manzocchi[1], T., Matthews[2], J. D., Strand[1,6], J.A., Carter[2], J. N., Skorstard[3], A., Howell[4], J.A., Stephen[5], K. D., and Walsh[1], J. J., 2008. A study of the structural controls on oil recovery from shallow-marine reservoirs. EAGE / Geological Society of London, v. 14. p. 55 – 70.

Maunde A[1], Henry U[2], Raji AS[1]., and Haruna IV[1]., 2013. Fault seal analysis: a regional calibration Nile delta,Egypt. International Research Journal of Geology and Mining (IRJGM) (2276-6618) v. 3(5) p. 190-194.

McClenaghan, R., Saikia, K., Mishra, S., Rao, C.G., Reddy, K., Gupta, M., Guttormsen, J., Josyula, S., and Burley, S.D., 2012. Integrated geoscience and 4D technology identifies potential to extend production life of the Ravva Field, K-G Basin, India. ICE 2012, AAPG, Singapore, extended abstract volume.

Naruk[1], S. J., Dula[1], W. F., Couzens-Schultz[1], B. A., Garmezy[1], L., Griffiths[2], H., Gunst[1], A. M., Hedlund[2], C. A., McAllister[1], E., Onyeagoro[1], U. O., Ozumba[3], B. M., and Younes[1], A., 2002. Common characteristics of proven sealing and leaking faults. American Association of Petroleum Geologists Hedberg Research Conference, p. 71-74.

Needham, D. T., Yielding, G., and Freeman, B., 1996. Analysis of fault geometry

and displacement patterns. In: Jolley[1], S. J., Dijk[1,2], H., Lamens[1,3,] J. H.,

Fisher[4], Q. J., Manzochi[5], T., Eikmans[1], H. and Huang[1,2], Y. (2007): Faulting

and fault sealing in production simulation models: Brent Province, northern

North Sea. Petroleum Geoscince, v. 13, p. 321-340.

Needham[1,3], T., Li1, A., Carr[2], C., Schorr[2], G., Benmahiddi[2], S., and Pena[2], J. L.,

2008. Faulting and fault sealing in the TAGI formation of the Ourhoud field,

Algeria. Petroleum Geoscience, v. 14. p.379 - 388.

Nysæther, E., 2006. Determination of overpressure in sandstones by fluid

modeling: the Haltenbanken area, Norway, In: B¡ørlykke, K., 2006.

Modeling of fluid flow and overpressure – A discussion, v. 86, p. 439 -441,

Norwagian journal of Geology.

Oluseye[1], E., Richard[1], E., Nick[1], F., Phil[2], R., jide[1,3], A., Gary[1], M., and Sankar[1,3],

M., 2008. Geological risk and uncertainty in the outer fold and trust belt-

deepwater, Niger Delta.

Pelosi, A. P. M[1]., 2009. Fault seal prediction and risk evaluation of exploratory

prospects: examples of Brazilian marginal basins. American Association of

Petroleum Geologists bulletin, v. 81, no. 6, p. 1023 – 1041.

Pevzner, R., Lumley, D., Urosevic, M., Gurevich, B., Bóna, A., Alajmi, M.A., Shragge, J., Pervukhina, M., Mueller, T., and Shulakova, V., 2013. Advanced   Geophysical Data Analysis at Harvey-1: Storage Site Characterization and   Stability Assessment. Anlec R&D Project Number 7-1111-0198.

Sapiie, B., Adiwibowo, R., and Imron, M., 2013. Fault Seal Analysis Application in Oblique Convergent Strike-Slip Fault Deformation. 75th EAGE Conference & Exhibition incorporating SPE EUROPEC 2013. Publication date: 10 June 2013. DOI: 10.3997/2214-4609.20130147.

Schowalter, T. T., 1979. Mechanics of secondary hydrocarbon migration and entrapment. In: Yielding, G. (2002): Shale gouge ratio – calibration by geohistory. Netherland, Elsevier, Norwegian Petroleum Society NPF Special Publication, 11, P. 1-15.

Shannon, P. M., and Naylor N., 1989. Petroleum Basin Studies: London, Graham and Trotman Limited, p 153-169.

Short, K. C., and Stauble, A. J., 1967. Outline of geology of Niger delta. In: Reijers, T. J. A., Petters, S. W., and Nwajide, C. S. The Niger delta basin. Selected chapters on geology. P. 103-117.

Skerlec, G. M., 1996. Evaluating top and fault seal. In: Dee, S. J., Yielding, G.,

Freeman, B. and Bretan, P. (2007): A comparison between deterministic

and stochastic fault seal techniques. Geological Society, London, Special

Publications, v. 292, p. 259-270.

Skorstad[1], A., Kolbjørnsen[1], Manzocchi[2], T., Carter[3], J. N., and Howell[4], J.

A., 2008. Combined effects of structural, stratigraphic and well controls on

production variability in faulted shallow-marine reservoirs. EAGE /

Geological society of London. V. 14. p. 45 – 54.

Sneder, R., Robert, M., and Vavra, C., 2000. Seal – A critical element to successful

exploration and production. From: Petroleum Technological council.

Sorkhabi, R., Hasegawa, S., Suzuki, K., Takahashi, M., Fujimoto, M., Sakuyama,

N., and Iwanaga, S., 2002. Modeling of shale smear parameters, fault seal

potential, and fault rock permeability. American Association of Petroleum

Geologists. p. 1-5.

Sperrevik[1,2], S., Færseth[3], R. B., and Gabrielsen[1],, R. H., 2000. Experiments on

clay smear formation along faults. EAGE / Geological Society, London. V. 6.

P. 113 -123.

Sperrevik, S., Gillepsie, P. A., Fisher, Q. J., Halvorson, T., and Knipe, R. J., 2002. Emperical estimation of the fault rock properties. In: Aref, L. and Muhamed, A. (2004): Juxtaposition and fault seal analysis of some mixed clastic reservoir in Egypt. Egyptian Geophysical Society Journal, v. 2, p. 165-184.

Stacher, P., 1995. Present understanding of the Niger delta hydrocarbon habitat. In: Oti, M. N., and Postma, G., eds., Geology of Deltas: Rotterdam, A. A. Balkema, p. 101-103.

Stoneley, E., 1966. The Niger delta region in the light of theory of Continental Drift. In: Etu-Efeotor, J. O., Fundamentals of petroleum geology. P. 110-142.

Strand1, J., Underschultz1, J., Michael1, K., Freeman2, B., and Yielding2, G., 2008. Effect of hydrodynamics and fault zone heterogeneity on membrane seal capacity. American Association of Petroleum Geologists, Search and Discovery article #40404 (2009).

Tearpock, D. J., and Bischke, R. E., Applied subsurface geological mapping. P. 95-131.

Tearpock, D. J., and Harris, J., 1987. subsurface geological mapping techniques –

A training manual, Tenneco Oil Co., Houston, TX. In: Tearpock, D. J., and

Bischke, R. E., Applied subsurface geological mapping. P. 95-131.

Tan C. H[1]., and Lothar S[2]., 2012. Fault Seal Prediction and Uncertainty

Estimation   of a Water Wet Fault. Search and Discovery Article #41029.

p.1-16.

Teige[1], G. M. G., Hermanrud[1], C., Thomas[2], W. H., Wilson[3], O. B., and Bolås[1], H.

M. N., 2005. Capillary resistance and trapping of hydrocarbons: a laboratory

experiment. EAGE / Geological Society of London, v. 11, p. 125 – 129.

Tveranger1, J., Howell1, J., Aanonsen1, S. I., Kolbjørnsen2, O., Semshaug, S. L.,

Skorstad2, A., and Ottesen3, S., 2008. Assessing structural controls on

reservoir performance in different stratigraphic settings. In: Robinson, A.,

Griffiths., Prince, S., Hegre, J., and Muggeridge, A. (eds) Thefuture

geological modeling in hydrocarbon development. The Geological Society,

London, Special Publications, v. 309, p. 51 – 66.

Vavra, C.L, J.G. Kaldi & R.M. Sneider (1992). Geological applications of

capillary pressure: a review. Bull. AAPG, 76 (6), pp. 840-850.

Vrolijk, P., James, B., Myers, R., Maynard, J., Sumpter, L., and Sweet, M., 2005.

Reservoir connectivity analysis – defining reservoir connections and

plumbing. Society of Petroleum Engineering, (ExxonMobil Upstream

Research Co), p.1-23.

Watts, N., 1987. Theoretical aspect of cap-rock and fault seals for single-and

two-phase hydrocarbon columns. In: Aref, L. and Muhamed, A. (2004):

Juxtaposition and fault seal analysis of some mixed clastic reservoir in

Egypt. Egyptian Geophysical Society Journal, v. 2, p. 165-184.

Weber, K. J., and Daukoru, E., 1975. Petroleum geology of the Niger delta. Proc.

Ninth World Petrol. Congr., 2: P. 209-221.

Weber, K. J., 1971. Sedimentological aspects of oil fields in Niger delta. In:

Reijers, T. J. A., Petters, S. W., and Nwajide, C. S. The Niger delta basin.

Selected chapters on geology. P. 103-117.

Weber, K. J., Mandl, G., Pilaar, F., Lehner, F., and Precious, R. G. 1978. The role

of faults in hydrocarbon migration and trapping in Nigerian growth fault

structures. 10th Annual Offshore Technology Conference Proceeding. V. 4.

P. 2643-2653.

Yielding, G., Badley, M. E., and Roberts, A. M., 1992. The structural evolution of

Brent Province. In: Harris1, D., Yielding1, G., Levine3, P., Maxwell2, G.,

Rose4, P. T. Nell1, P. (2002): Using shale gouge ratio (SGR) to model fault as

transmissibility barriers in reservoir: an example from the Strathspey Field,

North Sea. Petroleum Geoscience, v. 8, p. 167-176.

Yielding, G., Freeman, B., and Needham, D. T., 1997. Quantitative fault seal

prediction[1]. American Association of Petroleum Geologists Bulletin, v. 81, p.

897-917.

Yielding G., Boult P., Freeman B., Menpes S., Diekman L ., 2008. A minimum-strain

approach to reducing the structural uncertainty in poor 2D seismic data,

Gambier Embayment, Otway Basin, Australia. In: Strand1, J., Underschultz1,

J., Michael1, K., Freeman2, B., and Yielding2, G., 2008. Effect of

hydrodynamics and fault zone heterogeneity on membrane seal capacity.

American Association of Petroleum Geologists, Search and Discovery article

#40404 (2009).

Yielding, G., Overhand, J. A., and Byberg, G., 1999a. Characterization of fault

zones in the Gullfaks field for reservoir modeling. In: Harris1, D., Yielding1,

G., Levine3, P., Maxwell2, G., Rose4, P. T. Nell1, P. (2002): Using shale

gouge ratio (SGR) to model fault as transmissibility barriers in reservoir: an

example from the Strathspey Field, North Sea. Petroleum Geoscience, v. 8,

p. 167-176.

Yielding, G., Overhand, J. A., and Byberg, G., 1999b. Characterization of fault

Zones for reservoir modeling: An example from the Gullfaks Field, Northern

North Sea. In: Aref, L. and Muhamed, A. (2004): Juxtaposition and fault seal

analysis of some mixed clastic reservoir in Egypt. Egyptian Geophysical

Society Journal, v. 2, p. 165-184.

Yielding, G., 2002. Shale gouge ratio – calibration by geohistory. Netherland,

Elsevier, Norwegian Petroleum Society NPF Special Publication, 11, P. 1-15.

Yielding G., Jackson, M. D., Hampson, G. J., Saunders, J. H., El-Sheikh, A., and

Massart, B. Y. G. 2014. Surface-based reservoir modelling for flow

simulation. The Geological Society of London

Zhang, L., Luo, X., Liao, Q., Yang, W., Vasseur, G., Yu, C., Su, J., Yuan, S., Xiao, D.,

and Wang, Z., 2010. Quantitative evaluation of synsedimentary fault

opening and sealing properties using hydrocarbon connection probability

assessment. American Association of Petroleum Geologists Bulletin, v. 94,

p. 1379 - 1399.

APPENDIXES

Interpreted Isochore maps

Interpreted Depth Structural maps

Stratigraphic Correlations

3D Model Quality Control

Seismic Interpretation Quality Control

Interpreted Isochore Maps

F1000 Base – F1000 Top

G2000 Top – G2000 Base

G2000 Top – F1000 Base

G4000 Top – G2000 Base
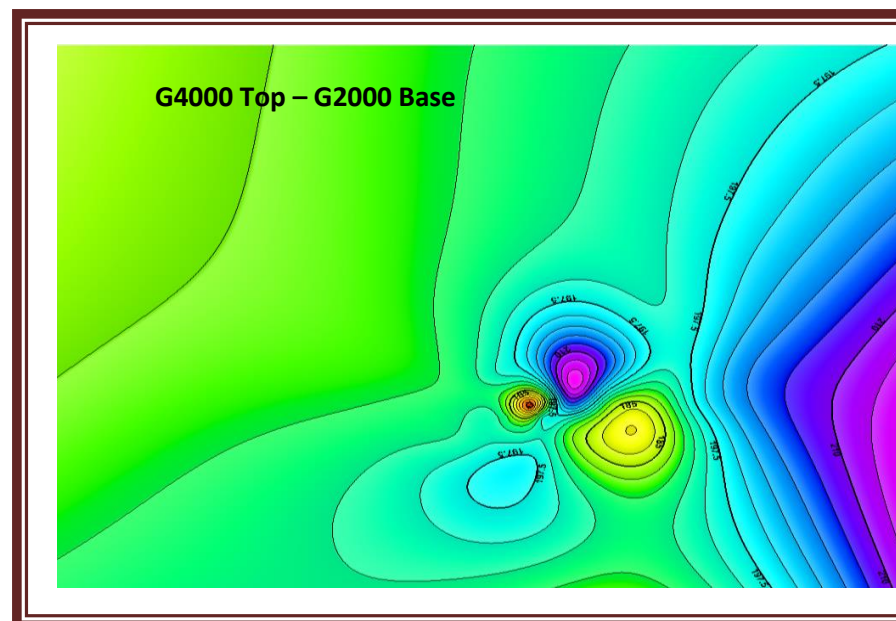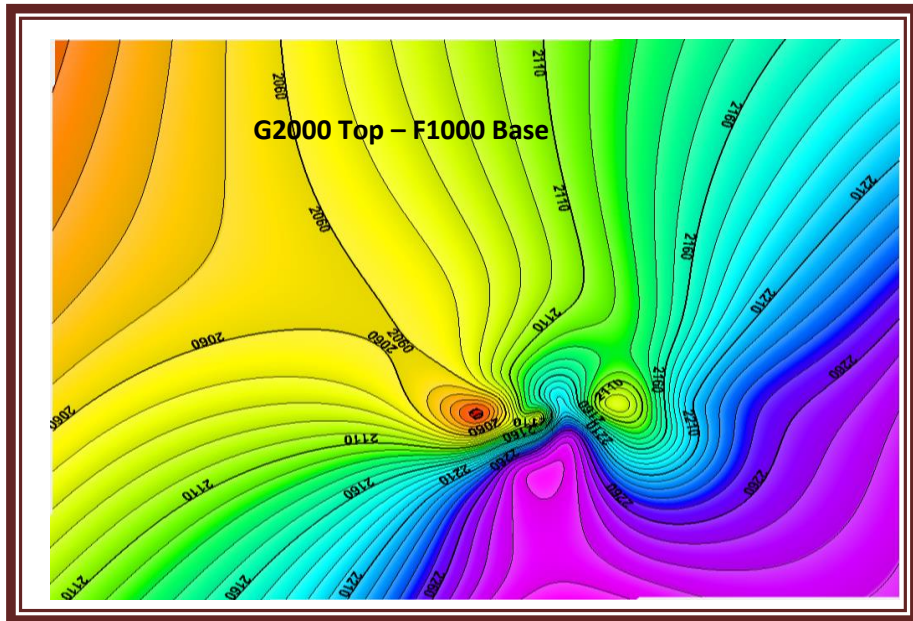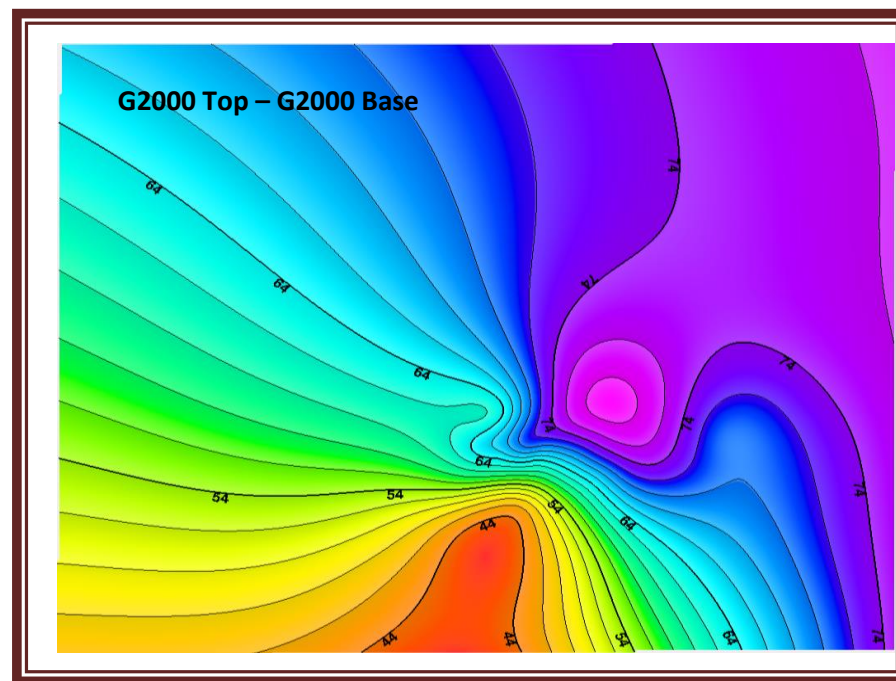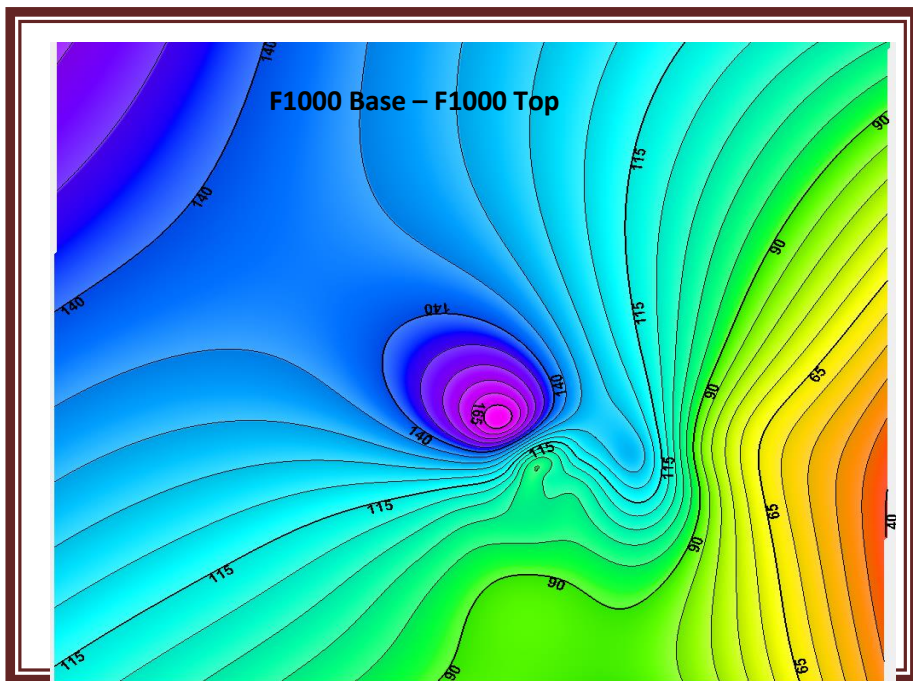
Appendix 1: F1000 Base – G4000 Top Isochore Maps

213
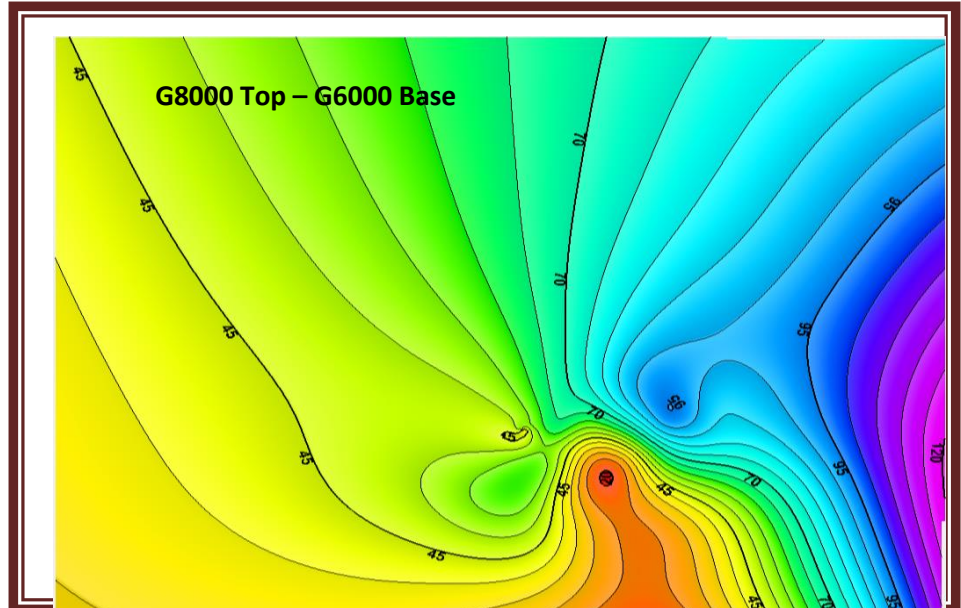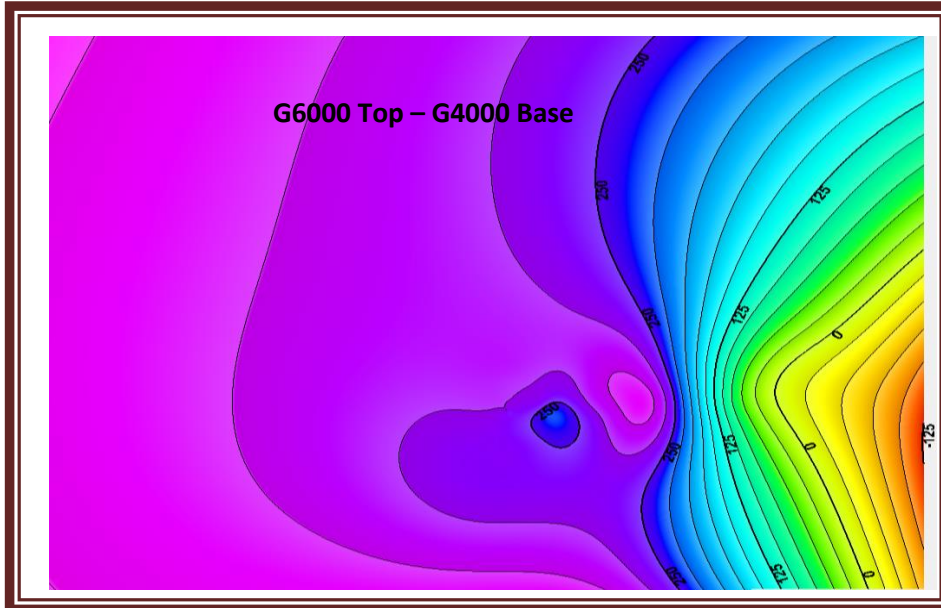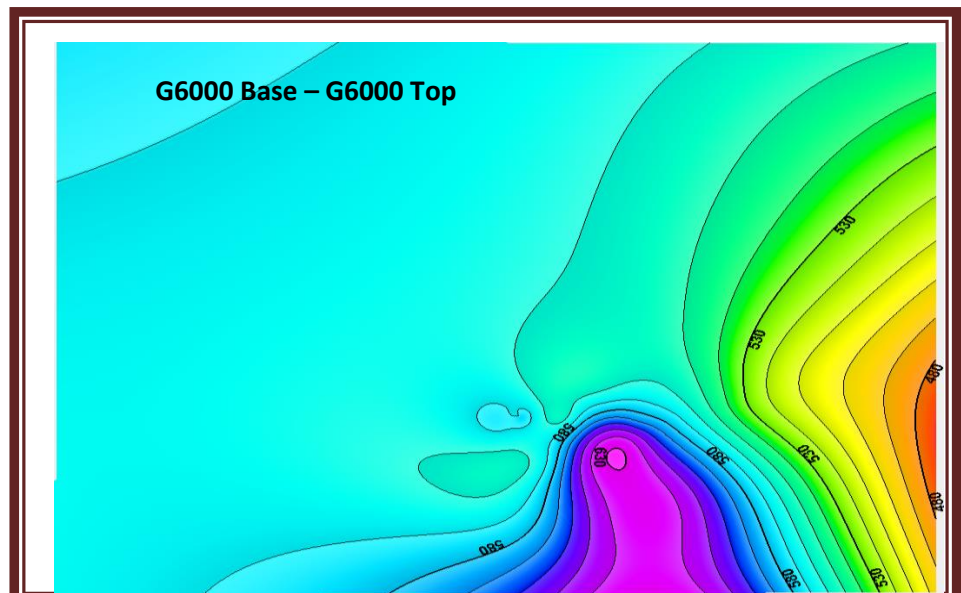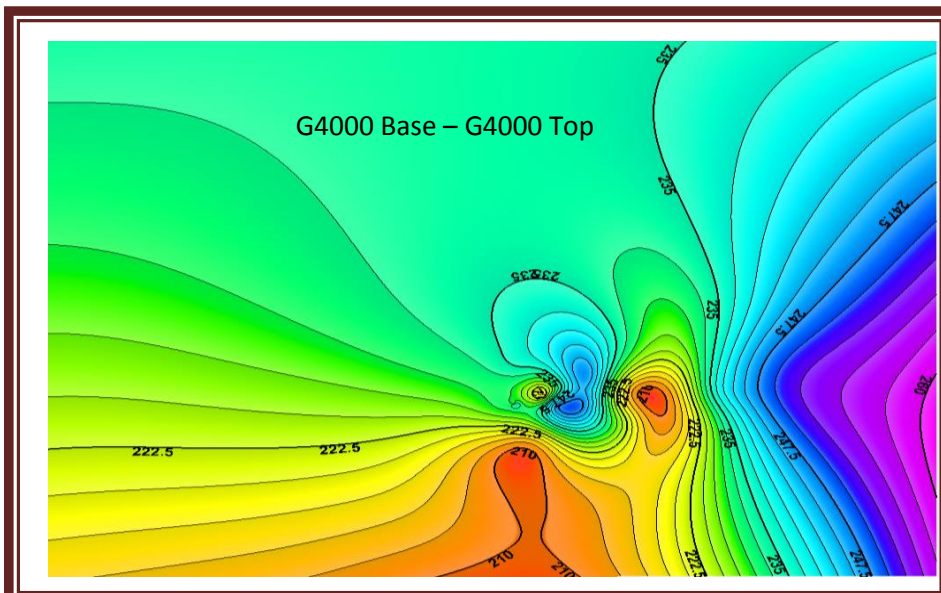
Appendix 2: G4000 Base – G8000 Top Isochore Maps
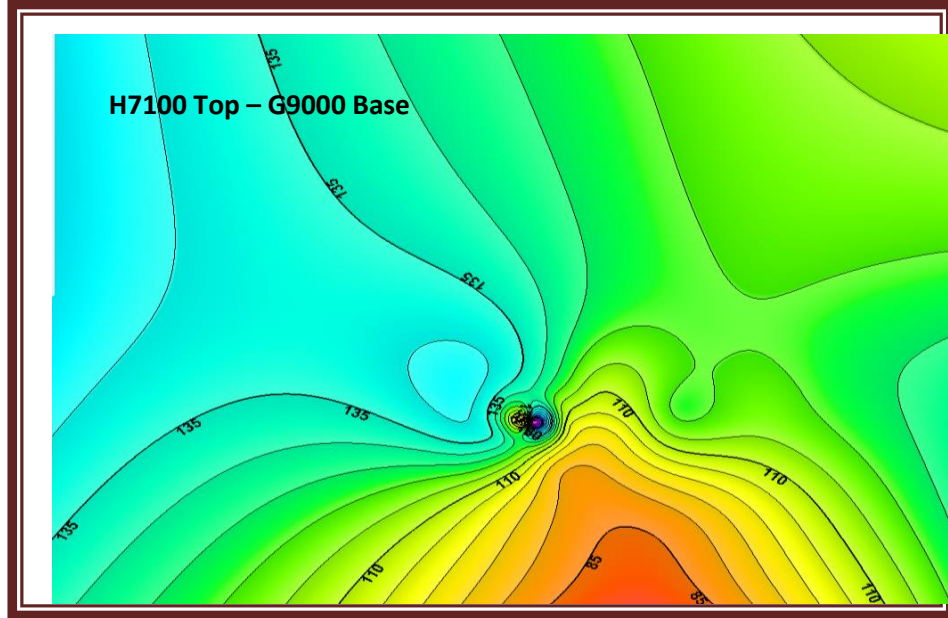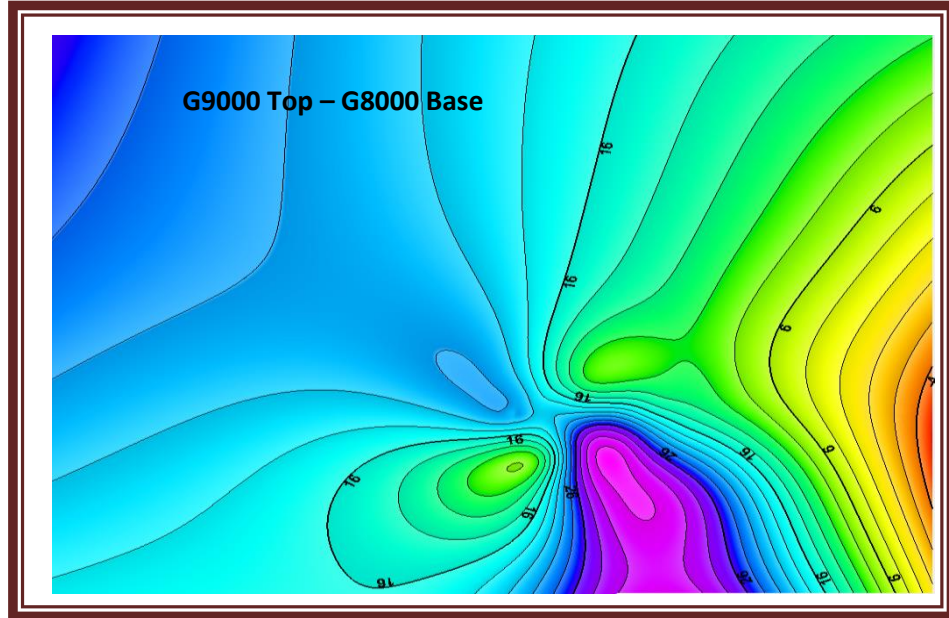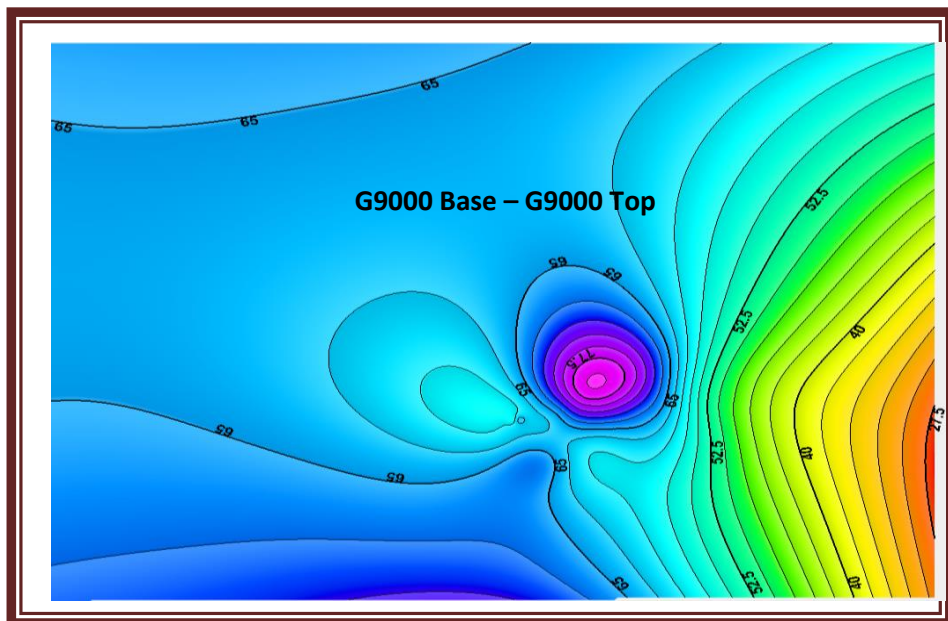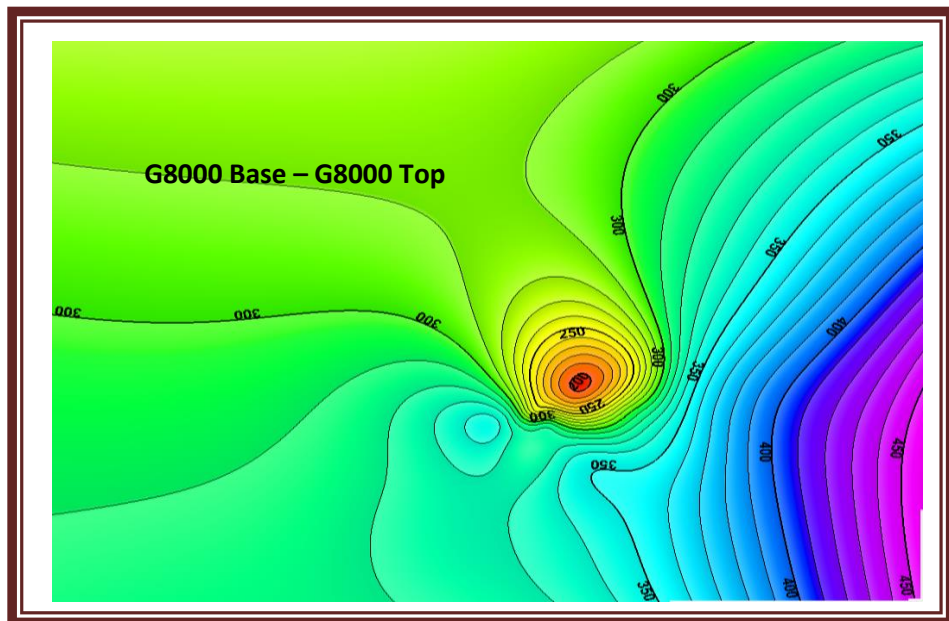
Appendix 3: G8000 Base – H7100 Top Isochore Maps
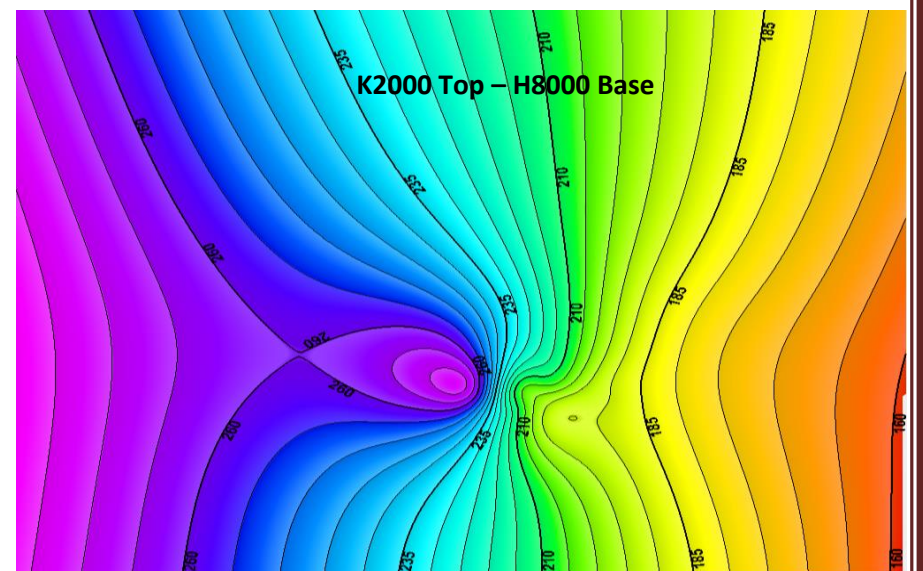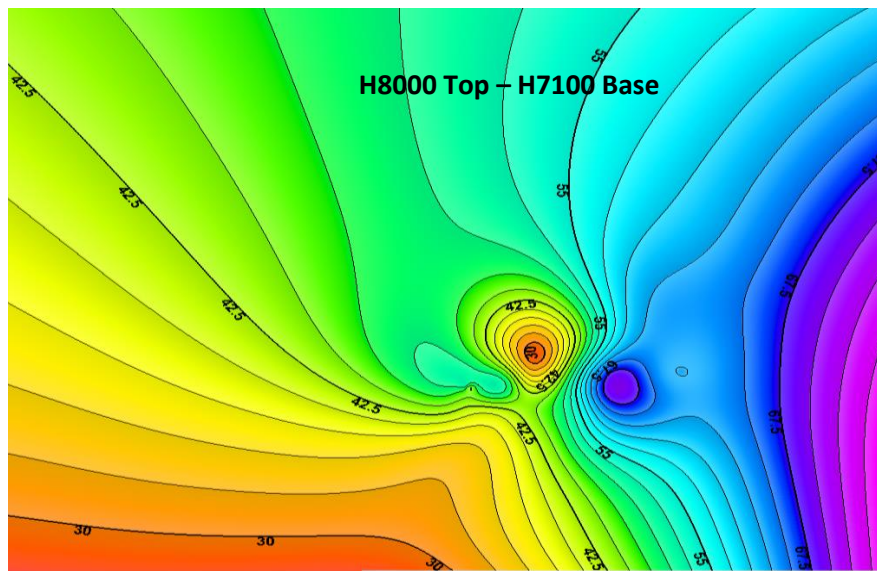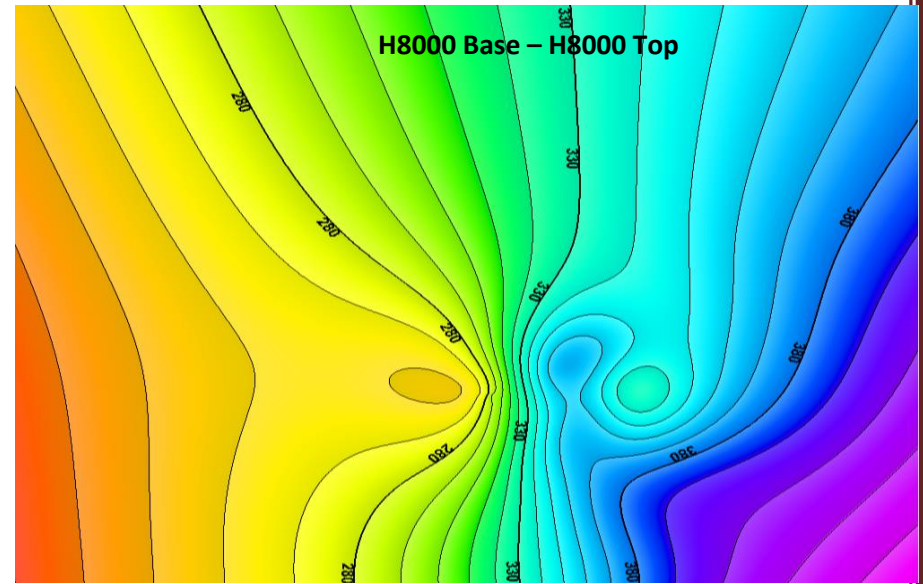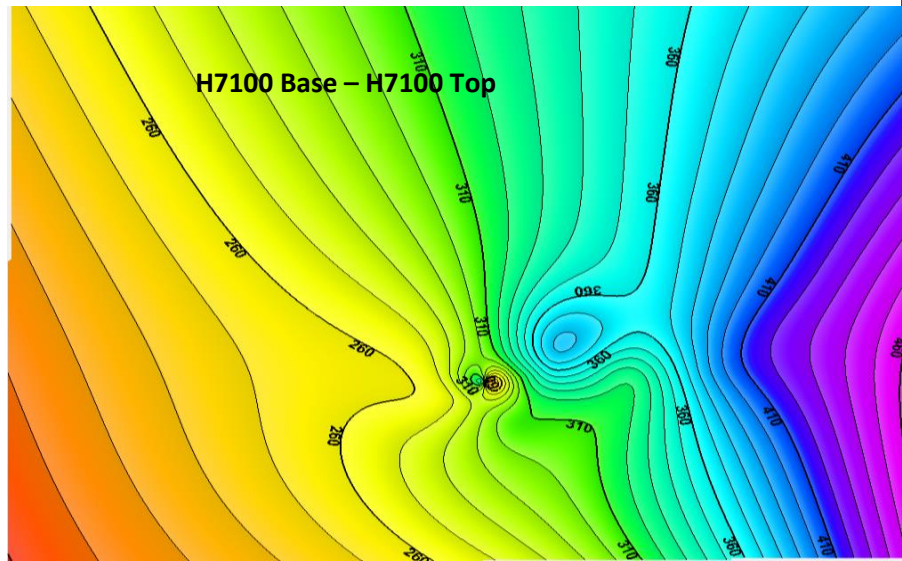
Appendix 4: H7100 Base – K2000 Top Isochors Maps

216
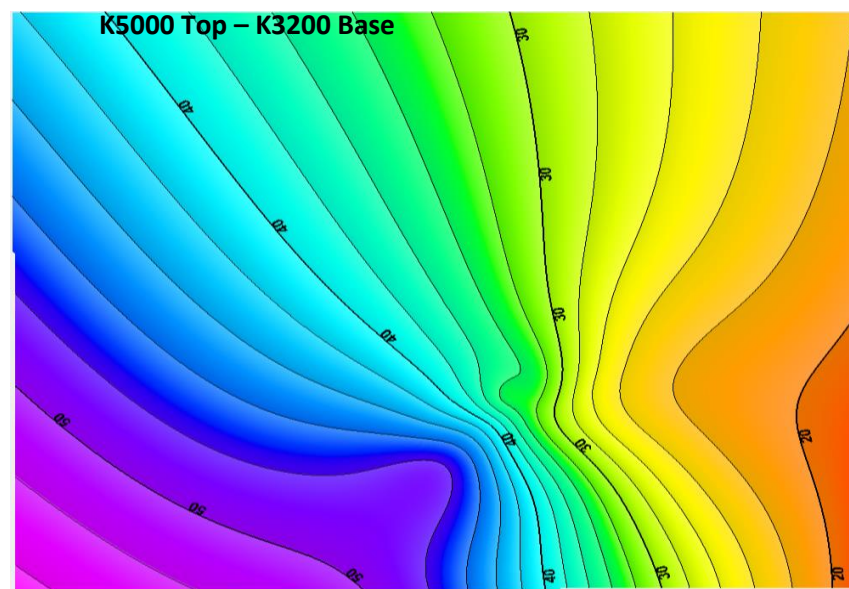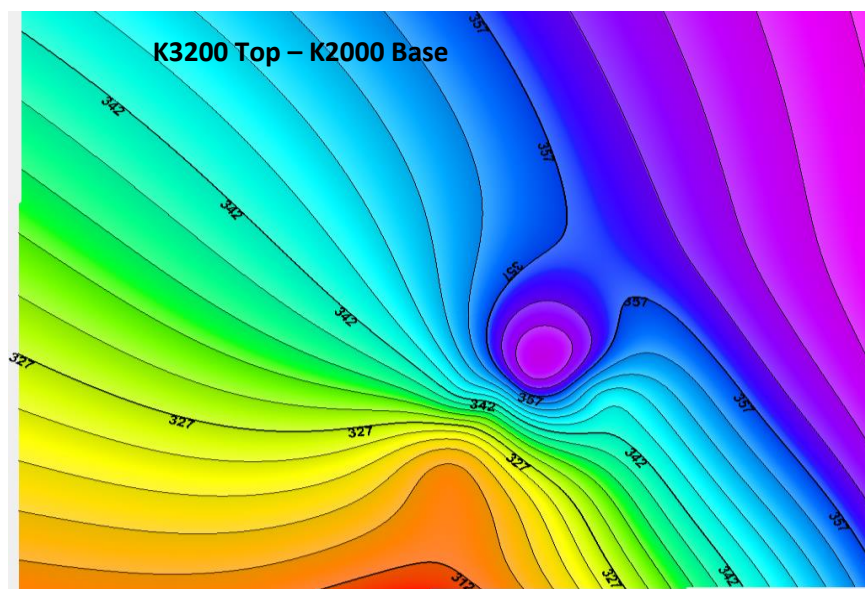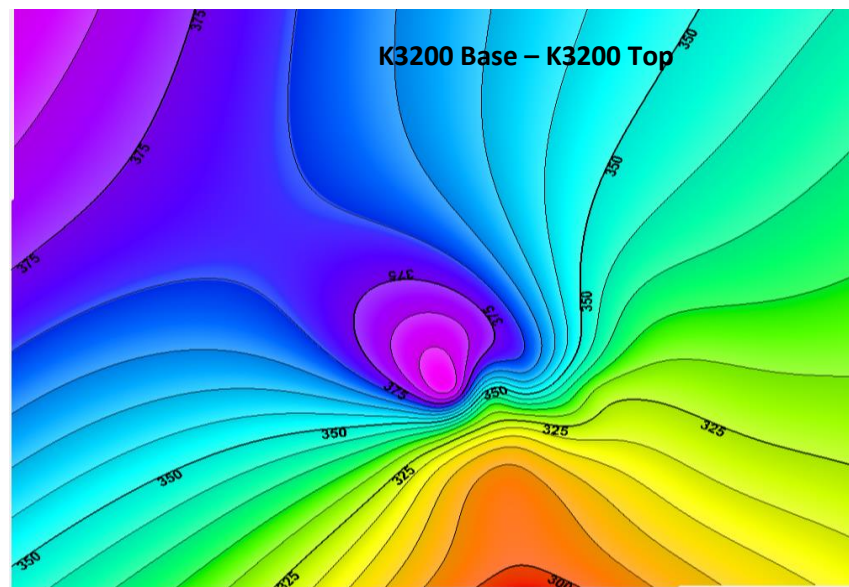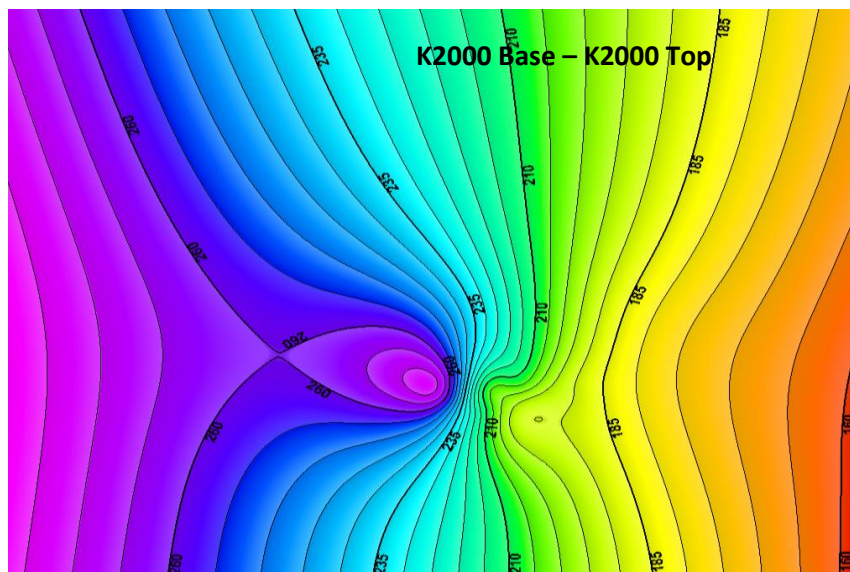
Appendix 5: K2000 Base – K5000 Top Isochore Maps
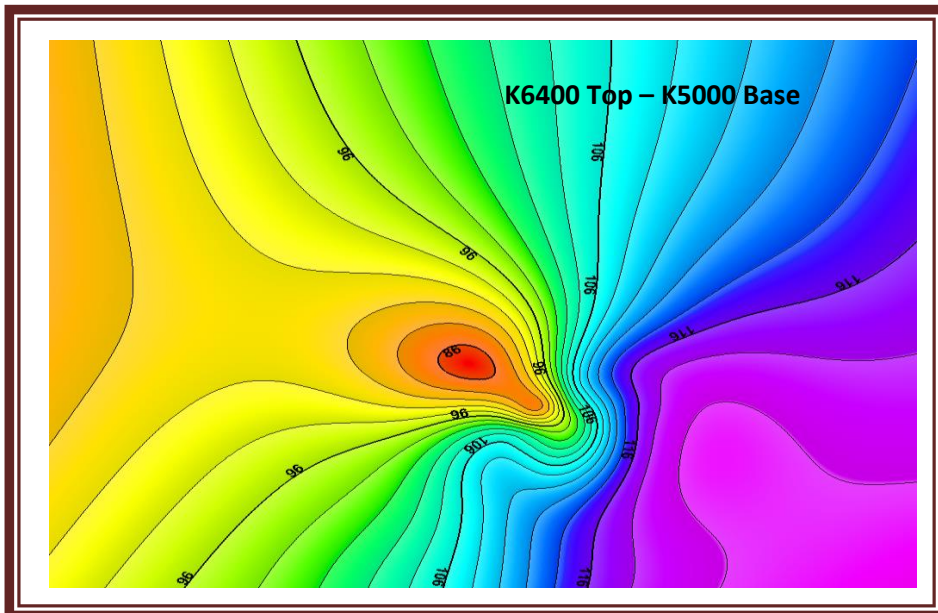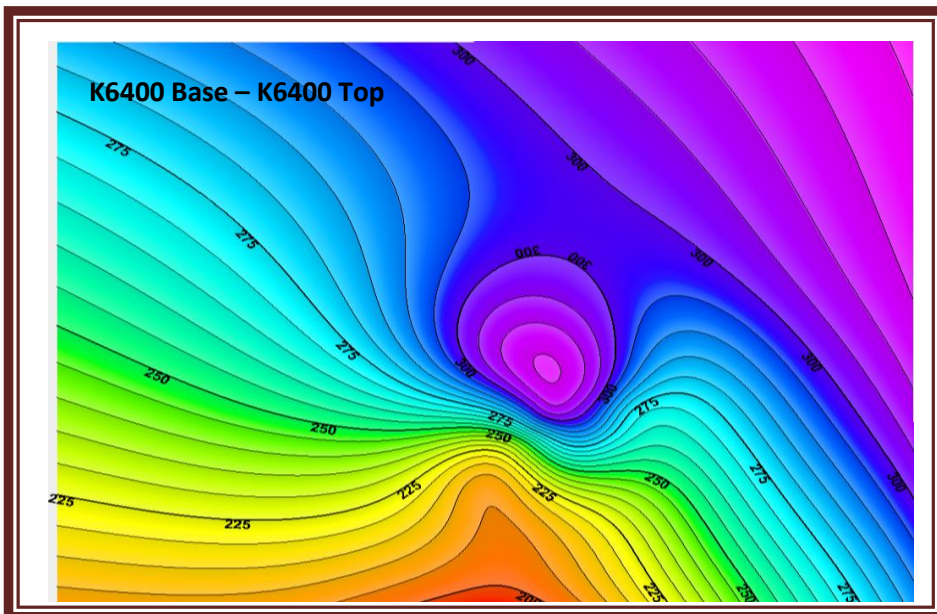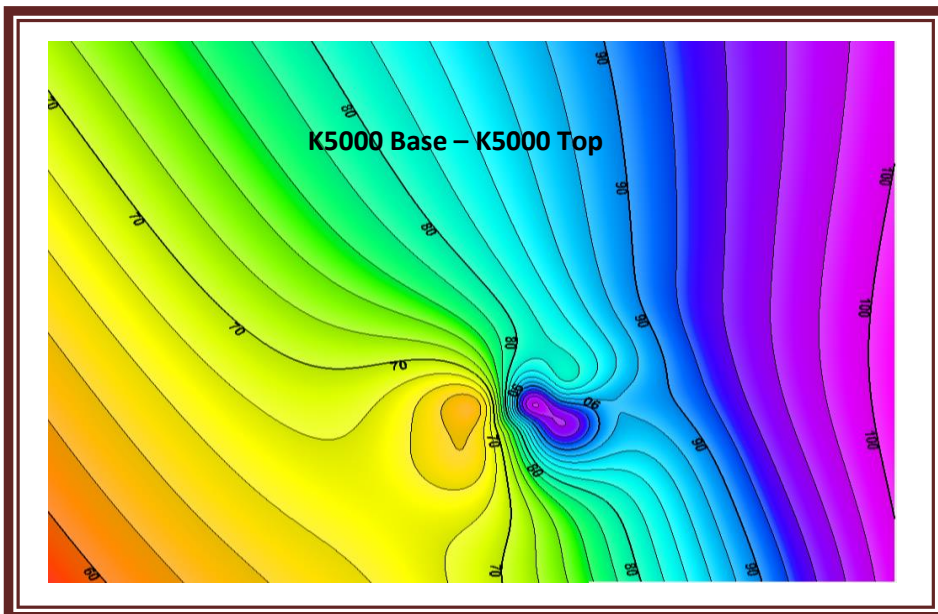
Appendix 6: K5000 Base – K7000 Top Isochore Maps
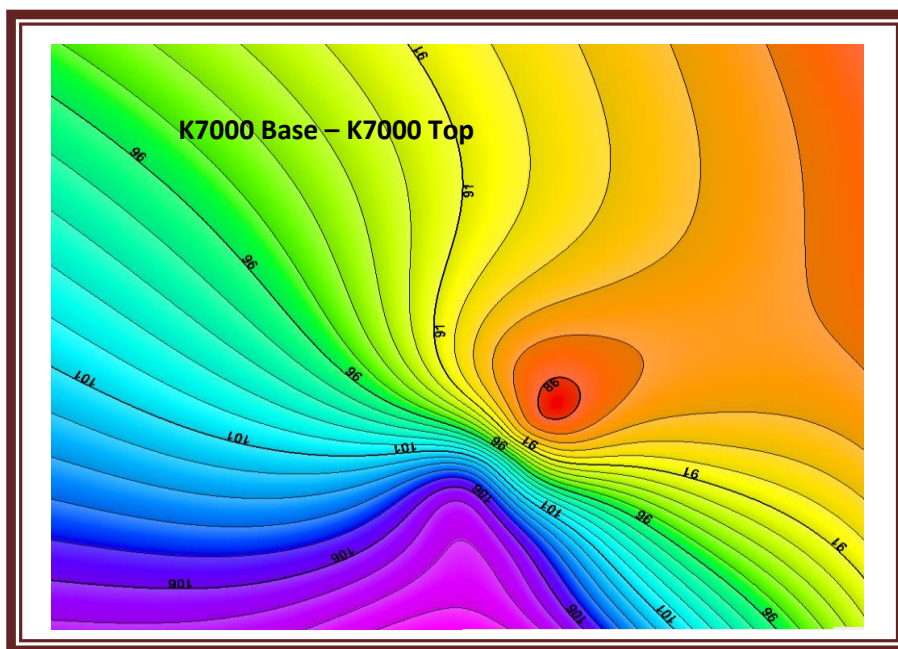
Appendix 7: K7000 Base – K7000 Top Isochore Map

Interpreted Depth Structural Maps
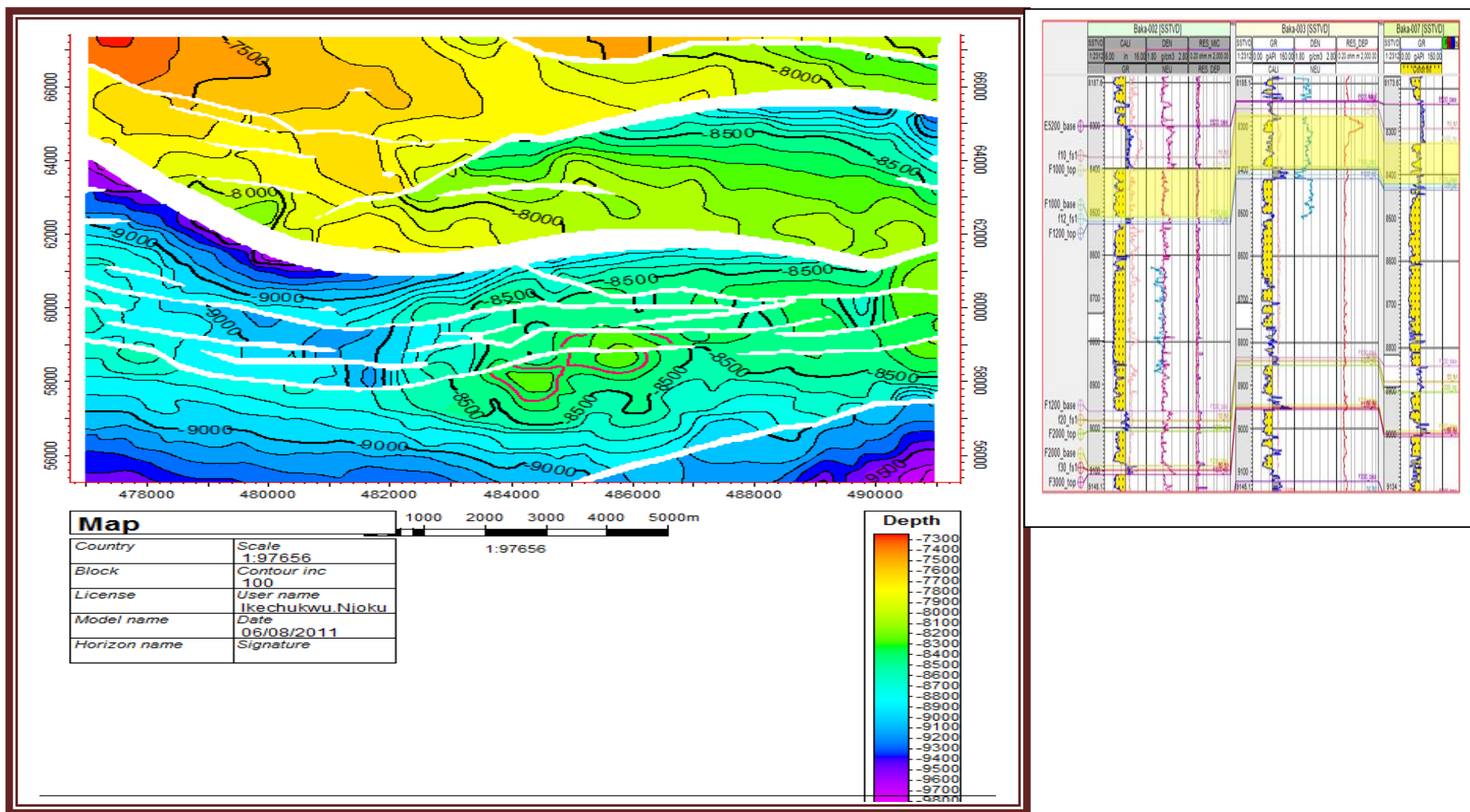
Appendix 8: F1000 Depth Structure Map and Typical Stratigraphic Correlation of F1000
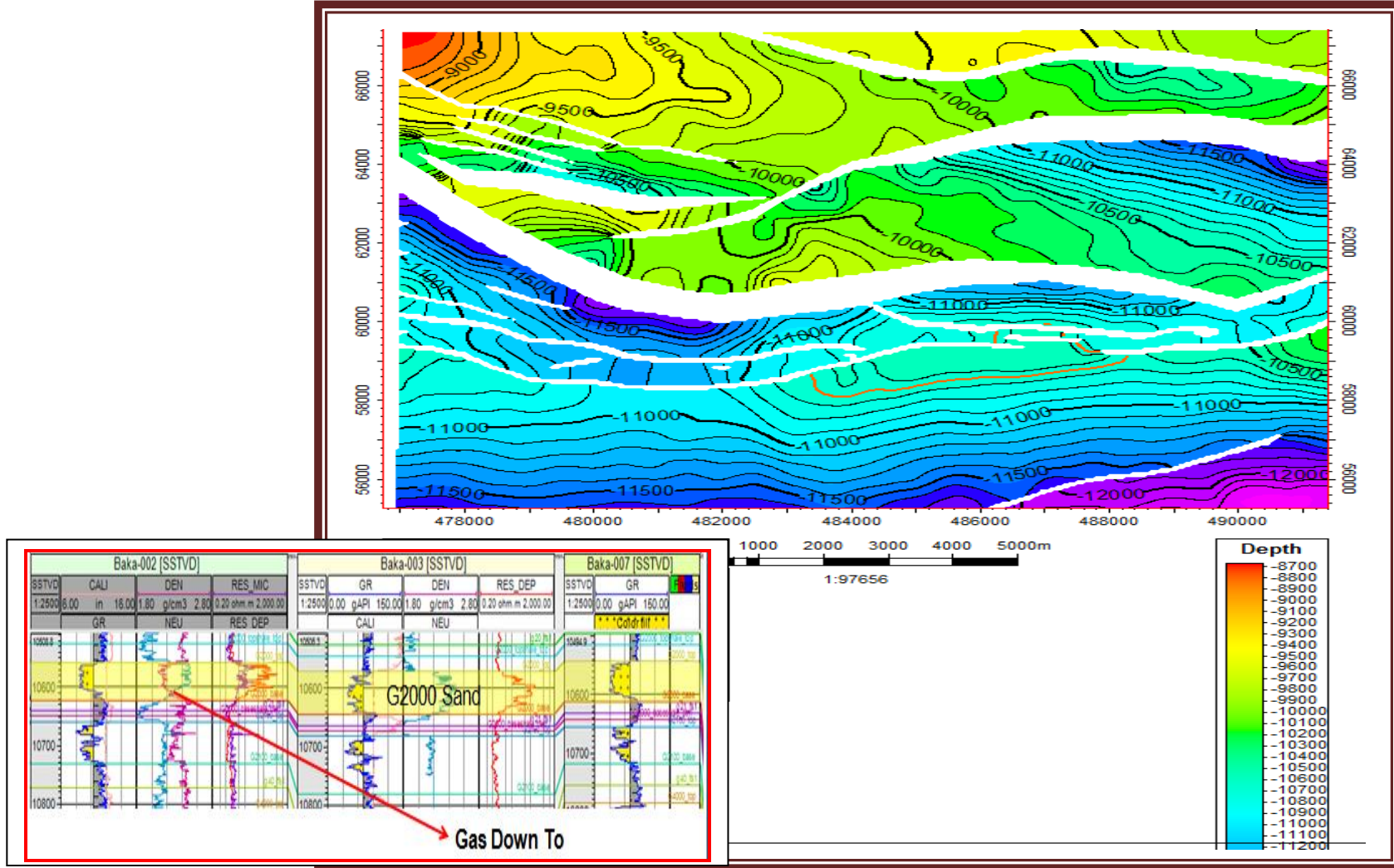
Appendix 9: G2000 Depth Structure Map and Typical Stratigraphic Correlation of G2000

222
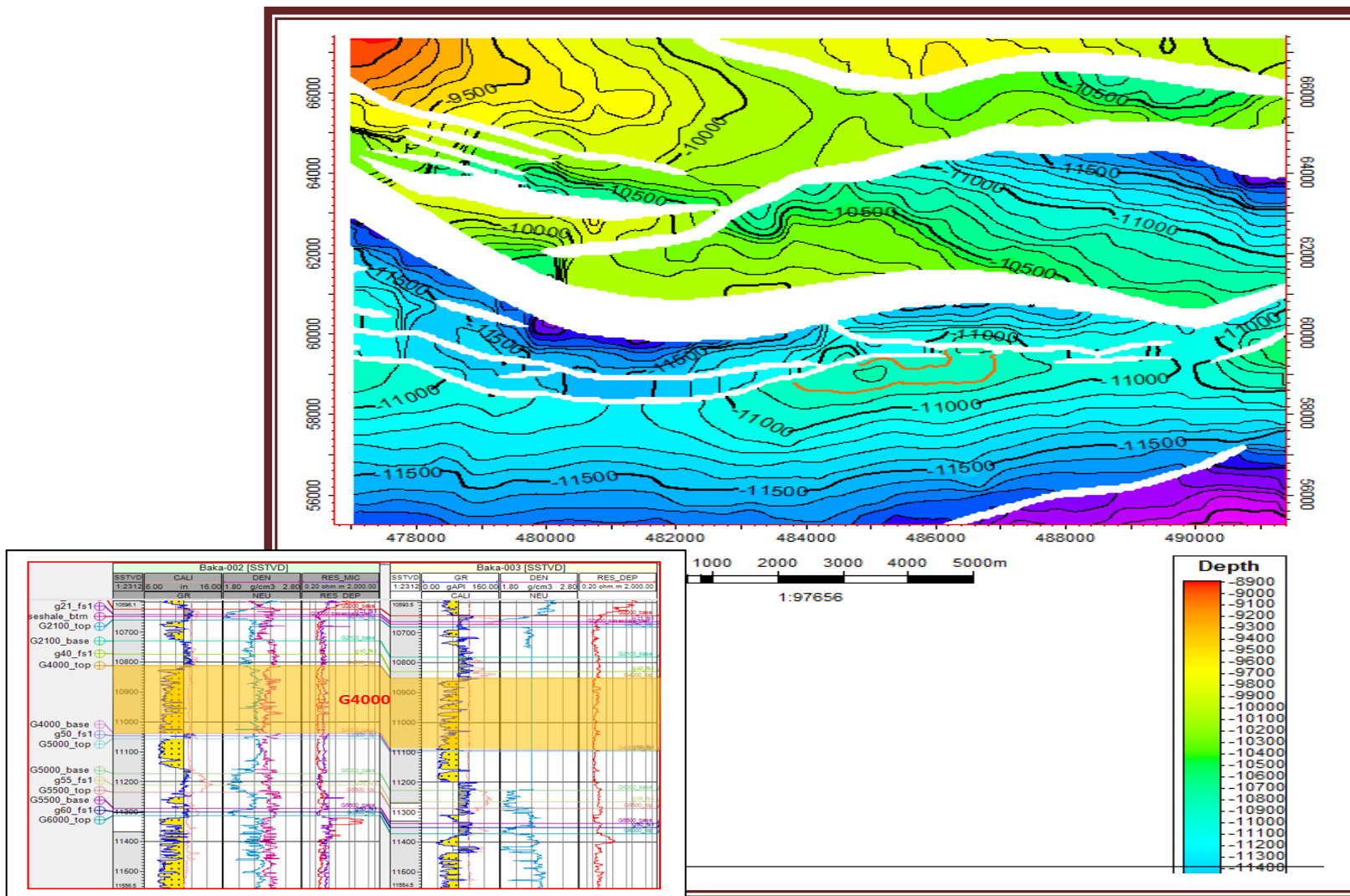
Appendix 10: G4000 Depth Structure Map and Typical Stratigraphic Correlation of G4000

223
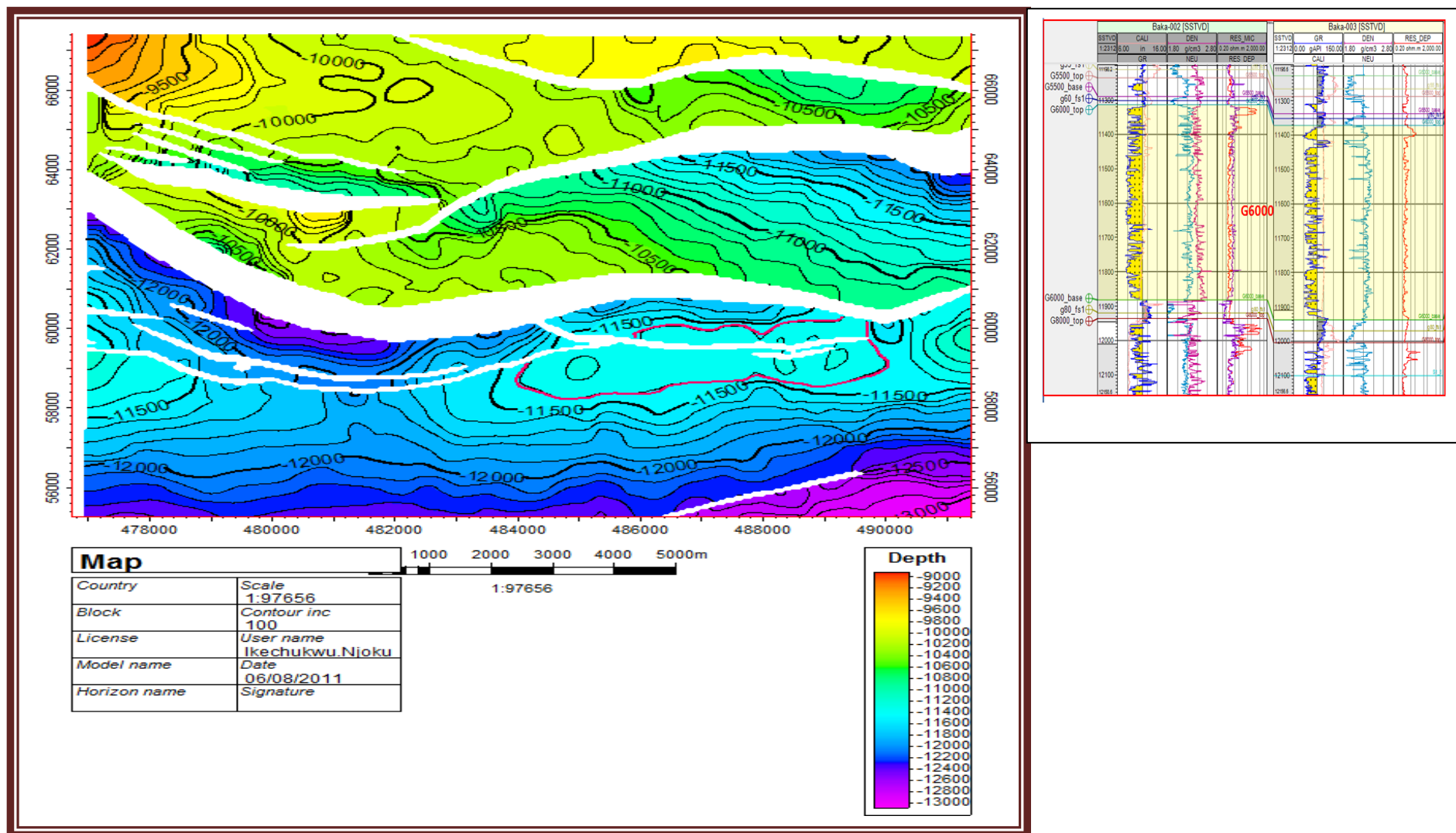
Appendix 11: G6000 Depth Structure Map and Typical Stratigraphic Correlation of G6000
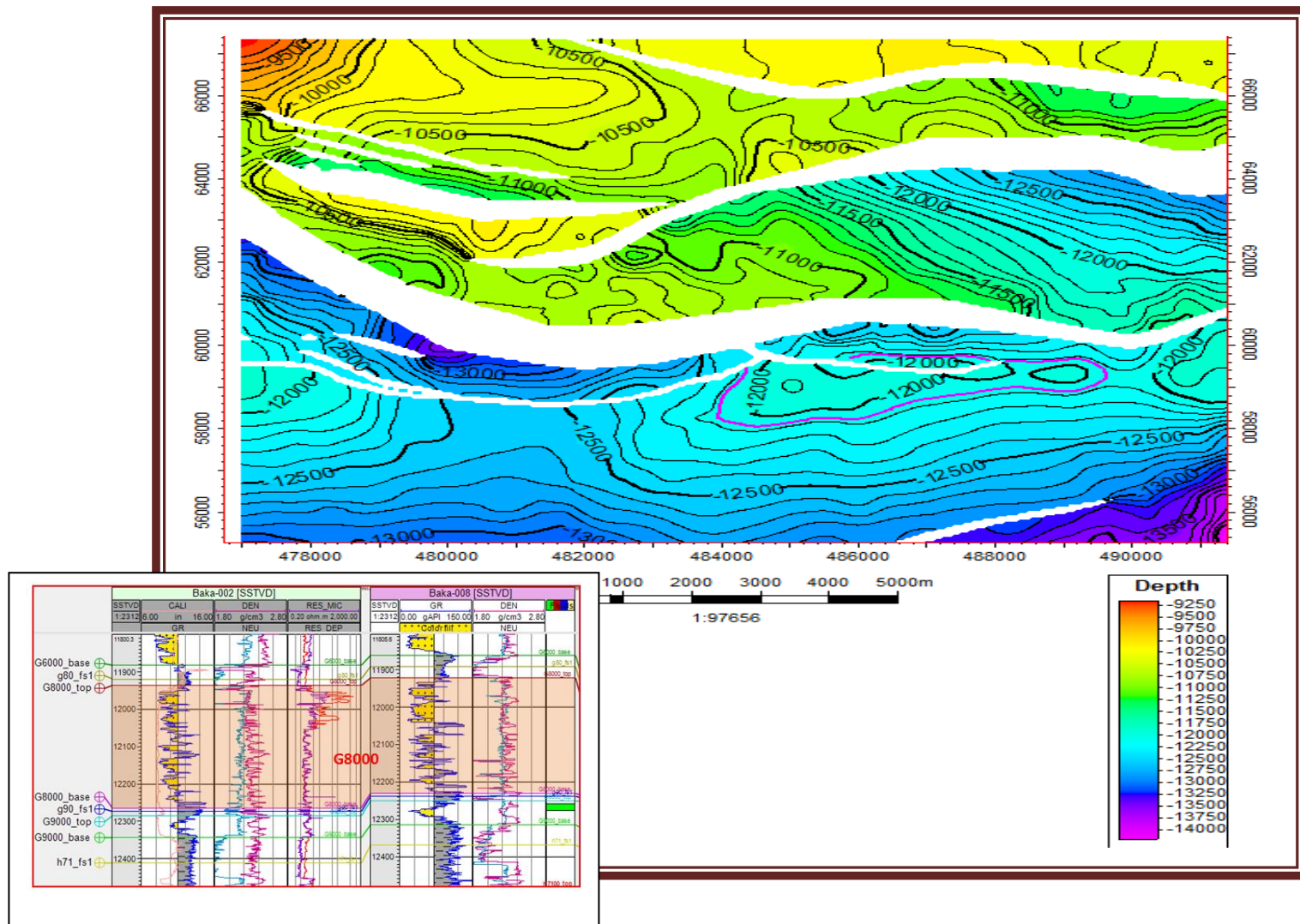
Appendix 12: G8000 Depth Structure Map and Typical Stratigraphic Correlation of G8000
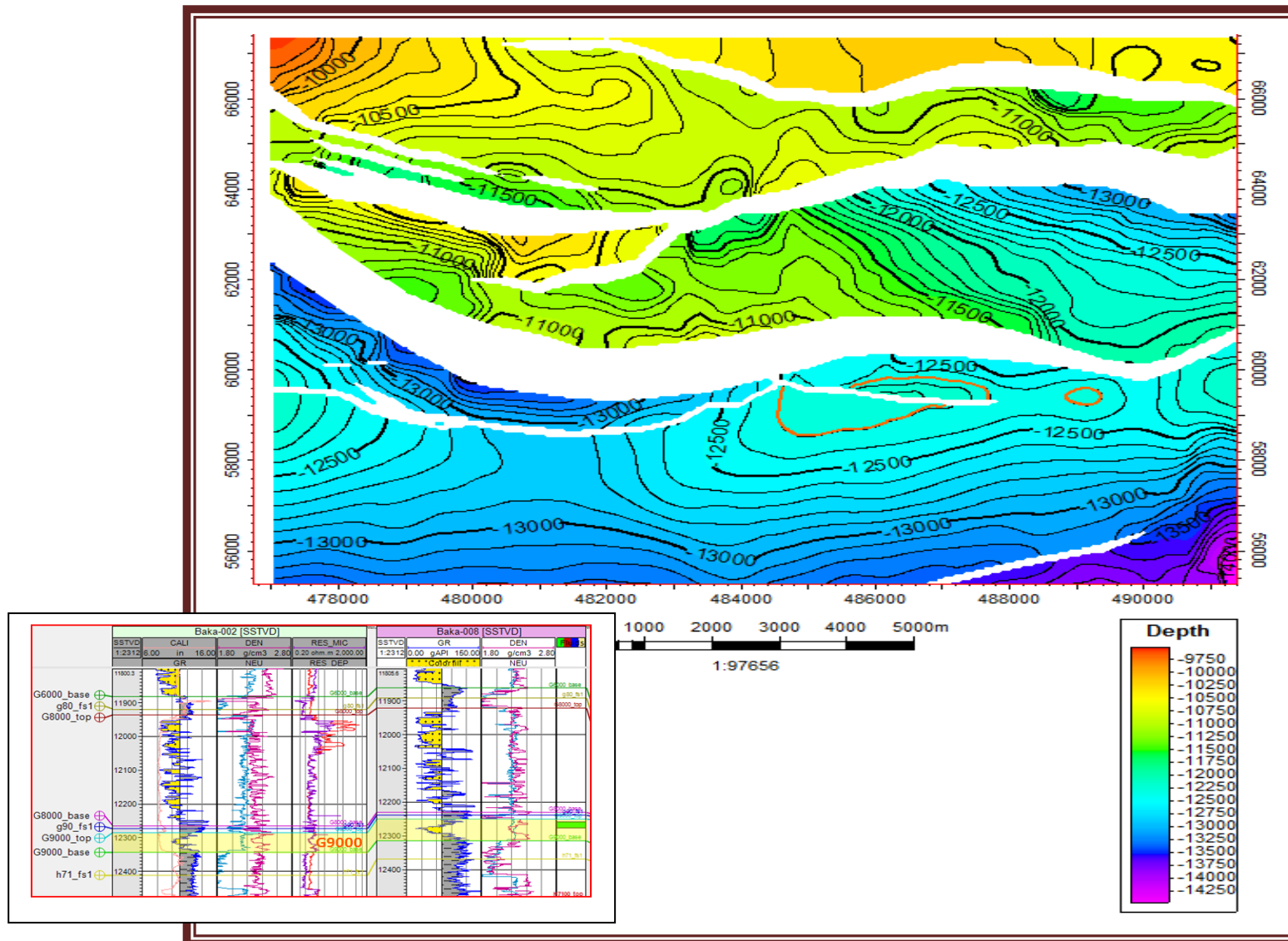
Appendix 13: G9000 Depth Structure Map and Typical Stratigraphic Correlation of G9000
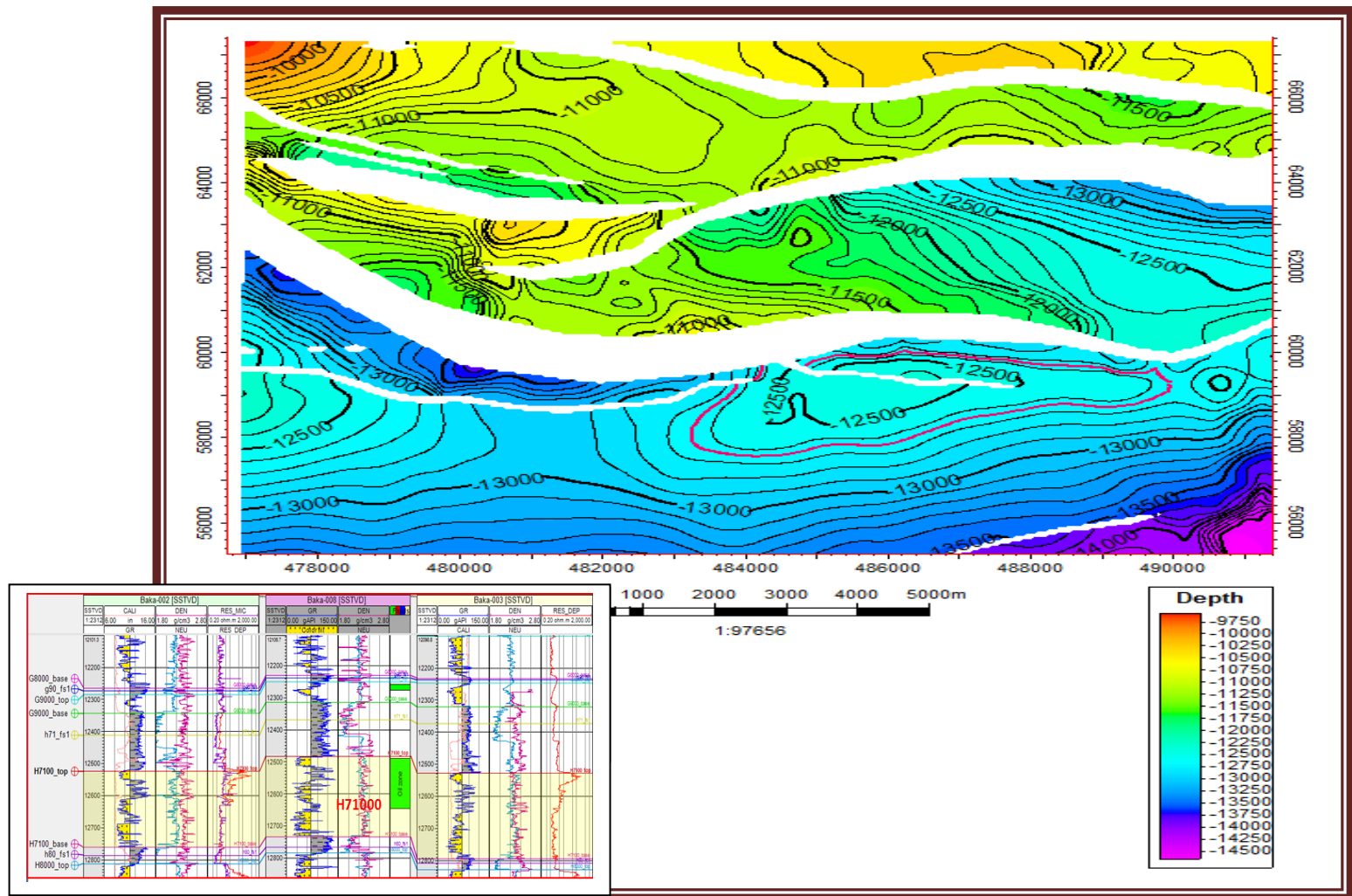
Appendix 14: H7100 Depth Structure Map and Typical Stratigraphic Correlation of H7100

Appendix 15: H8000 Depth Structure Map and Typical Stratigraphic Correlation of H8000

228

Appendix 16: K2000 Depth Structure Map and Typical Stratigraphic Correlation of K2000
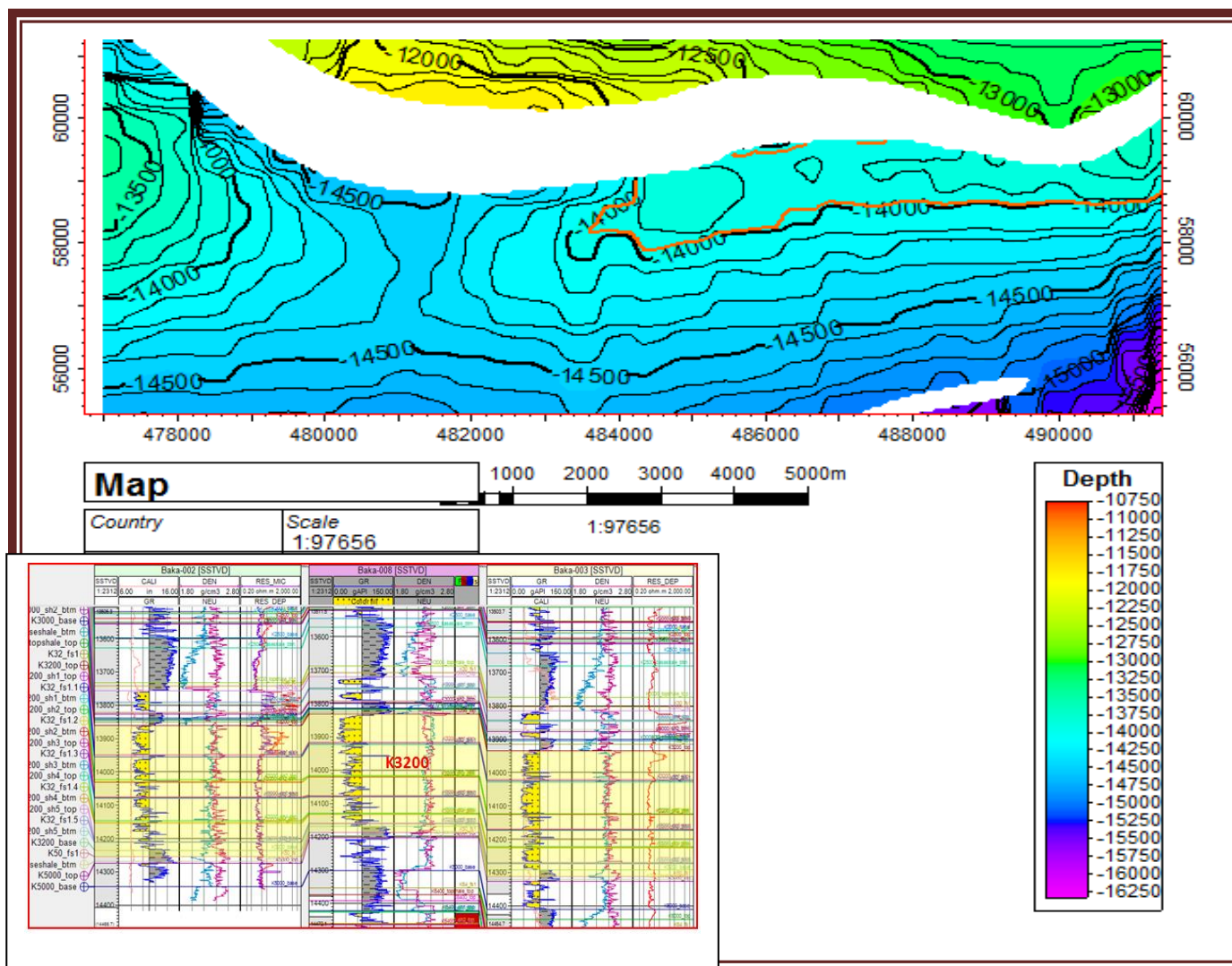
Appendix 17: K3200 Depth Structure Map and Typical Stratigraphic Correlation of K3200
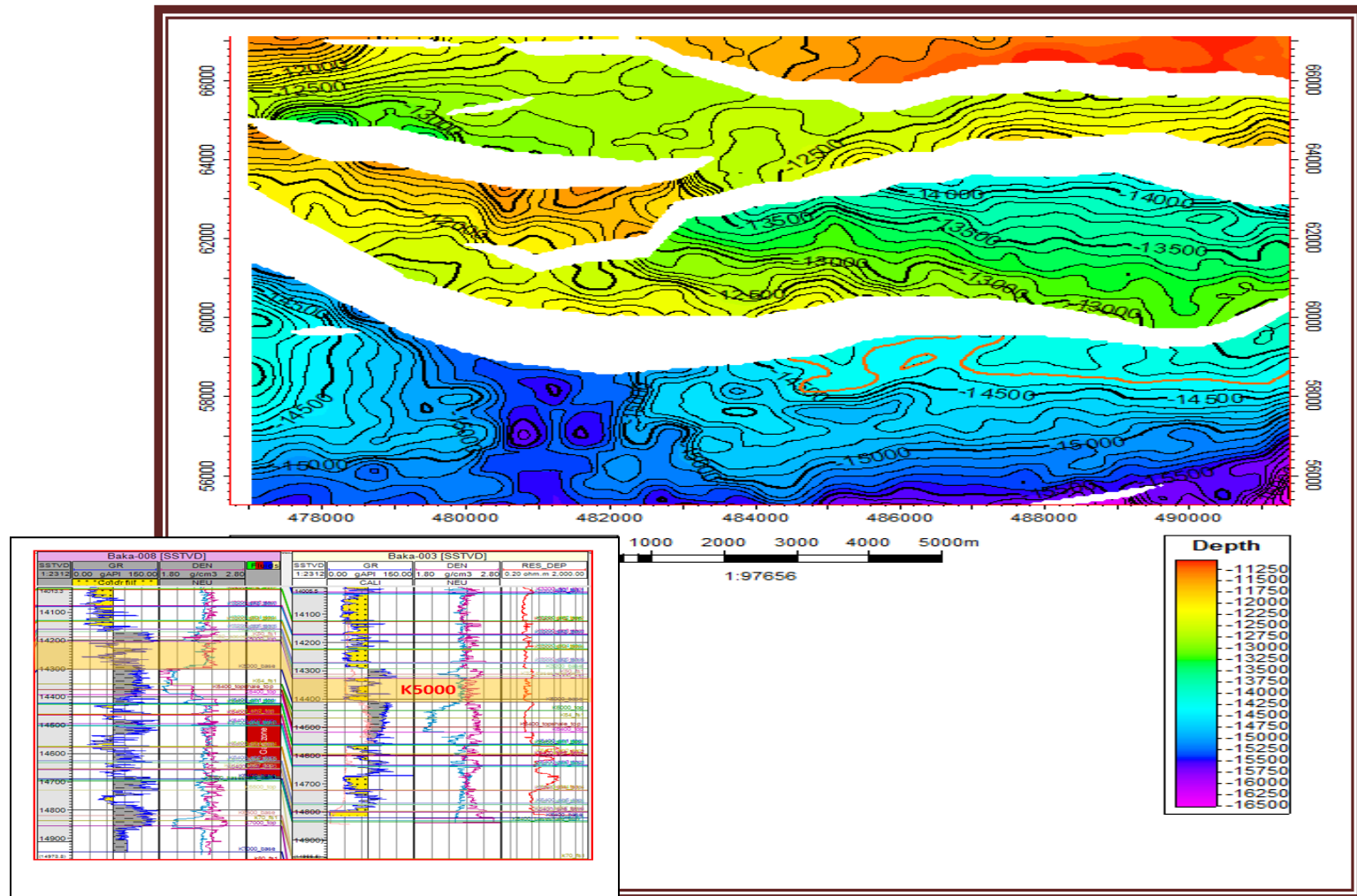
Appendix 18: K5000 Depth Structure Map and Typical Stratigraphic Correlation of K5000

Appendix 19: K6400 Depth Structure Map and Typical Stratigraphic Correlation of K6400
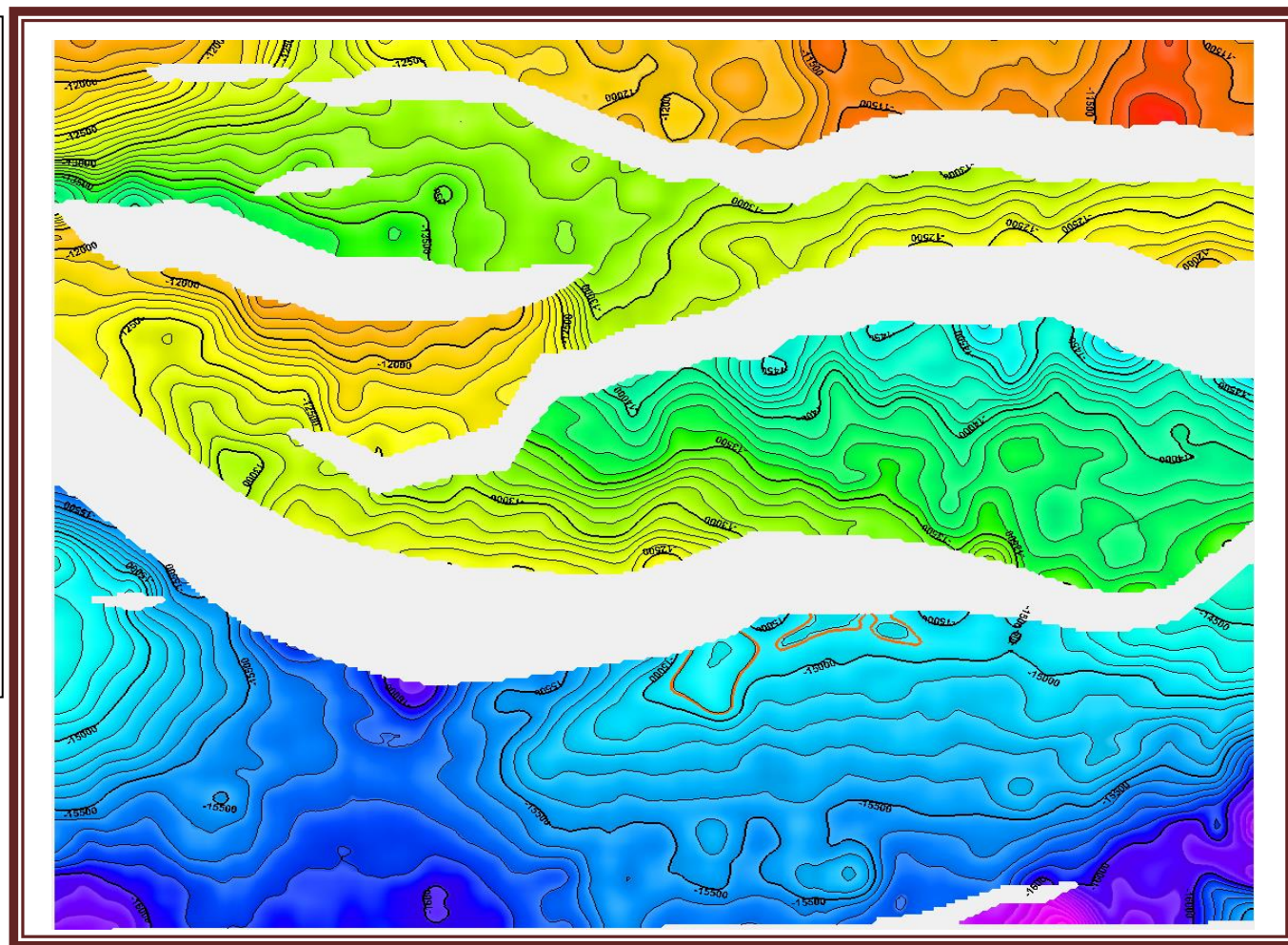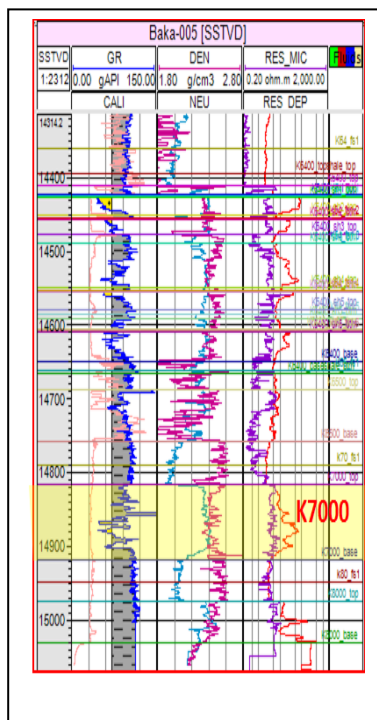
Appendix 20: K7000 Depth Structure Map and Typical Stratigraphic Correlation of K7000

Stratigraphic Correlations
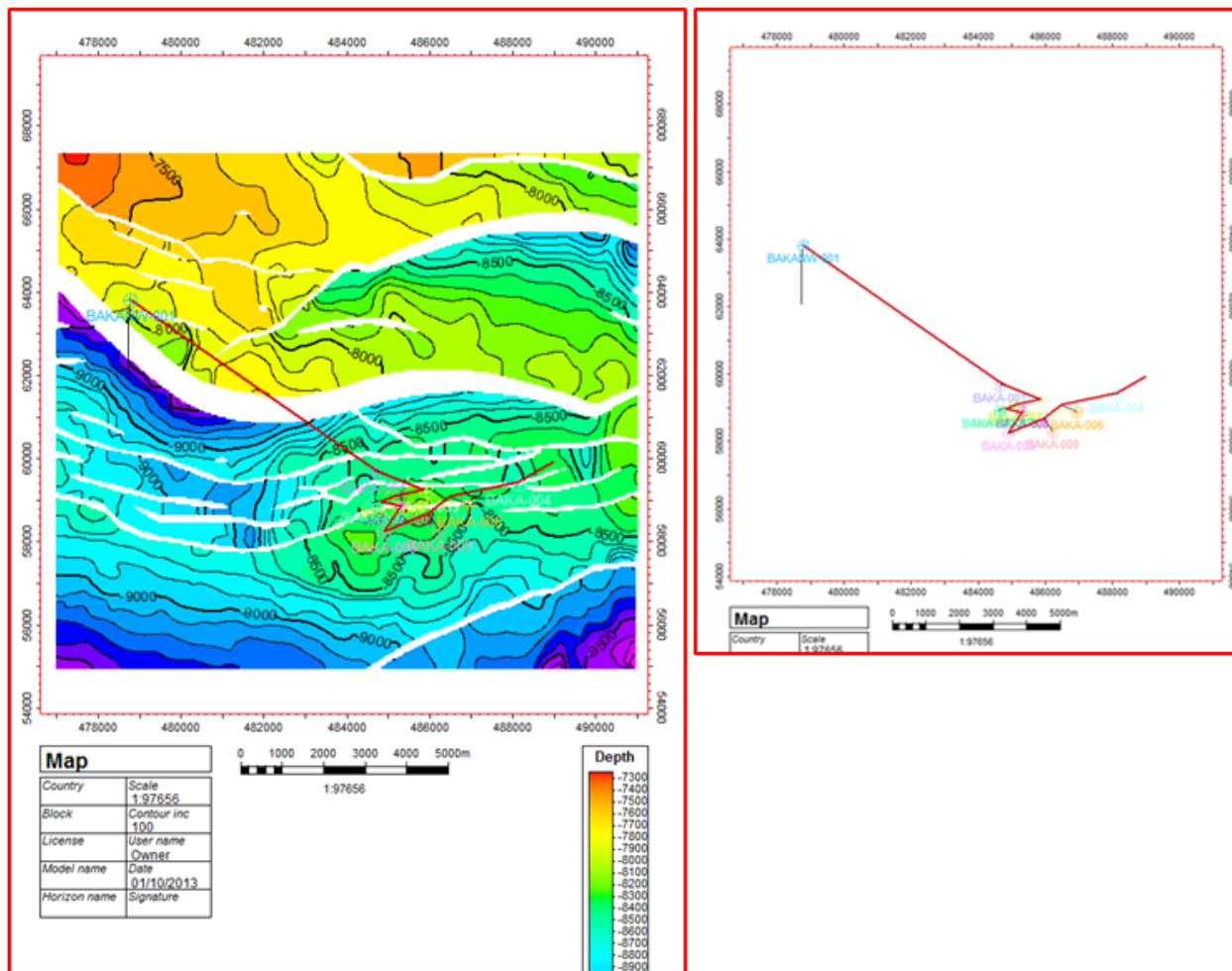
Appendix 21: Correlation Transect used for the study
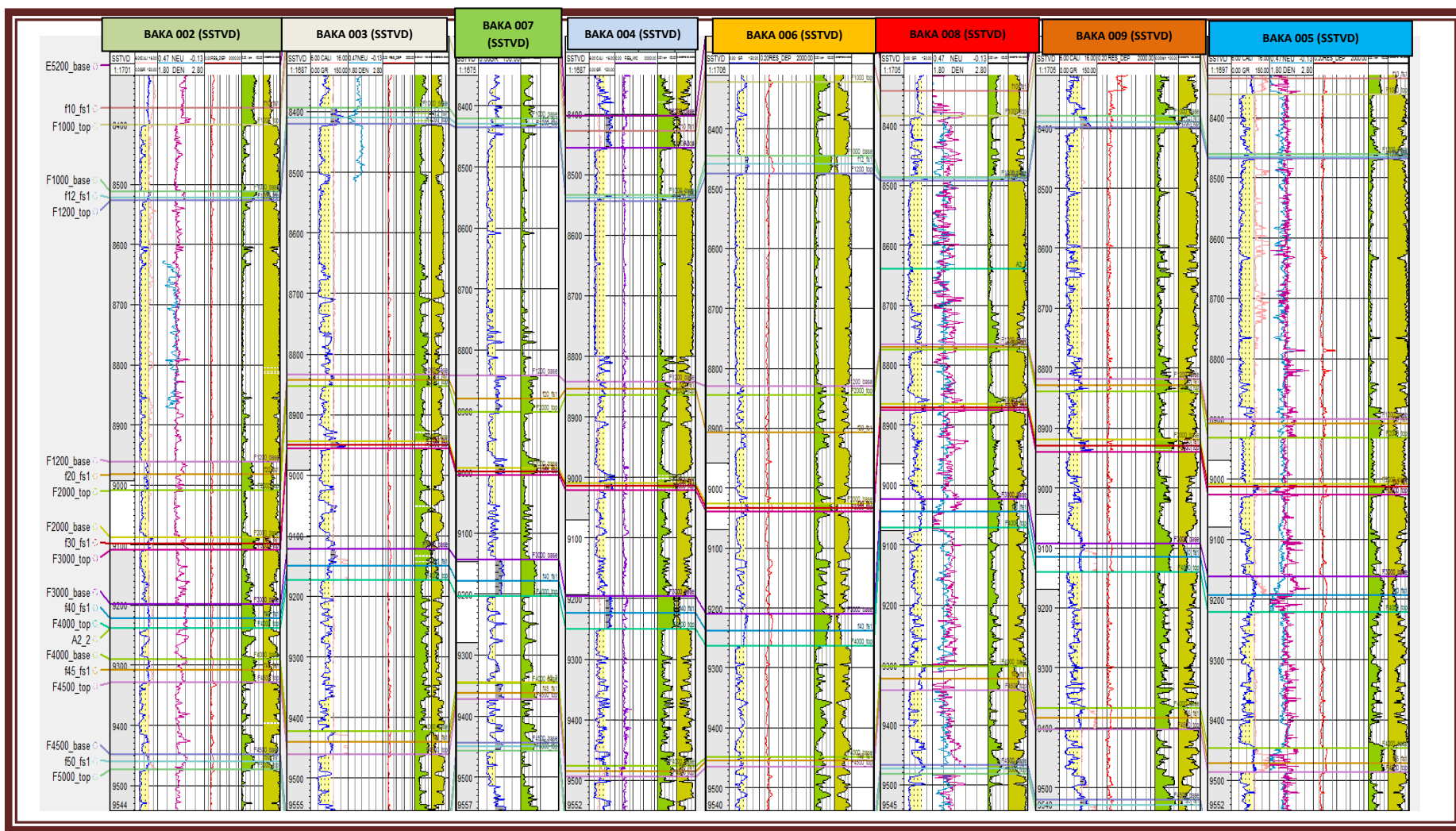
Appendix 22: Well Correlation showing F - Horizons
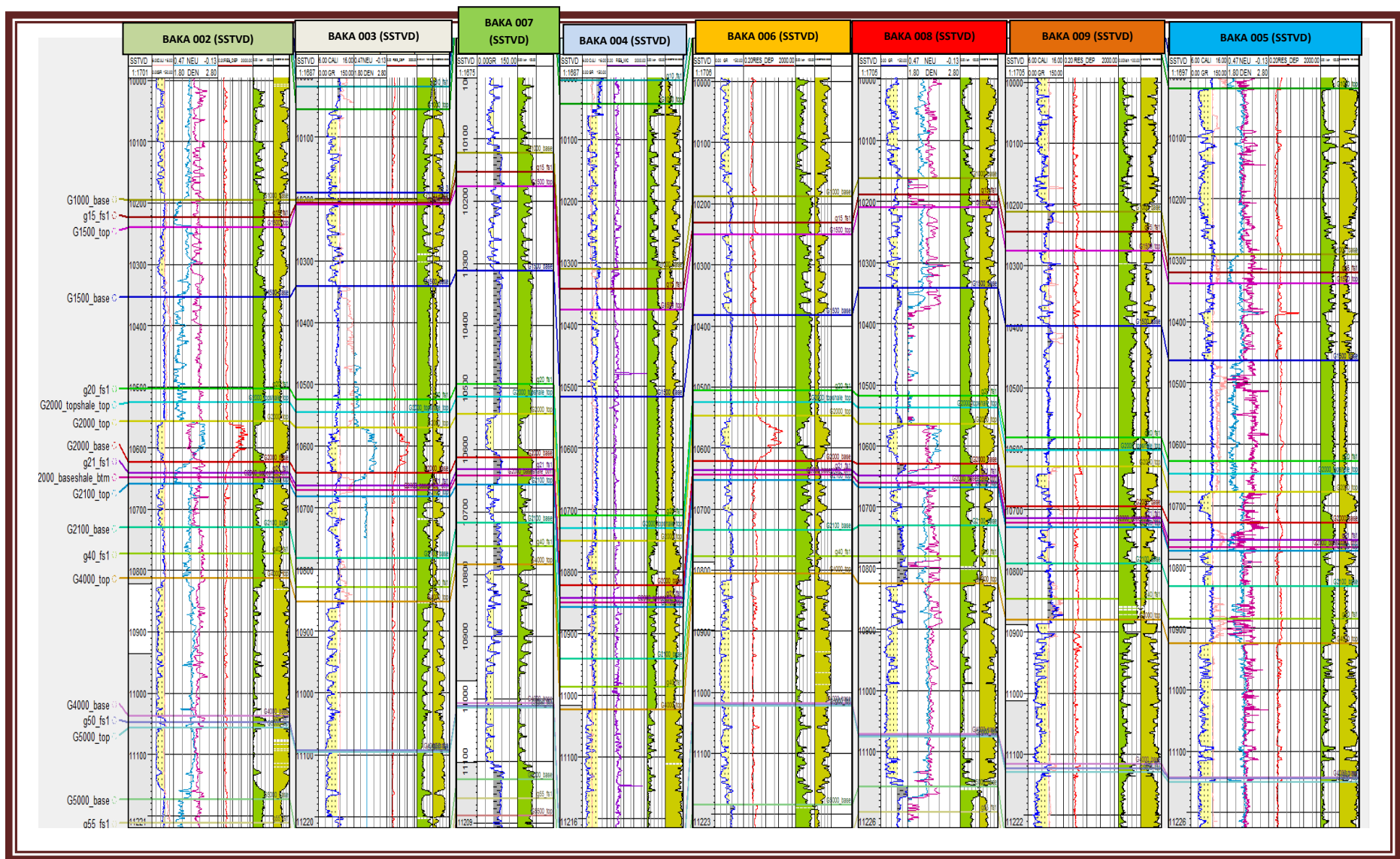
Appendix 23: Well Correlation showing G2000 and G4000

237
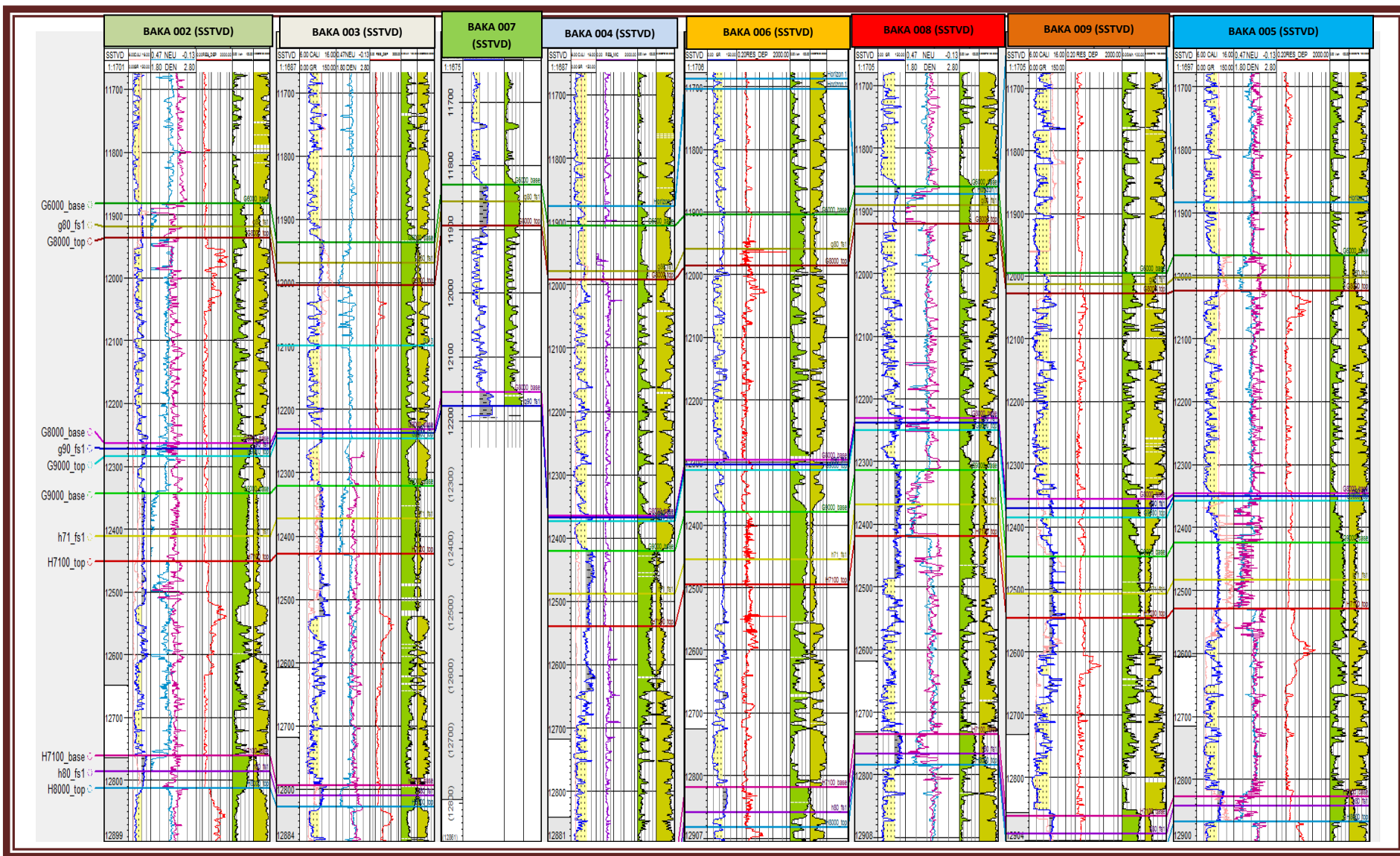
Appendix 24: Well Correlation showing G6000 and H7100
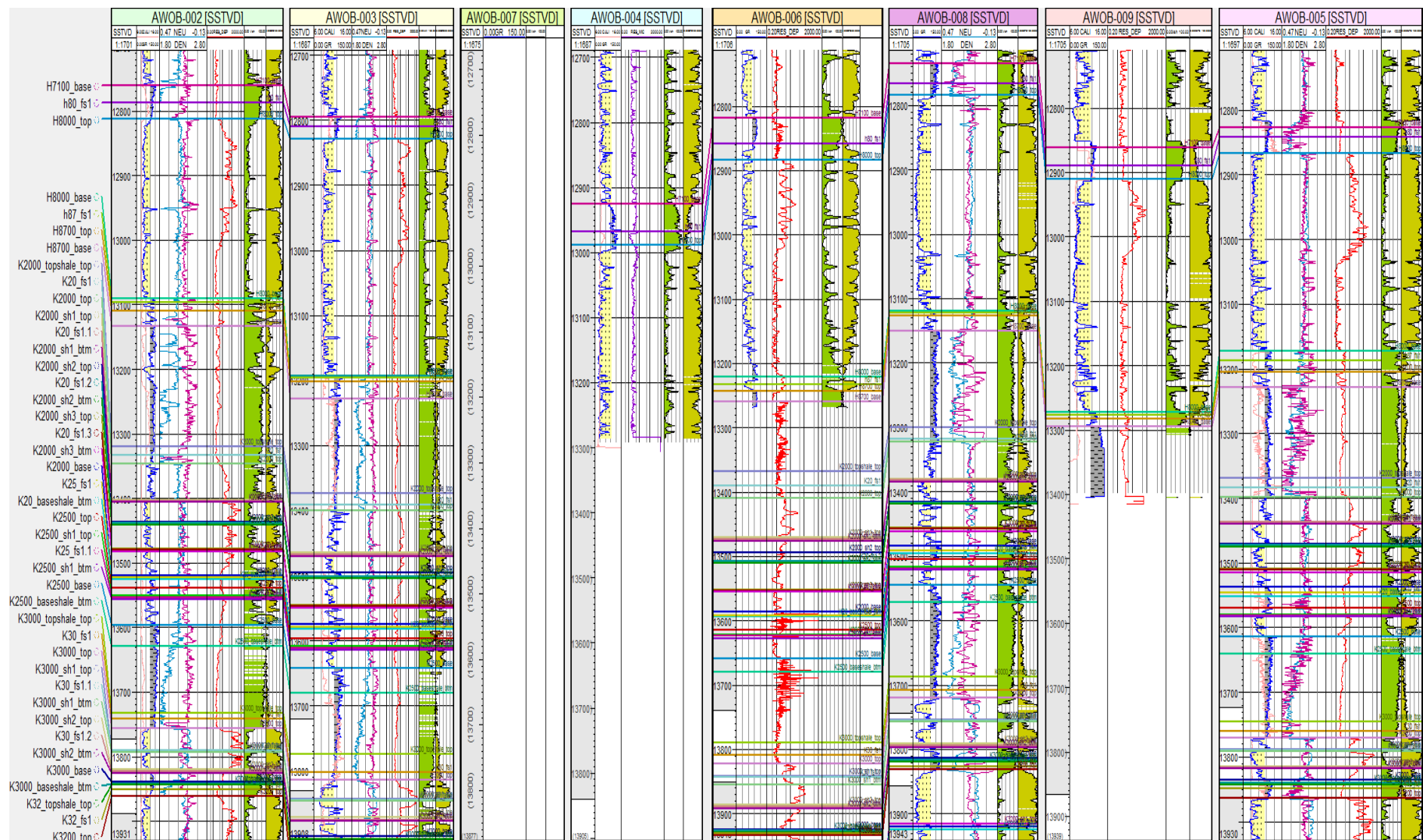
Appendix 25: Well Correlation showing H7100 Base and K3200 Top
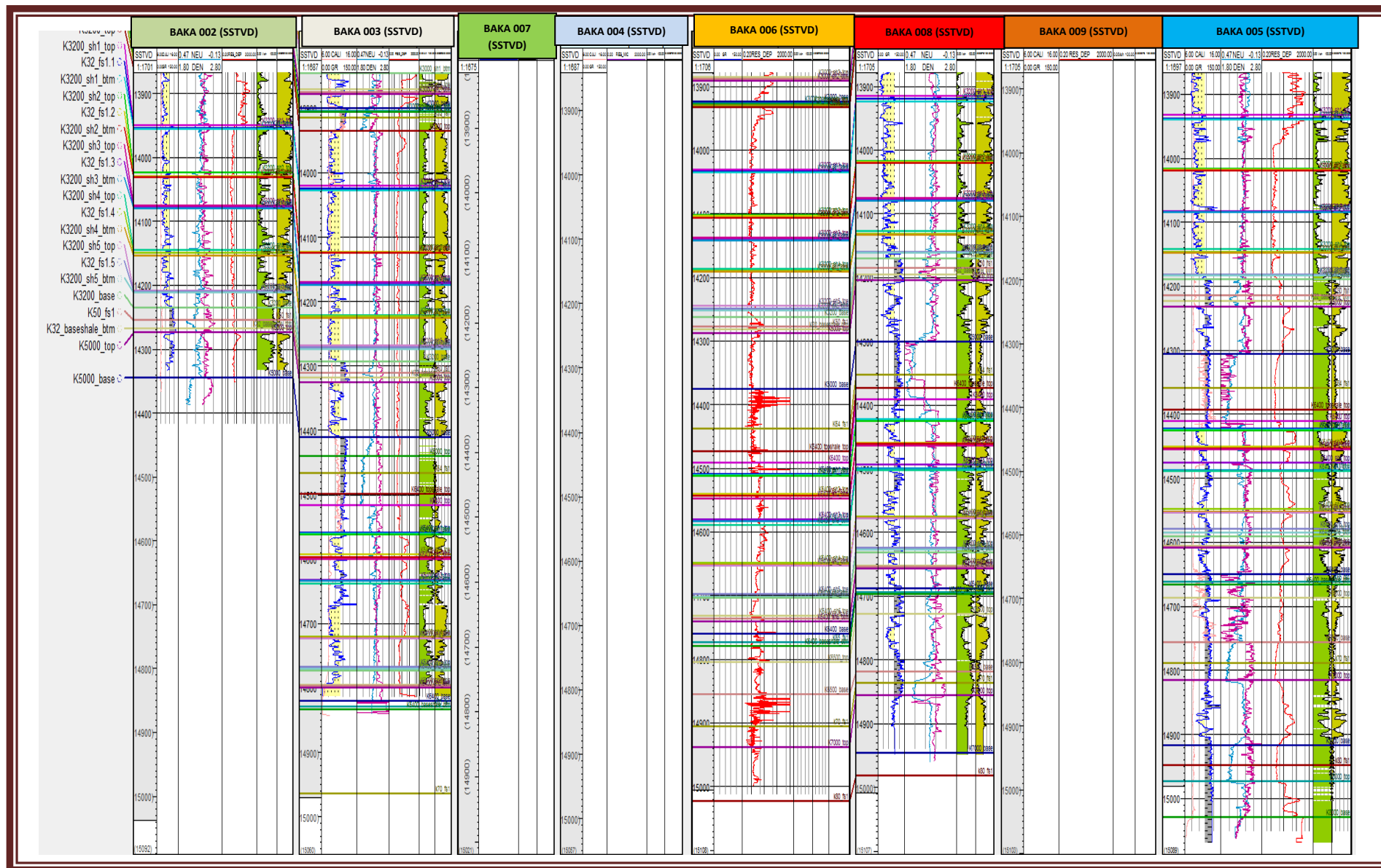
Appendix 26: Well correlation showing K3200 – K500 Base
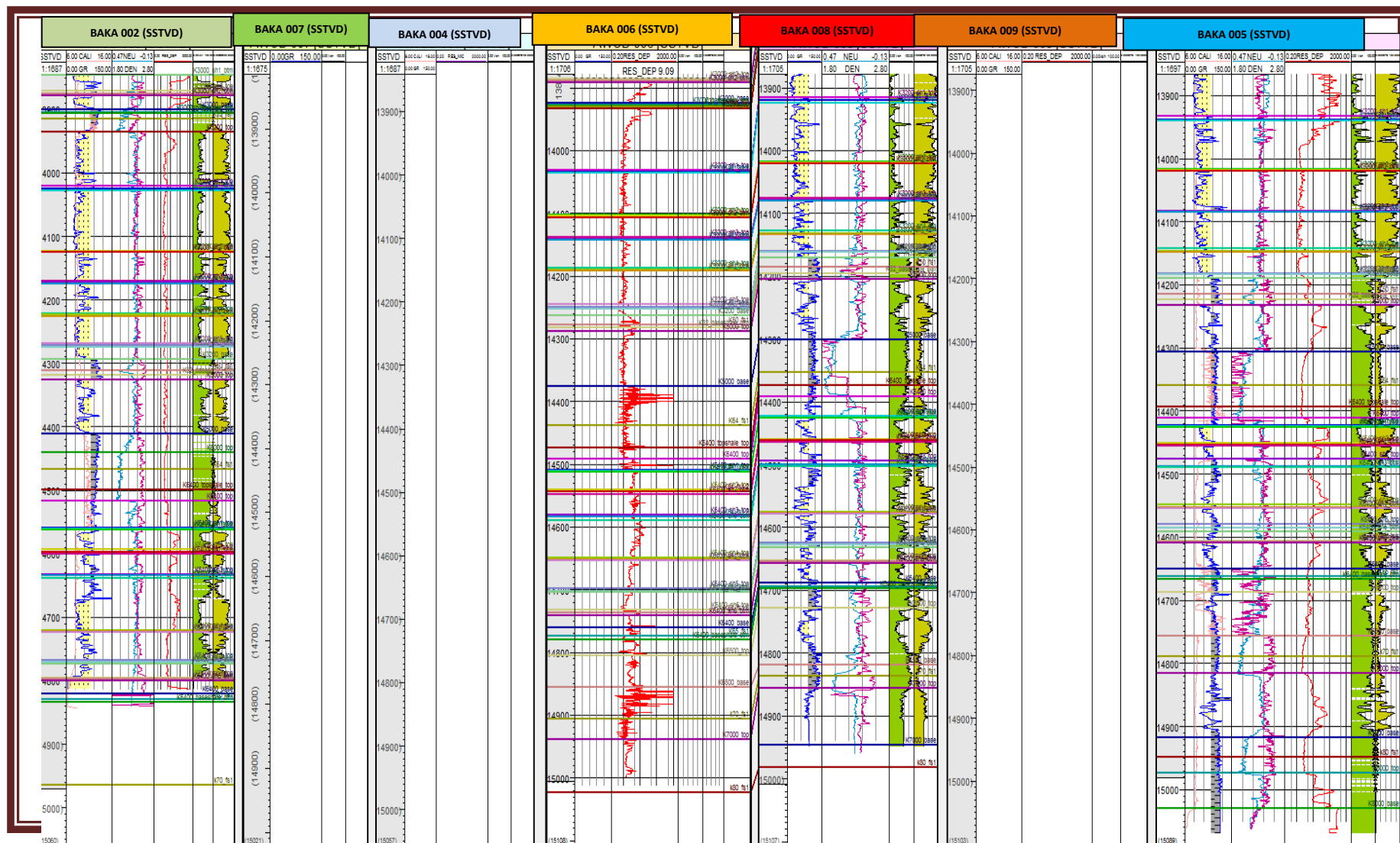
Appendix 27: Well Correlation showing K3000-K6400
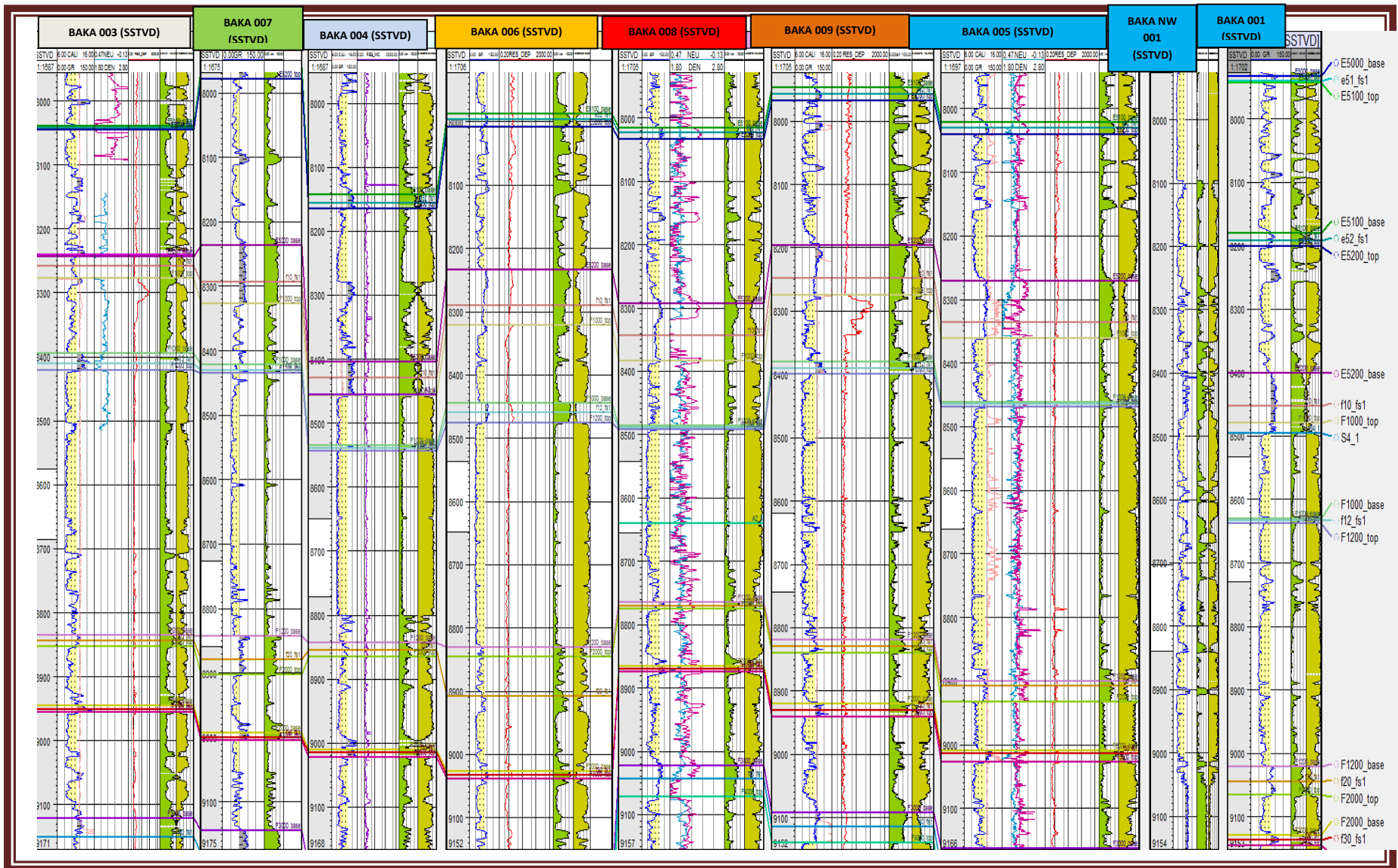
Appendix 28: Well Correlation showing F1000 at well 001 and other wells
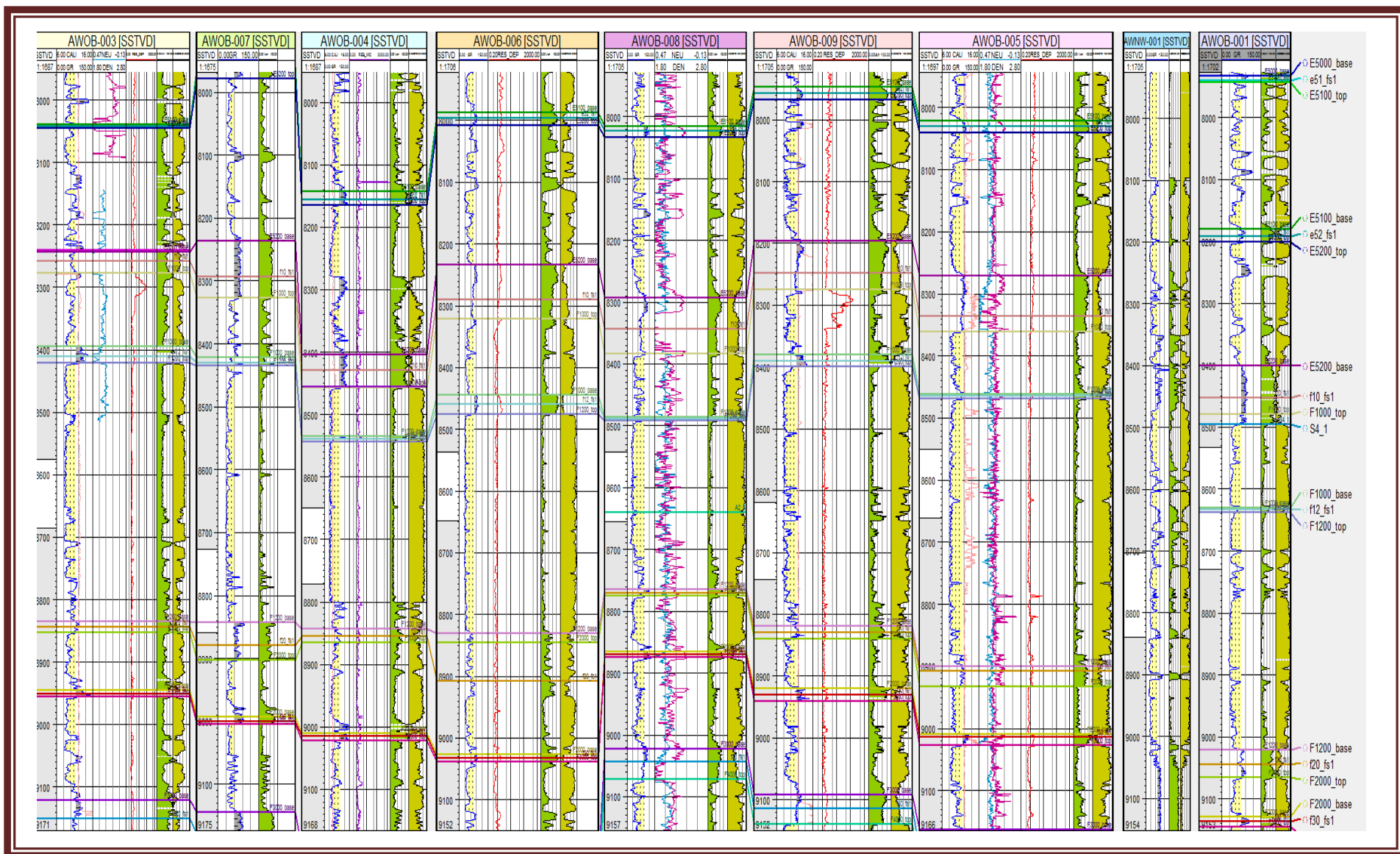
Appendix 29: Well Correlation showing G2000 Top - G6000 Top at well 001 and others

3D Structural Model Quality Control
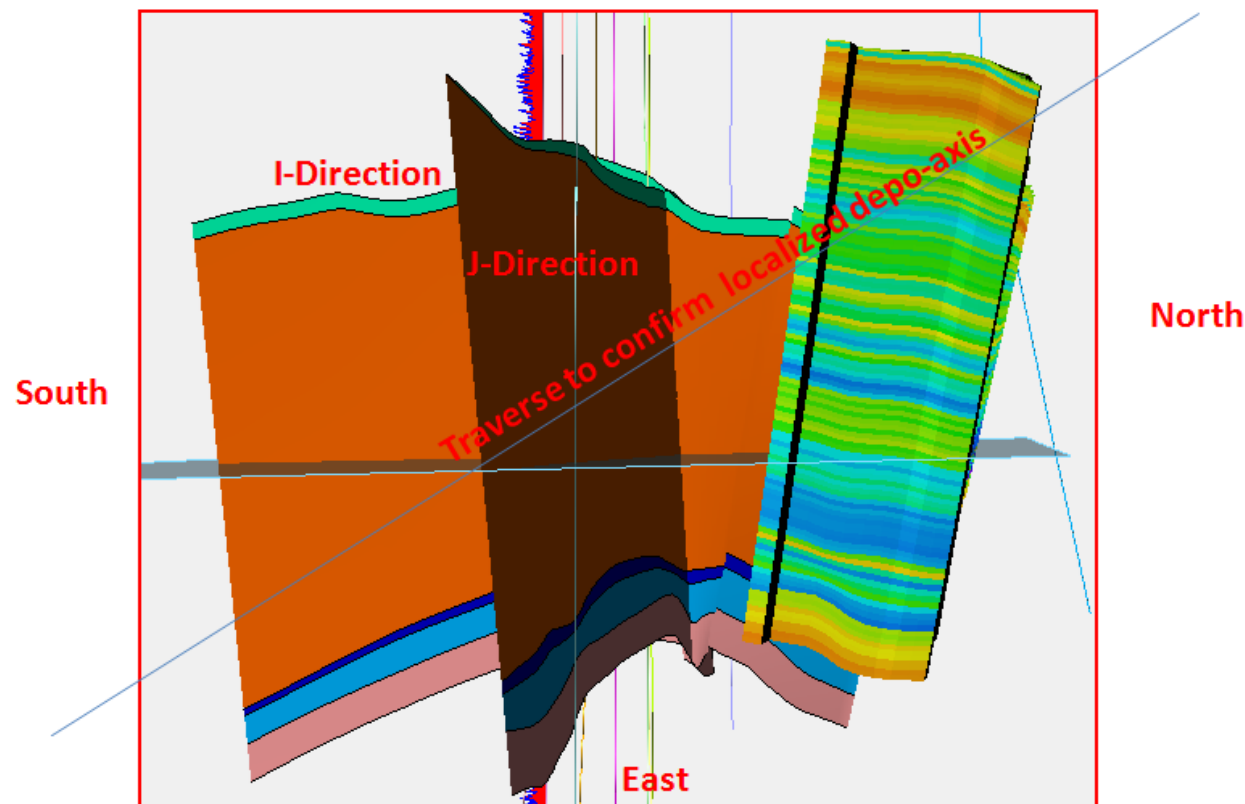
Appendix 30: Model QC using traverses in property Net-T0 -Gross reservoir Model
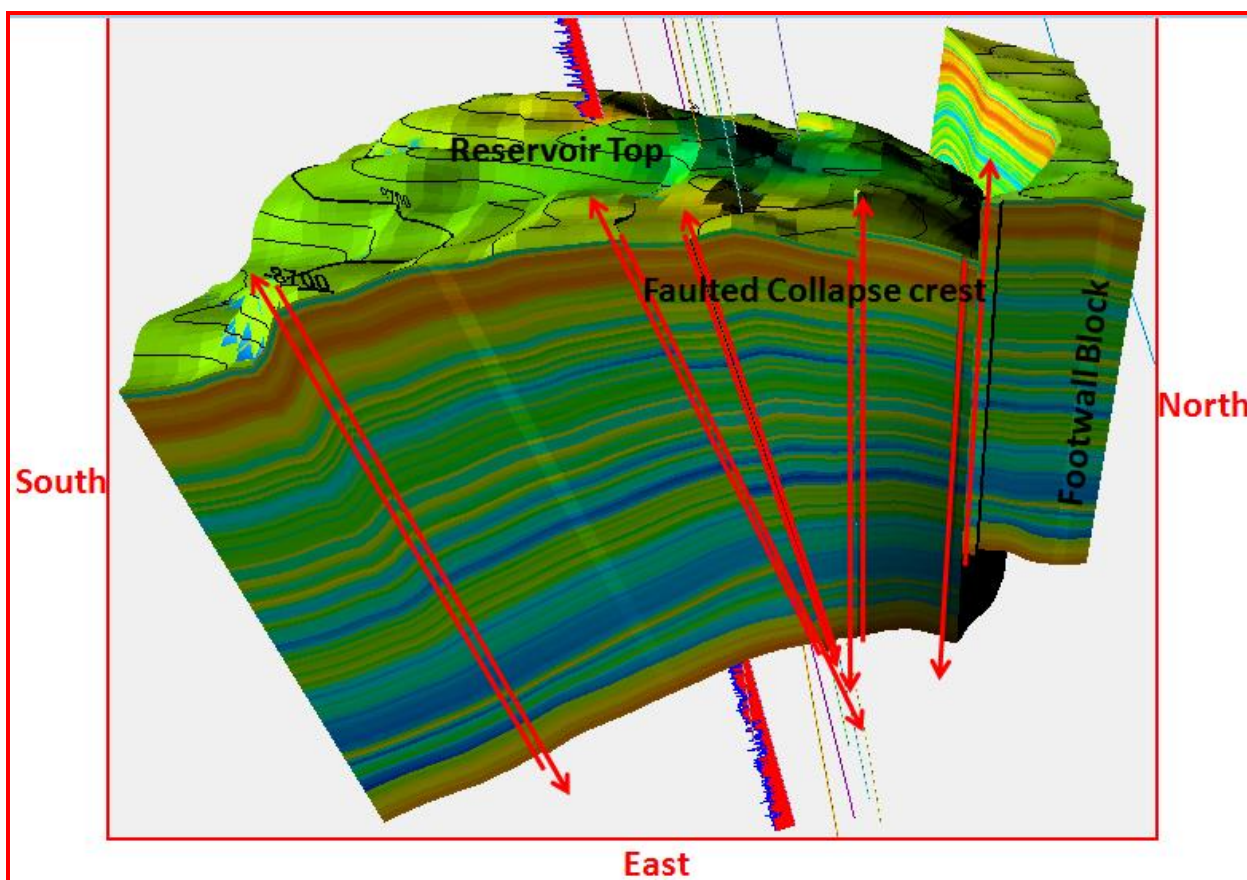
Appendix 31: 3D Structural Model showing Structural Styles of the Baka Field
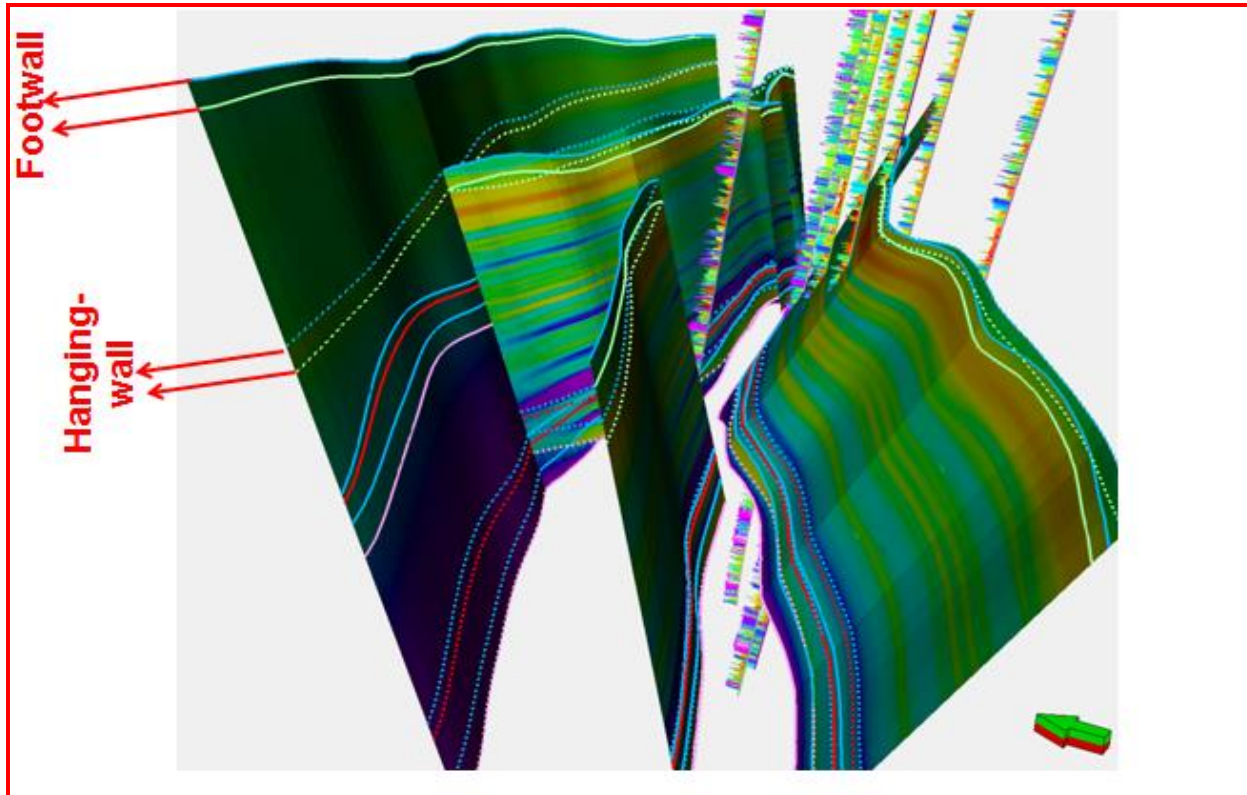
Appendix 32: Typical Hanging Wall - Footwall Fault Plane Interpretation
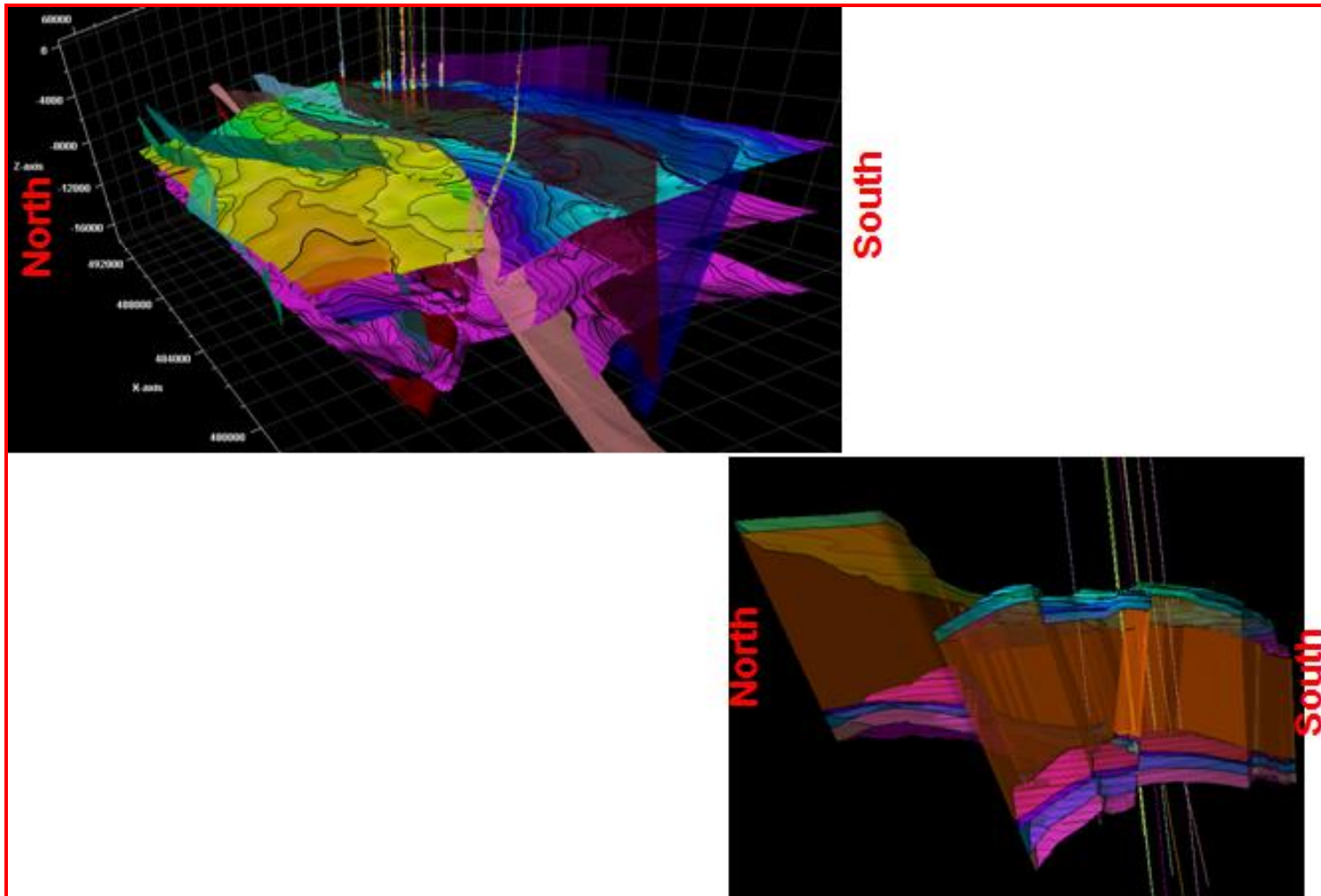
Appendix 33: Typical 3D Model QC using Transparent Model
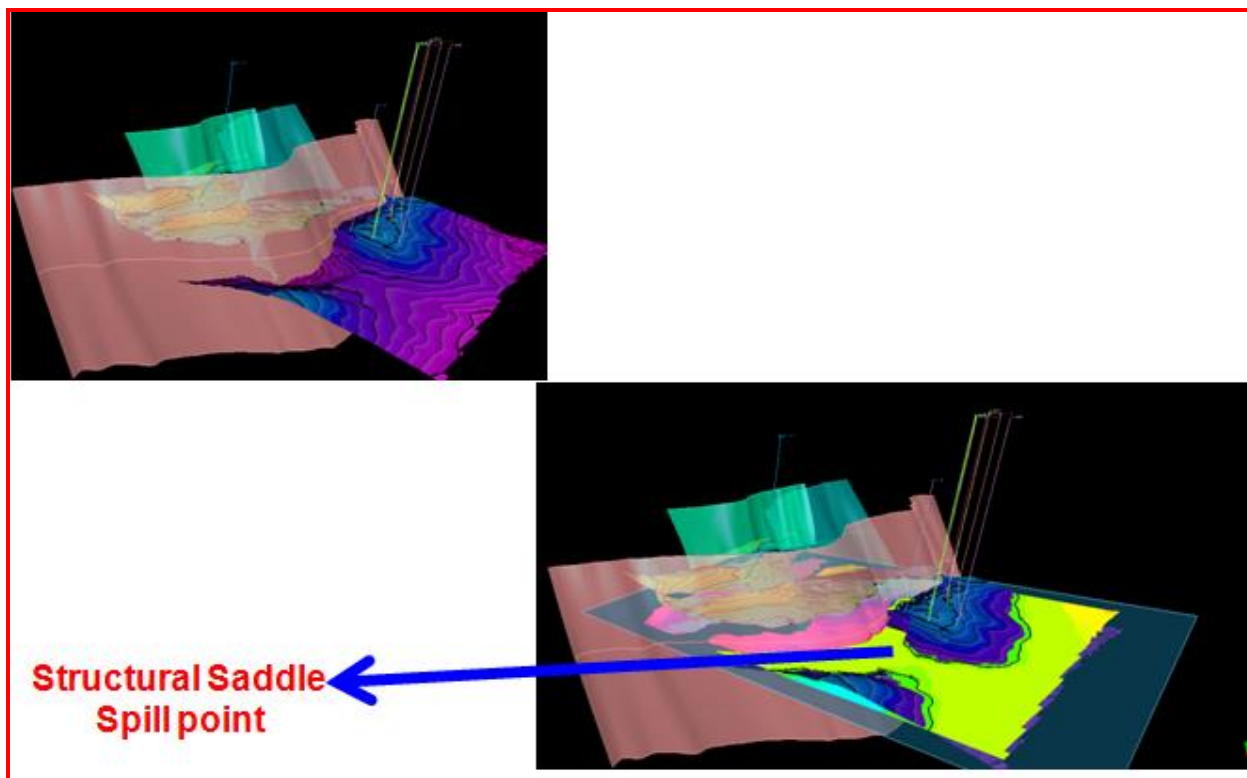
Appendix 34: Typical Structural Spill Point Interpretation using Intersection Plane on Seismic Grid G8000
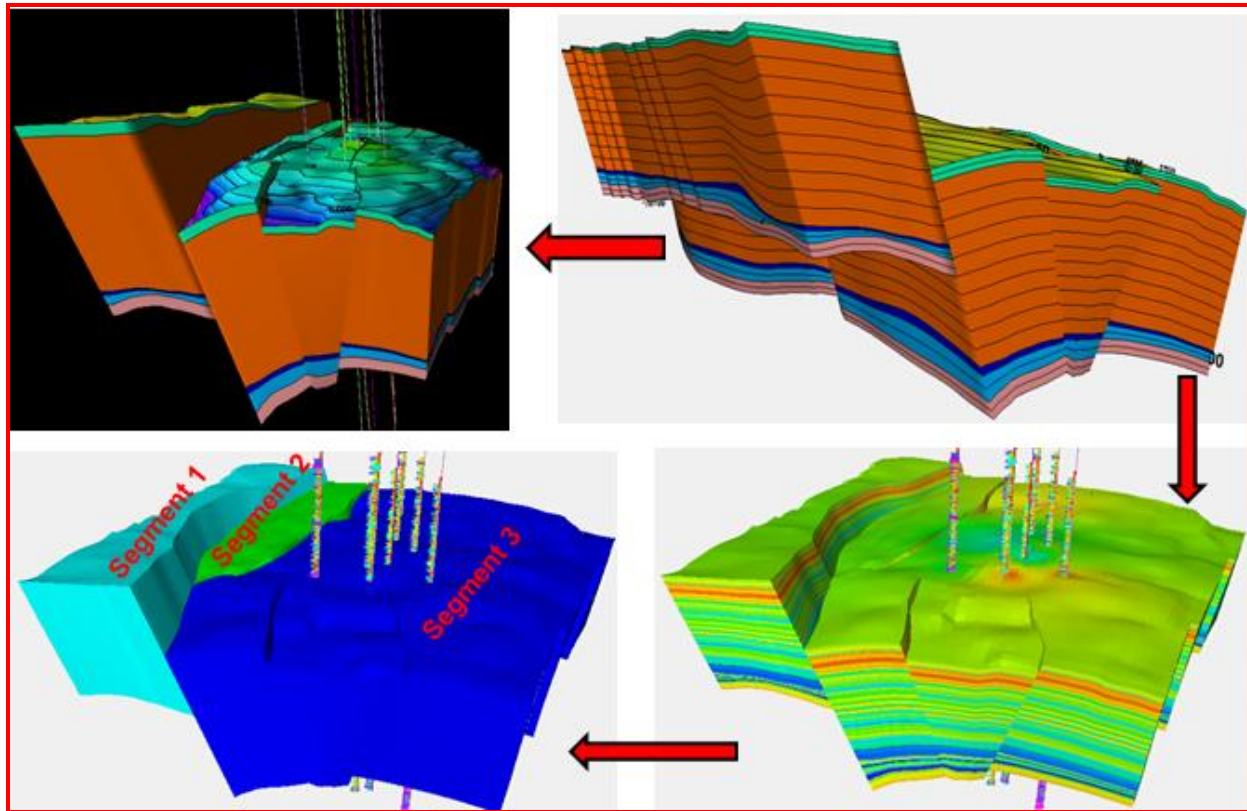
Appendix 35: Typical Interpreted 3D Model Showing Horizon, Zone, Property (Vsh) and Segment.
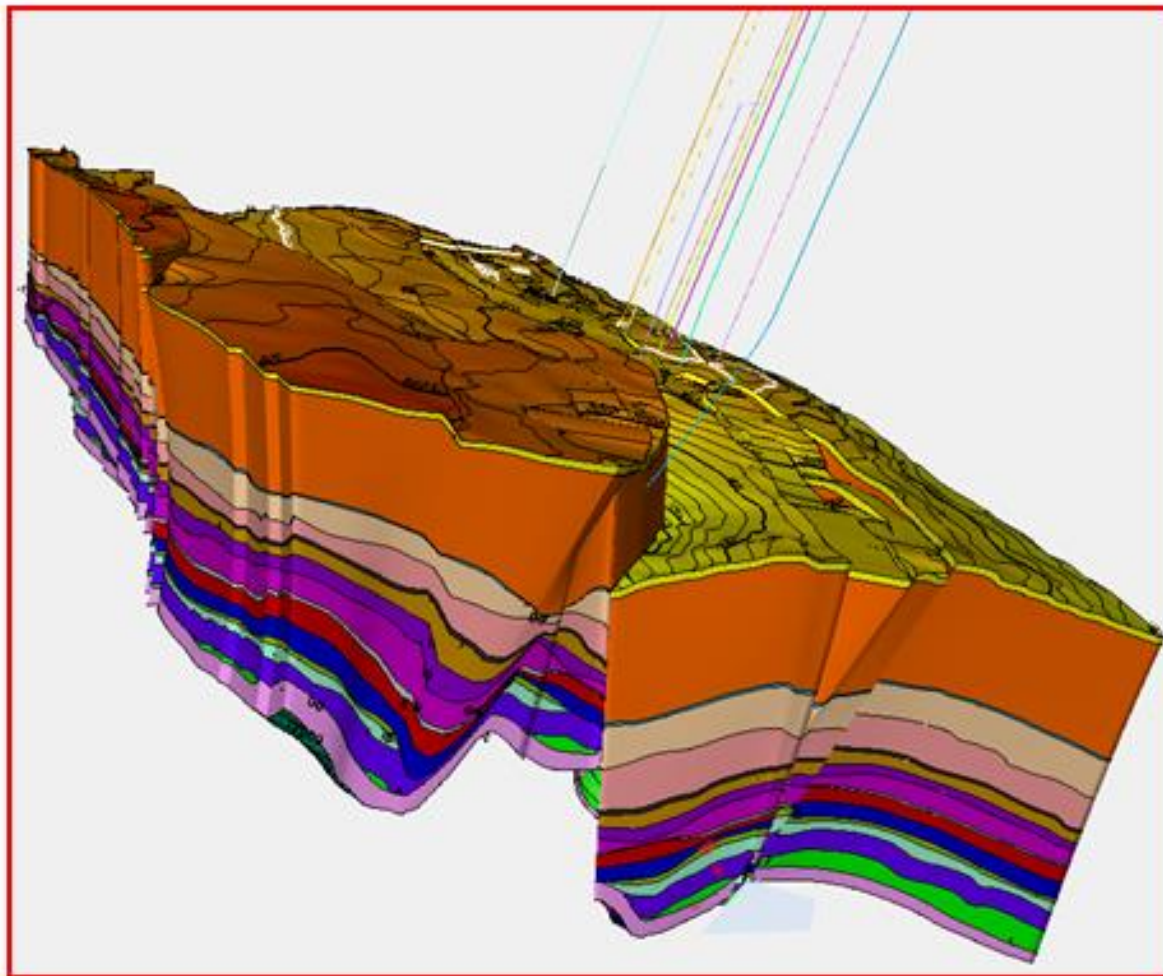
Appendix 36: 3D Structural Model of all Interpreted Horizon at Zone Model Stage showing North west
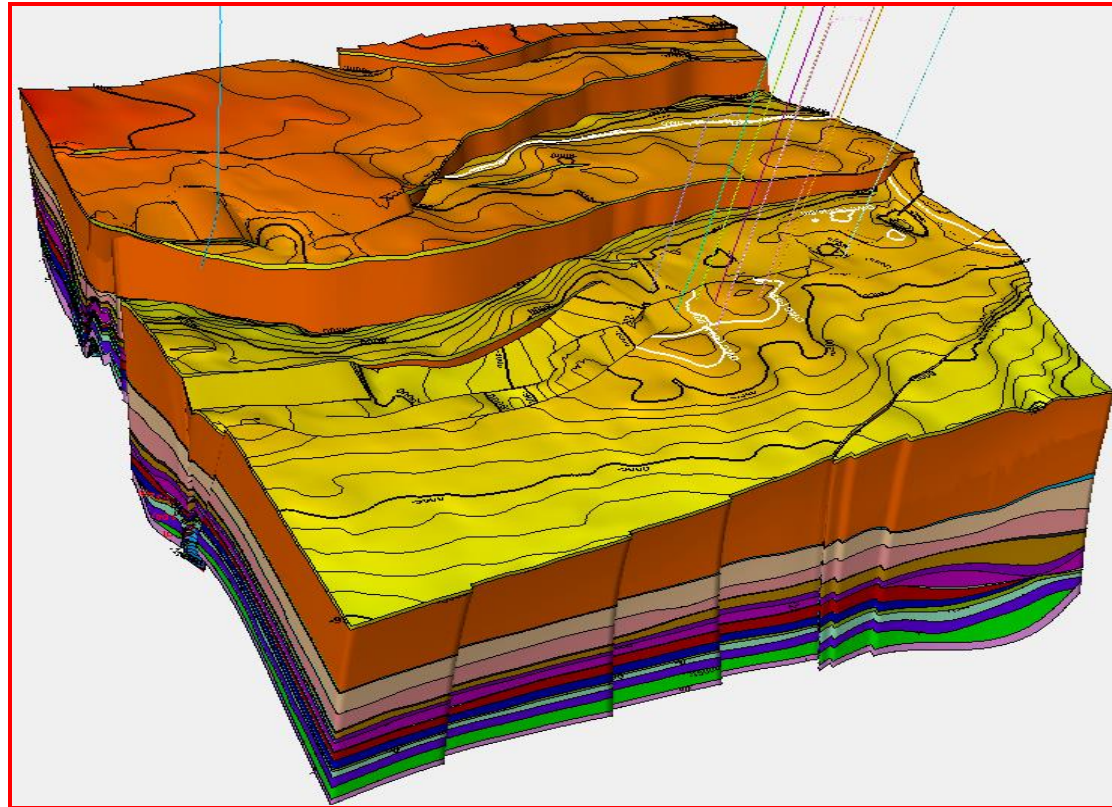
Appendix 37: 3D Structural Model of all Interpreted Horizon at Zone Model Stage showing South
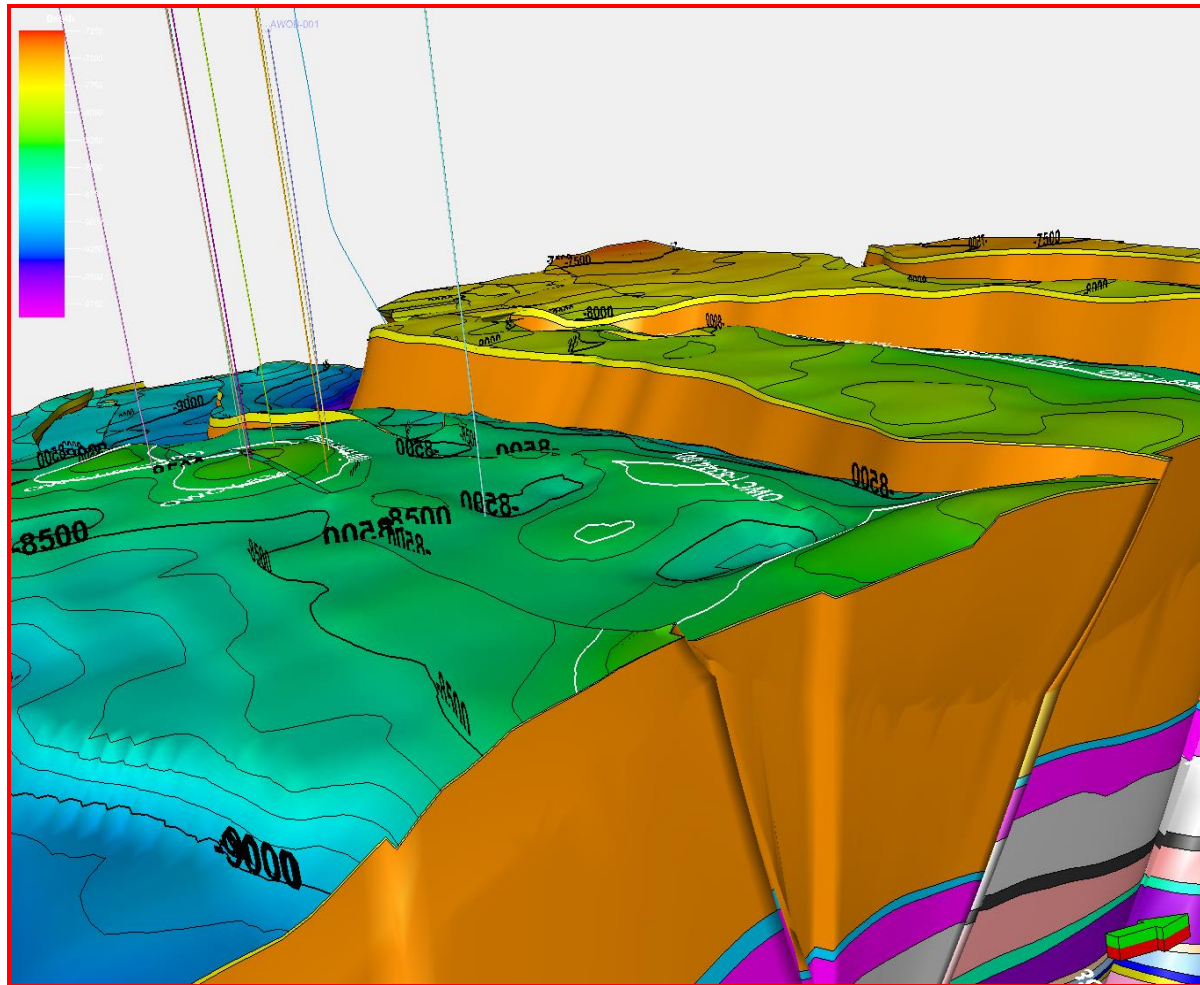
Appendix 38: 3D Structural Model of all Interpreted Horizon at Zone Model Stage showing East
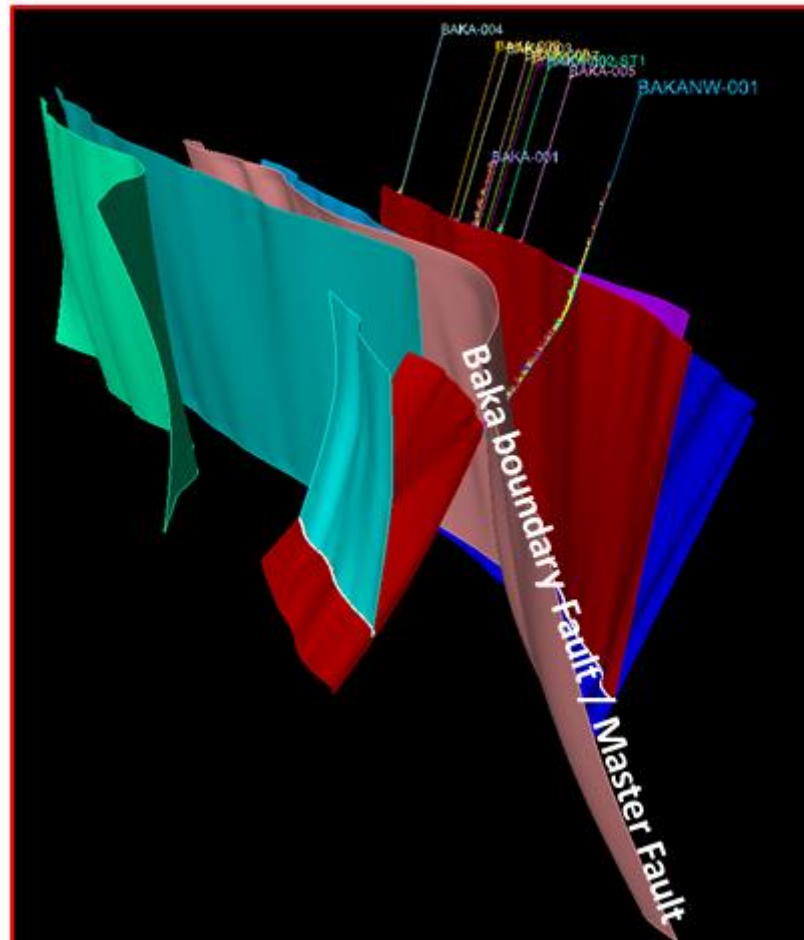
Appendix 39: Fault Structural Framework Model of the Baka Field
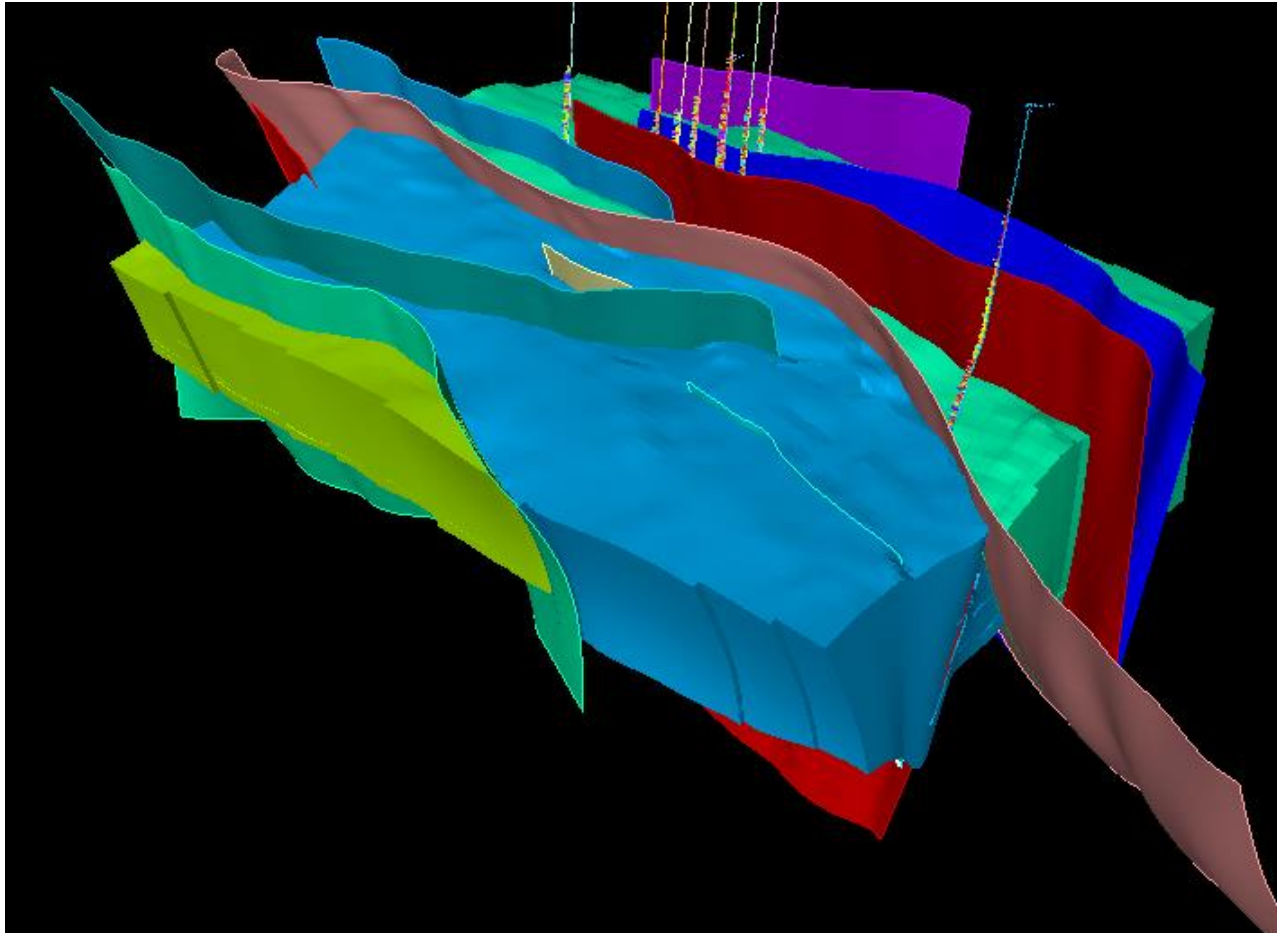
Appendix 40: 3D Structural Segment Model with Fault Structural Framework

Seismic Interpretation Quality Control
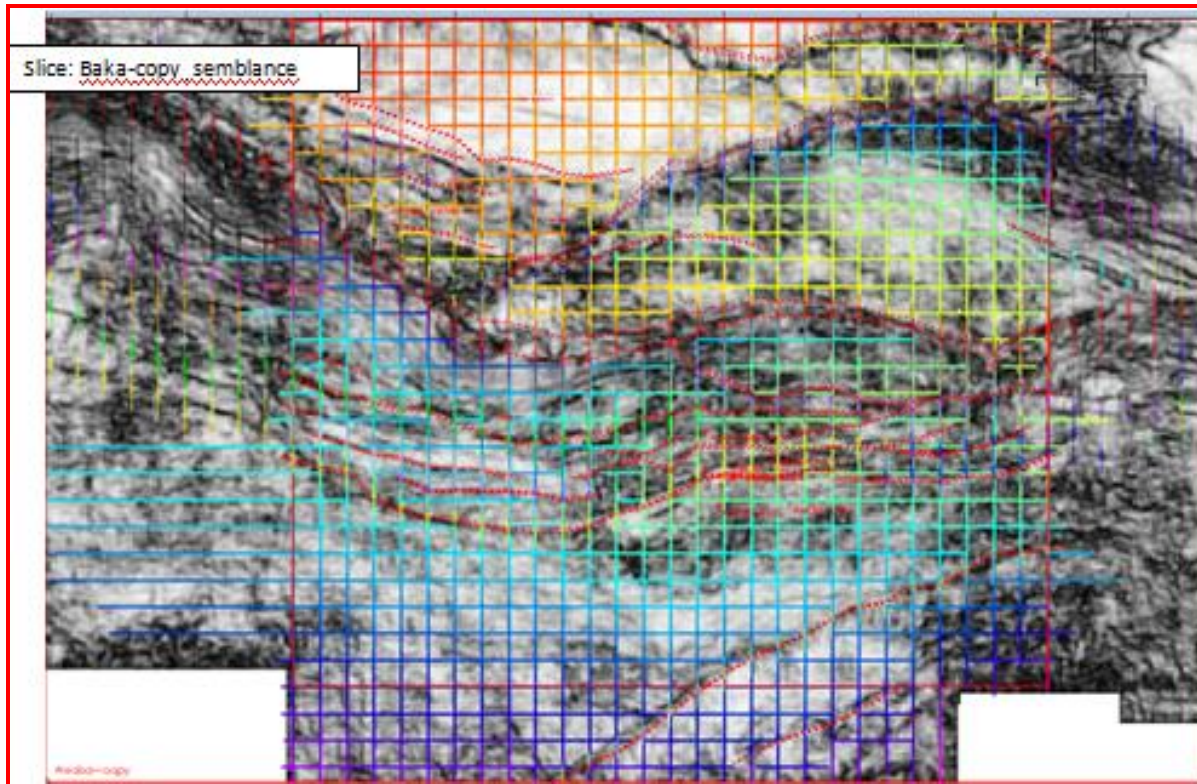
Appendix 41: Typical Seismic Interpretation Quality Control using Extracted Semblance Dip Guided Map
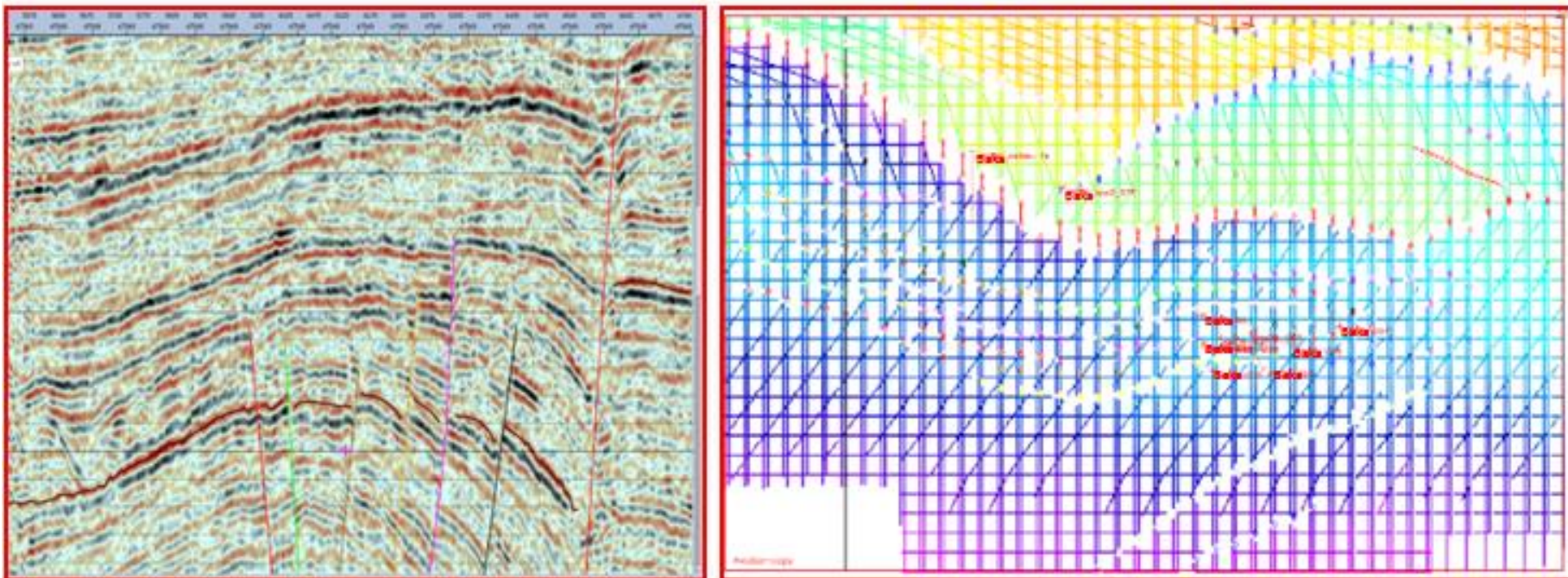
Appendix 42: Typical Seismic Interpretation using Inline, Cross Line and Arbitrary lines
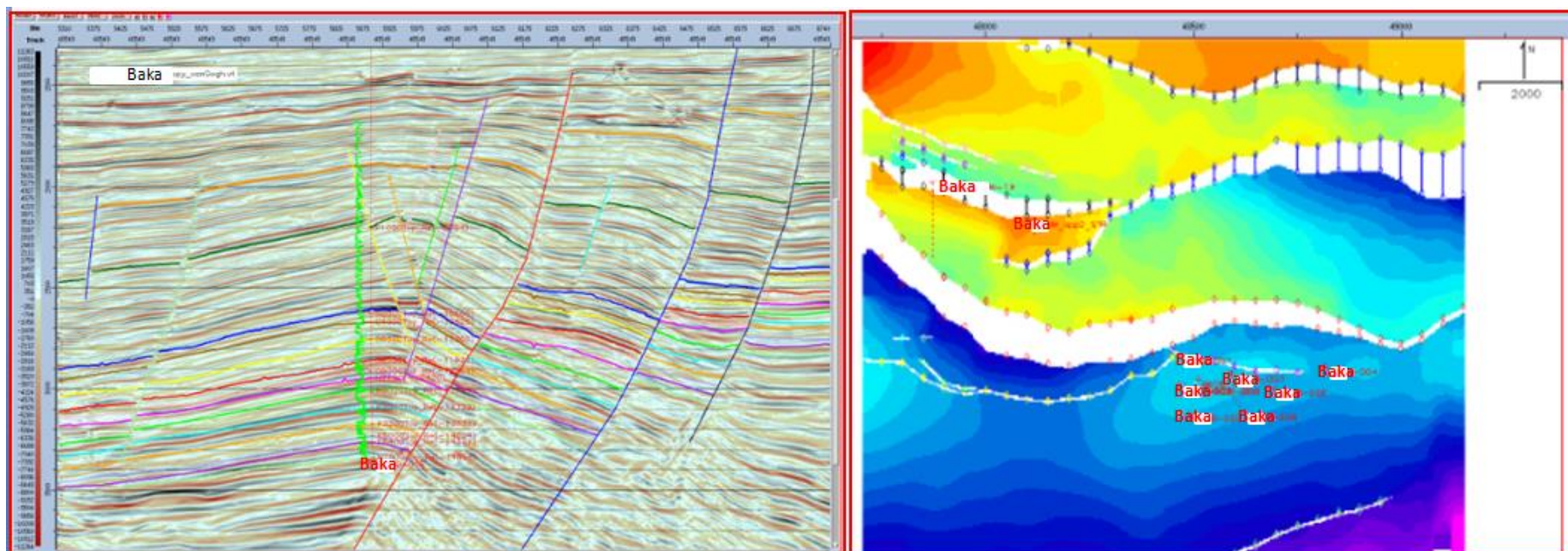
Appendix 43: Typical Interpreted Seismic and Time Structural Map
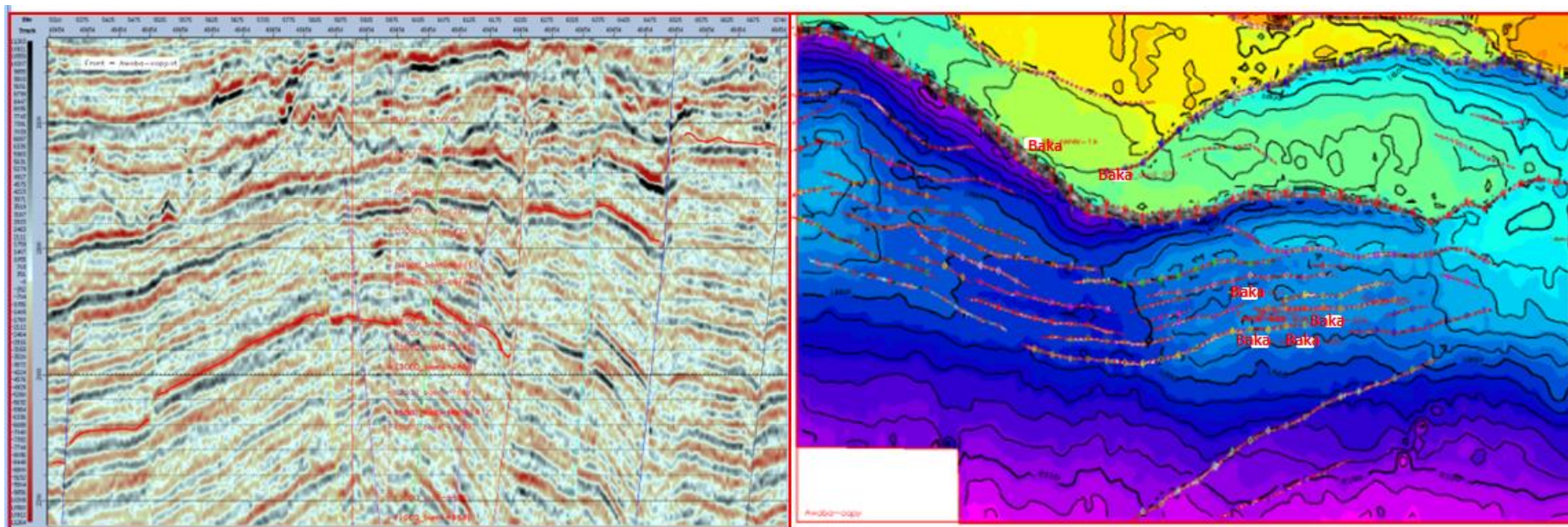
Appendix 44: Typical Interpreted Seismic and Contoured Time Structural Map
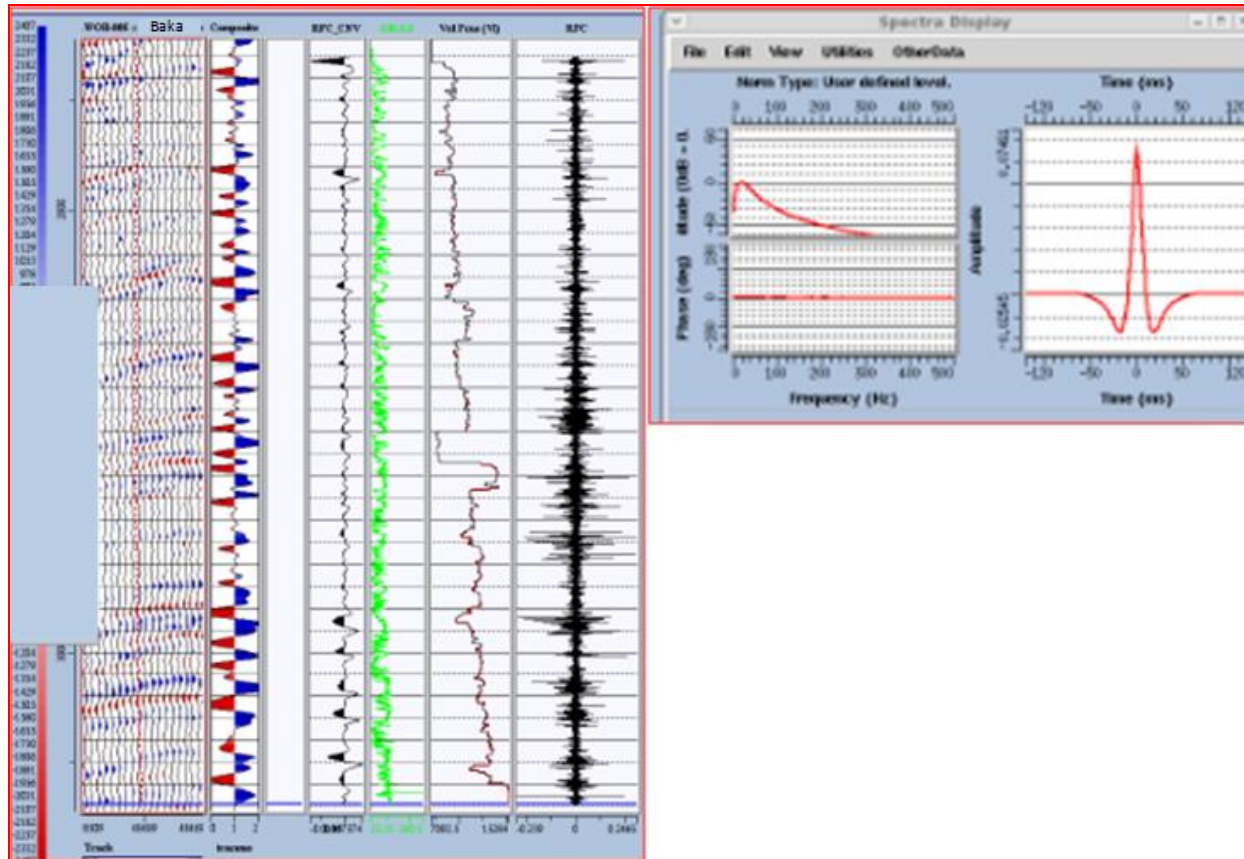
Appendix 45: Seismic To Well Tie of the Baka Field

Appendix 46: Cross Line Seismic Interpretation
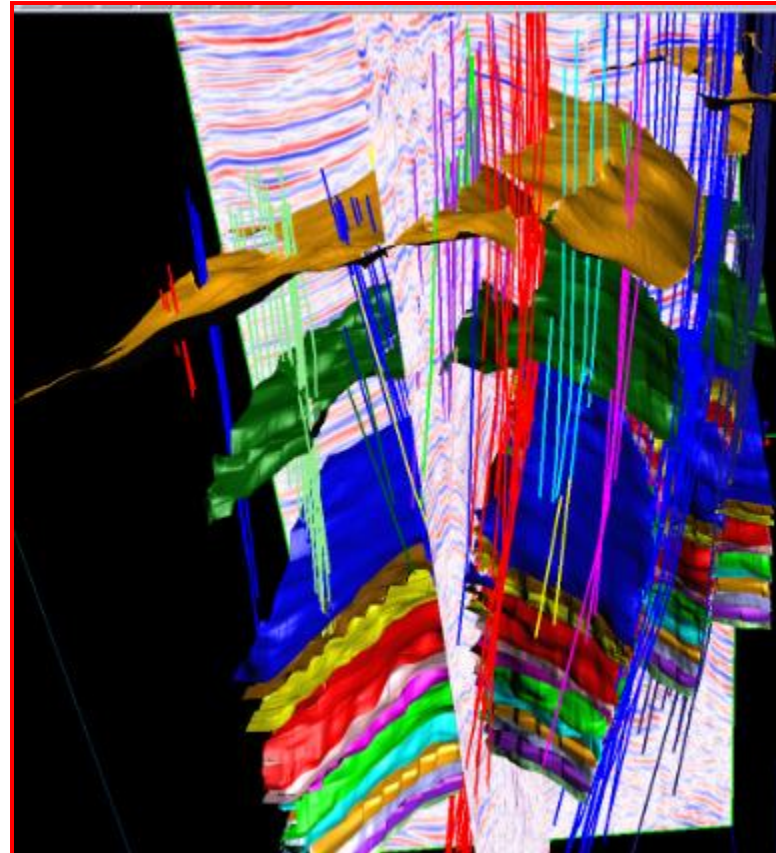
Appendix 47: Inline and Cross Line Seismic Interpretation showing Faulted Roll-Over Anticline
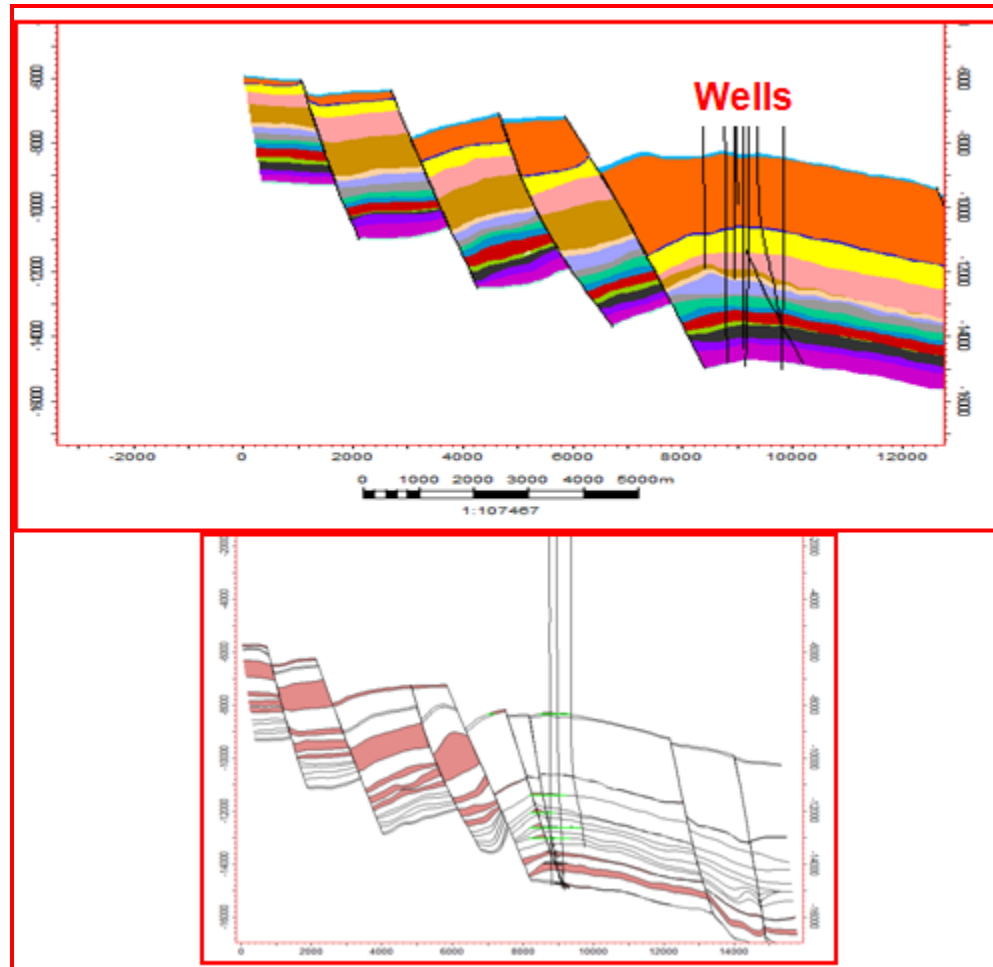
Appendix 48: Seismic versus Model Intersection Quality Control in all Interpreted Reservoir Level
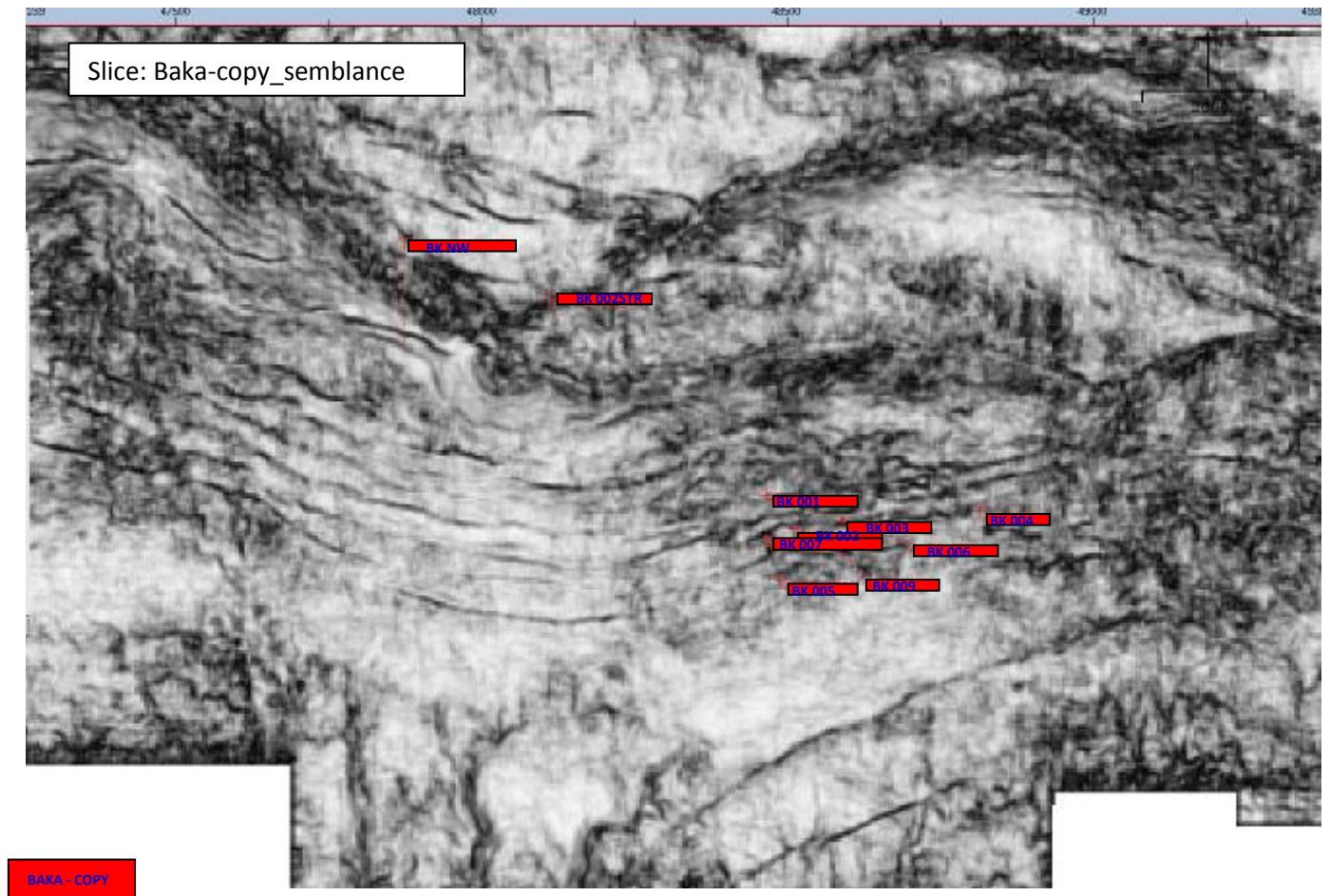
**Appendix 49: Extracted Dip Guided Semblance Map of Baka Field**
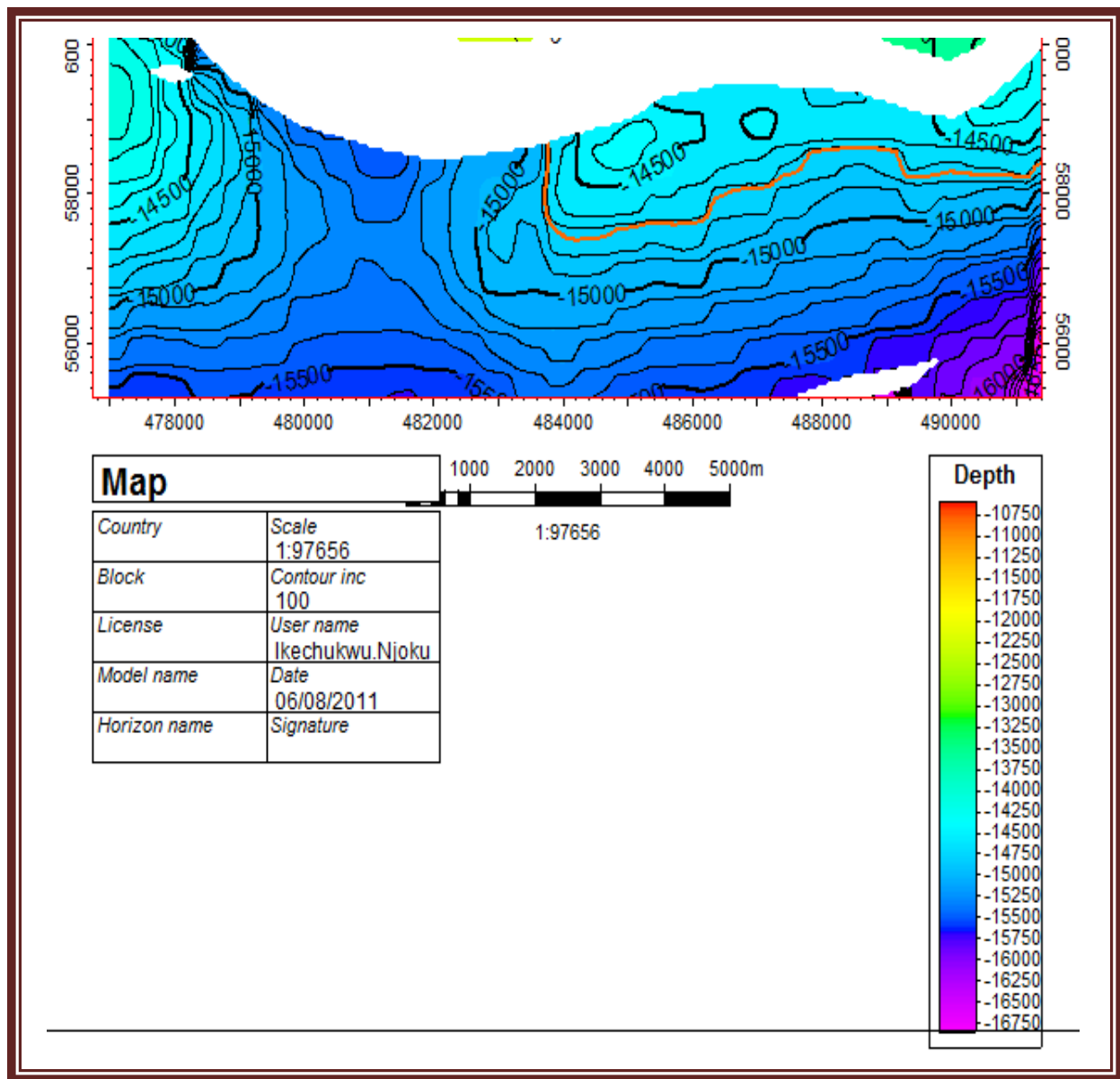
Appendix 50: F1000 In-lines and Cross-Lines Interpretation and Fault Polygons
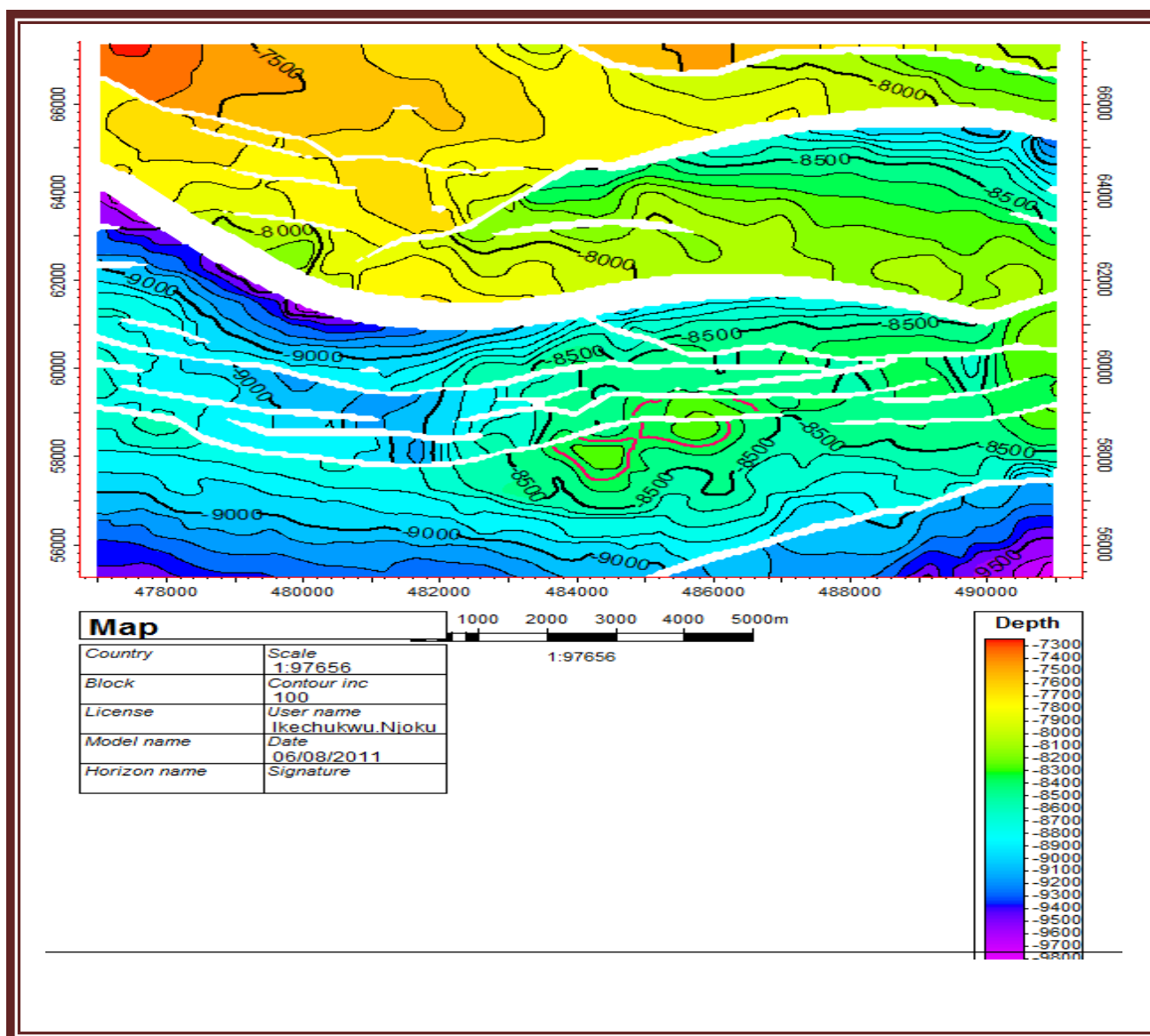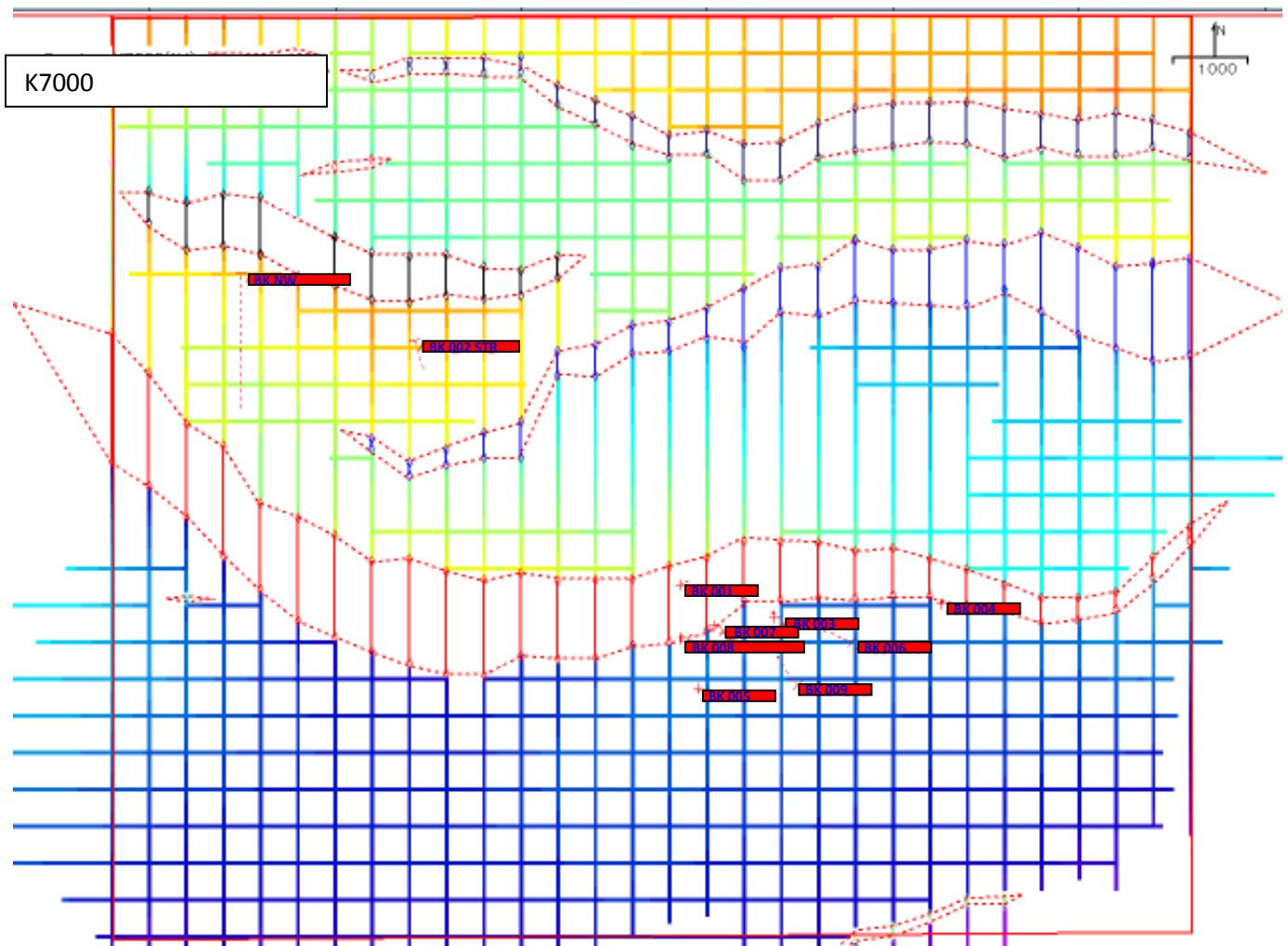
Appendix 51: Interpreted F1000 Horizon Depth Map and Oil Water Contact

Appendix 52: FG2000 In-lines and Cross-Lines Interpretation and Fault Polygons
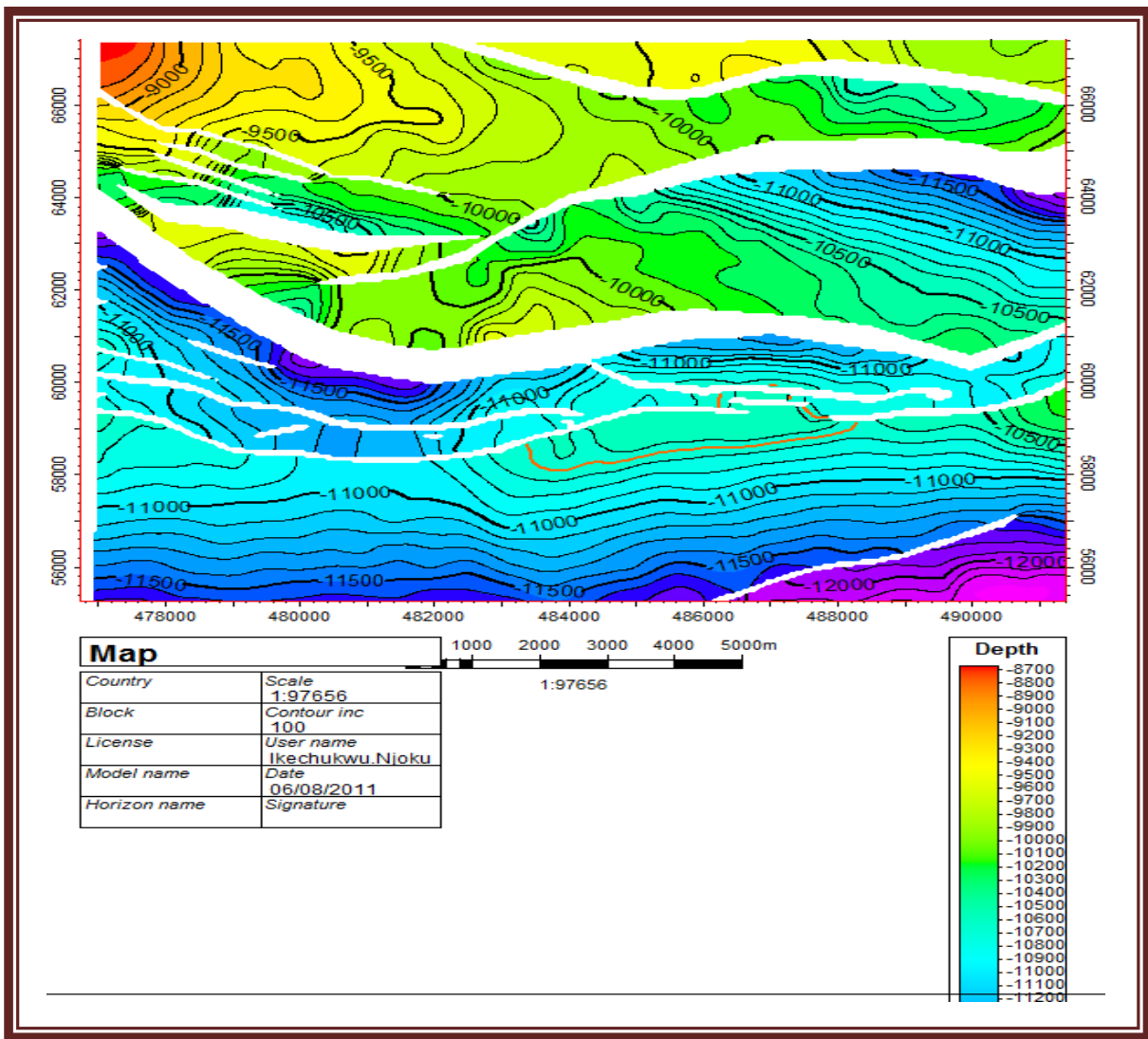
Appendix 53: Interpreted G2000 Horizon Depth Map and Gas Contact
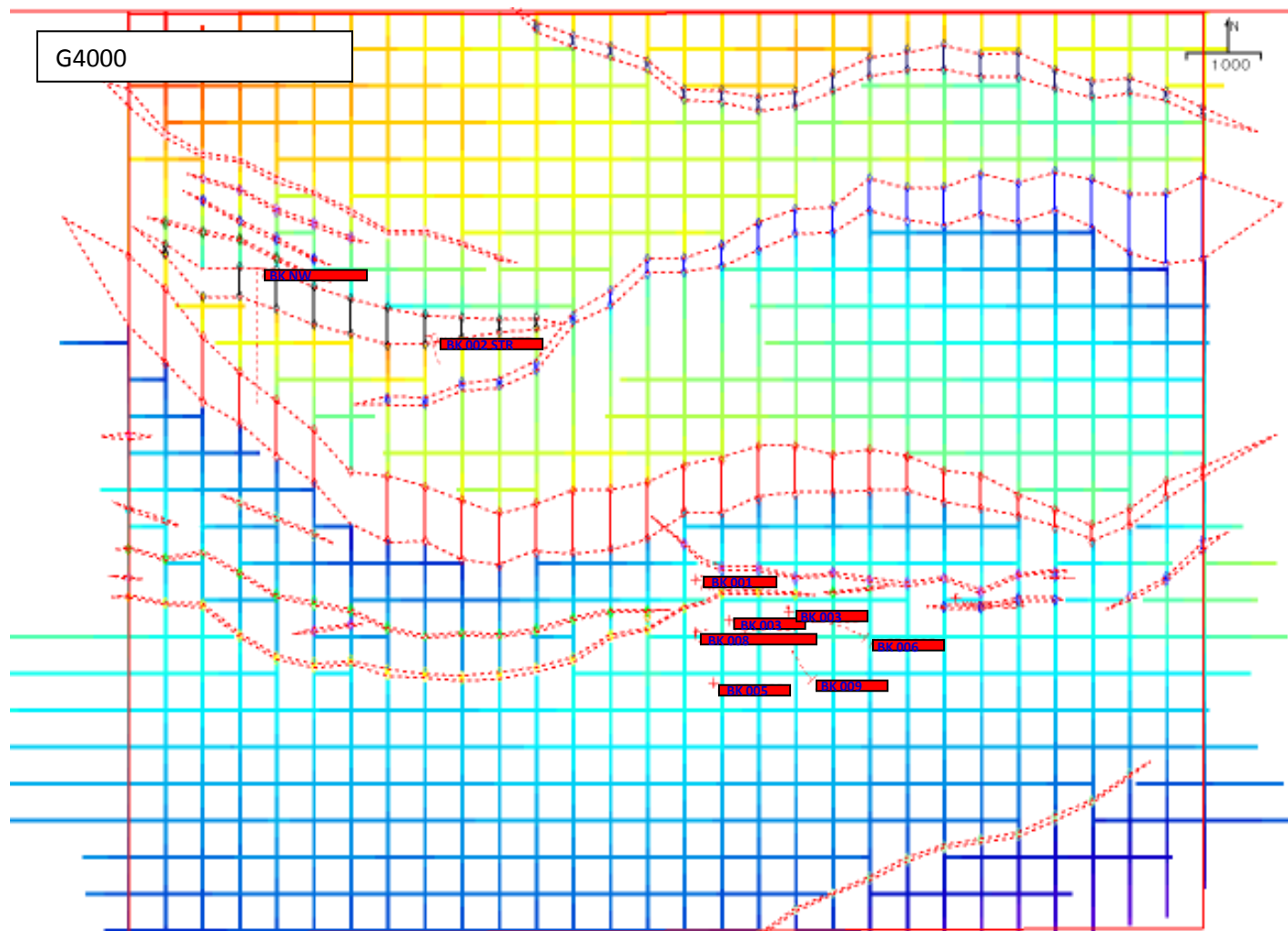
**Appendix 54: FG4000 In-lines and Cross-Lines Interpretation and Fault**
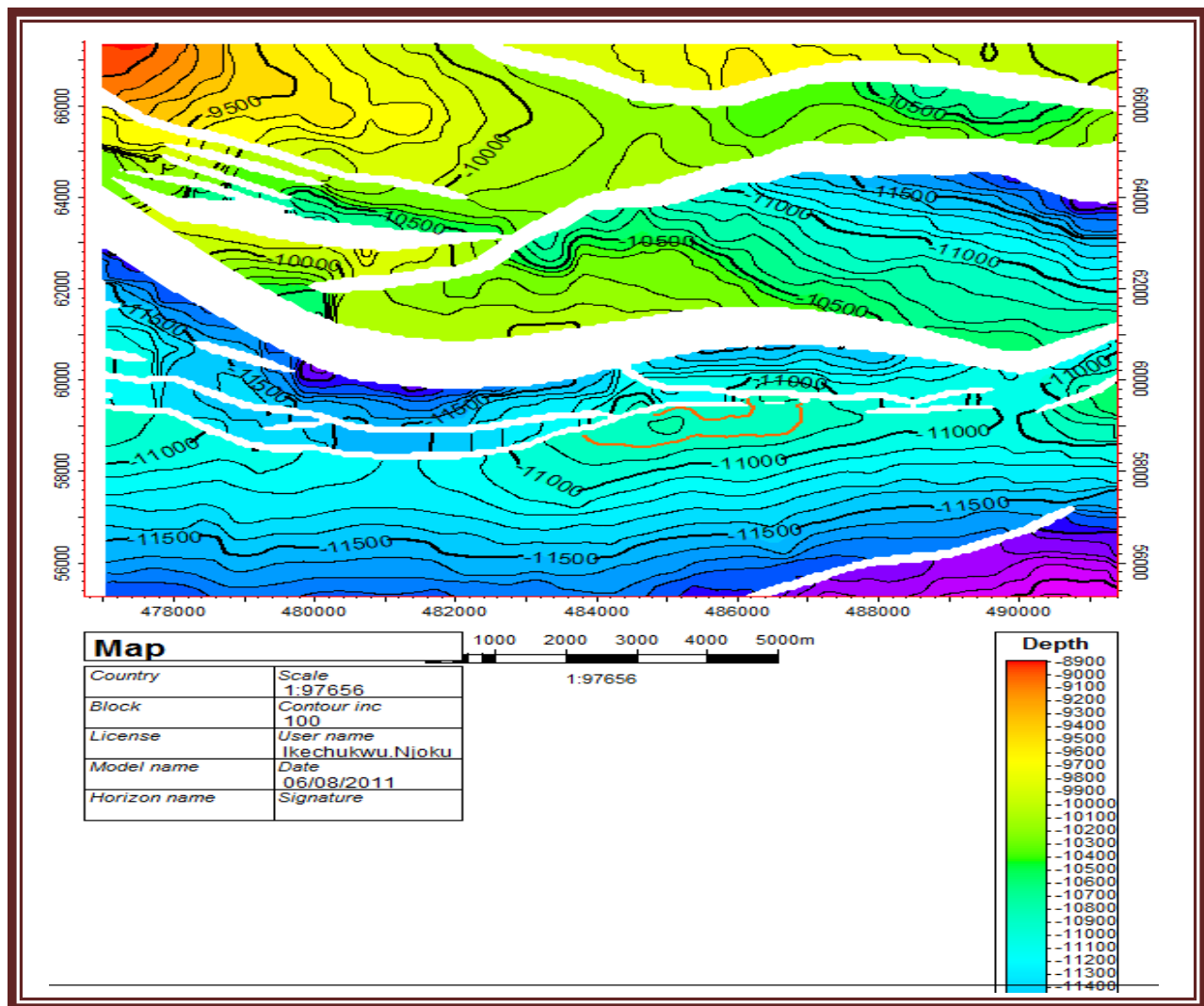
Polygons

Appendix 55: Interpreted G4000 Horizon Depth Map and Oil Water Contact
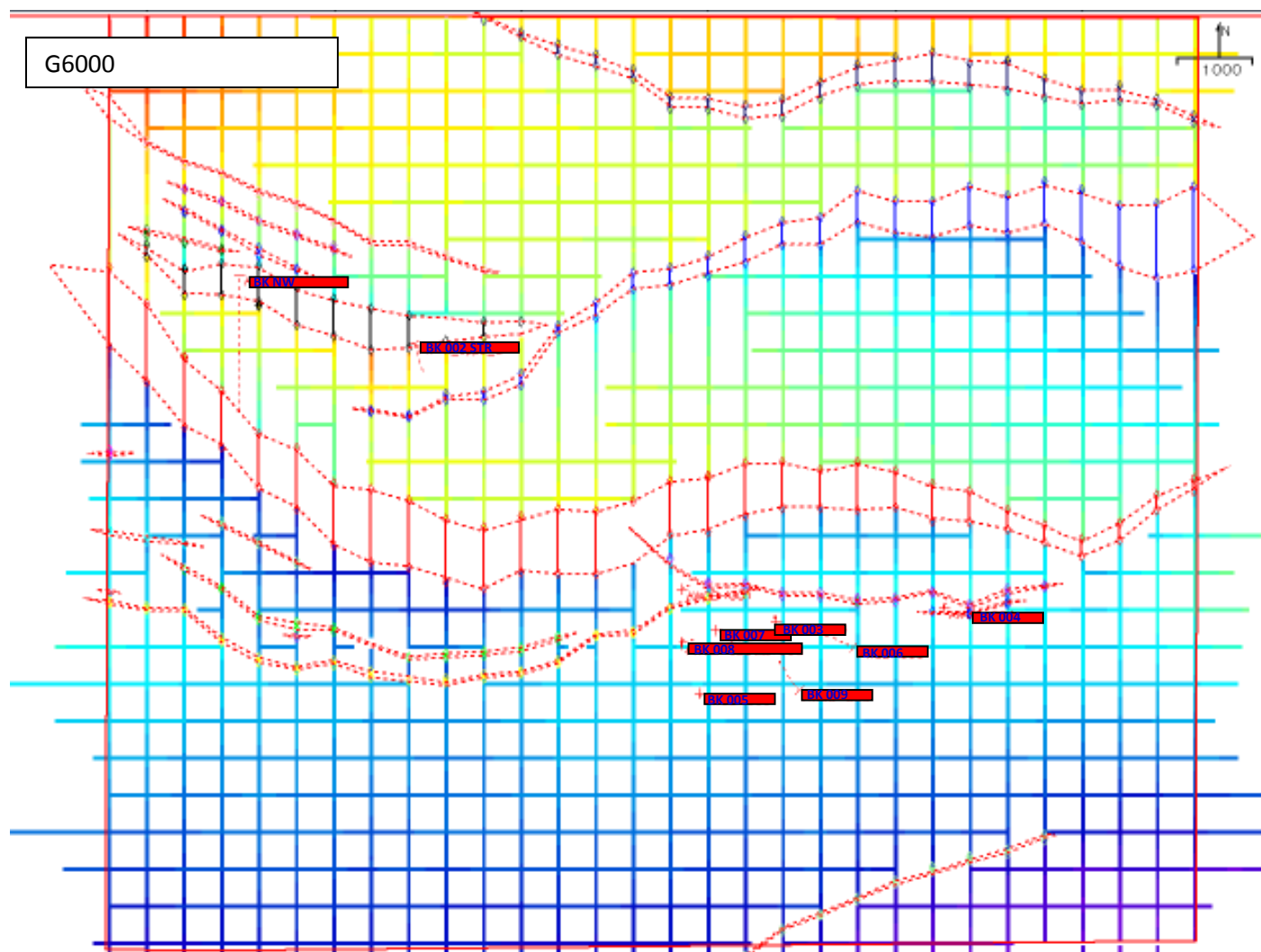
Appendix 56: FG6000 In-lines and Cross-Lines Interpretation and Fault
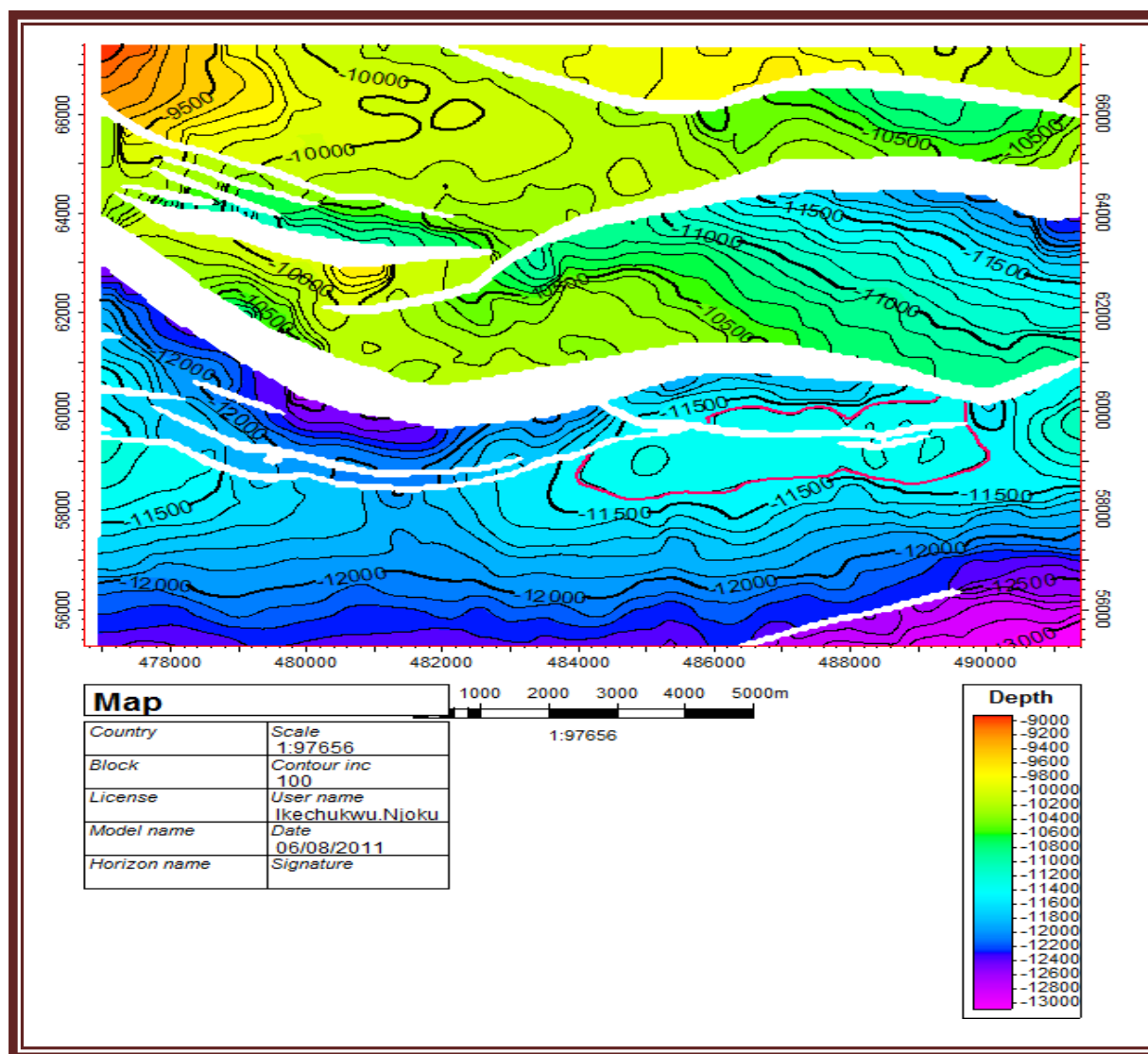
Polygons

Appendix 57: Interpreted G6000 Horizon Depth Map and Oil Contact

Appendix 58: G8000 In-lines and Cross-Lines Interpretation and Fault Polygons
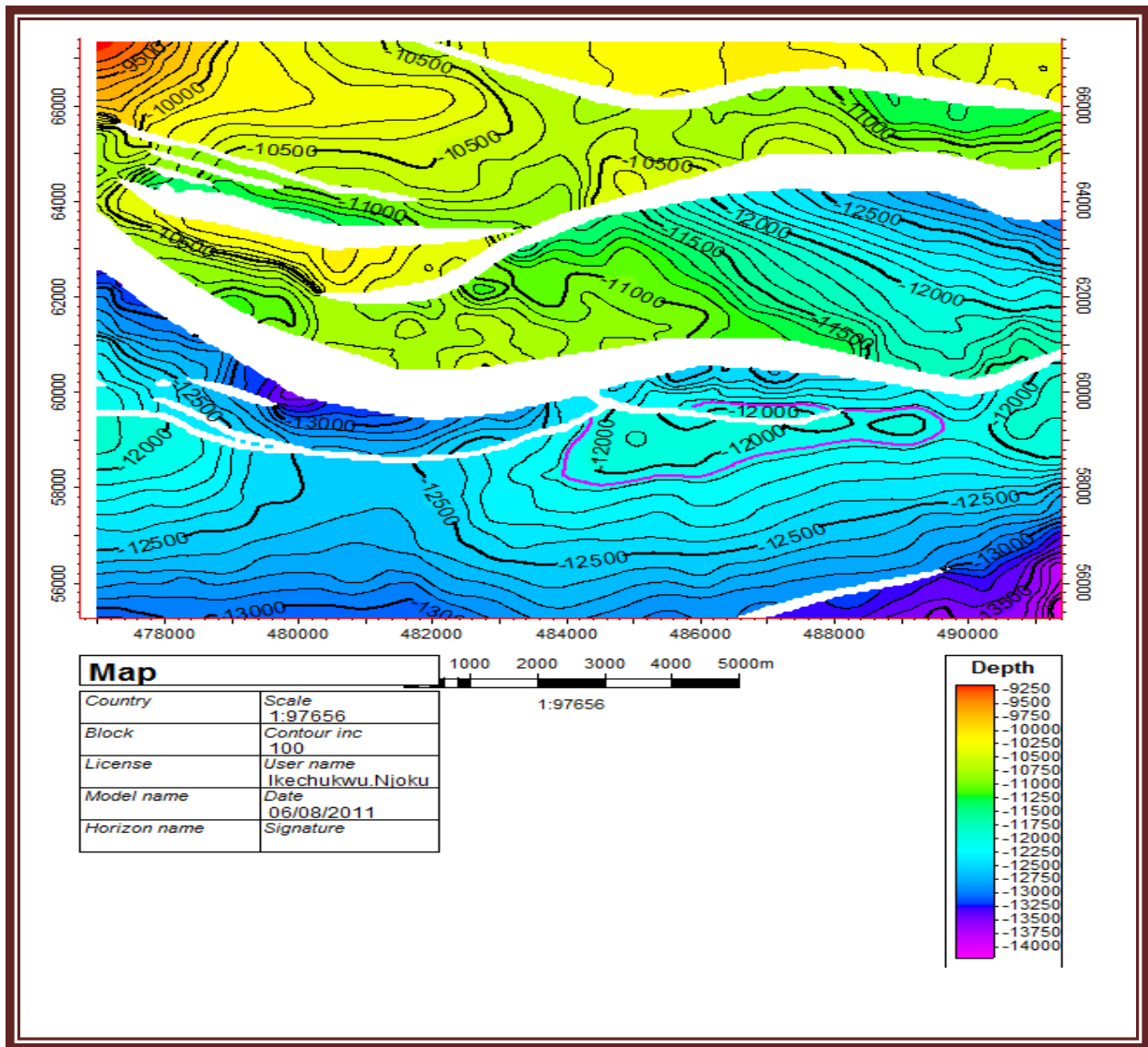
Appendix 59: Interpreted G8000 Horizon Depth Map and Oil Contact
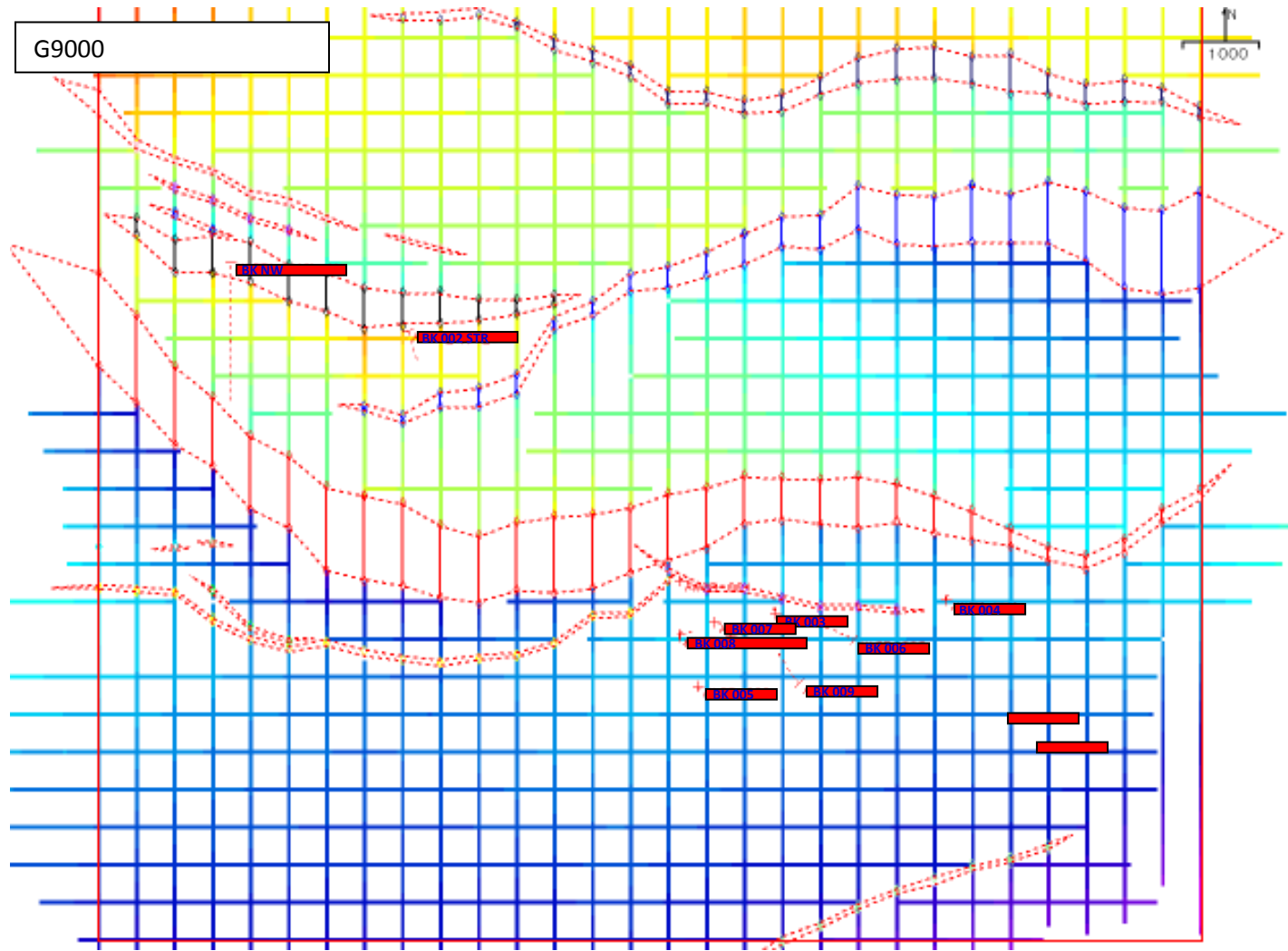
Appendix 60: FG9000 In-lines and Cross-Lines Interpretation and Fault Polygons
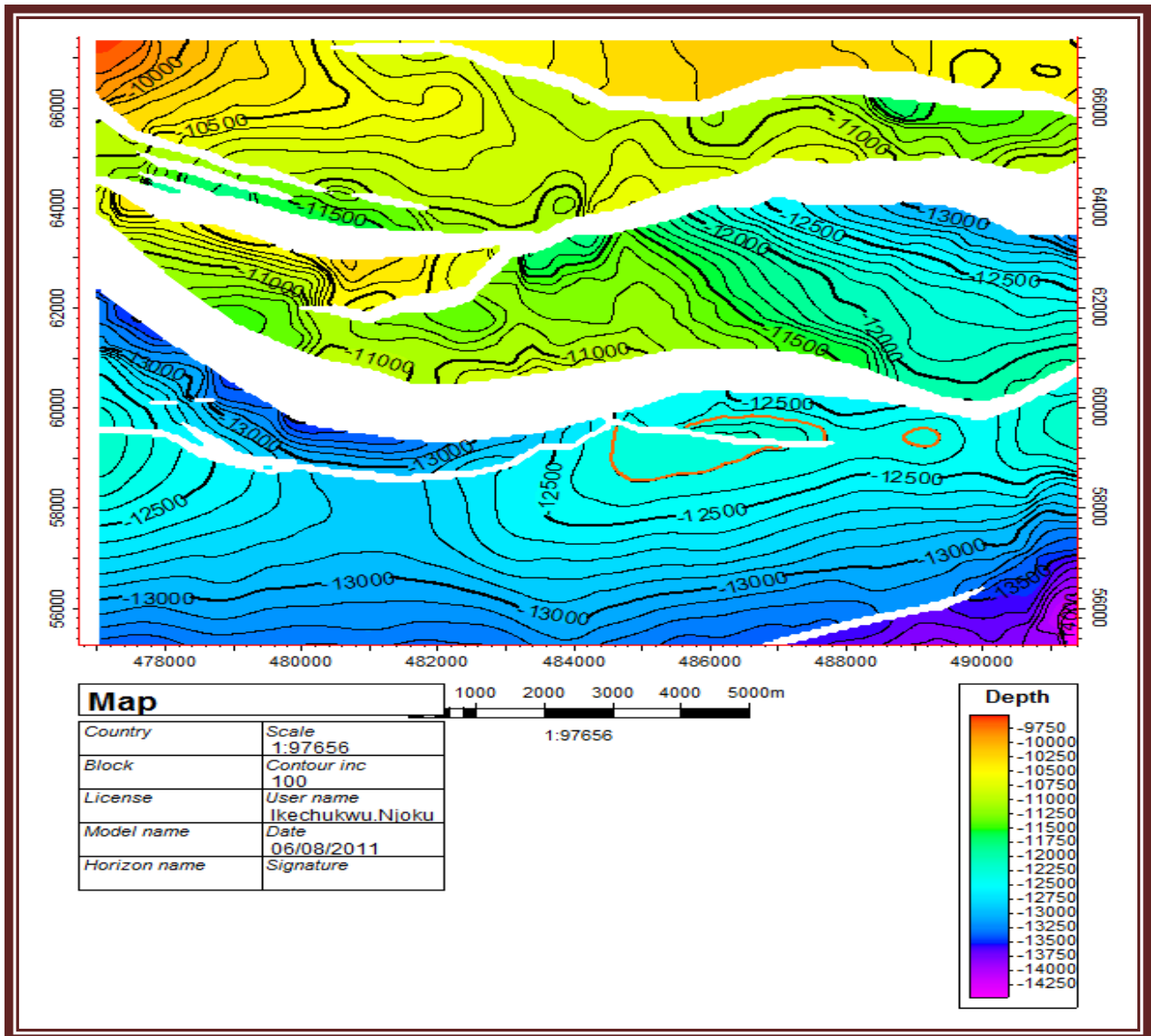
**Appendix 61: Interpreted G9000 Horizon Depth Map and Oil Water Contact**
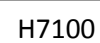
Appendix 62: H7100 In-lines and Cross-Lines Interpretation and Fault Polygons
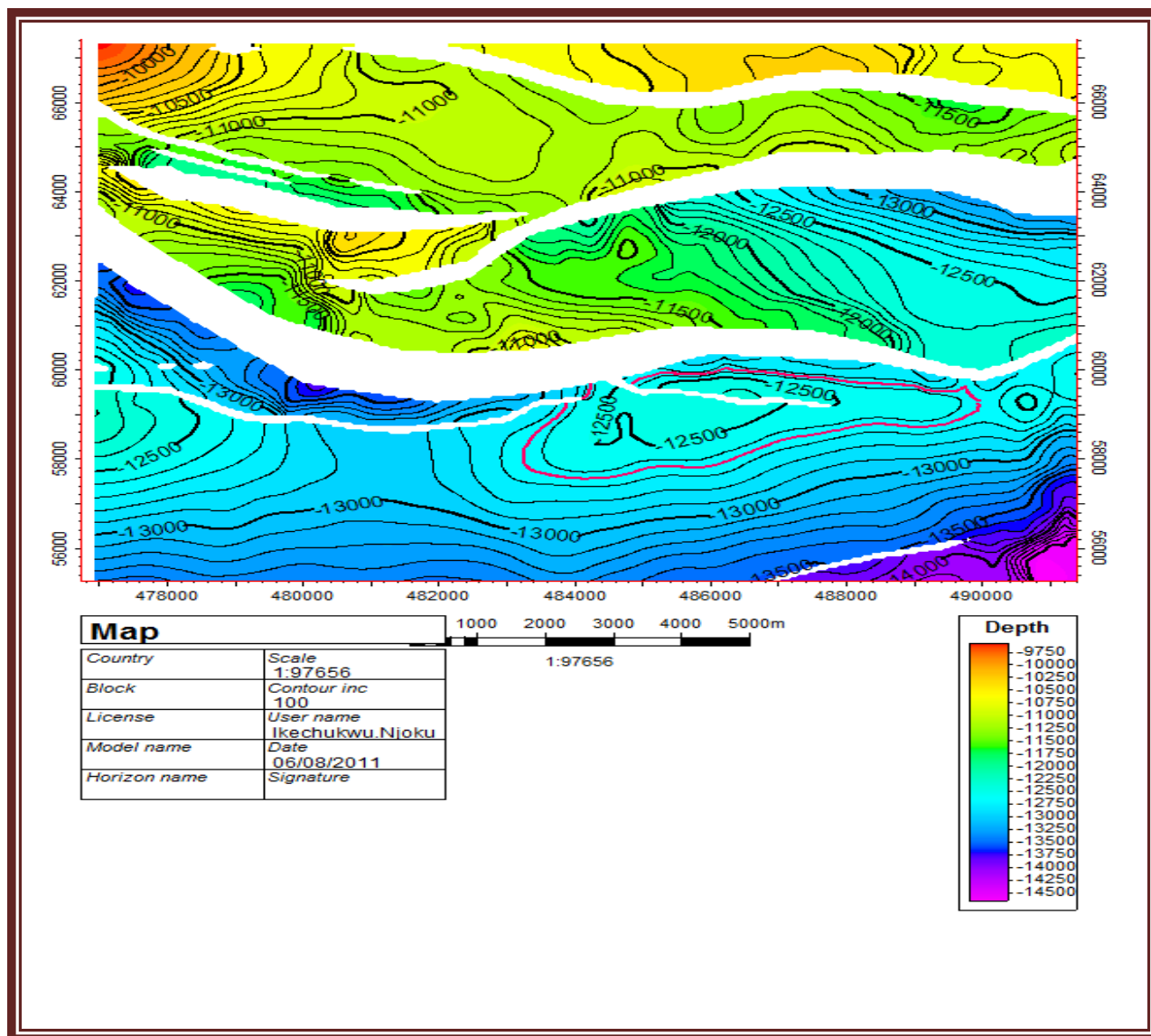
Appendix 63: Interpreted H7100 Horizon Depth Map and Oil Contact
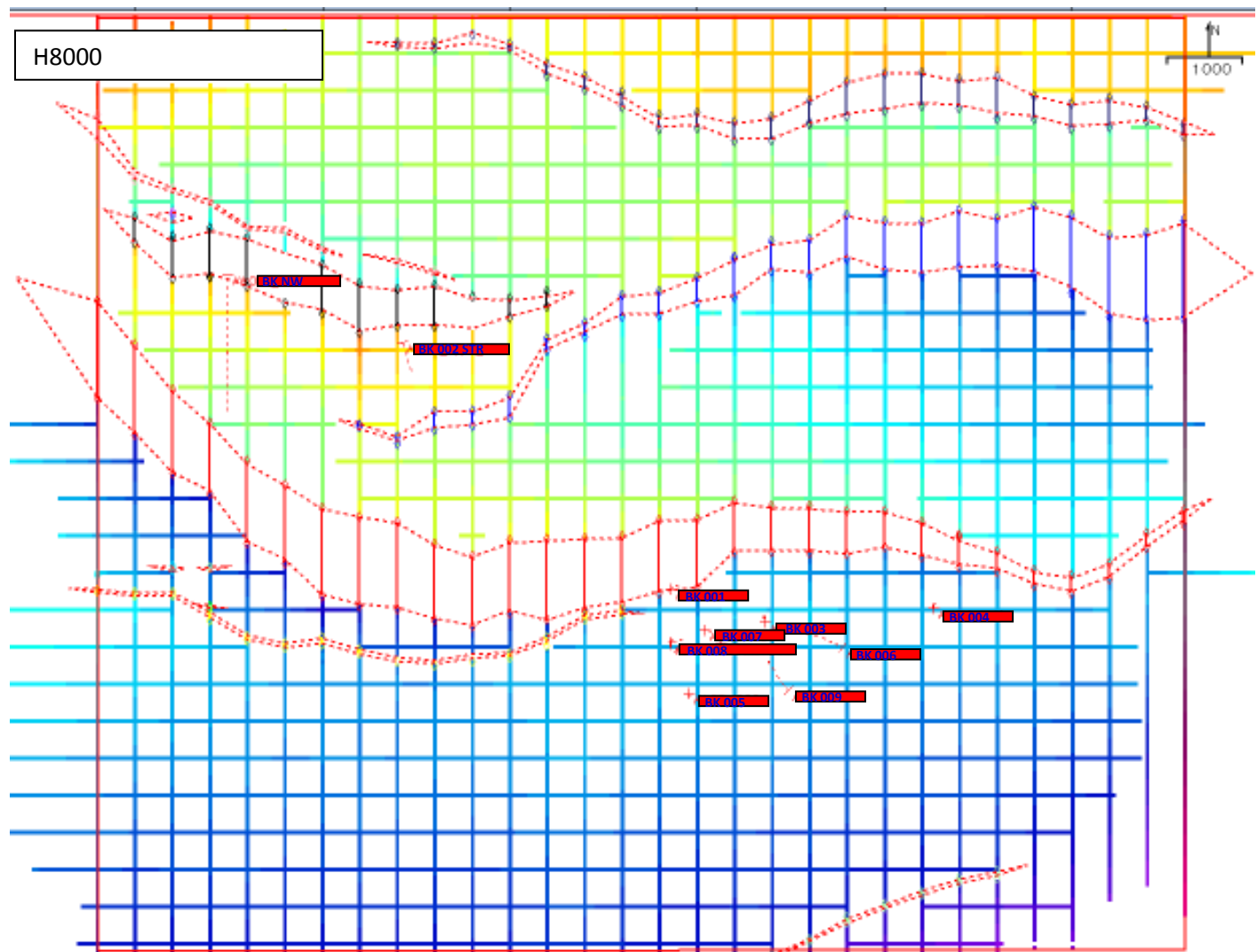
Appendix 64: H8000 In-lines and Cross-Lines Interpretation and Fault Polygons
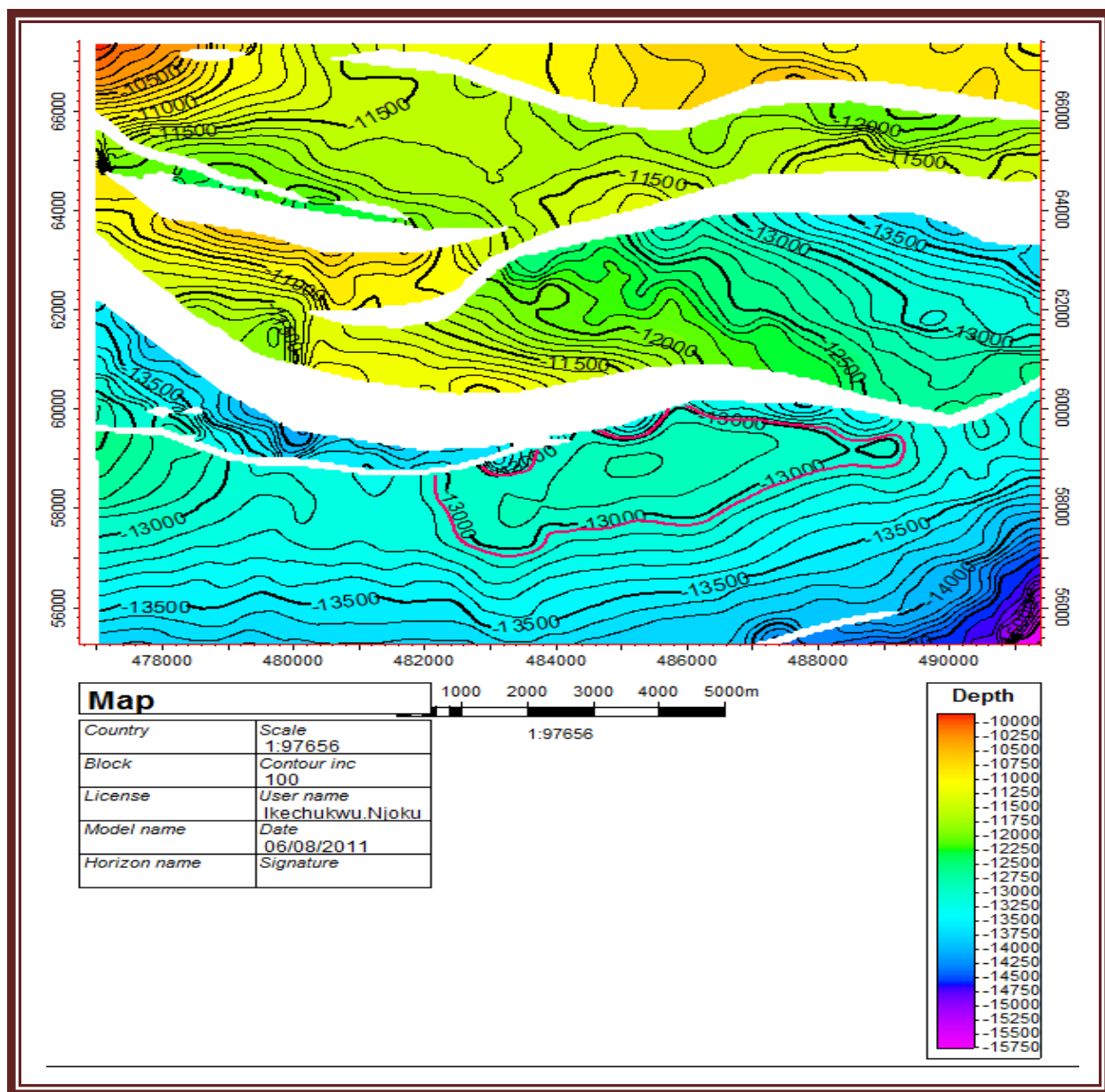
**Appendix 65: Interpreted H8000 Horizon Depth Map and Oil Water Contact**

Appendix 66: K2000 In-lines and Cross-Lines Interpretation and Fault Polygons
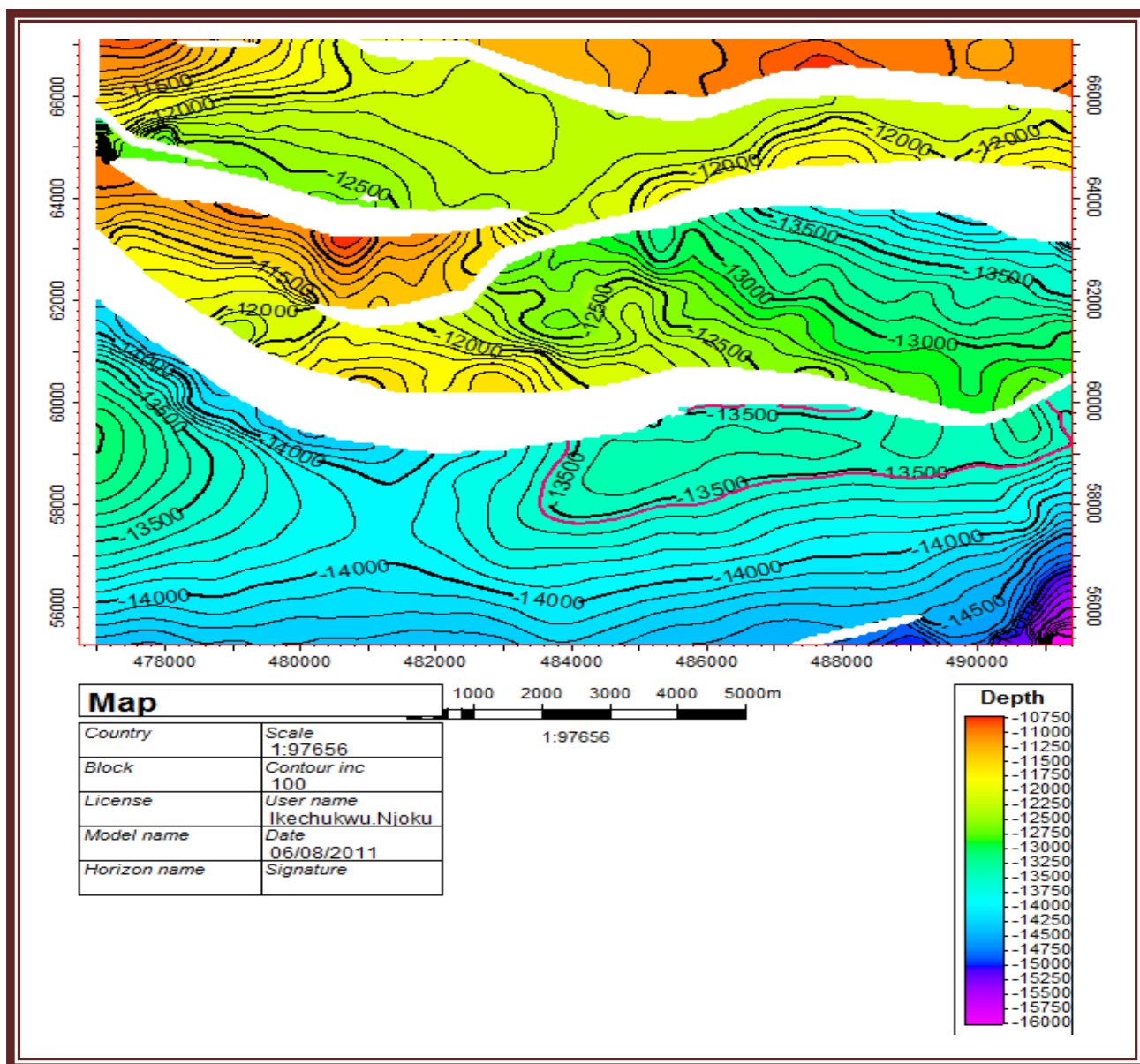
Appendix 67: Interpreted K2000 Horizon Depth Map and Gas Contact
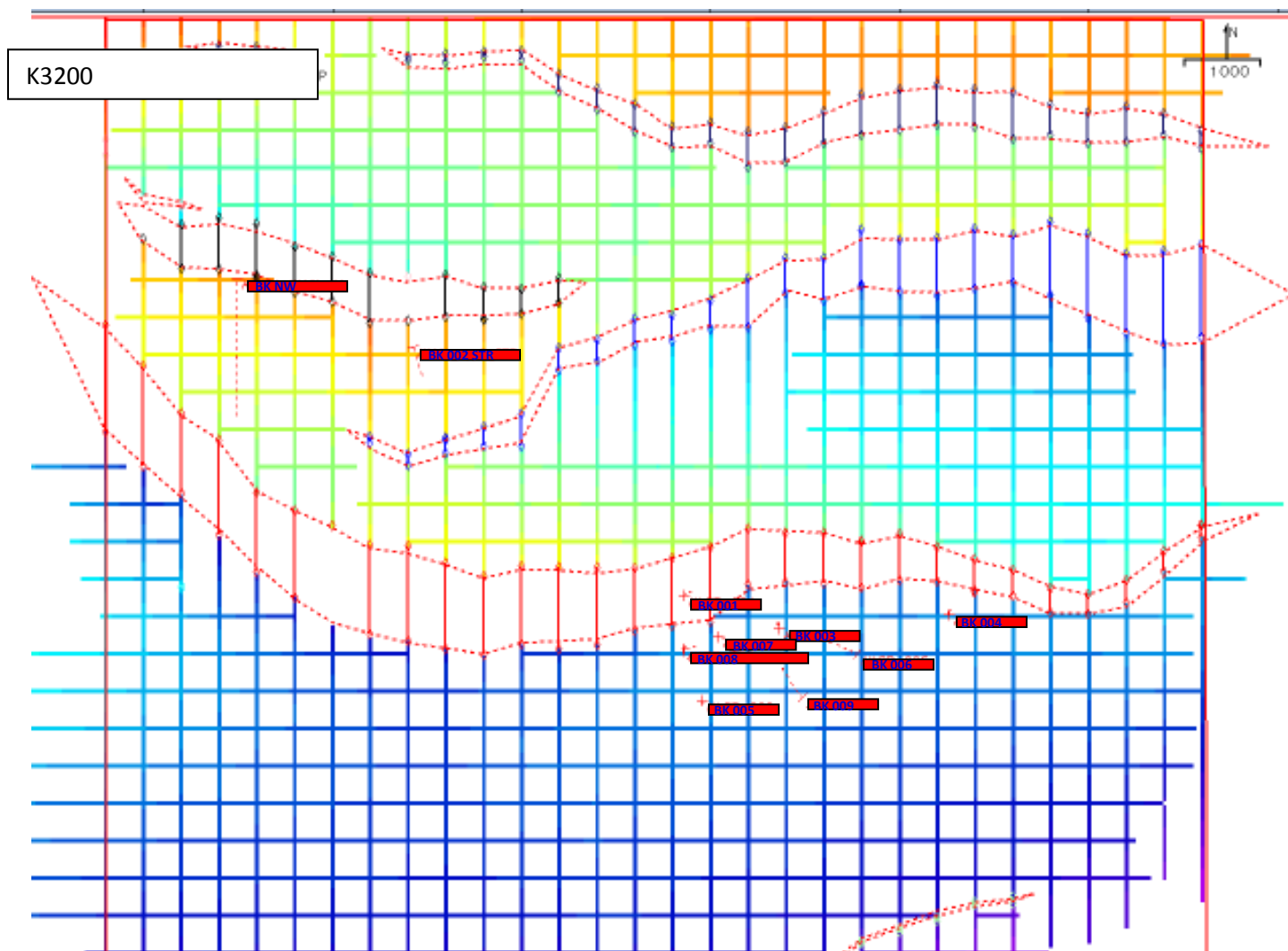
Appendix 68: K3200 In-lines and Cross-Lines Interpretation and Fault Polygons
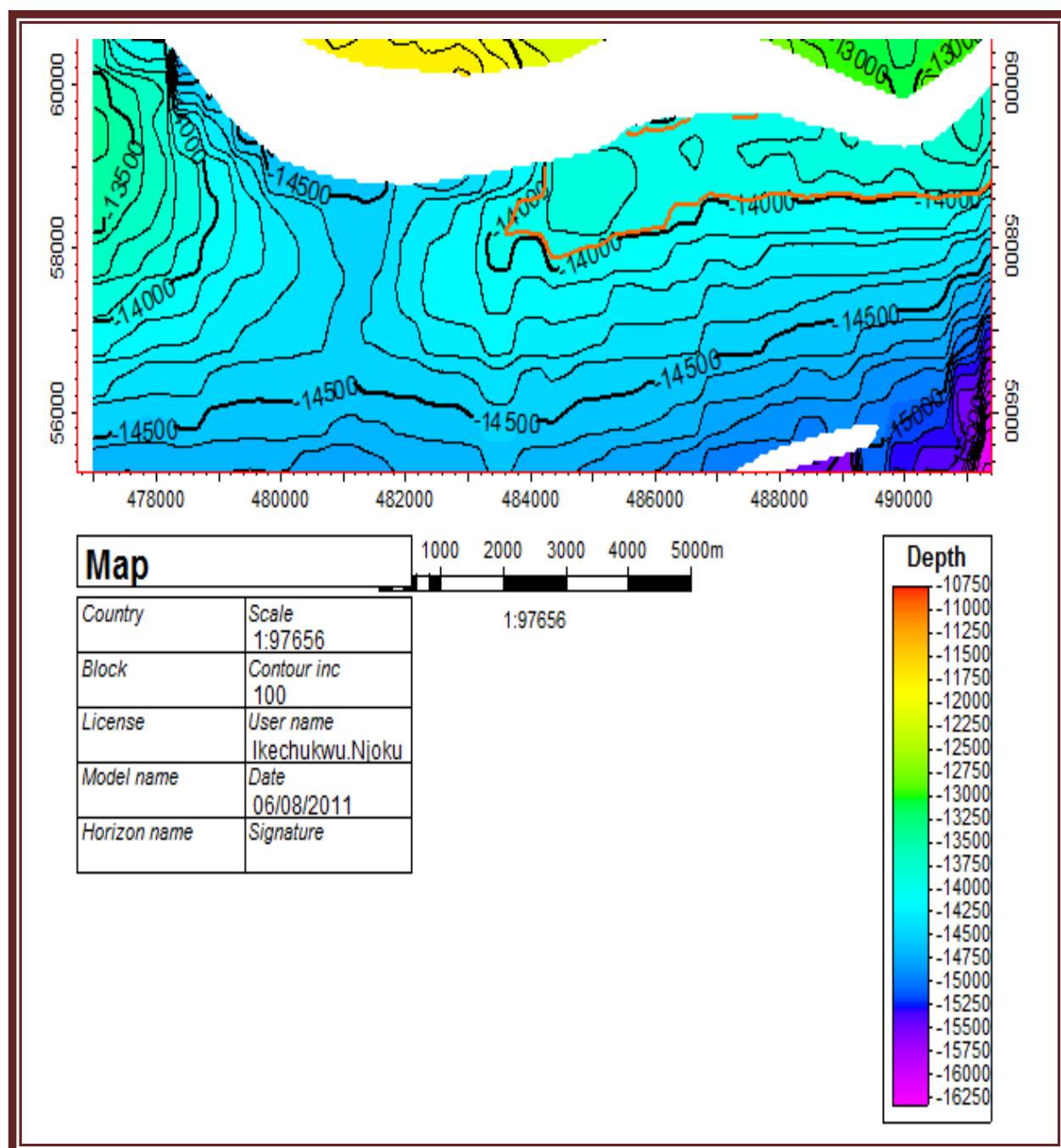
Appendix 69: Interpreted K3200 Horizon Depth Map and Gas Water Contact
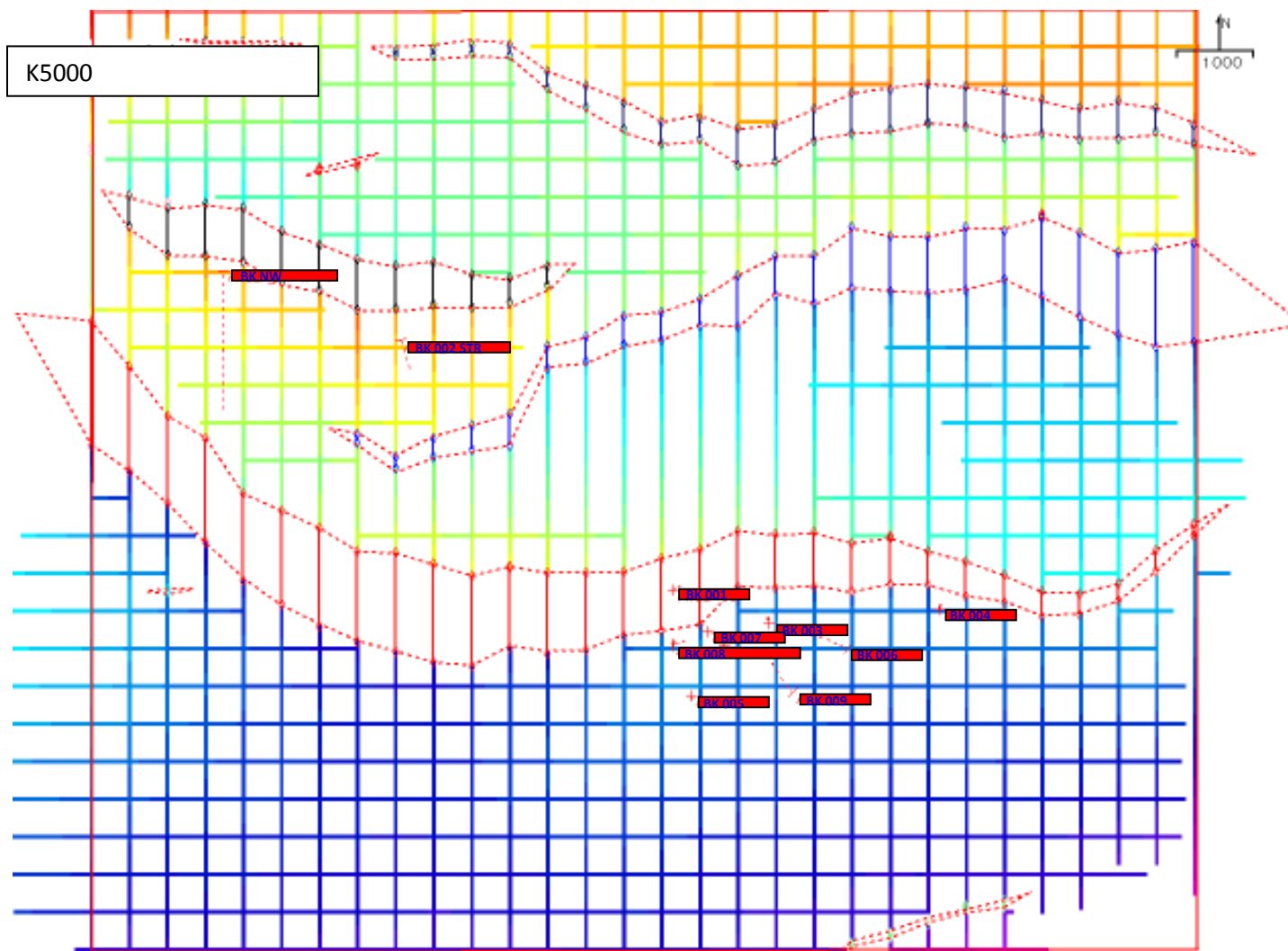
Appendix 70: K5000 In-lines and Cross-Lines Interpretation and Fault Polygons
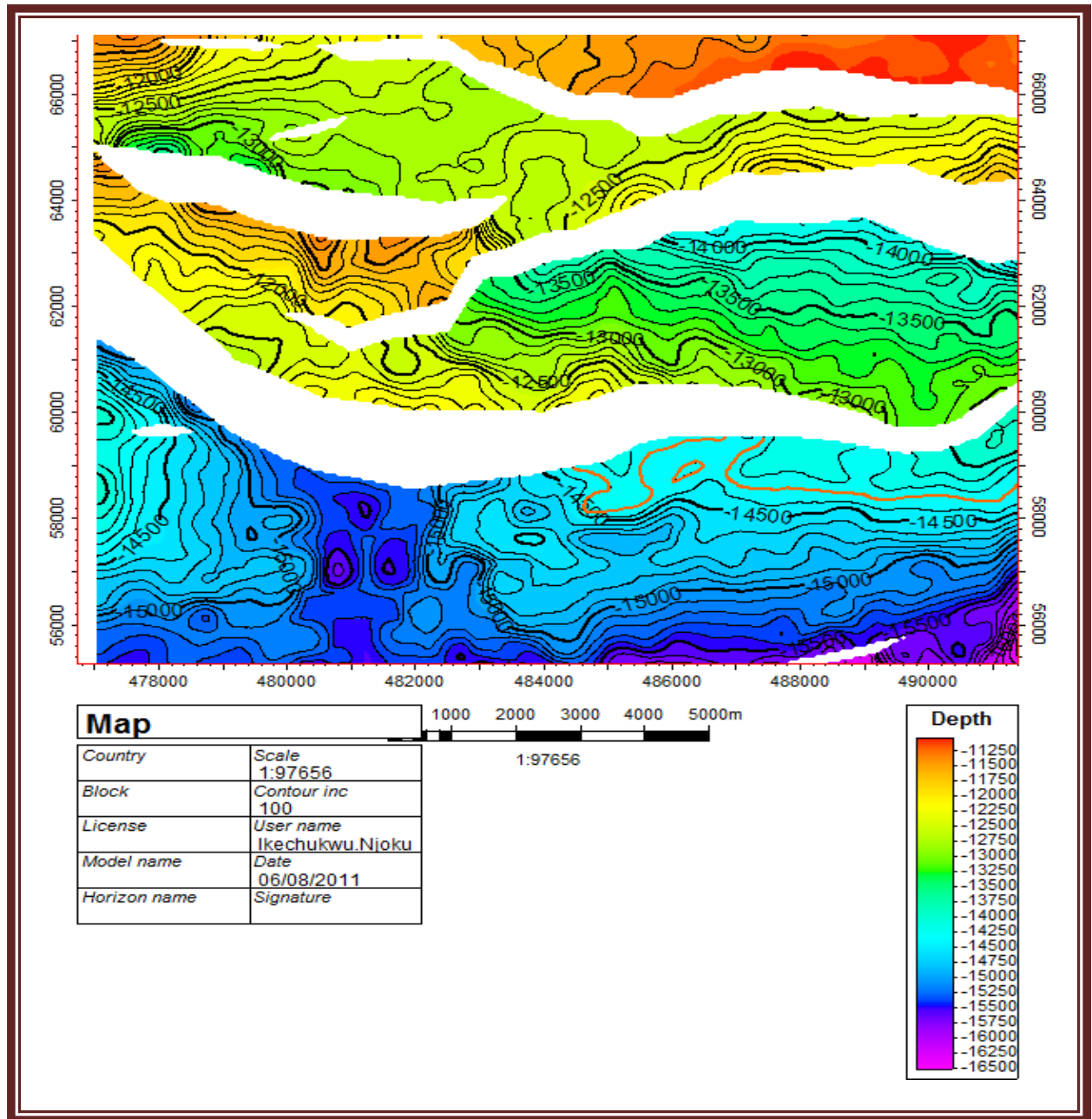
Appendix 71: Interpreted K5000 Horizon Depth Map and Gas Water Contact
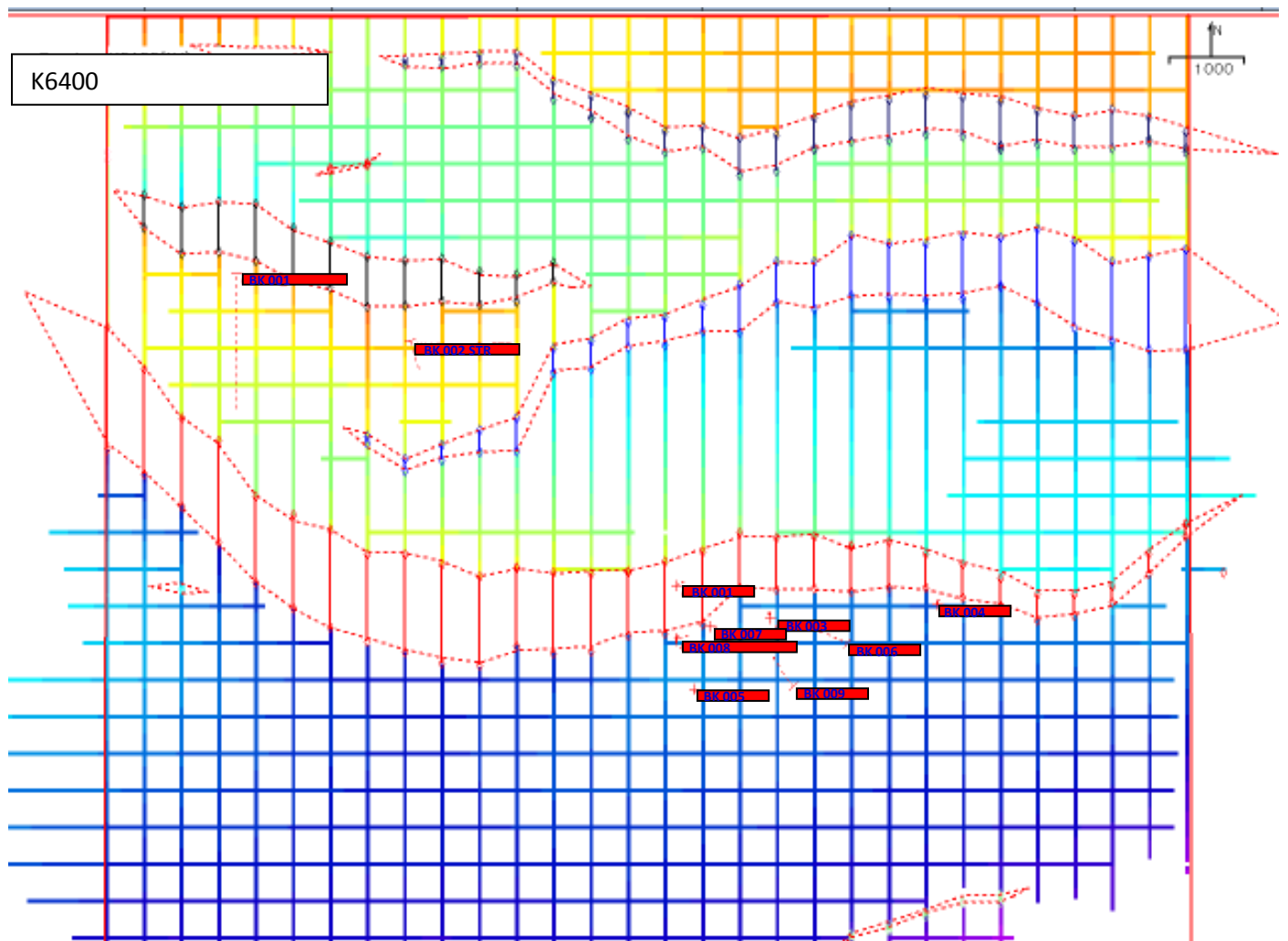
K6400

Appendix 72: K6400 In-lines and Cross-Lines Interpretation and Fault

Polygons

Appendix 73: Interpreted K6400 Horizon Depth Map and Gas Water Contact

K7000

Appendix 74: K7000 In-lines and Cross-Lines Interpretation and Fault Polygons
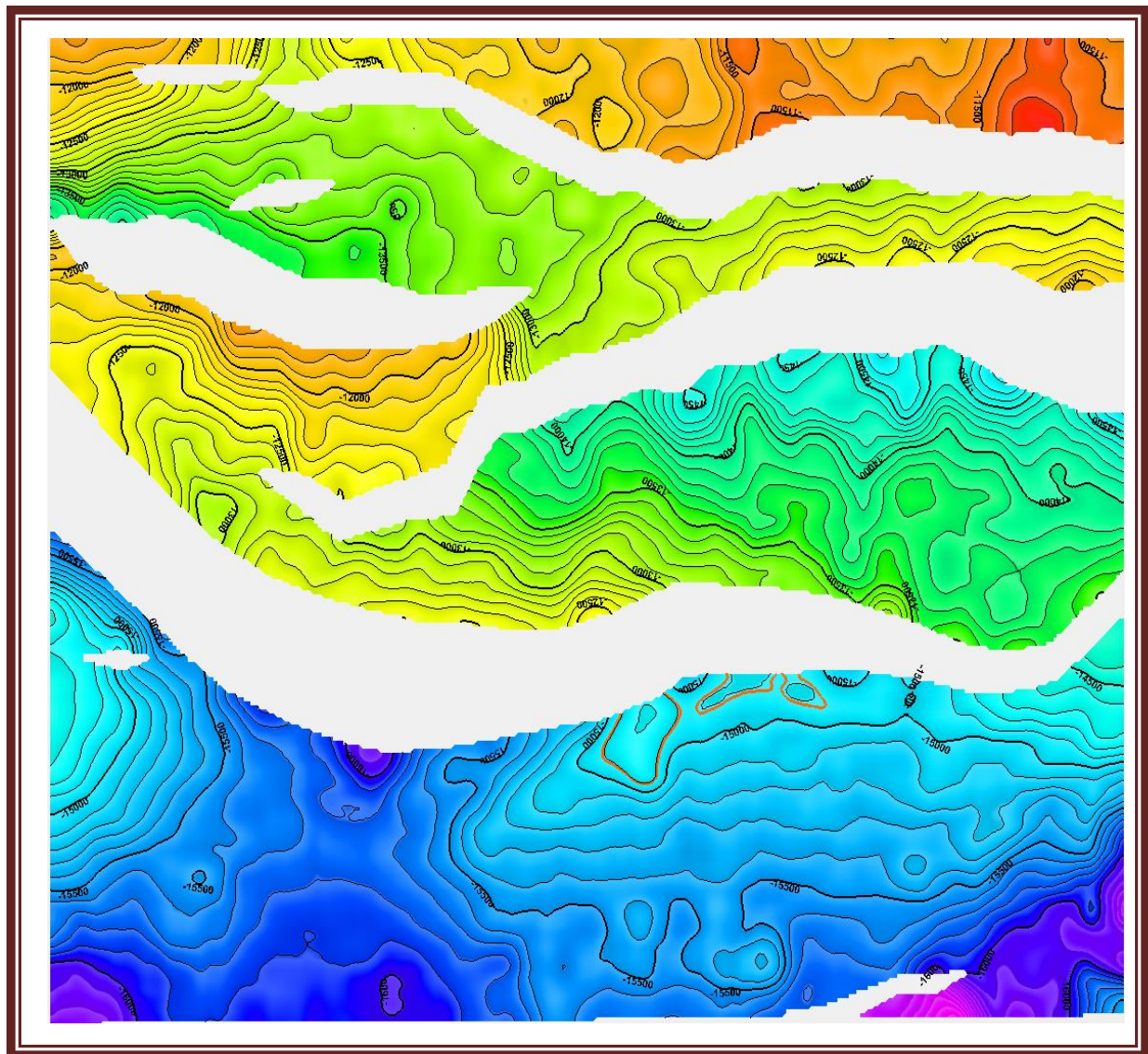
Appendix 75: Interpreted K7000 Horizon Depth Map and Gas Water Contact
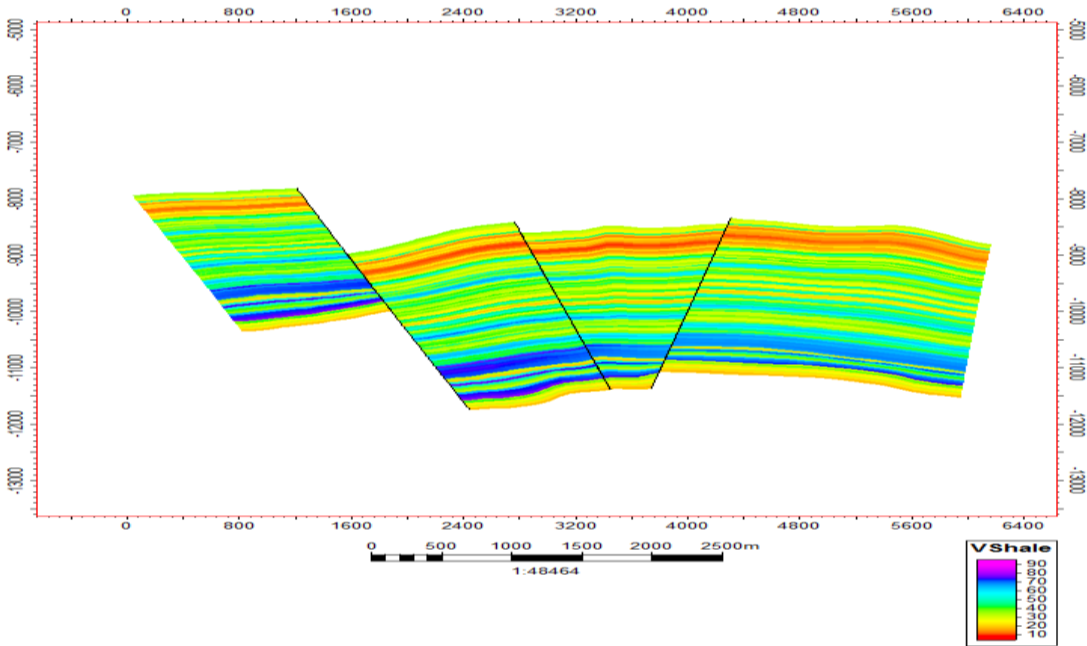
Appendix 76: Fault Horizon Intersection of V-Shale Model (Quality Control)
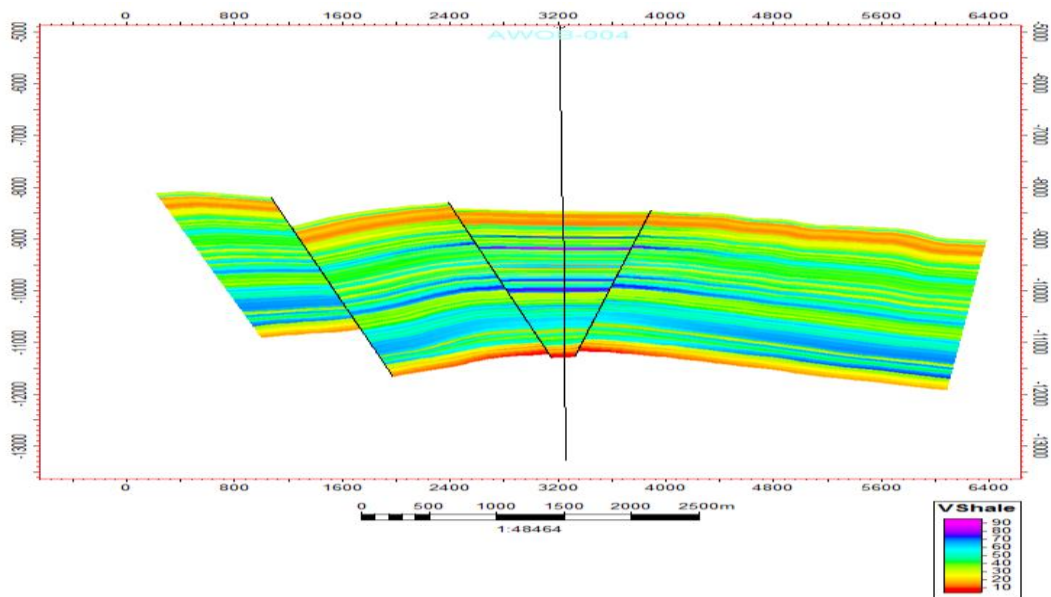
Appendix 77: Fault Horizon Intersection of V-Shale Model at well Location

(Quality Control)

292
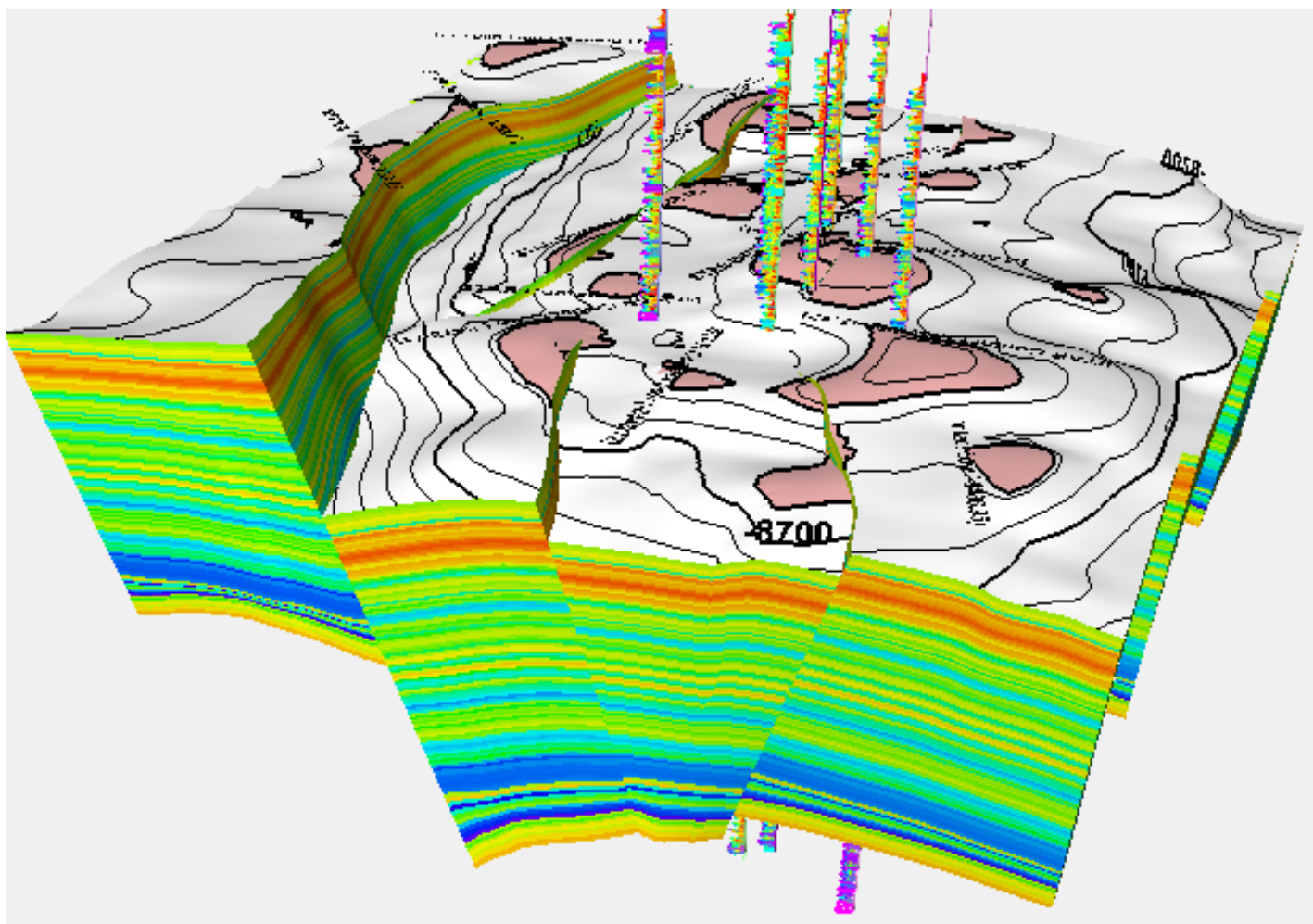
Appendix 78: Stochastic Trap Analysis and Risking Model Showing F1000

Reservoir Column Heights
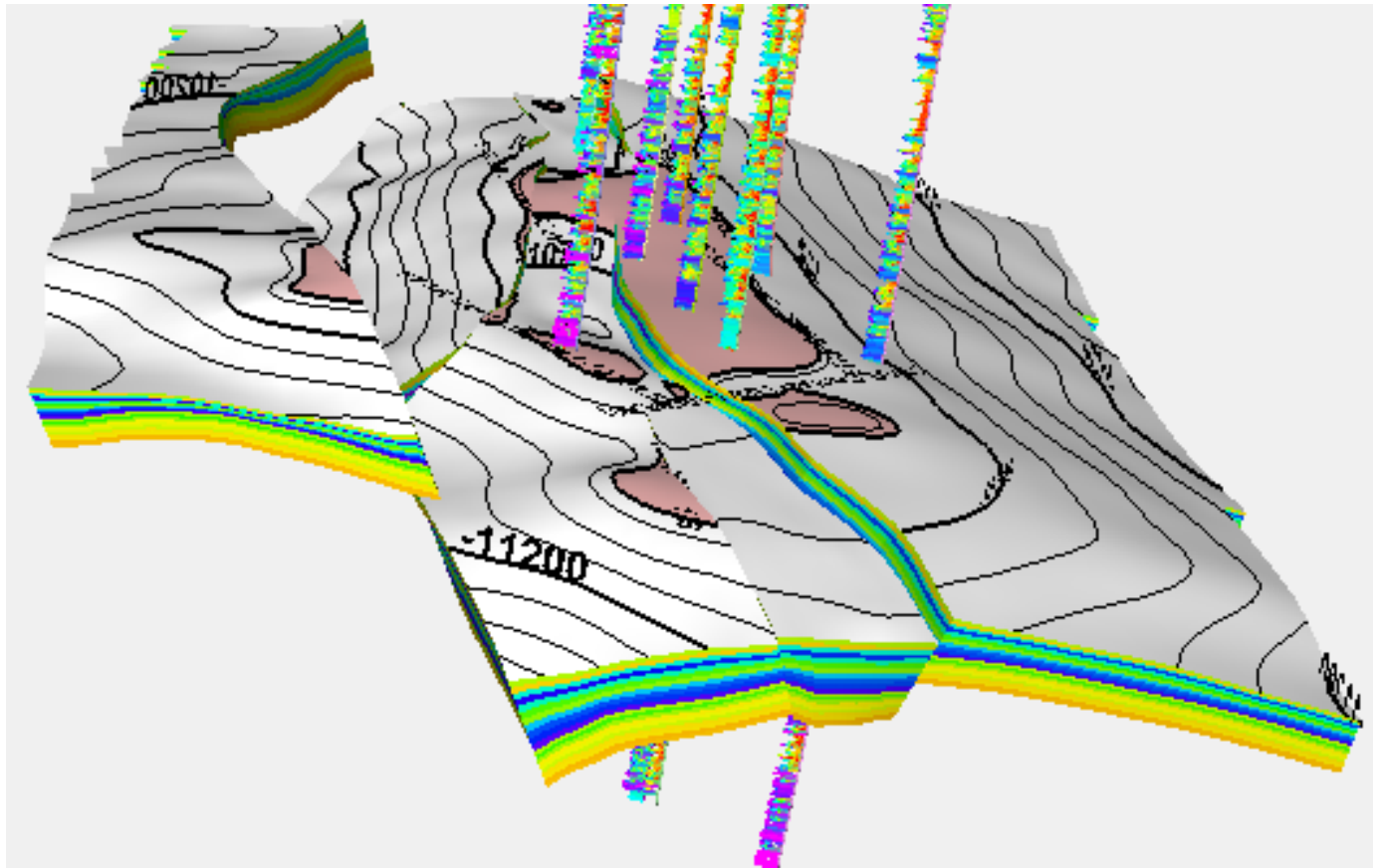
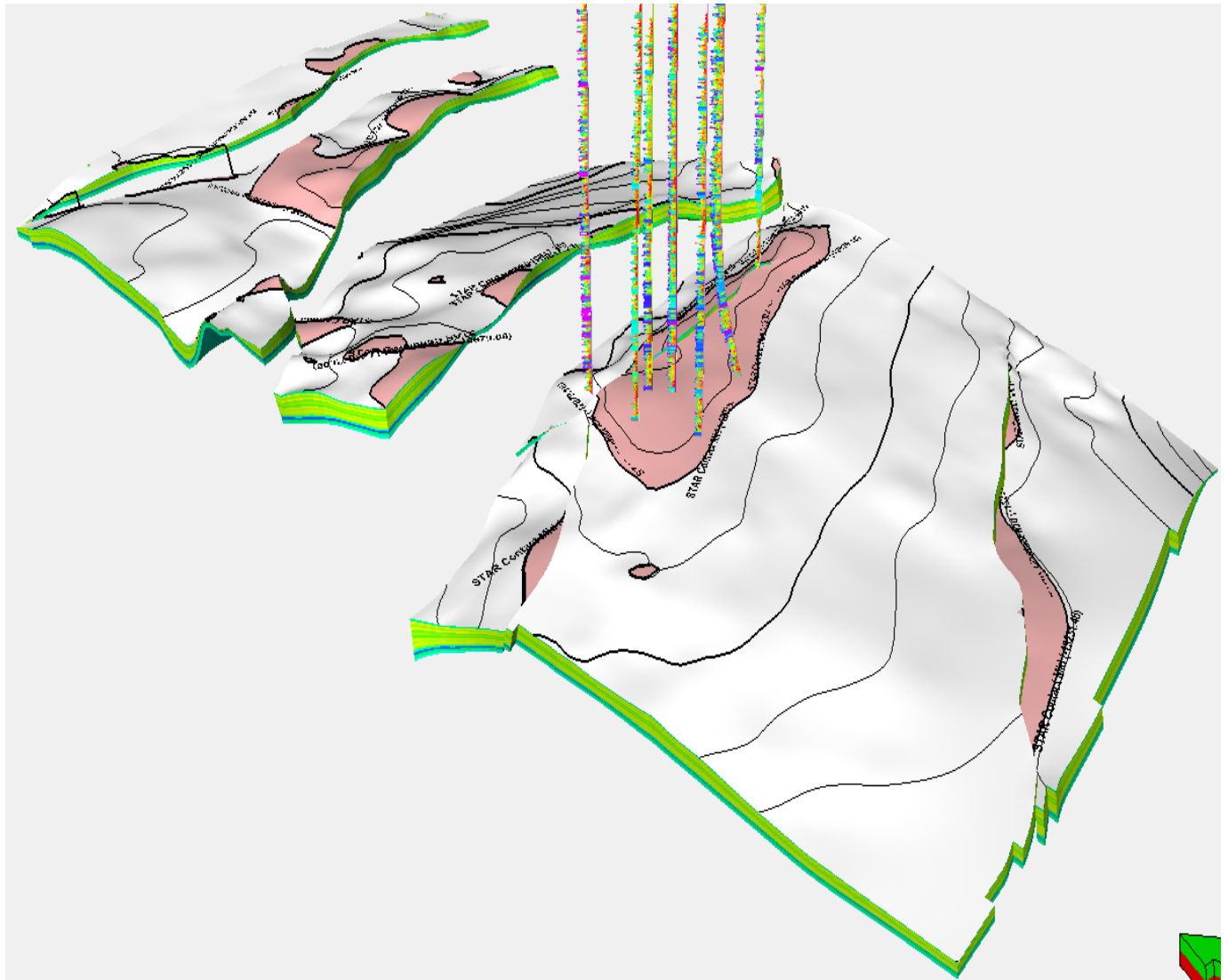**Appendix 79: Stochastic Trap Analysis and Risking Model Showing G2000**

Reservoir Column Heights
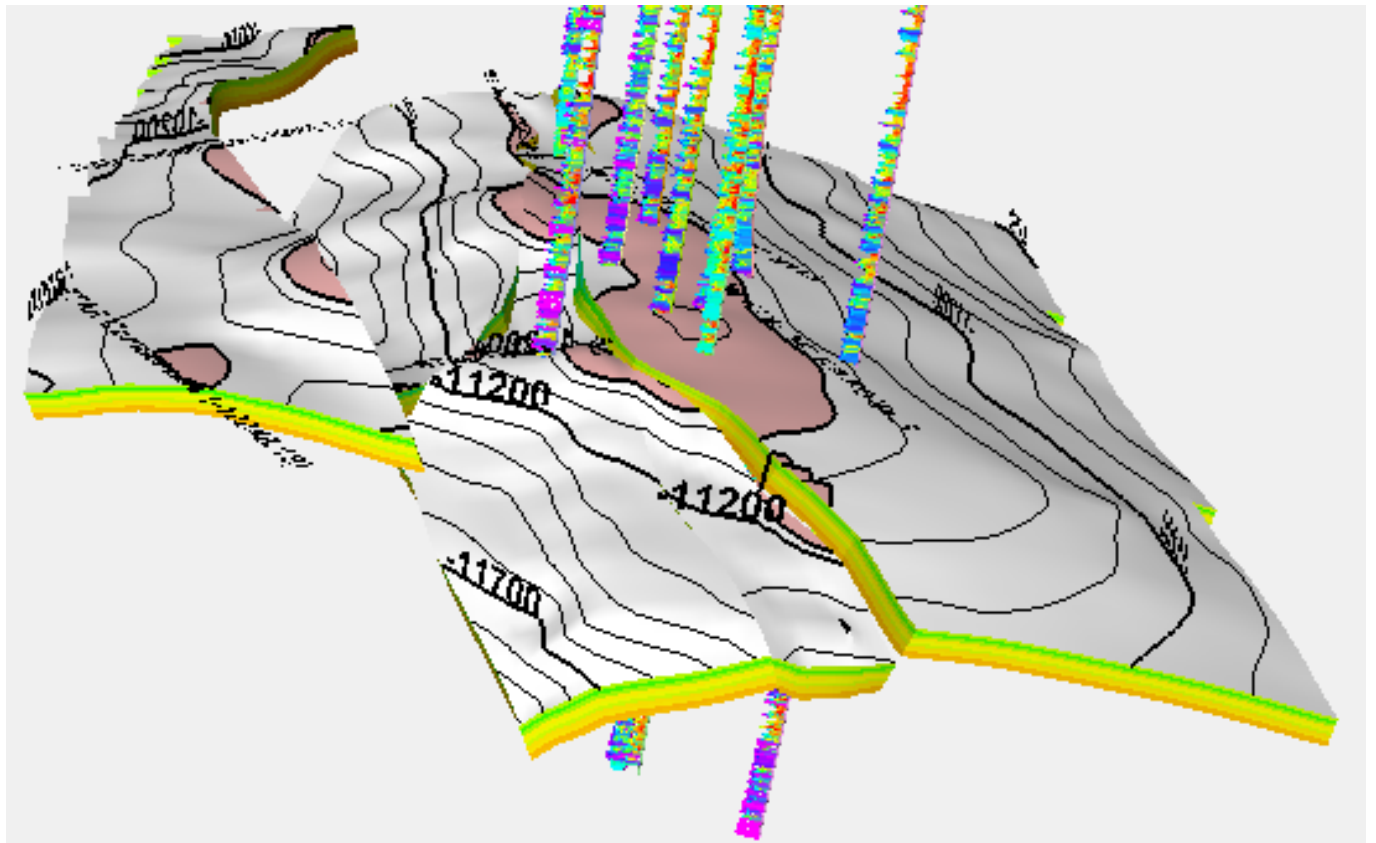
Appendix 80: Stochastic Trap Analysis and Risking Model Showing G4000
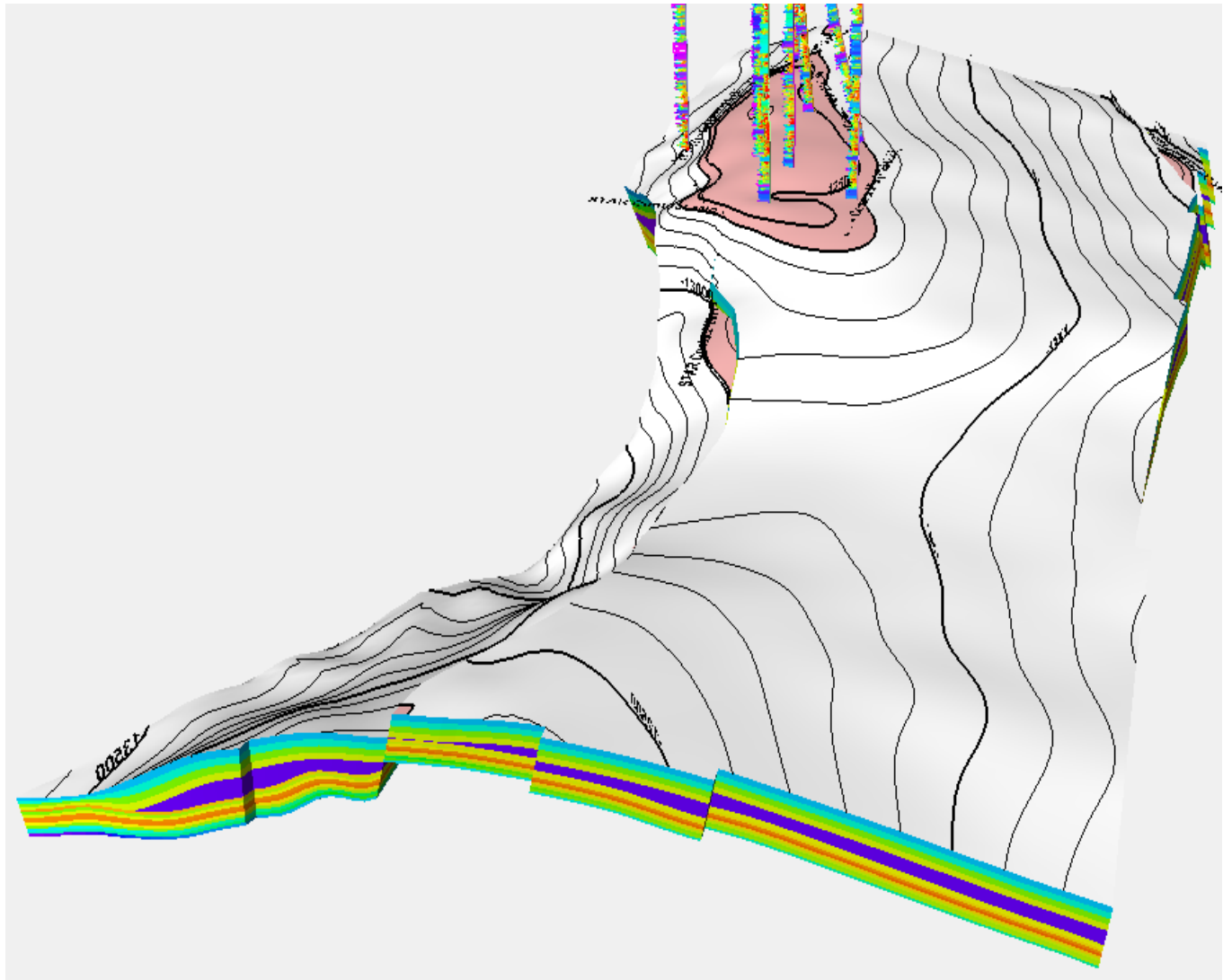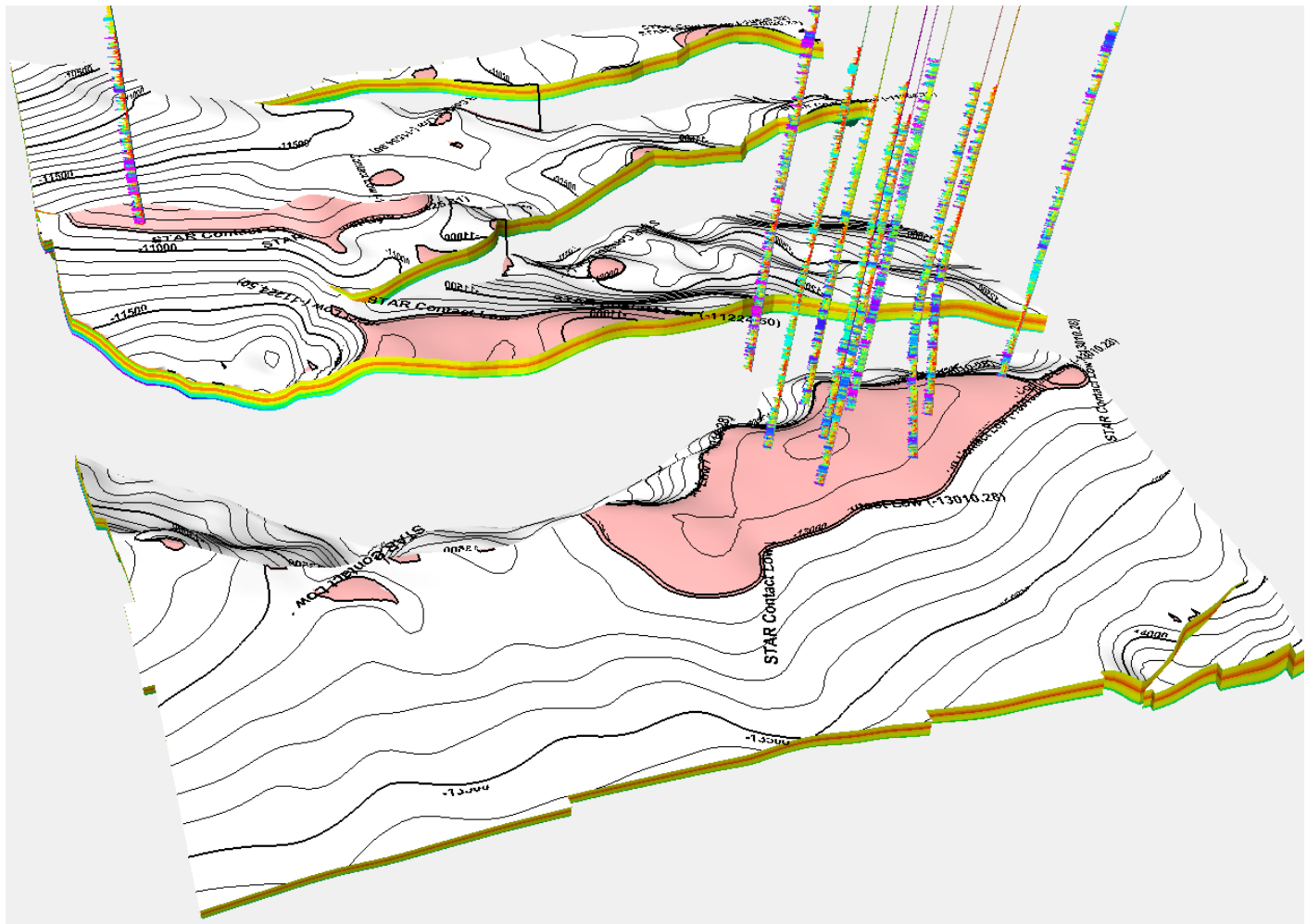
Reservoir Column Heights
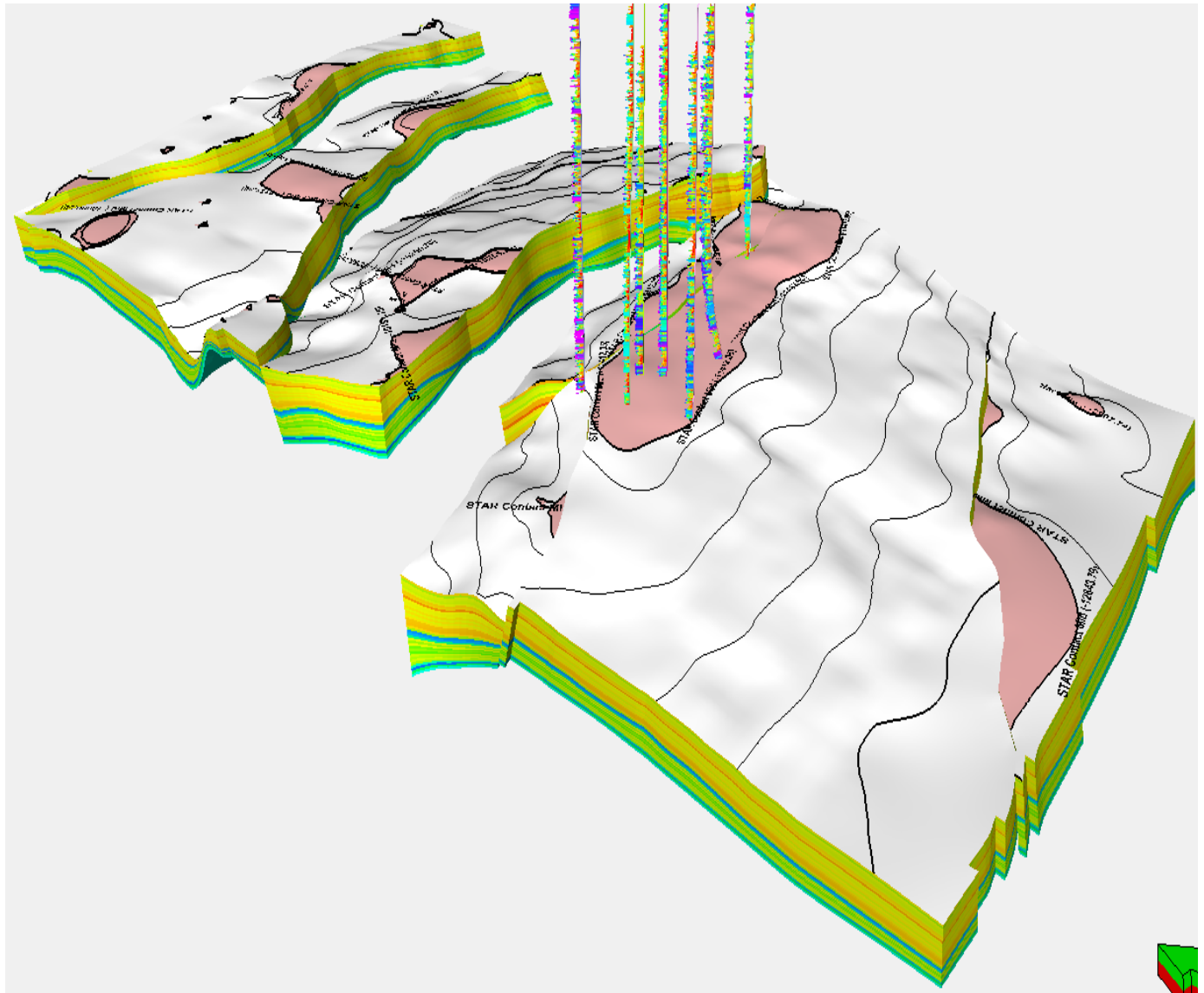
Appendix 81: Stochastic Trap Analysis and Risking Model Showing G6000
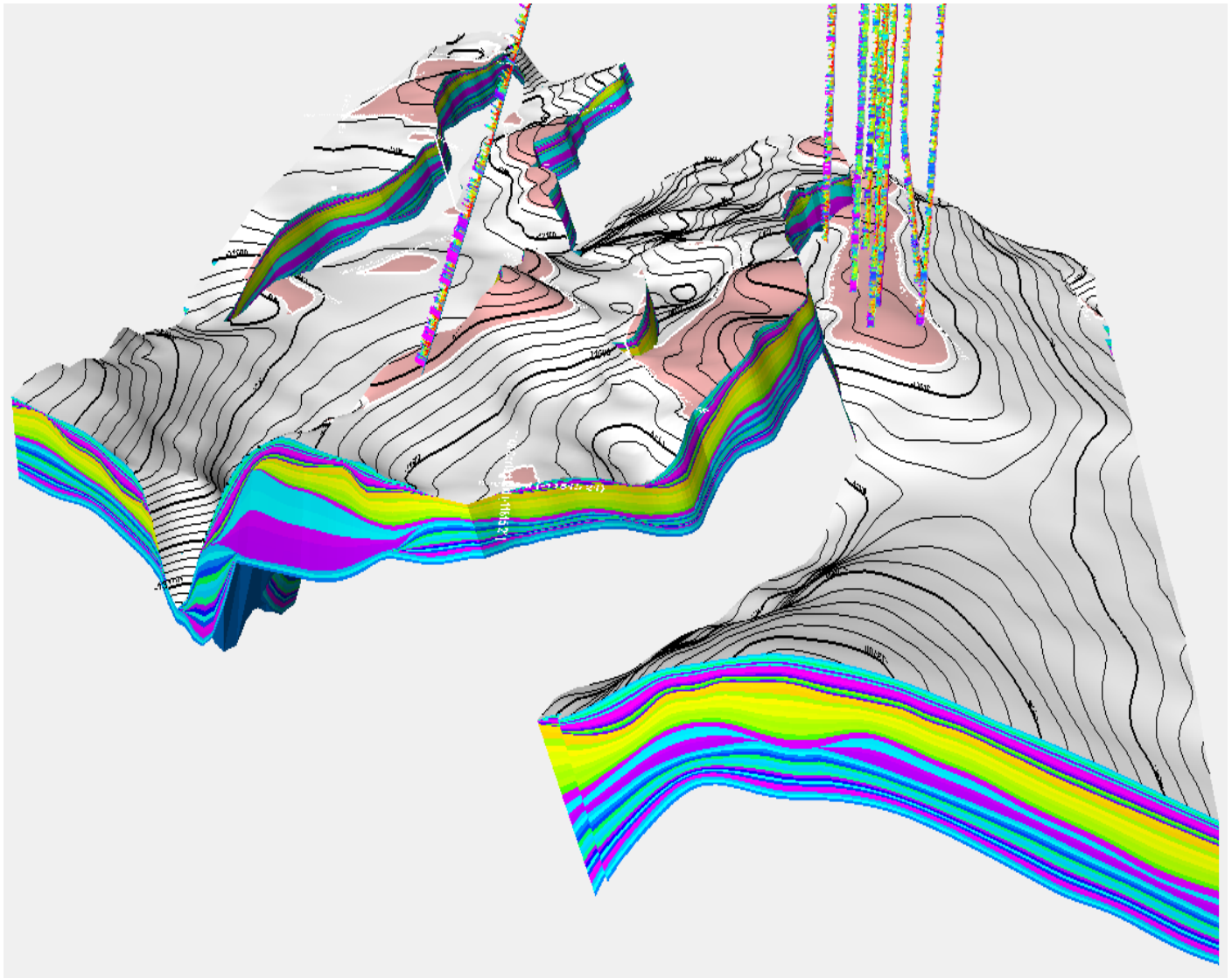
Reservoir Column Heights

Appendix 82: Stochastic Trap Analysis and Risking Model Showing G8000

Reservoir Column Heights

Appendix 83: Stochastic Trap Analysis and Risking Model Showing G9000

Reservoir Column Heights

Appendix 84: Stochastic Trap Analysis and Risking Model Showing H7100
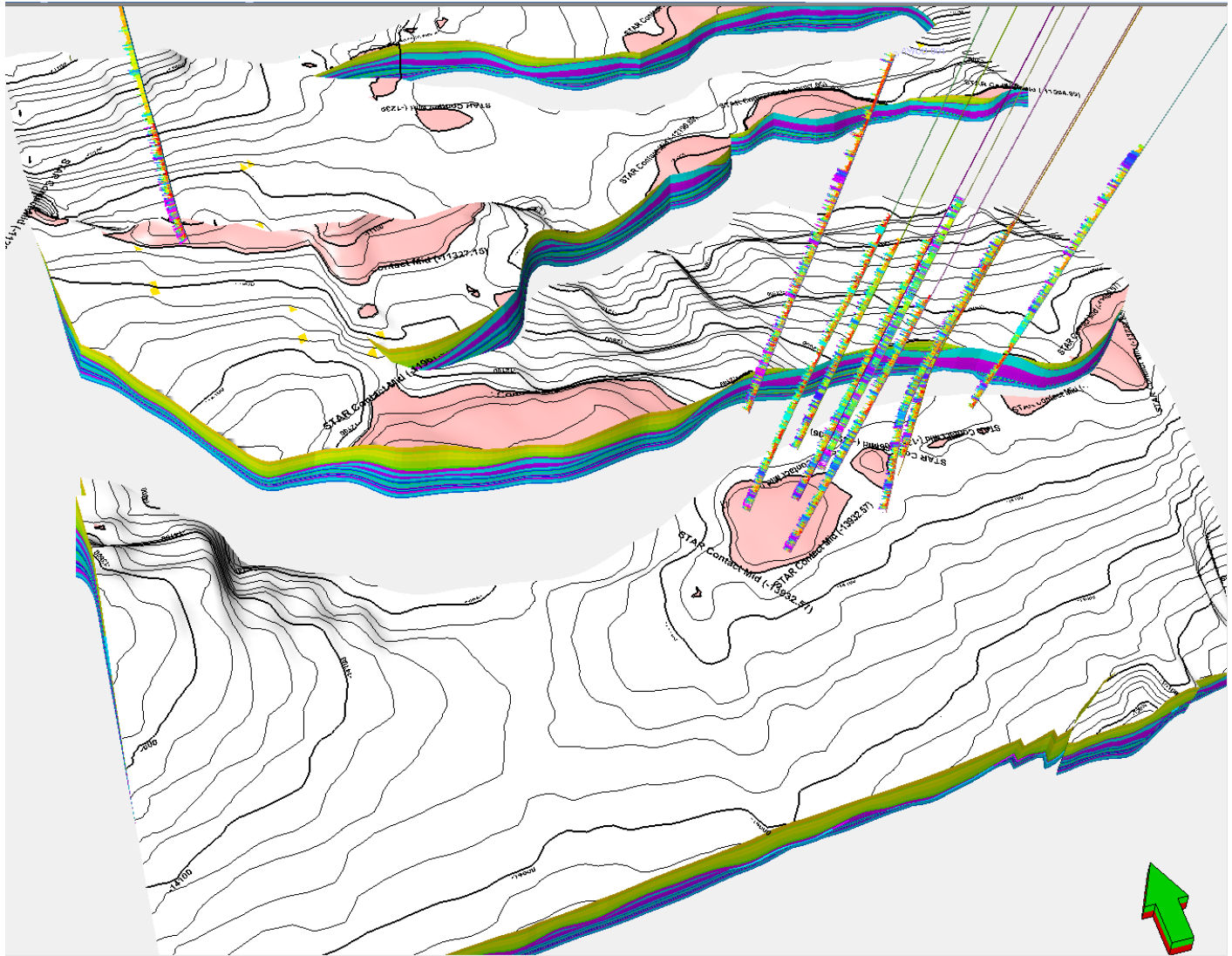
Reservoir Column Heights

Appendix 85: Stochastic Trap Analysis and Risking Model Showing H8000
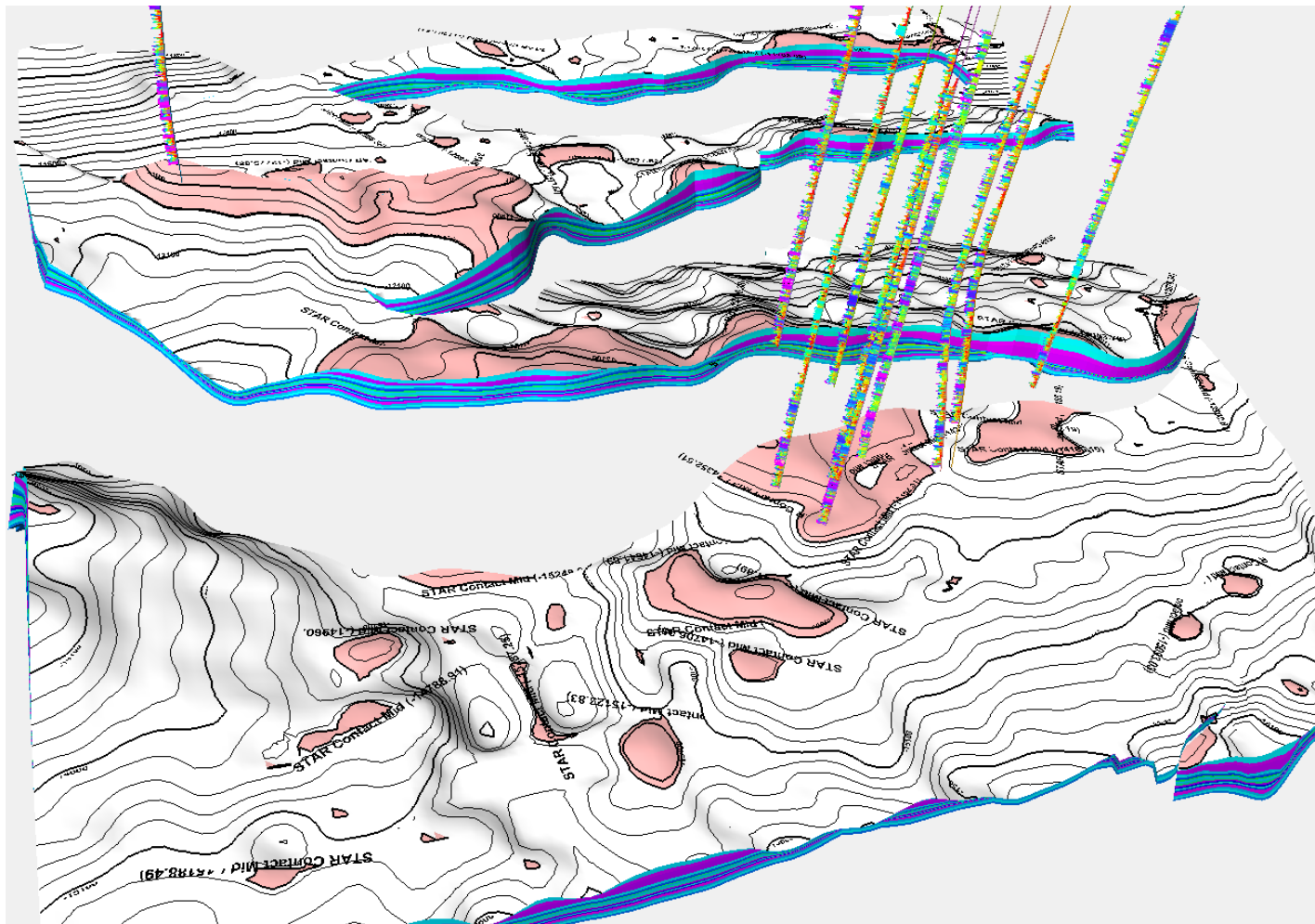
Reservoir Column Heights

Appendix 86: Stochastic Trap Analysis and Risking Model Showing K2000

Reservoir Column Heights

Appendix 87: Stochastic Trap Analysis and Risking Model Showing K3200

Reservoir Column Heights

Appendix 88: Stochastic Trap Analysis and Risking Model Showing K5000
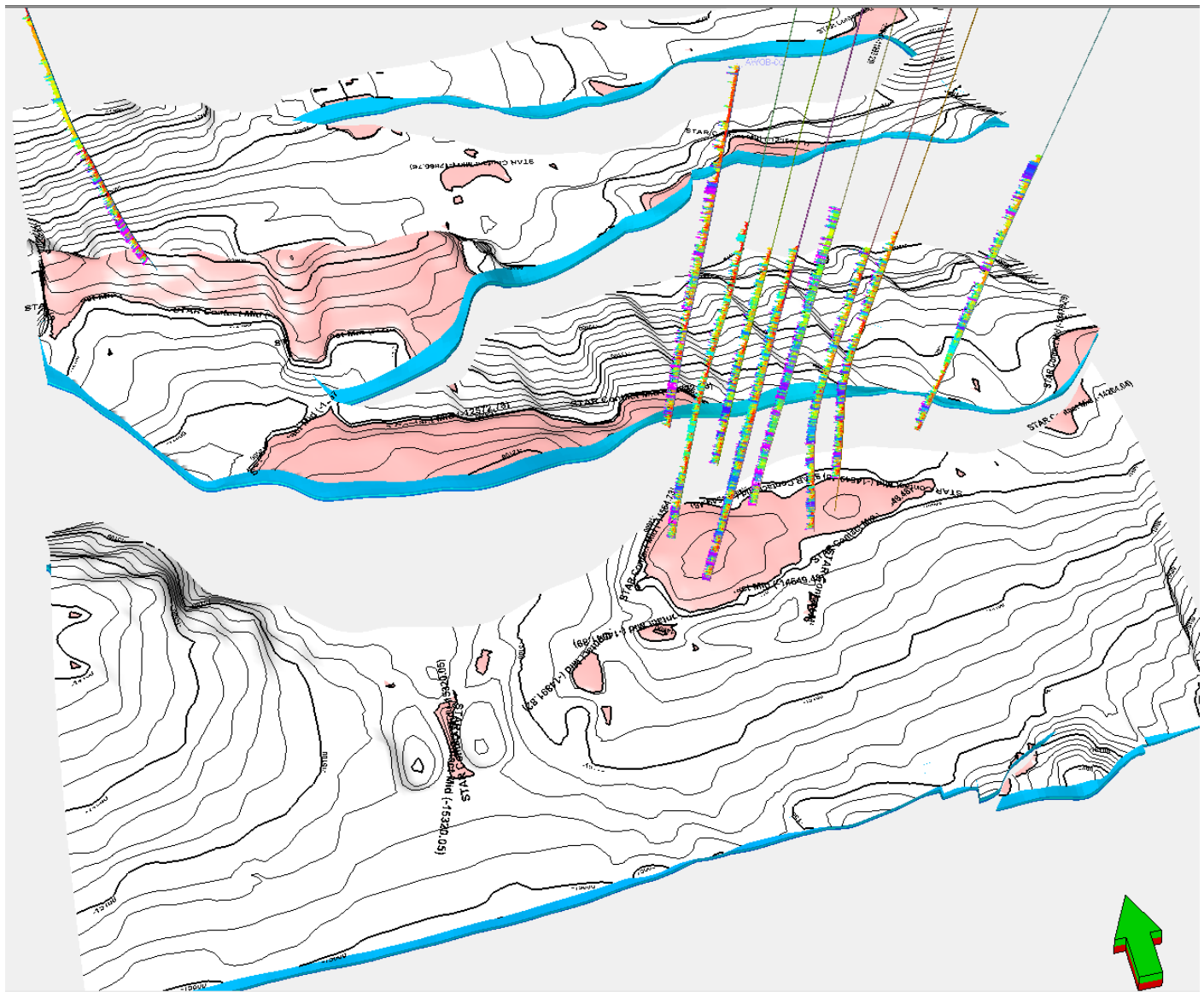
Reservoir Column Heights

Appendix 89: Stochastic Trap Analysis and Risking Model Showing K6400

Reservoir Column Heights

Appendix 90: Stochastic Trap Analysis and Risking Model Showing K7000

Reservoir Column Heights